Reuse of Produced Water from CO_2 Enhanced Oil Recovery, Coal-Bed Methane, and Mine Pool Water by Coal-Based Power Plants

Final Report

Reporting Period Start Date: October 1, 2008
Reporting Period End Date: April 30, 2012

Principal Authors:

Chad Knutson
Seyed A. Dastgheib (Principal Investigator)
Yaning Yang
Ali Ashraf
Cole Duckworth
Priscilia Sinata
Ivan Sugiyono
Mark A. Shannon
Charles J. Werth

Report Issued: July 2012
DOE Award number: DE-NT0005343

Submitted by:
Illinois State Geological Survey, Prairie Research Institute
University of Illinois at Urbana-Champaign
615 E Peabody Dr, MC-650
Champaign, IL 61820

Disclaimer

This report was prepared as an account of work sponsored by an agency of the United States Government. Neither the United States Government nor any agency thereof, nor any of their employees, makes any warranty, express or implied, or assumes any legal liability or responsibility for the accuracy, completeness, or usefulness of any information, apparatus, product, or process disclosed, or represents that its use would not infringe privately owned rights. Reference herein to any specific commercial product, process, or service by trade name, trademark, manufacturer, or otherwise does not necessarily constitute or imply its endorsement, recommendation, or favoring by the United States Government or any agency thereof. The views and opinions of authors expressed herein do not necessarily state or reflect those of the United States Government or any agency thereof.

Abstract

Power generation in the Illinois Basin is expected to increase by as much as 30% by the year 2030, and this would increase the cooling water consumption in the region by approximately 40%. This project investigated the potential use of produced water from CO_2 enhanced oil recovery (CO_2-EOR) operations; coal-bed methane (CBM) recovery; and active and abandoned underground coal mines for power plant cooling in the Illinois Basin. Specific objectives of this project were: (1) to characterize the quantity, quality, and geographic distribution of produced water in the Illinois Basin; (2) to evaluate treatment options so that produced water may be used beneficially at power plants; and (3) to perform a techno-economic analysis of the treatment and transportation of produced water to thermoelectric power plants in the Illinois Basin. Current produced water availability within the basin is not large, but potential flow rates up to 257 million liters per day (68 million gallons per day (MGD)) are possible if CO_2-enhanced oil recovery and coal bed methane recovery are implemented on a large scale. Produced water samples taken during the project tend to have dissolved solids concentrations between 10 and 100 g/L, and water from coal beds tends to have lower TDS values than water from oil fields. Current pretreatment and desalination technologies including filtration, adsorption, reverse osmosis (RO), and distillation can be used to treat produced water to a high quality level, with estimated costs ranging from $2.6 to $10.5 per cubic meter ($10 to $40 per 1000 gallons). Because of the distances between produced water sources and power plants, transportation costs tend to be greater than treatment costs. An optimization algorithm was developed to determine the lowest cost pipe network connecting sources and sinks. Total water costs increased with flow rate up to 26 million liters per day (7 MGD), and the range was from $4 to $16 per cubic meter ($15 to $60 per 1000 gallons), with treatment costs accounting for 13 – 23% of the overall cost. Results from this project suggest that produced water is a potential large source of cooling water, but treatment and transportation costs for this water are large.

Table of Contents

Disclaimer ii

Abstract iii

List of Tables vi

List of Figures ix

Executive Summary 1

Chapter 1 Introduction and objectives 3

1.1 Produced water 3

1.2 Water demand at coal-fired power plants 4

1.3 Project objectives 5

1.4 References 6

Chapter 2 Assessment of produced water in the Illinois Basin 8

2.1 Introduction 8

2.2 Produced water characterization 8

2.2.1 Geographic distribution 8

2.3 Produced water quantity 17

2.3.1 Produced water from oil fields and CO_2-EOR 17

2.3.2 Produced water from CBM 23

2.3.3 Produced water from coal mines 24

2.4 Produced water quality 26

2.4.1 Previous studies of produced water quality in the Illinois basin 27

2.4.2 Sample collection for this study 30

2.5 Conclusions 43

2.6 References 44

Chapter 3 Techno-economic assessment 47

3.1 Cooling and process water demand at Illinois Basin power plants to 2030 47

3.1.1 Current water demand by power plants in the Illinois Basin 47

3.1.2 Water demand projections for the Illinois Basin 51

3.2 Cost estimates for produced water treatment 56

3.2.1 Introduction 56

3.2.2 Cost estimations for treatment units 57

3.2.3 Treatment cost estimates for produced water 68

3.2.4 Comparison of costs to literature values 83
3.3 Treatment options for beneficial use of produced water at power plants 84
3.3.1 Water quality requirements 84
3.3.2 Treatment options results 87
3.4 Transportation cost estimate 92
3.4.1 Transportation cost methods 92
3.4.2 Transportation cost calculations 93
3.5 Optimization of the transportation network 100
3.5.1 Introduction 100
3.5.1.2 IL Basin produced water data 101
3.5.2 Optimization model analysis 109
3.5.3 Illinois basin optimization results 119
3.5.4 Electricity production increase allowed by produced water development 128
3.5.5 Paying for water treatment and transportation 128
3.5.6 Alternative cooling technologies 129
3.6 Conclusions 130
3.7 References 130
Chapter 4 Sulfate removal from produced water 134
4.1 Introduction 134
4.2 Sulfate reduction by zero-valent iron 134
4.2.1 Methods 134
4.2.2 Results from sulfate/nitrate reduction experiments with NZVI and iron powder 136
4.3 Sulfate removal by ion exchange 138
4.3.1 Introduction 138
4.3.2 Methods 139
4.3.3 Results 142
4.4 Conclusions 148
4.5 References 149
Appendix A Innovative water treatment 150

List of Tables

Table 2-1: Current active/developing CBM projects in the IL Basin (see Figure 2-5 for locations of Projects 1-9). 15
Table 2-2: Current coal production and produced water production from coal mining in the Illinois Basin. Coal production data were obtained from (DOE/EIA, 2009). Coal mine water production is from communications with mining companies. 17
Table 2-3: Oil and water production from EOR water flooding projects in Illinois. 18
Table 2-4: Produced water from EOR projects in different Illinois Counties in year 2005. 18
Table 2-5: Produced water re-injection for oil and gas recovery operations in Illinois during 2007. 19
Table 2-6: Estimated produced water production from oil recovery operations in IN and KY counties located in the Illinois Basin. 20
Table 2-7: Estimated oil and produced water potential of twenty largest oilfields in Illinois Basin. 22
Table 2-8: Produced water summary of CBM recovery in the U.S. (USGS FS-156-00). 24
Table 2-9: Produced water production from active coal mines in the Illinois Basin. 24
Table 2-10: Estimated void volume of abandoned coal mines in different counties of the Illinois Basin. Counties are ranked based on their estimated void volume. 26
Table 2-11: Compiled data from USGS and ISGS (1995) reports for the 20 largest oil fields in the Illinois Basin. Concentrations are in mg/L. Magnesium concentrations are reported as zero in the USGS report for oil fields in Illinois, so they were not included in tabulated results. 27
Table 2-12: Statistical summary of 1995 ISGS data from produced water sampled from the Aux Vases and Cypress Formations in the Clay City Consol., Lawrence, New Harmony, Dale, Sailor Springs, and Roland oil fields within Illinois. Additional measurements Pb, V, Cu, Zn, Zr, Cd, Be, Cr, As, Se, Mo, and Sb were below detection limits for nearly all samples from the fields of interest. All units, except pH, are in mg/L. 28
Table 2-13: Water quality parameters from existing CBM projects in the Illinois Basin. Concentrations are in mg/L. 29
Table 2-14: Statistics of 21 groundwater samples associated with Herrin coal in Illinois. 30
Table 2-15: List of sources for produced water samples obtained during this project. 32
Table 2-16: pH, turbidity, conductivity, TDS, TSS, alkalinity, DOC, and ammonia in produced water samples (mean values for each source with same letter are not significantly different). 34
Table 2-17: Compiled water quality data of produced water from the fields of interest in the Illinois Basin. Oilfield data represent calculated average water quality parameters of 20 largest oilfields in the Illinois Basin (Demir, 1995)). Coal mine data represent calculated average water quality parameters of 21 water samples from the Herrin coal seam (Gluskoter, 1965) (Concentrations in mg/L). 35
Table 2-18: Concentrations of major cations and anions in samples (concentrations in mg/L) (mean values for each source type with the same letter are not significantly different). 39
Table 2-19: Concentrations of trace elements in samples (concentrations in mg/L). 42
Table 3-1: Coal-based power generation in the US and Illinois Basin in 2007. 47
Table 3-2: Water withdrawal and consumption factors for different types of coal-based power plants. . 48
Table 3-3: Expected cooling and process water consumption factors of future power plants. 49

Table 3-4: Estimated yearly water withdrawal and consumption of current coal-based power plants with different cooling systems in the Illinois Basin. 50
Table 3-5: Classification of cooling systems of current coal-based power plants in the Illinois Basin. 50
Table 3-6: Water withdrawal and consumption by coal-based power plants in the Illinois Basin that use recirculating or once-through cooling systems. 51
Table 3-7: Projections for coal-based electricity generation capacity for Illinois Basin. 52
Table 3-8: Electric energy addition/retirement estimates (MWh) for future coal-based power plants in the Illinois Basin. 54
Table 3-9: Estimated additional water demand (Mgal) for future coal-based power plants in the Illinois Basin due to additions of new and retirements of old power plants, through 2030. Cumulative changes use 2005 as the starting point. 55
Table 3-10: DCC equations from Cost Estimation Manual excel model for water pumping. 59
Table 3-11: Components of raw and finished water pumping O&M cost. 59
Table 3-12: DCC equations from Cost Estimation Manual Excel model for various G values. 60
Table 3-13: Cost equations for sulfuric acid addition (before RO unit) in WaTER. 60
Table 3-14: Cost Equations for lime feed (before coagulation) in WaTER. 60
Table 3-15: Cost equations for iron coagulation in WaTER. 61
Table 3-16: Cost equations for antiscalant in WaTER. 61
Table 3-17: Cost-Capacity Equations Used in WaTER . 61
Table 3-18: Input parameters for gravity filtration system design in this report. 62
Table 3-19: Cost equations for gravity filtration unit in WaTER. 62
Table 3-20: Cost estimation equations for walnut shell and organoclay filtration units. 64
Table 3-21: Annual Cost of Concrete Contactor. 65
Table 3-22: Annual Cost of Onsite Infrared Reactivation. 65
Table 3-23: DCC equation for wash water surge basin and waste wash water storage in Cost Estimation Manual. 66
Table 3-24: MSF distillation-related costs obtained from McGivney and Kawamura (2008). 67
Table 3-25: MED distillation-related costs obtained from McGivney and Kawamura (2008). 67
Table 3-26: Stream specifications for Figure 3-3, for different water treatment scenarios of ACT (CBM) produced water. A total of ten treatment scenarios were considered: RO (only), MSF (only), RO&MSF, MED (only), RO&MED; all with and without crystallizer unit. 70
Table 3-27: Stream specifications for water treatment scenarios for Galatia (coal mine) produced water. A total of ten treatment scenarios were considered: RO (only), MSF (only), RO&MSF, MED (only), RO&MED; all with and without crystallizer unit. 71
Table 3-28: Stream specifications for Figure 3-4, for different water treatment scenarios of Louden (oilfield) produced water. A total of four treatment scenarios were considered: MSF (only), MED (only); both with and without crystallizer unit. 73
Table 3-29: Stream specifications for Sugar Creek (oilfield) produced water. A total of ten treatment scenarios are considered: RO (only), MSF (only), RO&MSF, MED (only), RO&MED; all with and without crystallizer unit. 74
Table 3-30: Direct capital cost (US$) of produced water treatment (ACT, 0.5 mgd). 77
Table 3-31: Total capital cost of produced water treatment (US$) (ACT, 0.5 mgd). 77

Table 3-32: Annual O&M cost of produced water treatment (US$) (ACT, 0.5 mgd). 78
Table 3-33: Total cost (US$/1000gal) of produced water treatment (ACT 0.5 mgd). 79
Table 3-34: Cost fraction of different produced water treatment units (ACT 0.5 mgd). 80
Table 3-35: Treatment costs of selected current produced water projects (from AGV (2004)). 83
Table 3-36: Cost estimation of representative produced water treatment systems (from Lawrence et al., 1995). 84
Table 3-37: Suggested guidelines for cooling water characteristics to reduce corrosion (from (EPRI, 2008)). 85
Table 3-38: Guidelines for power plant boiler feed water (from (GE, 2010)). 86
Table 3-39: ROSA model of full desalination system using SW30XHR membranes to treat ACT water. ... 91
Table 3-40: ROSA model of full desalination system using XLE membranes to treat ACT water. 91
Table 3-41: Components of pipeline water transportation cost. 95
Table 3-42: Pipeline right-of-way cost in the Illinois Basin. 97
Table 3-43: Cost components of water transportation by PVC pipelines for 1 mile (pump station cost estimated from power requirement). 99
Table 3-44: Cost of water transportation by PVC and DIP pipelines. 99
Table 3-45: Electric power production and water demand (assuming recirculating cooling) for power plants included in the study. 101
Table 3-46: Data for oil fields in the IL basin used for the optimization model. 103
Table 3-47: Locations of potential CBM projects in the IL basin used for simulations. 107
Table 3-48: Computational performance of permutation code using Matlab/Windows Vista. 110
Table 3-49: Total water costs for the IL basin using all CBM sources broken down by sink and demand. Flow rate (q) is kgal/day and cost is $/kgal. 126
Table 4-1: APS and NZVI experiments. 136
Table 4-2: Experimental results for Re-NZVI + DMAP system designed to reduce sulfate. 137
Table 4-3: Resin characteristics. 140
Table 4-4: Isotherm constants for real and synthetic Galatia produced water 147

List of Figures

Figure 2-1: A conceptual integrated CO_2 and produced water system for electricity generation and oil production. 9
Figure 2-2: Geographic distribution and estimated amount of CO_2-EOR from oilfields in the Illinois Basin (twenty largest oilfields are ranked and shown). From (Finley, 2005). 11
Figure 2-3: Original Oil In Place (OOIP) of oilfields in the Illinois Basin. Twenty largest oilfields are ranked and shown on this map. Derived from Finley (2005). 12
Figure 2-4: Field miscibility classification of oilfields in the Illinois Basin for CO_2-EOR. Twenty largest oilfields are ranked and shown on this map. Derived from Finley (2005). 13
Figure 2-5: Estimated coal bed methane original gas in place for major coal seams in the Illinois Basin (ISGS/MGSC, 2005). Current active/developing CBM projects are shown on the map. 14
Figure 2-6: Areas of active and historical coal mining in the Illinois Basin. 16
Figure 2-7: Concentration distributions for (a) TDS and (b) Cl^- for the USGS and 1995 ISGS data sets. There are 279 and 29 data points for the USGS and ISGS (1995) reports, respectively. 29
Figure 2-8: Water sampling locations of oil fields, coal mines, and CBM projects in the Illinois Basin. 31
Figure 2-9: A schematic diagram of produced water sample preparation and analysis. 33
Figure 2-10: TPH contents in selected samples before and after filtration (0.7 µm). 38
Figure 3-1: Projections for cumulative additional annual water consumption and withdrawals of coal-based power plants in the Illinois Basin. 56
Figure 3-2: A summary of the approach to estimating produced water treatment costs. 57
Figure 3-3: Conceptual process flow diagram (PFD) for treating produced water from CBM and coal mines. 69
Figure 3-4: Conceptual process flow diagram for treating produced water from oilfields (Louden and Sugar Creek). 72
Figure 3-5: Estimated produced water treatment cost of different cases without including the salt sale credit for ZLD processes. 81
Figure 3-6: Estimated produced water treatment for ZLD processes considering the salt sale credit. 82
Figure 3-7: Permeate TDS values as a function of recovery for ACT produced water (feed TDS = 19 g/L) with XLE and SW30XHR membranes. 88
Figure 3-8: Permeate TDS values obtained at maximum recovery for the 3 produced waters. XLE (circles) and SW30XHR (diamonds) membranes are used in the simulations. Target TDS values for permeate are shown by the red and green dashed lines. 89
Figure 3-9: Permeate TDS values for ACT produced water with (filled circles) and without (open circles) booster pumps. Dashed line denotes target TDS value for cooling make-up water. 90
Figure 3-10: ROSA results for membrane treatment of ACT produced water using (a) SW30XHR and (b) XLE membranes. 92
Figure 3-11: Locations of power plants (green stars) , oil fields (black O), coal mines (red O), and potential coal bed methane projects (cyan O) used for the optimization model. 104
Figure 3-12: Cumulative raw water production of the modeled sources plotted as a function of distance from the Gibson (blue), Powerton (green), and Coffeen (red) power plants. 105
Figure 3-13: Total flow rate as a function of the distance from sources to the closest sink in IL basin. 105

Figure 3-14: Cost of water management for RO treatment of produced water. Curves show costs for RO treatment only, RO treatment plus concentrate disposal, and direct disposal of all produced water. ... 109
Figure 3-15: Model results from randomly generated locations and flow rates for 7 produced water sources (circles). Sinks (x) are located at (0,0) and (1,1). Transport cost is given by power law cost function. Optimal pipe network solution (left) and histogram of the costs for all feasible solutions (right). ... 110
Figure 3-16: Total water costs (treatment and transportation) for two different distances and raw water TDS values using a single sink and source. ... 111
Figure 3-17: Pipe length at which transportation costs are equal to treatment plus disposal costs. Black lines indicate RO treatment, red lines indicate thermal treatment, and flow rates are 20, 100, and 500 kgal/d (solid, dashed, and dash-dot, respectively). ... 112
Figure 3-18: Distance differences for equal water costs, comparing sources with different values of TDS. Circles denote RO treatment for both sources, diamonds denote thermal treatment for both sources, and squares one source with RO and one with thermal, where RO treats a source with TDS equal to 20 (red), 40 (cyan), and 60 (black) g/L. ... 113
Figure 3-19: Costs for water treatment and pipe network configurations for the sample square problem. ... 114
Figure 3-20: Source configuration problem. Each source (blue circles) has the same flow rate and TDS value. a: sources are equidistant from the sink (red). b: Linked linear pipe network. c: Linked fractal pipe network. ... 115
Figure 3-21: Linearly located sources linked along a single pipeline with distances between sources equal to 1(o), 2 (diamonds), 5 (+), and 10 (squares) miles. ... 116
Figure 3-22: Incremental costs for each additional water source added for the single pipeline case. (Same distance symbols as in Figure 3-21). ... 116
Figure 3-23: Cost of water from sources equidistant from the sink that have TDS concentrations that increase by 5 g/L with each source. The blue curve is for using separate pipelines, with the green curve us a single pipe connects all the sources to the sink. Linear disposal costs are included. ... 117
Figure 3-24: Water costs for linear chain (O), fractal (diamond), independent constant distance (red), and independent increasing distance (blue). ... 118
Figure 3-25: Number of connections in the fractal network varied (2 (blue O), 3 (red squares) or 4 (green diamonds) sources sent to each source in the network), but the flow rate as a function of distance is equal for all cases. ... 119
Figure 3-26: Optimal pipe network for water sent to Gibson only, where total flow rate is 3087 kgal/d. Oil fields (black O), CBM projects (cyan O), coal mines (red O), send produced water to Gibson power plant (green star). ... 120
Figure 3-27: Optimal pipe network for water sent to Clifty Creek only, where total flow rate is 3126 kgal/d. Symbols are the same as used in Figure 3-26. ... 121
Figure 3-28: Optimal pipe network for water sent to Marion only, where total flow rate is 3347 kgal/d. Symbols are the same as used in Figure 3-26. ... 121
Figure 3-29: Water costs for demand at a single sink, where blue diamonds and red squares indicate Gibson and Clifty Creek, respectively. ... 122

Figure 3-30: Degree of branching as a function of the number of sources connected to Gibson (blue) and Clifty Creek (red) power plants, and the theoretical branching of a binary fractal network (green)..... 123
Figure 3-31: Optimal pipe network for a single realization using large scale CBM development where all sinks demand water. Oil fields (black O), CBM projects (cyan O), coal mines (red O), send produced water to power plants (green stars). 124
Figure 3-32: Water costs for delivery of produced water to all sinks, with minimal (blue diamonds) and large-scale (brown squares) CBM development. 125
Figure 3-33: Water flow rates and costs at individual sinks for all sinks simulations. Sinks are Gibson (blue diamonds), Clifty Creek (red squares), Powerton (green triangles), and Marion (x). 125
Figure 3-34: Water cost versus flow rate averaged over a set of realizations. Results are for all-sinks (solid line), Gibson (solid blue diamonds), and Clifty Creek (solid brown squares). Open symbols denote data from single sink simulations. 127
Figure 3-35: Degree of branching at several sinks for the all-sinks case. Sinks are Gibson (blue diamonds), Clifty Creek (red squares), Powerton (green triangles), and Marion (x)..... 127
Figure 3-36: Percentage of total water cost comprised of transportation costs for Gibson only (blue diamonds), Clifty Creek only (red squares), and all-sinks (green triangles). 128
Figure 4-1: APS experiments shown with two controls. 138
Figure 4-2: Effects of resin pretreatment on sulfate uptake for weak base resins. 143
Figure 4-3: Sorption isotherms for commercially available weak base and strong base anion exchange resins. Inset plot shows strong base resin isotherms expanded. 144
Figure 4-4: Chloride's effects on sulfate uptake by resins WBG-30 and R402. 145
Figure 4-5: Sulfate removal for waters with similar chloride concentrations but differing chloride to sulfate ratios. 146
Figure 4-6: Chloride effect on retardation (R). 148

Executive Summary

Because thermoelectric power generation requires large volumes of water, future increases of power production may require more water than is available from current water sources, even in water-rich regions such as the Illinois Basin. This project investigated the potential use of water derived from the production of fossil fuels, including oil, coal, and coal-bed methane (CBM), to supplement freshwater cooling sources at power plants in the Illinois Basin. Current annual electric power production from coal-fired power plants in the Illinois Basin is 200 million megawatt-hours, and this number is expected to increase by 30% by the year 2030. The expected increase in electricity generation may increase the current annual water consumption of the coal-based power plants in the Illinois Basin by 40% within the next 20 years.

Large volumes of produced water may be available depending on the future production of fossil fuels. For oil fields, CO_2-enhanced oil recovery (CO_2-EOR) could produce large volumes of water for cooling, especially if the objective is to maximize subsurface CO_2 storage. Potential water production from CO_2-EOR in the Illinois Basin is estimated to be between 15 and 110 million liters per day (4 and 29 MGD). Water production from active coal mines is approximately 4 million liters per day (1 MGD), and only three mines report significant water production. Voids in abandoned mines are estimated to have a total volume of 1.2 billion cubic meters, some of which may be filled with water that can potentially be used. Currently, CBM production in the Illinois Basin is very small, but methane may be produced in conjunction with CO_2 sequestration within coal beds. If large-scale CBM production occurs over a time period of the next 50 years, we estimate that the produced water flow rate will be as large as 144 million liters per day (38 MGD) during this time frame. Current volumes of produced water are not large, but up to 257 million liters per day (68 MGD) could be available if CO_2-EOR and coal-bed methane are practiced extensively.

Produced water samples were collected from thirteen different sources and analyzed for water quality. Produced water from oil fields in the Illinois Basin tends to be highly saline; total dissolved solids (TDS) concentrations commonly are 100 g/L, although TDS values near 30 g/L have been observed. A challenge for treating produced water from oil fields is to ensure that all the oil droplets are removed from the water, as entrained oil droplets may affect water treatment processes. Produced water from coal mines and coal bed methane projects generally have TDS values closer to 20 g/L, and concentrations of suspended solids tend to be small.

Treatment of produced waters to the required levels is possible with existing technology. We propose different desalination treatment processes depending on the TDS concentration of the raw produced water. For TDS values less than 60 g/L, reverse osmosis can be used for desalination; distillation is needed for produced waters with larger TDS values. Pre-treatment steps include flocculation, filtration, and treatment with activated carbon (typically for oil-field produced water only). Concentrate from the desalination process may either be pumped into deep saline aquifers or sent to a crystallizer when zero liquid discharge is indicated by the economics. Salts generated during the crystallizer process may be an additional revenue stream for the water treatment facility. Costs for produced water treatment,

including concentrate disposal, are in the range of $2.6 to $10.5 per cubic meter ($10 to $40 per 1000 gallons). These costs are larger than for sea water desalination because the concentrate must either be pumped underground or crystallized, and potential produced water treatment plants have small capacities (typically less than 2 million liters per day (0.5 MGD)), which increases unit costs.

Sulfate removal by both catalytic reduction and ion exchange processes was investigated in this project. Sulfate removal from produced water may be significant for some produced water sources because sulfate can cause formation of stress-induced cracks in stainless steel and can corrode concrete. To test catalytic reduction for sulfate removal, zero-valent iron was doped with electron transfer agents and mixed with solutions containing sulfate. Some sulfate sorbed to the iron complex, but no redox reactions were observed for a range of experimental conditions. As an alternative method, weak base anion exchange resins were found to effectively remove sulfate even when chloride/sulfate ratios in the produced water approached 100 to 1.

Treated produced water must be piped to a nearby power plant if it is to be used for cooling. Transportation costs depend on the flow rate and distance, but can be approximated as $0.16 per cubic meter per kilometer ($1 per 1000 gallons per mile). For the distances that produced water must travel within the Illinois Basin, transportation costs can be more than twice the cost for treatment.

An optimization algorithm was developed to minimize the overall costs of using produced water at power plants in the basin. The objective of the solver is to determine the least cost pipe network that distributes produced water to power plants within the Illinois Basin. The 20 largest oil fields, three coal mines, and either 2 or 20 potential CBM projects in the basin were sources of produced water, and 11 power plants were sinks. The pipe network connects sources to other sources or sinks (power plants). Cost functions for water treatment and transportation were power law functions of the TDS concentration and flow rate, and disposal costs for post-treatment concentrates were neglected. Produced water flow rates from between 4 and 27 million liters per day (1 and 7 MGD) were obtained by adjusting the maximum cost of produced water. Total water costs, including treatment and transportation, ranged from $4 to $16 per cubic meter ($15 to $60 per 1000 gallons). Treatment costs accounted for 13 - 21% of the total cost. Somewhat counter-intuitively, the total cost of produced water treatment and transportation increased nearly linearly with flow rate. The reason for this increase is that the distance traveled between sources and sinks increases with increasing flow rate. Transportation costs tend to be much larger than treatment costs.

Results from this project suggest that produced water is a large potential resource for cooling water systems at power plants. However, using this water resource will be much more expensive than the water currently used, and the primary cost component is transportation from sources to power plants. Perhaps a solution to this problem would be to build future power plants much closer to regions with large volumes of produced water.

Chapter 1 **Introduction and objectives**

1.1 Produced water

Produced water is defined as the water from geological formations that is brought to the surface during production of fossil fuels (i.e. oil, gas, and coal). It is also referred to as production water, co-produced water, or formation water by different researchers. Produced water constitutes the single largest waste stream in the oil and gas industry (Sirivedhin and Dallbauman, 2004).

The national average water-to-oil ratio estimated from the onshore production-weighted ratios of 14 states was 7.6 barrel per barrel (bbl/bbl) and the national average water-to-gas ratio estimated from the onshore production-weighted ratios of 11 states was about 41.3 cubic meters of water per 28,000 cubic meters of gas (260 barrels per million cubic feet (bbl/Mmcf)) (Clark and Veil, 2009). The estimated yearly amount of produced water generated from onshore oil and gas activities in the United States from 1988 to 2007 varied between 2.226 and 3.340 billion cubic meters (14 and 21 billion bbl (1 bbl = 42 U.S. gallons) (API, 1988, 2000; Veil et al., 2004; Clark and Veil, 2009).

National data for produced water from coal mines are not available, but it has been reported that some mines in different coal basins produce or contain a considerable volume of water. For example, the estimated water discharge from 130 coal mines in the Appalachian basin is 72.3 million cubic meters (19.1 billion gallons) per year (Veil et al., 2003). A large volume of water is produced during coal bed methane (CBM) recovery. For example, the estimated volume of water produced for CBM recovery in the Powder River Basin of Wyoming is 945,000 cubic meters (250 million gallons) per day (Gillette and Veil, 2004). The U. S. Geological Survey (USGS) (2000) reported average water-to-gas ratios of about 0.4 cubic meters of water per 28,000 cubic meters of gas (2.75 bbl water/Mmcf of gas) in five coal basins.

Depending on the produced water quality, current practice for produced water management includes reinjection into underground formations, surface discharge into receiving waters, and beneficial reuse. Water from surface mines and overflowing underground mines typically is discharged to surface streams, whereas reinjection is the most common approach for managing onshore oil and gas produced water. More than 98% of produced water from onshore wells was injected underground in 2007 (Clark and Veil, 2009). Approximately 59% was injected into producing formations to maintain reservoir pressure and for enhanced oil recovery (EOR); while another 40% was injected into nonproducing formations for disposal (Clark and Veil, 2009).

The major constituents in produced water include suspended solids, dispersed oil and grease (from oilfields), dissolved organic compounds, and various cations and anions. The physical and chemical properties of produced water vary widely depending on the geographic location of the field, the geological formation from which the water is pumped, and the composition of hydrocarbon products being produced. In recent years, the feasibility of reusing produced water for agricultural, industrial, and potable uses has been studied (Tao et al., 1993; Koren and Nadav, 1994; Doran et al., 1999). About 37% of the produced water sources from the oil and gas industry documented in the USGS's Produced Waters Database were deemed to be treatable (EPRI, 2006). Considering the finite availability of freshwater resources and increasing demand for water in thermoelectric, agricultural, domestic, and

industrial sectors (including emerging biofuel and hydrogen production plants), in addition to possible water shortages due to climate change, new restrictions on water use, even in non-arid areas, seem likely to be enacted. Non-traditional sources of water such as treated wastewater and produced water may potentially become significant supplements to current freshwater sources for thermoelectric, industrial, and agricultural applications.

Produced water quality and local water demand and supply are important factors that influence water management. The feasibility of reclaiming produced water primarily depends on the water's quality and quantity, which determines the appropriate treatment technologies and costs. Although produced water quantity plays an important role in selecting the best approaches for water management, it is difficult to reliably predict the quantity of water production that will result from future development of fossil fuel resources. Knowledge of physical and chemical properties of a produced water source is needed for regulatory compliance and for selecting proper management options such as secondary recovery (in the case of oilfields), disposal, or reuse.

1.2 Water demand at coal-fired power plants

Current annual electricity consumption in the United States is approximately 4 billion megawatt-hours, and the demand is predicted to increase 20% by 2035 (EIA, 2010). About 68% of the total electric power in the U.S. is generated from fossil fuels (about 46% from coal, 21% from natural gas, and 1% from petroleum).

Thermoelectric power generating systems, including fossil-based and nuclear plants, use steam cycles for electric power generation. Water is used in wet cooling systems to condense steam at the back end of the turbine generator. There are two main wet cooling systems: open-loop and closed-loop. About 31% of current U.S. electricity generation capacity is from thermoelectric plants that use the open-loop cooling system (U.S. DOE, 2006).

An open-loop, or once-through system, withdraws water from a source (e.g., a river or lake) and returns the heated water to the source. Average estimated amounts of water withdrawal and consumption to generate 1 kWh of electricity in an open-loop system is ≈0.14 m^3 and 380 cm^3 (≈38 and ~0.1 gallons), respectively. In comparison, the corresponding values in a closed-loop (circulating) system are about 4,500 and 4,200 cm^3 (1.2 and 1.1 gal) per kWh (Feeley et al., 2006). Another DOE publication reports that total water consumption in different coal-fueled power plants (equipped with closed-loop cooling systems) varies from 2,700 cm^3 (0.714 gal) per kWh in PC boilers to 1600 to 1900 cm^3 (0.433-0.510 gal) per kWh in Integrated Gasification Combined Cycle (IGCC) processes (Klett et al., 2007). In coal-based power plants, 74 to 78% of the total water consumed is converted to water vapor and lost either in a cooling tower or with flue gas.

A significant amount of water is required to operate a thermoelectric power plant. In the U.S., thermoelectric power generation accounts for about 40% of the total freshwater withdrawals (1.31 billion m^3 [346 billion gallons] per day) and about 3% of the total water consumption (378.5 million m^3 [100 billion gallons] per day) (EIA, 2010; Solley et al., 1998; Hutson et al., 2004). In Illinois, about 82% of the estimated 53 million m^3 (14 billion gallons) per day of fresh water withdrawals in 2000 were used in

the thermoelectric power sector, which is more than twice the average percentage of withdrawals for the U.S. Freshwater consumption by the thermoelectric industry in Illinois is approximately one-third of the state's total 3.785 million m^3 (1 billion gallons) of daily freshwater consumption (Solley et al., 1998; Hutson et al., 2004).

A recent DOE/National Energy Technology Laboratory (NETL) scenario study of freshwater demand by the thermoelectric generation sector predicts that by 2030, the sector's water consumption will increase by 30-50%. During the same time frame, total water withdrawals by the sector change within a range of −20% to +7% (DOE/NETL, 2007). Most new power plants are expected to use recirculating cooling systems, which reduce withdrawal, but increase consumption. If CO_2 capture systems are installed at fossil fuel power plants, water consumption increases. Depending on the energy source and carbon capture technologies, water consumption can increase from 40 to 120% (DOE/NETL, 2007). According to the same study, by 2030, for a region that includes Illinois, water consumption by the thermoelectric generation sector increases by 55 to 160%, but water withdrawal changes by −16% to +14%.

Current freshwater demand has resulted in over-pumping from available water resources in some regions of the U.S. The groundwater elevation in some areas near Chicago drops as much as 5.2 m (17 feet) per year (U.S. DOE, 2006). Considering the limited availability of water resources and the potential for increased water demand by the domestic, agricultural, and industrial sectors, it is likely that the coal-based power generation industry will face restrictions on water use.

Non-traditional sources of water, including produced water from CBM recovery, oil recovery, and coal mines, are potential sources to meet the water needs of power generation plants. Argonne National Laboratory (ANL) and West Virginia University recently evaluated the feasibility of using coal mine water for cooling operations of power plants in the Appalachian Basin (Feeley et al., 2006; Veil et al., 2003). The combined water storage volume of these mines could be up to 250 billion gallons (Veil et al., 2003). ANL's research suggests that mine pool water can be a potential source of industrial cooling water if some technical, policy, and regulatory issues are resolved. Two other studies investigated the use of mine pool water for power plant cooling. West Virginia University and the University of Pittsburgh/Carnegie Mellon studied locations of pools and distances to power plants in the Appalachian Basin. Additionally, they investigated treatment requirements of the water and regulations for its use at power plants. Large mine pools have been considered as heat sinks for power plants (DOE/NETL, 2009).

Sandia National Laboratories are studying the use of water from saline aquifers used as sequestration sites for carbon dioxide disposal. The sequestration potential of various aquifers is being examined, and the water treatment methods allowing water usage at power plants are being determined. They are considering using waste heat from power plants to reduce the energy needed to remove dissolved solids from the water (DOE/NETL, 2009). Details of recent and previous research by the national laboratories on utilization of non-traditional sources of water for power plants can be found in DOE/NETL (2009).

1.3 Project objectives

This project was supported by the US Department of Energy (DOE) (cooperative agreement DE-NT0005343, from 10/1/08 through 4/30/12) and the Illinois Clean Coal Institute (ICCI) (project 08-1/US-

3). Participants of this project are: (1) Illinois State Geological Survey (ISGS); (2) Illinois Department of Commerce and Economic Opportunity, ICCI; (3) Midwest Geological Sequestration Consortium (MGSC); (4) Center for Advanced Materials for the Purification of Water with Systems (WaterCAMPWS*),* University of Illinois at Urbana-Champaign; and various CBM and coal mining companies in the Illinois Basin. The main goal of this project was to evaluate the feasibility of reusing three types of non-traditional water sources for cooling or process water for existing and future (up to 2030) coal-based power plants in the Illinois Basin. The sources were: (1) produced water from CO_2 enhanced oil recovery (CO_2-EOR) operations; (2) coal-bed methane (CBM) recovery; and (3) active and abandoned underground coal mines. Specific objectives of this project were: (1) to characterize the quantity, quality, and geographic distribution of produced water in the Illinois Basin; (2) to evaluate treatment options so that produced water may be used beneficially at power plants; and (3) to perform a techno-economic analysis of the treatment and transportation of produced water to thermoelectric power plants in the IL basin.

1.4 References

American Petroleum Institute (API) Production Waste Survey prepared by Paul G. Wakim, June 1988.

American Petroleum Institute (API) Overview of Exploration and Production Waste Volumes and WasteManagement Practices in the United States, prepared by ICF Consulting for the American Petroleum Institute, Washington, DC, May 2000.

Clark, C. E., Veil J. A., Produced Water Volumes and Management Practices in the United States, ANL/EVS/R-09/1, prepared by the Argonne National Laboratory for the U.S. Department of EnergySeptember 2009.

DOE/NETL, Estimated Freshwater Needs to Meet Future Thermoelectric Generation Requirements, DOE/NETL-400/2007/1304, September 24, 2007.

DOE/NETL, Use of Non-traditional Water for Power Plant Applications: An Overview of DOE/NETL R&D efforts, DOE/NETL-311/040609, November 1, 2009.

Energy Information Administration, www.eia.doe.gov, accessed 2010.

Feeley T. J., Green L., McNemar A., Carney B. A., Pletcher S., Department of Energy/Office of Fossil Energy's Water-Energy Interface Research Program, DOE/FE's Power Plant Water Management R&D Program Summary, April 2006.

Gillette J. L., Veil J. A., Identification of Incentive Options to Encourage the Use of Produced Water, Coal Bed Methane Water, and Mine Pool Water. Prepared by Argonne National Laboratory for U.S. Department of Energy, Office of Fossil Energy, National Energy Technology Laboratory, 2004.

Hutson S. S., Barber N. L., Kenny J. F., Linsey K. S. , Lumia D. S., Maupin M. A., Estimated Use of Water in the United States in 2000, U.S. Geological Survey 1268, 2004.

Klett M. G., Kuehn N. J., Schoff R. L., Vaysman V., White J. S., Power Plant Water Usage and Loss Study, prepared for the United States Department of Energy, National Energy Laboratory, August 2005, Revised May 2007.

Solley W. B., Pierce R. R., Perlman H. A., Estimated Use of Water in the United States in 1995, U.S. Geological Survey 1200; 1998.

Sirivedhin T., Dallbauman L., Organic matrix in produced water from the Osage-Skiatook Petroleum Environmental Research site, Osage county, Oklahoma. *Chemosphere* **57**, 463-469, 2004.

USGS, Water Production with Coal-bed Methane, Fact Sheet FS-156-00, November 2000.

Veil J. A., Kupar J. M., Puder M. G., Feeley T. J., Beneficial Use of Mine Pool Water for Power Generation, Ground Water Protection Council Annual Forum, Niagara Falls, NY, September 13-17, 2003.

Veil J. A., Puder M. G., Elcock D., Redveik R. J., Jr. A white paper describing produced water from production of crude oil, natural gas, and coal bed methane. U.S. Department of Energy, National Energy Technology Laboratory, 2004.

Chapter 2 Assessment of produced water in the Illinois Basin

2.1 Introduction

The Illinois Basin encompasses northwestern Kentucky, southeastern Indiana, and all but the northern and eastern most portions of Illinois. The Illinois Basin, a large intracratonic sedimentary basin, contains some of the largest bituminous coal deposits and oil reservoirs in the U.S. (USGS, 1996) and has a long history of fossil-fuel production.

Produced water in the Illinois Basin has been investigated previously by the ISGS. Concentrations of inorganic species in the produced water from oilfields and coal seams were measured by Meents et al. (1952); Gluskoter (1965) and Demir (1995). To the best of our knowledge, no study of the quality of water produced from CBM recovery in the Illinois Basin is available in the literature. Produced water flow rates and their geographical distribution have not been well characterized previously.

In this chapter, the geographic distribution, quantity and quality of produced water in the IL Basin are described.

2.2 Produced water characterization

2.2.1 Geographic distribution

2.2.1.1 Produced water from oil fields and CO_2-EOR

In a majority of oil and gas reservoirs, 20-40% of the total amount of original oil in place (OOIP) can be recovered by standard petroleum extraction methods (EPRI, 1999). Several different enhanced (or tertiary) oil recovery technologies, including CO_2 flooding EOR, are available to recover the residual oil. Generally, about 10% of OOIP can be recovered through a CO_2-EOR technology (Baviere, 1991). It is estimated that 223 million m^3 (1.4 billion barrels) of crude oil can be recovered in Illinois by CO_2-EOR (Baviere, 1991; Frailey, 2005). CO_2-EOR technology requires about 0.5 metric tons of CO_2 for each barrel of oil recovered.

The costs of crude oil, CO_2, and produced water management are major economic factors in the EOR industry. It is estimated that an EOR project can break even at a CO_2 price of $20/metric ton and an oil price of $157/$m^3$ ($25/barrel) (Winter and Chen, 1997; Holtz et al., 1999; Holtz et al., 2001). At the current crude oil price of ~$100/barrel, EOR should be profitable if sufficient oil is produced. Figure 2-1 shows a conceptual integrated water-energy system that uses concentrated and pressurized CO_2 from coal-based power plants for EOR at an oil field. The produced water from EOR is treated and used as process or cooling water at the power plant.

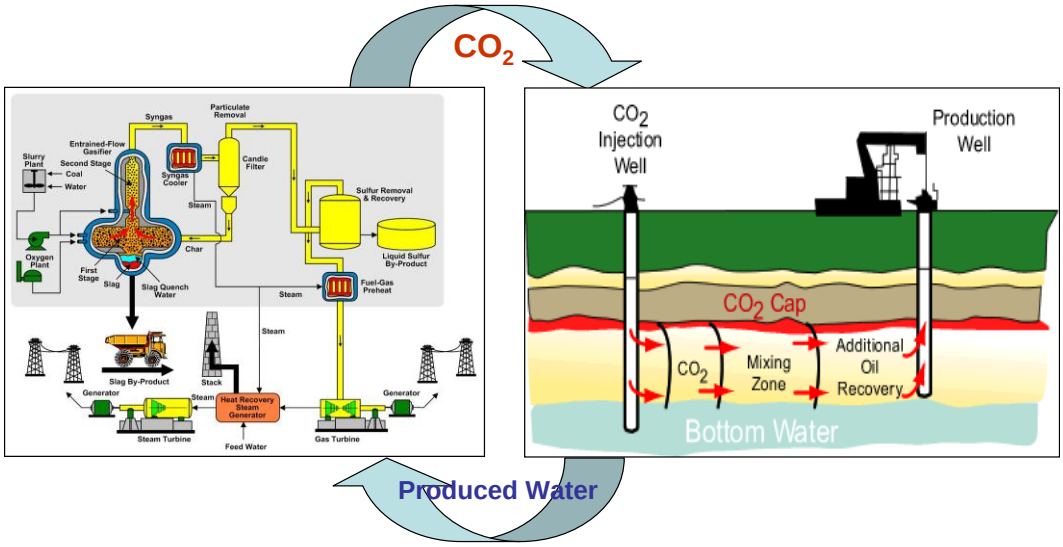

Figure 2-1: A conceptual integrated CO_2 and produced water system for electricity generation and oil production.

Potential sources of produced water from future CO_2-EOR operations in the Illinois Basin were identified and mapped. Details of the methodology for produced water data collection, analysis, and estimation are described below.

The first objective was to collect available geographic distribution data and quantity of produced water from oil recovery. There is a limited amount of published data (and these data are based on estimates) on the quantities of produced water from oil recovery operations in the Illinois Basin.

Oil producing companies in Illinois are required to annually report oil and produced water data from their water-flooding EOR operations to the Illinois Department of Natural Resources (IDNR) by submitting Form OG-17. They also are required to report their brine disposal volume through Class II wells by submitting Form OG-18 to IDNR. However, data are needed to confirm this and to quantify volumes of disposed produced water. The ISGS receives and compiles data from OG-17 Forms and makes the information partially available to the public through its interactive mapping system. However, brine disposal data (from Form OG-18) generally are not recorded.

More than 4000 OG-18 forms were obtained from IDNR. Data from these forms were compiled into a database about produced water injection into Class II injection wells in Illinois. This database includes each well's name, location, permit number, operator, water injection formation and depth, average monthly water injection rate, and total yearly water injection volume. According to the IDNR these forms cover approximately 90% of all produced water injection operations in Illinois, predominantly from oil recovery operations. Therefore, the total reported produced water values for each county were divided by 0.9 to take into account the remaining 10% of unreported data and estimate the total current production of produced water in Illinois.

Based on communications with the Kentucky and Indiana Geological Surveys, no produced water data from oil recovery operations in these states were available. Therefore, for those counties of the Illinois Basin located in Kentucky and Indiana, the produced water production from oil recovery was estimated from the available oil production data, using the oil-to-water ratio estimated from Illinois data.

A large quantity of EOR water flooding and oil production data from ISGS databases for 2001-2006 was analyzed to estimate the average ratio of produced water to oil. The average water-to-oil ratio was used to estimate the potential amount of water that can be produced from future CO_2-EOR operations.

Several maps were prepared to show geographic distribution and quantity of OOIP and CO_2-EOR (also sources of produced water from CO_2-EOR) in the Illinois Basin. The largest 20 oilfields in the Illinois Basin are identified on these maps. Geographic distributions of the largest oilfields, and estimated amounts of CO_2-EOR of oilfields determined by the Midwest Geological Sequestration Consortium (Finley, 2005) are shown in Figure 2-2. The OOIP of Illinois Basin fields and the field miscibility classifications for CO_2-EOR, are shown in Figure 2-3 and Figure 2-4, respectively.

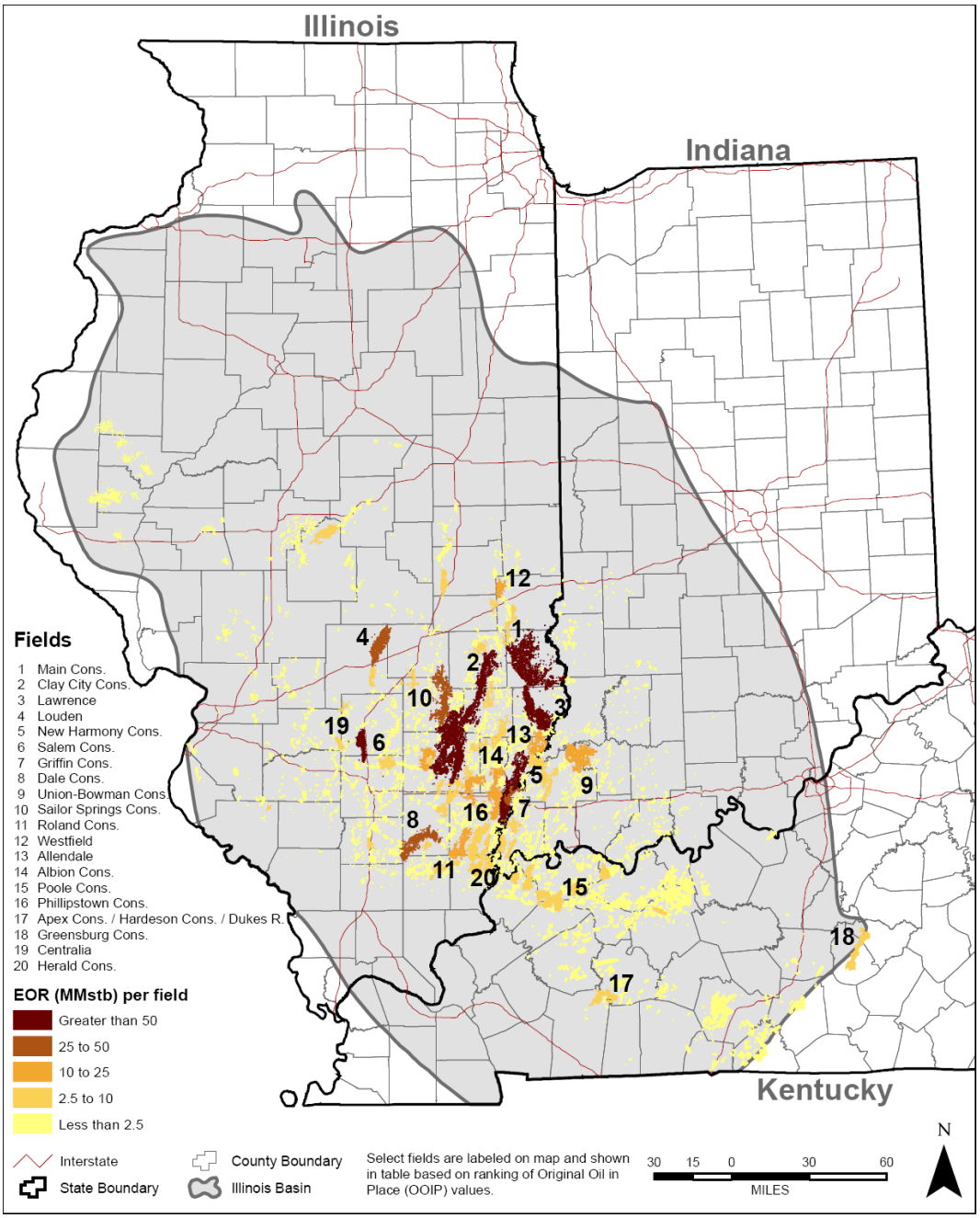

Figure 2-2: Geographic distribution and estimated amount of CO_2-EOR from oilfields in the Illinois Basin (twenty largest oilfields are ranked and shown). Derived from (Finley, 2005).

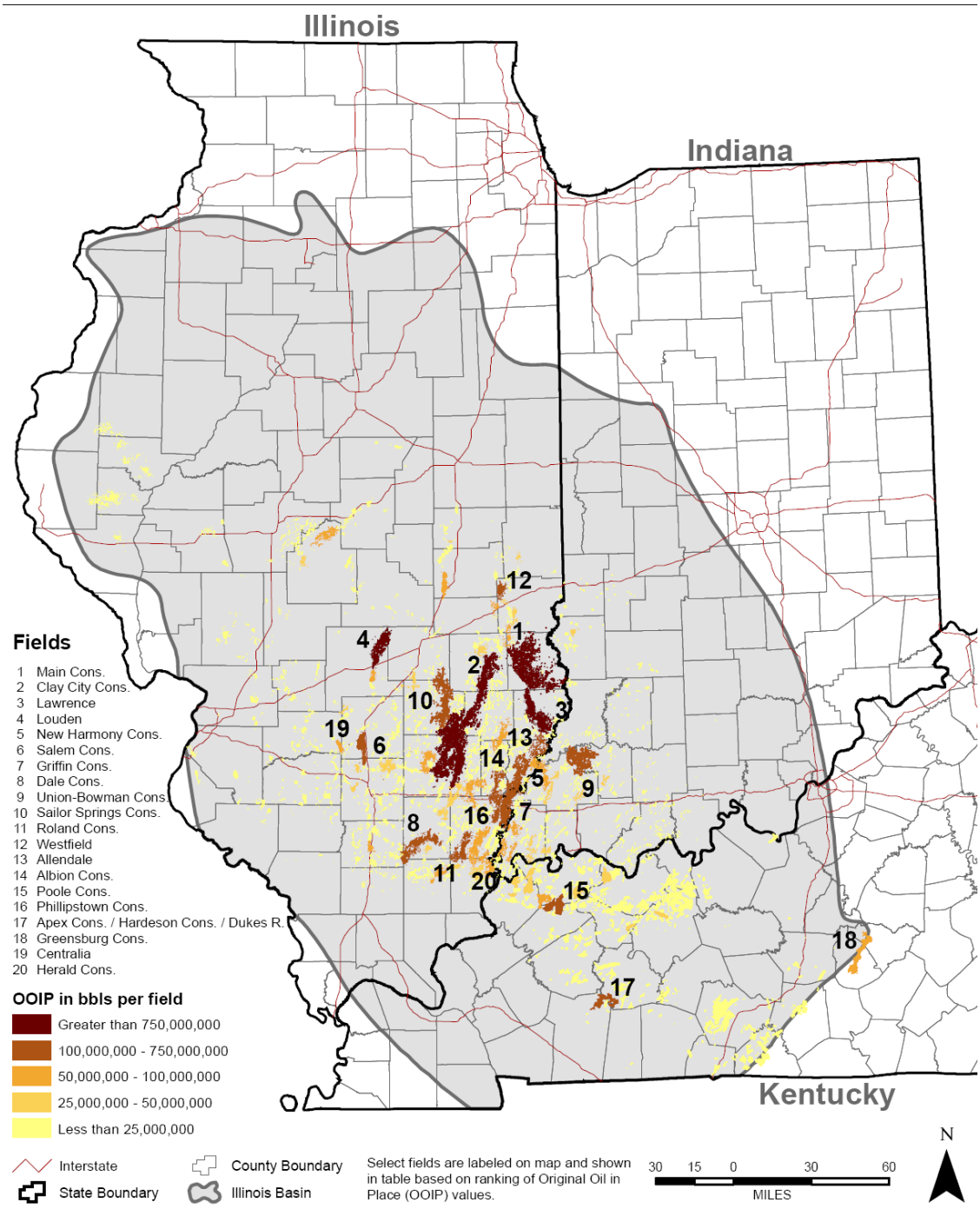

Figure 2-3: Original Oil In Place (OOIP) of oilfields in the Illinois Basin. Twenty largest oilfields are ranked and shown on this map. Derived from Finley (2005).

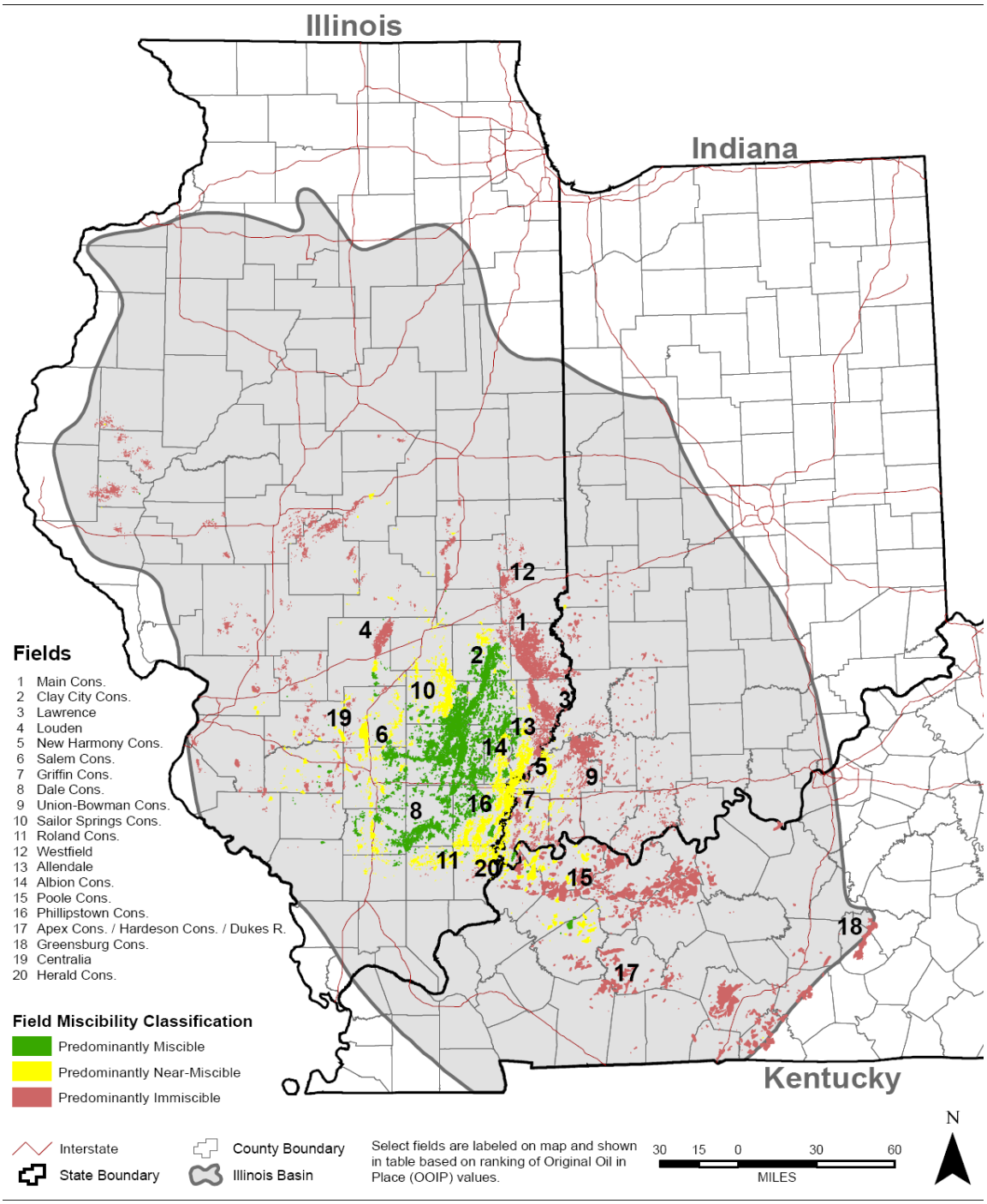

Figure 2-4: Field miscibility classification of oilfields in the Illinois Basin for CO_2-EOR. Twenty largest oilfields are ranked and shown on this map. Derived from Finley (2005).

2.2.1.2 Produced water from CBM

Based on the previous ISGS/MGSC studies (Finley, 2005), the potential amount of entrapped methane in coal seams or Original Gas In Place (OGIP) was estimated. Active/developing CBM projects in the Illinois

Basin are identified and produced water data (i.e., geographic distribution and quantity) are summarized in this report.

The potential amount of produced water from future CBM operations in the Illinois Basin was predicted based on the OGIP values and an average water-to-gas ratio that was estimated from USGS data (USGS, 2000).

A previous study by ISGS/MGSC generated a map of OGIP as shown in Figure 2-5. Active/developing CBM projects in the Illinois Basin are denoted on the map. A limited amount of information from the projects is presented in Table 2-1. The largest CBM project to date is BPI's Delta Project, with 122 wells and 23,000 m^3 (0.8 million cubic feet) of gas production per day. Most other projects were undergoing initial development during this study.

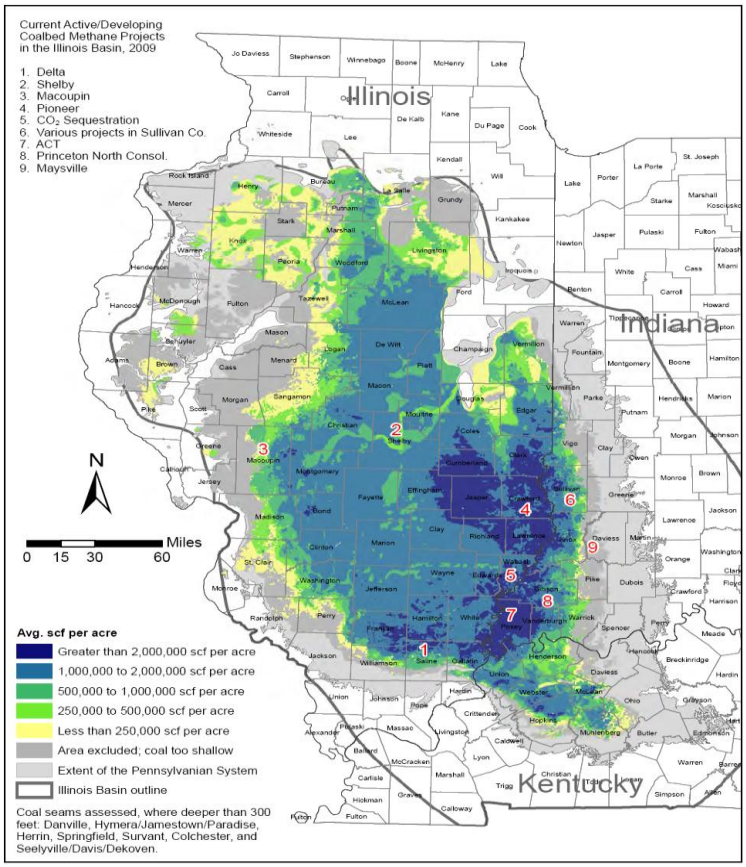

Figure 2-5: Estimated coal bed methane original gas in place for major coal seams in the Illinois Basin (ISGS/MGSC, 2005). Current active/developing CBM projects are shown on the map.

Table 2-1: Current active/developing CBM projects in the IL Basin (see Figure 2-5 for locations of Projects 1-9).

	Project	State	County	Name of Company	# of Wells	Water Production (bbl/day)	Gas Production (1000 scf/day)	Year Drilled
1	Delta	IL	Saline	BPI Energy	122	3400	800	2004-2008
2	Shelby	IL	Shelby	BPI Energy	10	capped	capped	2004-2005
3	Macoupin	IL	Macoupin	BPI Energy	10	capped	capped	2004-2005
4	Pioneer	IL	Crawford	Pioneer Oil Comp.	12	293	Not Available	2008
5	CO_2 Sequestration	IL	Wabash	ISGS	3	0	0	2008
6	Sullivan Co. Projects	IN	Sullivan	Various companies	59	Not Available	Not Available	Not Determinable
7	ACT	IN	Posey	ACT	5	100	0	2007
8	Princeton North Consol	IN	Gibson	Hydrocarbon Investments	3	Not Available	Not Available	2005
9	Maysville	IN	Daviess	Horizontal Systems Inc	1	Not Available	Not Available	2004

	Data sources
1	BPI website - communications with the BPI staff
2	BPI website - communications with the BPI staff
3	BPI website - communications with the BPI staff
4	Communications with the Pioneer Oil staff
5	ISGS/MGSC
6,7,8	http://igs.indiana.edu/geology/coalOilGas/CBM/index.cfm http://igs.indiana.edu/pdms/Query/Search/MainQuery.cfm
7	Communications with the ACT staff

2.2.1.3 Produced water from coal mines

A total of 1615 abandoned and inactive underground mines were surveyed to determine historic production quantities in Illinois. Coal Mine Quadrangle Maps and Directories available on the ISGS website were used. The 7.5 minute (1:24,000 scale) quadrangle maps show both active and abandoned mines. A coal directory gives a brief history of mining for each quadrangle and lists the following for each mine: name, thickness, and depth of coal seams, production history, geologic problems reported, company names, mine names, type of mine, years operated, coal seam mined, and mine location. Production from some mines was not reported, and some mines are not mapped. The maps do not include production data for currently active mines.

The Indiana Geological Survey provided a database from their coal mine information system with production data sheets for mines located in the 13 Indiana counties located within the Illinois Basin. Data included mine name, type of mine, county in which the mine is located, and production each year in operation. A total of 851 mines are represented in the Indiana mine void data. Kentucky data were obtained using the Kentucky Geological Survey Coal Production Search website. Approximately 1000

underground mines are represented in the Kentucky mine void data. Data provided included total production for each county in the western Kentucky region that is in the Illinois Basin.

Active coal mines in the Illinois Basin were contacted to obtain information about mining activities and produced water status and quantities. Coal mining databases of the Illinois, Indiana, and Kentucky Geological Surveys were also searched to find produced water information. However, except for a few notes regarding the existence of water in some mines, no information about the quantity of produced water was found in the literature.

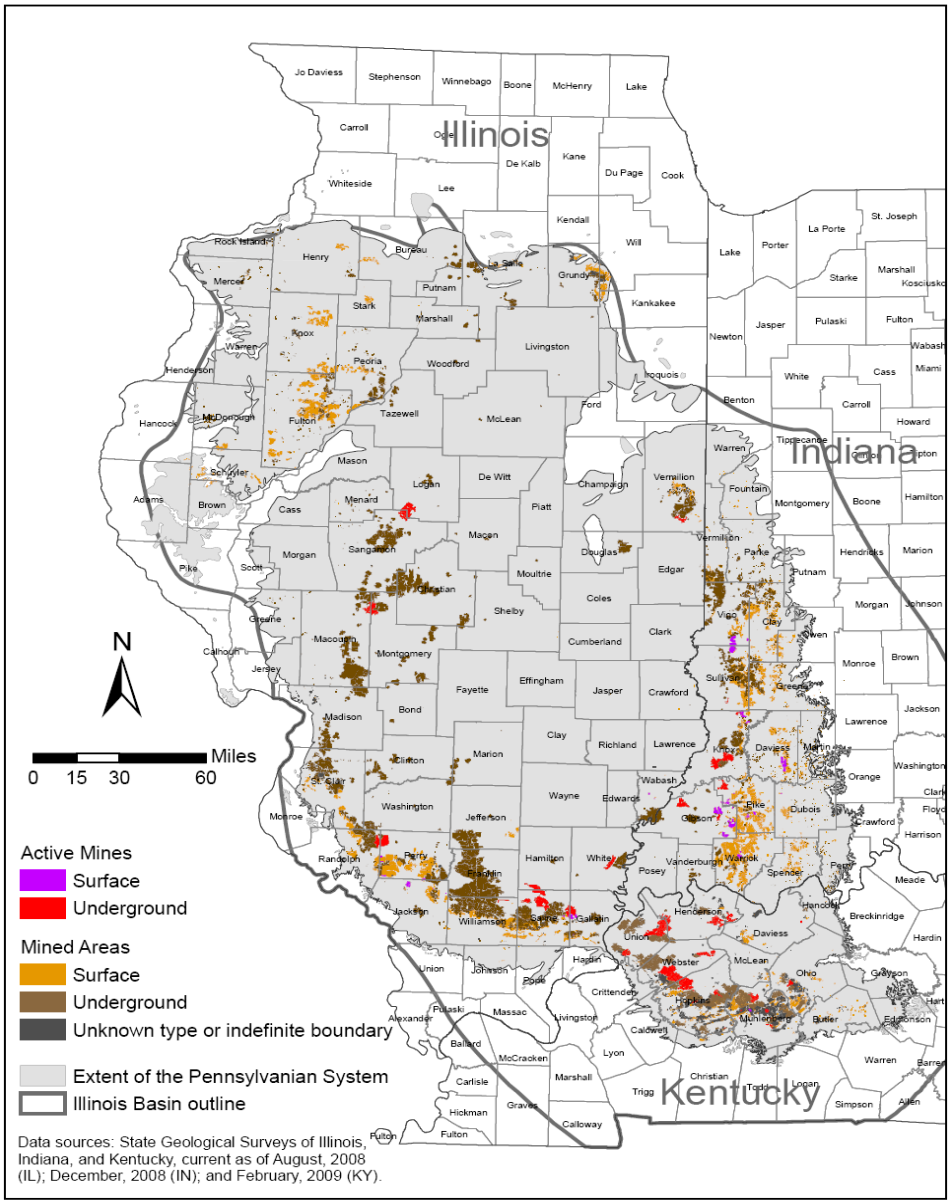

Figure 2-6: Areas of active and historical coal mining in the Illinois Basin.

The Illinois Basin has abundant coal resources that can last for centuries at current production rates. DOE/EIA data indicate that the Illinois Basin's coal reserve is approximately 120 billion metric tons (132

billion short tons), of which 46 billion metric tons (51 billion short tons) is estimated to be recoverable. Coal mining activities in the Illinois Basin have been reported since the early years of the 19th century. Coal mining throughout the Illinois Basin involves both underground and surface mines. A map of active and abandoned (or inactive) coal mines in the Illinois Basin is shown in Figure 2-6. The latest DOE/EIA data indicated that a total of 31 active underground mines and 40 surface mines produced a total of 87,606,000 metric tons (95,659, 000 short tons of coal in the Illinois Basin in year 2007 (Table 2-2).

Table 2-2: Current coal production and produced water production from coal mining in the Illinois Basin. Coal production data were obtained from (DOE/EIA, 2009). Coal mine water production is from communications with mining companies.

Coal production is in thousand short tons per year							
Coal-Producing	Underground		Surface		Total		Total
State and County	Number of Mines	Production	Number of Mines	Production	Number of Mines	Production	Water Production (million barrels / year)
Illinois	**14**	**26,807**	**7**	**5,638**	**21**	**32,445**	**9.5**
Gallatin	-	-	1	2,070	1	2,070	A (only undeterminable amounts in abandoned mines)
Jackson	1	19	2	1,579	3	1,598	1.5
Macoupin	3	4,488	-	-	3	4,488	N (negligible)
Perry	1	447	3	1,051	4	1,498	0
Randolph	1	2,695	-	-	1	2,695	0
Saline	3	11,334	-	-	3	11,334	4.3
Sangamon	1	2,090	-	-	1	2,090	N
Vermilion	1	1,375	-	-	1	1,375	N
Wabash	1	386	1	938	2	1,324	N
White	1	2,897	-	-	1	2,897	3.7
Williamson	1	1,076	-	-	1	1,076	A
Franklin	0	0	0	0	0	0	A
Jefferson	0	0	0	0	0	0	A
Indiana	**7**	**10,604**	**20**	**24,399**	**27**	**35,003**	N
Daviess	-	-	2	3,556	2	3,556	N
Dubois	-	-	1	674	1	674	N
Gibson	3	4,313	4	9,722	7	14,034	N
Knox	2	2,628	4	3,346	6	5,974	N
Pike	1	2,624	6	2,312	7	4,936	N
Sullivan	1	1,039	-	-	1	1,039	N
Vigo	-	-	2	4,063	2	4,063	N
Warrick	-	-	1	727	1	727	N
Kentucky (Western)	**10**	**24514**	**13**	**3699**	**23**	**28211**	N
Daviess	-	-	1	232	1	232	N
Henderson	1	1,357	2	1,217	3	2,574	N
Hopkins	3	7,702	2	306	5	8,007	N
Muhlenberg	1	2,974	7	1,941	8	4,915	N
Union	2	5,065	1	3	3	5,067	N
Webster	3	7,416	-	-	3	7,416	N

2.3 Produced water quantity

2.3.1 Produced water from oil fields and CO_2-EOR

Oil and produced water data from water flooding EOR projects in Illinois during years 2001 to 2006 were analyzed (Table 2-3). Produced water flow rates during 2005 are tabulated by county in Table 2-4. The average oil production from water flooding EOR is about 525,000 m^3 (3.3 million barrels) per year, which is about 30% of the total Illinois oil production. The total average yearly production of produced water from EOR water flooding activities is about 22 million m^3 (138 million barrels). Almost all of the produced water (>99%) from water flooding projects is re-injected into oilfields to continue oil

production. The average water-to-oil ratio for all EOR water flooding activities for the six studied years was about 41.2.

Table 2-3: Oil and water production from EOR water flooding projects in Illinois.

Year	Produced Water, bbls	Injected Water, bbls	Produced Oil, bbls	Water:Oil Ratio
2001	119,889,840	119,275,591	3,562,633	33.7
2002	172,161,034	168,518,968	4,075,405	42.2
2003	158,847,814	151,815,401	3,950,238	40.2
2004	152,657,496	154,184,593	3,475,996	43.9
2005	156,694,313	156,037,618	3,118,536	50.2
2006	66,477,070	71,631,708	1,811,062	36.7
Average	137,787,928	136,910,647	3,332,312	41.2

Table 2-4: Produced water from EOR projects in different Illinois Counties in year 2005.

County	Water production*, bbls	County	Water production*, bbls
Bond	401,540	Lawrence	47,735,388
Christian	63,137	Macoupin	292,000
Clark	2,616,773	Madison	811,907
Clay	4,318,154	Marion	33,749,806
Clinton	290,861	Monroe	36,500
Coles	21,900	Montgomery	12,600
Crawford	1,988,307	Peoria	2,500
Edgar	978,620	Richland	1,793,525
Edwards	666,133	Saline	335,500
Fayette	47,014,582	Shelby	25,550
Franklin	166,851	Wabash	809,630
Gallatin	726,441	Washington	281,370
Hamilton	398,215	Wayne	5,265,466
Jasper	1,902,440	White	3,862,540
Jefferson	60,377	Williamson	65,700
Total			156,694,313

* Reported water production from EOR water flooding projects in Illinois in year 2005.

The produced-water database that was developed by compiling data from more than 4000 OG-18 forms filed at the IDNR showed that the total yearly water production from all oil and gas recovery operations in 75 counties in Illinois was estimated to be about 62.6 million m^3 (394 million barrels) (Table 2-5). Based on the Illinois 2007 county oil production data, only 43 counties produced oil. These counties produced an estimated volume of 346 million barrels of water in 2008 (Table 2-5). The average yearly water injection rate for EOR projects in Illinois (Table 2-3) is about 21.8 million m^3 (137 million barrels). The difference between these values indicates that about 40% of total water production from oil recovery operations in Illinois is injected for EOR operations. Unless there is an accounting error, this suggests that the remaining 40.7 million m^3 (256 million barrels) of water produced per year, or about 110,000 m^3 (29 million gallons) per day, are disposed into a different formation than oil producing formations. This disposed water, therefore, may become available for beneficial use.

Table 2-5: Produced water re-injection for oil and gas recovery operations in Illinois during 2007.

County	Reported Water Injection, Mbbl/yr	Estimated Total Water Injection, Mbbl/yr	Oil Producing	County	Reported Water Injection, Mbbl/yr	Estimated Total Water Injection, Mbbl/yr	Oil Producing	County	Reported Water Injection, Mbbl/yr	Estimated Total Water Injection, Mbbl/yr	Oil Producing
Adams	2.162	2.402	Yes	Fulton	0.148	0.165	No	Mclean	3.021	3.357	No
Alexander	0.071	0.079	No	Gallatin	1.758	1.954	Yes	Monroe	0.729	0.810	Yes
Bond	5.026	5.585	Yes	Grundy	0.055	0.061	No	Montgomery	0.036	0.040	Yes
Brown	2.003	2.226	Yes	Hamilton	4.529	5.032	Yes	Morgan	0.202	0.224	No
Carroll	0.088	0.098	No	Hancock	0.345	0.383	No	Moultrie	0.015	0.016	Yes
Cass	0.007	0.008	No	Henderson	0.154	0.171	No	Perry	0.194	0.216	Yes
Champaign	3.596	3.995	No	Jackson	0.043	0.048	No	Randolph	0.061	0.067	Yes
Christian	9.008	10.009	Yes	Jasper	3.235	3.594	Yes	Richland	11.509	12.788	Yes
Clark	13.471	14.967	Yes	Jefferson	6.095	6.773	Yes	Saline	0.741	0.823	Yes
Clay	19.712	21.903	Yes	Jo Daviess	0.333	0.370	No	Sangamon	1.008	1.120	Yes
Clinton	3.570	3.966	Yes	Kane	0.586	0.651	No	Schuyler	0.061	0.067	Yes
Cloes	0.686	0.762	Yes	Kankakee	30.551	33.946	No	Shelby	0.444	0.493	Yes
Cook	0.383	0.425	No	Knox	0.076	0.084	No	St.Clair	0.151	0.168	Yes
Crawford	52.400	58.223	Yes	Lake	0.291	0.324	No	Stephenson	0.161	0.179	No
Cumberland	0.211	0.234	Yes	Lasalle	0.033	0.037	No	Tazewell	0.038	0.042	No
Dekalb	0.128	0.143	No	Lawrence	31.466	34.962	Yes	Vermilion	0.087	0.097	No
Dewitt	0.830	0.922	Yes	Livingston	1.544	1.715	No	Wabash	4.322	4.803	Yes
Douglas	0.757	0.841	Yes	Logan	0.067	0.075	No	Warren	0.012	0.013	No
Dupage	0.015	0.016	No	Macon	0.212	0.235	Yes	Washington	2.583	2.870	Yes
Edgar	1.482	1.647	Yes	Macoupin	0.359	0.398	Yes	Wayne	5.199	5.777	Yes
Edwards	1.705	1.895	Yes	Madison	10.394	11.549	Yes	White	13.010	14.456	Yes
Effingham	2.113	2.348	Yes	Marion	45.597	50.663	Yes	Williamson	0.401	0.445	Yes
Fayette	49.089	54.544	Yes	Marshall	0.057	0.063	No	Winnebago	0.015	0.017	No
Ford	0.010	0.012	No	Mason	0.092	0.102	No	Woodford	0.068	0.076	No
Franklin	3.293	3.659	Yes	McDonough	0.118	0.131	Yes	Unknown	0.511	0.567	

Illinois 2008 Reported Produced Water Production = 354.532 million barrels
Illinois 2008 Estimated Total Produced Water Production = 393.924 million barrels
Illinois 2008 Estimated Total Produced Water Production from Oil Producing Counties = 346.382 million barrels

Considering the total 2008 Illinois oil production of 1.5 million m^3 (9.4 million barrels), and assuming that water production from gas recovery operations in oil-producing counties is negligible, the average oil-to-water production ratio in Illinois can be estimated as 37. By using this estimated water-to-oil ratio and the latest available county oil production data, yearly produced water production from oil recovery operations in the Indiana and Kentucky counties in the Illinois Basin can be estimated as 9.6 and 7.1 million m^3 (60.3 and 44.5 million barrels), respectively (Table 2-6).

Table 2-6: Estimated produced water production from oil recovery operations in IN and KY counties located in the Illinois Basin.

Kentucky (IL Basin)			Indiana (IL Basin)		
County	2006 Oil Production, bbl	Estimated Produced Water, 1000 bbl	County	2006 Oil Production, bbl	Estimated Produced Water, 1000 bbl
Allen	5,222	193	Clay	14,659	541
Barren	10,477	387	Daviess	63,790	2,354
Breckinridge	823	30	Dubois	2,336	86
Butler	5,414	200	Gibson	197,376	7,283
Caldwell	186	7	Greene	101,641	3,751
Christian	17,545	647	Knox	40,989	1,512
Daviess	64,967	2,397	Pike	131,642	4,858
Edmonson	14,578	538	Posey	808,447	29,832
Green	4,920	182	Spencer	74,489	2,749
Hancock	5,719	211	Sullivan	41,206	1,521
Hart	12,582	464	Vanderburgh	63,653	2,349
Henderson	316,298	11,671	Vigo	58,665	2,165
Hopkins	92,634	3,418	Warrick	34,620	1,277
Logan	604	22			
Mclean	55,147	2,035			
Muhlenberg	108,672	4,010		**bbl Oil**	**1000 bbl Water**
Ohio	51,767	1,910	**Indiana**	**1,633,513**	**60,277**
Simpson	860	32	**Kentucky**	**1,205,621**	**44,487**
Todd	2,157	80			
Union	283,368	10,456			
Warren	50,336	1,857			
Webster	101,346	3,740			

There are more than 1000 oil fields in the IL basin that are potentially available for CO_2-EOR application. The potential amount of produced water from each oilfield depends on a variety of factors including geological characterization of the oilfields and specifications of the EOR technology. Total OOIP of the Illinois Basin is estimated as 2.2 billion m^3 (14.1 billion barrels) and approximately 10% of this amount can be potentially recoverable by CO_2-EOR.

The twenty largest oilfields that initially contained 1.3 billion m^3 (8.2 billion barrels), or ≈58% of the total OOIP, were selected for this study. Detailed information about these oilfields is provided in Table 2-7. This includes reservoir ranking, location, area of coverage, number of formations, estimated OOIP, estimated CO_2-EOR, estimated OOIP from the most important formations, depth of the formations, and estimated produced water from each oilfield and its most important formations.

The total produced water flow rate was calculated by estimating the maximum volume of CO_2 that may displace water during oil production. After primary and secondary oil recovery, approximately 40% of OOIP is removed, and water from the producing formation fills regions previously occupied by oil. During CO_2-EOR, an additional ≈10% of OOIP is recovered, and the entire region once occupied by oil is filled with CO_2. The estimate of water produced during CO_2-EOR is the total volume of oil removed from the reservoir. The OOIP of an oilfield (or formation) is multiplied by 0.5 to determine the volume of produced water. Based on these results a potential maximum amount of 652 million m^3 (4.1 billion barrels) of water may be produced from the twenty largest oilfields in Illinois Basin during CO_2-EOR oil recovery (Table 2-7).

Two different water production rates from CO_2-EOR were considered: a slow case and a fast case. For the slow case, CO_2-enhanced oil production is assumed to continue at the same rate until 10% of OOIP is obtained. The flow rate of water is estimated by dividing the total volume available from above by the

duration of oil production. Assuming that oil production is constant at the 2008 production rate, the oil production time from slow CO_2-EOR is 119.4 million m^3 / 922,000 (751 million bbls oil / 5.8 million bbls per year) = 124 years. Total CO_2-EOR potential (751 million bbls) is obtained from Table 2-7. The 2008 oil production from the 20 largest oilfields in the Illinois Basin was estimated by multiplying total Illinois Basin 2008 oil production (≈10 million bbls) times 0.58 (fraction of OOIP in the 20 largest oilfields). The annual water production from slow CO_2-EOR, thus, is 651 million m^3 (4.1 billion bbls water) / 124 years ≈ 5.1 million m^3 (32 million barrels) per year.

For the fast case, the same oil production rate is assumed, but the current water to oil ratio is assumed constant during CO_2-EOR. Oil production is assumed to continue until all available water is extracted. The produced water flow rate is the oil flow rate times the water to oil ratio {922,000 m^3 (5.8 million bbls per year)} × 41 = 37.8 million m^3 (238 million barrels of water) per year. The duration of oil production is {652 million m^3 (4.1 billion bbls water)} / {37.8 million m^3 (238 million bbls per year)} = 17 years. In this case, the total oil produced is just 1.2% of OOIP, rather than 10% of OOIP.

The three estimates for the daily flow rates of water potentially available for industrial use are 110,000; 102,000 and 15,000 m^3 per day (29, 27, and 4 MGD). The first estimate is for currently disposed water, and the second two numbers are from the estimates for potential large scale CO_2-EOR development. The amount of available water for cooling systems at power plants will depend on the treated water recovery rate of the treatment systems, which is discussed in the techno-economics chapter of this report. To put these flow rates in context, a 200 MW power plant consumes water at a rate of 13,600 m^3 per day (3.6 MGD) (assuming a water consumption rate of 2,650 cm^3 (0.7 gallons) per kWh electricity generated).

Table 2-7: Estimated oil and produced water potential of twenty largest oilfields in Illinois Basin.

Rank	Oil Field	State	Acres	# of Formations	Cumulative Production (1998), bbls	OOIP, bbls	CO2 EOR Potential, bbls	Oilfield Estimated Produced Water Potential [OOIP * 0.5], bbls	Formation	Formation Top Depth, ft	Formation OOIP, bbls	Formation Estimated Produced Water Potential [OOIP * 0.5], bbls
1	Main Consol.	IL	81,390	15	264,301,200	1,403,036,544	98,215,563	701,518,272	Robinson	950	1,212,968,404	606,484,202
									Paint Creek	1,280	85,987,316	42,993,658
									Aux Vases	1,430	31,946,094	15,973,047
2	Clay City Consol.	IL	164,359	14	374,548,256	1,249,116,058	188,101,964	624,558,029	Aux Vases	2,940	376,134,659	188,067,330
									Ohara	3,020	357,707,208	178,853,604
									Cypress	2,635	187,108,394	93,554,197
3	Lawrence	IL	44,211	25	427,862,592	1,046,043,854	66,065,370	523,021,927	Cypress	1,400	489,528,469	244,764,234
									Buchanan	1,250	199,640,834	99,820,417
									Bridgeport	800	106,069,946	53,034,973
4	Louden	IL	29,783	11	399,088,928	784,900,365	46,839,645	392,450,182	Cypress	1,500	471,036,094	235,518,047
									Bethel	1,540	164,561,353	82,280,676
									Benoist	1,550	103,652,281	51,826,140
5	New Harmony Consol.	IL	38,157	22	161,517,280	643,358,898	59,438,017	321,679,449	Sample	2,660	160,019,891	80,009,945
									Cypress	2,570	159,604,324	79,802,162
									Aux Vases	2,800	95,004,943	47,502,472
6	Salem Consol.	IL	16,681	11	397,881,344	512,239,343	52,236,779	256,119,672	Benoist	1,780	202,699,263	101,349,632
									McClosky	2,050	108,336,227	54,168,114
									Devonian	3,440	71,060,582	35,530,291
7	Griffin Consol.	IN	10,372	71	84,162,272	340,066,073	33,015,994	170,033,037	Aux Vases	2,788	108,776,541	54,388,271
									Cypress	2,499	56,124,775	28,062,388
									Waltersburg	2,433	42,484,883	21,242,441
8	Dale Consol.	IL	32,619	12	105,909,056	328,846,650	48,576,269	164,423,325	Aux Vases	3,150	243,777,275	121,888,638
									Bethel	2,975	29,052,025	14,526,013
									Ohara	3,110	21,401,287	10,700,643
9	Union-bowman Consol.	IN	30,534	158	29,901,836	325,006,485	20,841,719	162,503,243	Pennsylvanian	1,089	38,508,010	19,254,005
									Jackson	1,242	28,218,053	14,109,026
									St Louis	2,077	20,373,329	10,186,664
10	Sailor Springs Consol.	IL	38,358	13	70,815,312	273,733,893	25,840,343	136,866,947	Cypress	2,550	149,334,088	74,667,044
									Aux Vases	2,825	39,764,542	19,882,271
									Ohara	2,900	25,592,495	12,796,248
11	Roland Consol.	IL	20,843	19	64,718,392	202,222,865	19,916,958	101,111,433	Aux Vases	2,880	60,790,339	30,395,169
									Cypress	2,700	34,439,450	17,219,725
									Ohara	3,020	24,096,484	12,048,242
12	Westfield	IL	8,191	9	40,389,149	179,571,933	12,747,212	89,785,967	Westfield	335	109,863,399	54,931,700
									Trenton	2,300	29,831,198	14,915,599
									Pennsylvanian	280	29,385,957	14,692,978
13	Allendale	IL	13,401	18	28,229,000	160,921,503	10,669,130	80,460,752	Biehl	1,450	88,879,161	44,439,581
									Cypress	1,920	26,744,188	13,372,094
									Bethel	2,010	16,177,117	8,088,559
14	Albion Consol.	IL	13,998	19	36,148,288	144,045,761	14,744,588	72,022,880	Aux Vases	3,045	36,291,654	18,145,827
									Biehl	2,000	28,040,731	14,020,366
									Bethel	2,960	17,017,882	8,508,941
15	Poole Consol	KY	9,848	7	8,399,268	124,654,416	8,792,524	62,327,208	Chester	2,030	86,227,187	43,113,594
									Aux Vases	1,775	24,635,388	12,317,694
									St Genevieve	2,560	8,978,856	4,489,428
16	Phillipstown Consol.	IL	15,107	22	41,105,916	117,974,150	11,718,952	58,987,075	Tar Springs	2,295	20,436,597	10,218,299
									Aux Vases	2,880	19,902,306	9,951,153
									Cypress	2,720	13,884,864	6,942,432
17	Apex Cons / Hardeson Cons	KY	3,662	5	5,116,863	116,436,435	8,168,393	58,218,217	Chester	715	99,977,008	49,988,504
									St Genevieve	934	16,312,039	8,156,020
									Vienna	875	70,510	35,255
18	Greensburg Consol	KY	22,740	2	2,386	94,919,223	6,739,265	47,459,612	Laurel Dol	442	94,904,490	47,452,245
									Fort Payne	324	14,733	7,367
19	Centralia	IL	4,176	5	59,045,076	92,081,931	9,286,769	46,040,965	Devonian	2,870	39,317,073	19,658,536
									Benoist	1,355	31,664,110	15,832,055
									Cypress	1,200	11,921,347	5,960,674
20	Herald Consol.	IL	15,383	19	22,293,352	91,512,614	9,201,977	45,756,307	Aux Vases	2,920	40,419,046	20,209,523
	TOTAL				2,621,435,766	8,230,688,994	751,157,432	4,115,344,497			6,396,696,702	3,198,348,351

2.3.2 Produced water from CBM

The major coal seams buried deeper than 91 m (300 feet) beneath the surface which were considered for OGIP estimation were the Danville; the Hymera/Jamestown/Paradise; the Herrin; the Springfield; the Survant, Seelyville/Davis/Dekoven, and the Colchester. The estimated amount of OGIP varies from 250,000 scf/acre to more than 2,000,000 scf/acre, and the total amount of OGIP of the Illinois Basin is estimated as 22.1 trillion scf (tscf) (Finley, 2005). ISGS/MGSC study indicated that approximately 70-78% of the OGIP can be recovered and approximately 41% of the total OGIP can be considered for Enhanced (e.g., CO_2-enhanced) Coal Bed Methane (ECBM) recovery. CBM in shallow (i.e., <152 m (500 ft)) and deep (i.e., >152 m (500 ft)) coal seams can be recovered by conventional and enhanced (ECBM) technologies, respectively. Assuming an average recovery factor of 74%, an estimated amount of 464 billion m^3 (16.4 tscf) of CBM can be potentially recovered by both conventional and enhanced methods.

The amount of CBM-produced water is variable in space and time. Produced water production is at the highest level at the early (de-watering) stages of operation when there is little or no gas production and decreases with time. The USGS has reported CBM produced-water volumes ranging from 0.005 m^3 (0.03 bbl) (San Juan, NM) to 0.44 m^3 (2.75 bbl) (Powder River, MT) per 28.3 m^3 (thousand cubic feet) of recovered methane. Few CBM explorations have occurred in the Illinois Basin, limiting our ability to predict produced water production over a long period of time. Current active/developing Illinois Basin CBM projects are at early stages of gas production and de-watering. The largest CBM project in the Illinois Basin (Delta project) has about 122 active wells with an approximate daily production of 540 m^3 (3400 bbl) of water and 22,600 m^3 (800 mscf (mscf is 1000 scf)) of gas. This gives a water-to-gas ratio of 4.25 bbl/mscf. This calculation likely overpredicts produced water generation because the project was not completed. In the absence of reliable and conclusive water-to-gas ratios for the Illinois Basin, we performed an analysis of all other major CBM activities in the U.S. to estimate an average water-to-gas ratio. Five Coal Basins (Black Warrior, Powder River, Raton, San Juan and Uinta) that have more than 9500 CBM wells were considered (Table 2-8). These five basins have an average water/gas ratio of 1.02 bbl/mscf.

By multiplying the assumed water/gas ratio (i.e., 1.02 bbl/mscf) by the OGIP values, geographic distribution of the potential amount of produced water from future CBM operations can be roughly estimated. A map of CBM produced water is identical to that of the map shown in Figure 2-5 with potential produced water volumes ranging from less than 255 to greater than 2,040 bbl/acre. This indicates that the majority of CBM resources can potentially generate more than 1000 bbl/acre produced water over the life time of the CBM recovery.

Considering the estimated potential amount of 464 billion m^3 (16.4 tscf) of CBM production in the Illinois Basin, and an assumed average water-to-gas ratio of 1 bbl/mscf, the potential volume of produced water can be estimated as 2.6 billion m^3 (16.4 billion barrels; 689 billion gallons). If this water is available over a lifetime of fifty years, the potential amount of available produced water per year is 52.2 million m^3 (13.8 billion gallons), or about 144,000 m^3 per day (38 MGD). This volume of water is sufficient to provide water for eleven 200 MW coal-fired power plants.

Table 2-8: Produced water summary of CBM recovery in the U.S. (USGS FS-156-00).

Basin	State	No of wells	Avg. Water Production (Bbl/day/well)	Water/gas ratio (bbl/Mscf)
Black Warrior	Alabama	2917	58	0.55
Powder River	Wyoming, Montana	2737	400	2.75
Raton	Colorado	459	266	1.34
San Juan	New Mexico	3089	25	0.03
Uinta	Utah	393	215	0.42
				1.018 (Average)

2.3.3 Produced water from coal mines

Most mines in the Illinois Basin are considered dry compared to Appalachian coal mines. Western Kentucky mines in the Springfield seam are particularly noted for being free of water except where mine shafts penetrated sandstone formations saturated with groundwater. Water comes from three sources in association with coal mines: (1) coal seam water, similar to water found with CBM; (2) groundwater in various overlying geologic formations that migrates into coal mines; and (3) surface water in surface mines. Information obtained from coal mine geologic reports suggests that most of the water found in Illinois Basin mines is groundwater. The majority of mines report little if any water directly associated with the coal seam. Several mines reported using water pumped from the mine in their coal processing plants. Excess water is discharged to surface runoff.

Active underground and surface mines throughout the Illinois Basin were contacted to obtain information about discharge of produced water. Surface mines reported having water only from surface runoff. Surface runoff from rain was accumulated in holding ponds and either used for coal processing or discharged to local stream channels. While most underground mines reported no water, there were three underground mines, located in different counties in southern Illinois along the Cottage Groove Fault System, which reported a significant amount of water discharge (Table 2-9).

Table 2-9: Produced water production from active coal mines in the Illinois Basin.

Owner/ operator	Mine	Mine type	County	Produced water (gal/d)	Comments
American Coal Company	Galatia and Millenium	Underground	Saline, IL	500,000	Producing 1.5 million gallons per day between Galatia and Millenium mines but using approximately 1 million gallons in coal processing. Discharging approximately half million gallons per day to surface discharge.
White County Coal, LLC	Pattiki II Mine	Underground	White, IL	432,000	Water discharged to Wabash River.
Knight Hawk Coal, LLC	Royal Falcon	Underground	Jackson, IL	168,000	

Produced water resources from Galatia/Millenium Mines (Saline County) and Pattiki Mine (White County) are sufficient to potentially provide supplemental sources of water to two 200 MW power plants by supplying more than 10% of the plants' water demand (assuming a water consumption rate of 0.7 gallons per kWh electricity generated). Produced water from Royal Falcon Mine (Jackson County) could provide about 5% of the water demand of a 200 MW power plant.

Depending on the geologic characteristics of abandoned coal mines, void volumes from underground coal mining potentially can be filled with water that can be used to supplement the water demand of power plants. Void volumes can also be potentially used as geothermal cooling sinks for the power plants.

Available historic coal mining data in the Illinois Basin was reviewed to estimate the void volume created by underground coal mining. Geographic distribution and quantities of void volume in selected counties of the Illinois Basin are shown in Table 2-10. This summary indicates an estimated total volume of 4.1 billion m^3 (5.3 billion cubic yards) void space in 60 counties in Illinois, Indiana and Kentucky.

Several mines along the Rend Lake Fault Line, part of the Cottage Grove Fault System, and mines located below Rend Lake in southern Illinois reported having water under the "Geologic Problems Reported" in the directory of coal mines in Illinois. Mine operators contacted also noted from personal experience that these mines were the wettest in Illinois. These mines are located in Franklin, Saline, Williamson, Jefferson, Gallatin, Jackson, and Hamilton counties and the counties rank 1, 3, 6, 18, 22, 30, and 41, respectively, in coal mine void volume for the Illinois Basin. The total void volume in these counties is about 1.2 billion m^3 (about 1.6 billion cubic yards or 314 billion gallons). It is possible that a considerable fraction of this void is filled with water. Further study is needed to estimate flux of water into these voids when water is actively pumped out.

Table 2-10: Estimated void volume of abandoned coal mines in different counties of the Illinois Basin. Counties are ranked based on their estimated void volume.

County	Abandoned mine voids (yd^3)	County	Abandoned mine voids (yd^3)
IL – Franklin	648,846,221	IN – Vermillion	30,688,241
IL - Christian	453,673,965	IL – Peoria	21,737,866
IL – Saline	406,297,472	IN – Pike	17,918,101
KY - Hopkins	391,326,263	IN – Parke	11,374,619
IL - Macoupin	359,084,947	IL – Marshall	10,809,680
IL - Williamson	339,522,380	IL – Macon	9,467,056
KY – Union	270,180,764	IL – Tazewell	9,197,949
KY - Muhlenburg	253,380,242	IL – Menard	8,720,336
KY - Webster	252,348,484	KY – Daviess	6,172,789
IL - St. Clair	212,736,197	IL – Livingston	6,024,257
IL - Sangamon	203,288,072	IL – Hamilton	5,535,747
IN – Vigo	158,437,166	IL – Will	5,396,782
IN – Sullivan	141,260,071	IL – McLean	4,850,504
IL - Vermillion	127,641,786	KY – Mclean	4,634,126
IL – Madison	118,436,387	IL – Woodford	3,716,406
IN – Daviess	103,683,187	KY – Butler	3,238,446
IN – Knox	102,953,961	KY – Christian	2,691,619
IL – Jefferson	73,130,592	IL – Moultrie	1,829,012
KY – Ohio	56,938,171	IL – Kankakee	1,729,607
IL - La Salle	56,145,553	IL – Henry	1,590,788
IL – Clinton	53,750,519	IL – White	1,509,067
IL – Gallatin	51,149,455	IL – Montgomery	1,163,045
IL – Logan	47,684,288	KY – Hancock	599,104
KY – Henderson	42,800,461	IL – McDonough	561,262
IN – Gibson	38,020,442	IN – Dubois	252,456
IN – Warrick	37,908,137	KY – Edmonson	154,883
IN – Greene	37,795,307	KY – Crittenden	126,691
IL – Grundy	34,699,248	IL - Rock Island	26,123
IN – Clay	34,113,322	IN – Perry	8,943
IL – Jackson	31,811,979	KY – Grayson	4,500
Illinois Basin total estimated mine void = 5,310,775,037 cubic yards			

2.4 Produced water quality

Research activities for produced water quality assessment included: (1) compilation of the available produced water quality data from literature; (2) collection of current produced water quality data from oil, CBM, and coal mining companies; and (3) sampling and characterization of produced water from selected locations.

A comprehensive search for oilfield produced water quality data in the Illinois Basin was undertaken. The USGS website provides the largest database of produced water quality for all oil producing states (USGS, 2010). The USGS database provides the locations of the samples including the names of oil fields in some cases, and pH values and concentrations of total dissolved solids (TDS), Na, Ca, Mg, Si, Al, Fe, Mn, Cl, and SO_4. The database contains sample data from the following formations: Aux Vases, Benoist, Bethel, Bridgeport Sandstone, Buchanan, Cypress, Devonian, Fort Payne, Hardinsburg, Harrodsburg, Lime Devonian, McClosky, O'Hara, Osage, Paint Creek, Palestine, Pennsylvanian, Rosiclare, Salem, Silurian, St. Peter, St. Genevieve, Stein, Tar Springs, Trenton, Waltersburg, and Weiler. The Illinois data are from a 1952 ISGS study (Meents et al., 1952). Additional data for the Aux Vases and Cypress Formations is available from a 1995 ISGS study (Demir, 1995).

Published data about produced water from underground coal mines in the Illinois Basin were also summarized and discussed. BPI Energy, a major CBM company in the Illinois Basin and one of the industrial collaborators of this project, and Pioneer Oil provided some CBM produced water quality data from some fields. Available water quality data of oil fields, coal mines, and CBM projects were summarized and compared with our measured water quality data in this report.

2.4.1 Previous studies of produced water quality in the Illinois basin

2.4.1.1 Oil field produced water

The USGS and ISGS databases/reports were searched to obtain water quality data from the selected twenty largest potential CO_2 EOR oil fields in the Illinois Basin. Data from these fields was compiled, and the statistics obtained from the data are presented in Table 2-11. Produced water from these oil fields tends to be highly saline. The TDS values for produced water ranged from 6,000 to 210,000 mg/L, with a large fraction of the TDS comprised of sodium and chloride ions. Most of the produced water samples with smaller TDS concentrations were collected from Pennsylvanian formations that are shallow compared to other formations. The produced water from the Roland Consolidated oil field within the Waltersburg formation had one of the lowest TDS values. The Sailor Springs field has TDS concentration in the range of 17,000 mg/L in the Tar Springs formation. The Clay City Consolidated oil field has some of the highest (>150,000 mg/L) observed concentrations of TDS, in samples collected from the Ohara and McClosky formations.

Table 2-11: Compiled data from USGS and ISGS (1995) reports for the 20 largest oil fields in the Illinois Basin. Concentrations are in mg/L. Magnesium concentrations are reported as zero in the USGS report for oil fields in Illinois, so they were not included in tabulated results.

	pH	TDS	Na	Ca	Mg	HCO_3	Cl	SO_4
Mean	6.6	110,000	37,000	4,300	1,300	220	68,000	810
Min	5.2	6,000	0	5	380	0	2,800	0
Max	8.0	210,000	73,000	26,000	2,300	1,800	130,000	4,900
Std dev	0.6	34,000	11,000	2,600	490	230	21,000	890

Statistical data for the concentrations of additional species reported in Demir (1995) are shown in Table 2-12. Water quality data were averaged over the fields that are among the selected 20 fields in the Illinois Basin for two oil-producing formations (Aux Vases and Cypress). Concentrations of TDS and of various other ions are similar to values reported in the USGS database. Valuable metals such as Li generally have small concentrations (less than 10 mg/L). Although the concentration of silicon in most cases is less than 10 mg/L, fouling problems may occur during desalination.

Table 2-12: Statistical summary of 1995 ISGS data from produced water sampled from the Aux Vases and Cypress Formations in the Clay City Consol., Lawrence, New Harmony, Dale, Sailor Springs, and Roland oil fields within Illinois. Additional measurements Pb, V, Cu, Zn, Zr, Cd, Be, Cr, As, Se, Mo, and Sb were below detection limits for nearly all samples from the fields of interest. All units, except pH, are in mg/L.

Aux Vases Formation													
	pH	TDS	Cl	Br	I	SO_4	NO_3	CO_3	HCO_3	Na	Ca	Mg	K
Mean	6.7	125,634	73,996	154	8.6	612	0.4	0.17	122	44,193	4721	1,488	222
Min	5.3	43,325	25,000	65	3.2	1	0.0	0.00	30	16,290	1140	452	79
Max	8.0	146,456	85,000	220	15.0	1,800	1.3	1.00	190	53,780	6,350	2,190	356
SD	0.6	24,472	14,608	43	3.1	572	0.3	0.26	53	8,554	1,348	438	66
	Sr	NH_4	Ba	Li	Fe	Mn	B	Si	Al	Ti	Co	Ni	
Mean	265	30	3.3	7.6	7.6	0.86	4.19	4.53	0.0	0.0	-	-	
Min	117	6	0.1	2.2	0.0	0.33	3.00	0.60	-	0.0	-	-	
Max	958	46	16.3	15.0	52.3	2.25	9.21	7.40	0.3	0.2	0.0	0.4	
SD	206	8	4.5	3.0	14.4	0.62	1.42	1.58	0.3	0.1	0.0	0.1	

Cypress Formation													
	pH	TDS	Cl	Br	I	SO_4	NO_3	CO_3	HCO_3	Na	Ca	Mg	K
Mean	6.4	106,041	62,333	127	4.4	551	0.9	0.21	202	38,347	3,079	1,075	128
Min	5.7	48,460	28,000	60	2.4	1	0.3	-	20	18,400	633	378	70
Max	7.7	140,537	83,000	190	8.2	1,100	4.7	0.81	690	50,700	5,150	1,400	213
SD	0.6	25,218	14,822	35	1.6	471	1.3	0.23	170	8,943	1,427	296	42
	Sr	NH_4	Ba	Li	Fe	Mn	B	Si	Al	Ti	Co	Ni	
Mean	132	22	18.3	5.3	6.6	1.90	2.68	5.50	0.1	0.0	-	-	
Min	32	10	0.1	1.7	0.1	0.43	2.20	-	-	0.0	-	-	
Max	315	41	183.0	15.6	18.7	4.84	3.46	15.40	0.3	0.0	0.1	0.2	
SD	94	9	52.2	3.6	6.0	1.52	0.37	3.78	0.2	0.0	0.1	0.1	

The quality of produced water from oil fields in the Illinois Basin has significant variability. Figure 2-7 shows the cumulative distribution of histograms of TDS and Cl^- concentrations for produced water from the top 20 oil fields, using data from the USGS database and the 1995 ISGS publication. The cumulative distribution is calculated by dividing the number of samples with concentrations less than a given value by the total number of samples. Cumulative distributions are calculated separately for the ISGS data (29 samples) and the USGS data (279 samples). Most produced waters samples have TDS concentrations in the range of 100,000 to 150,000 mg/L, but a few samples (4%) have concentrations less than 30,000 mg/L. The chloride concentration distribution shown in Figure 2-7b and the high chloride and sodium concentrations listed in Table 2-11 and Table 2-12 show that most of the TDS is composed of sodium chloride.

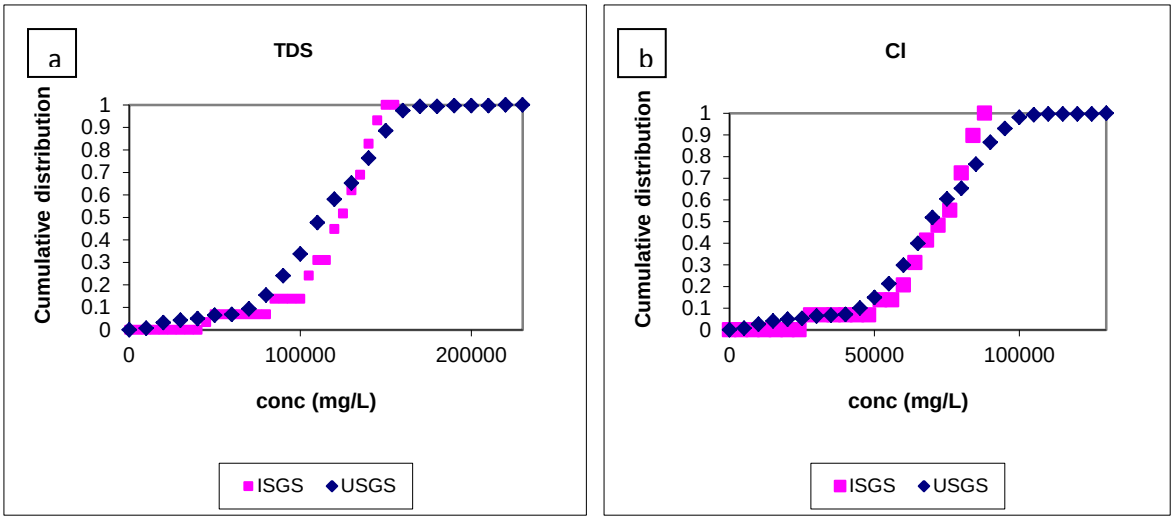

Figure 2-7: Concentration distributions for (a) TDS and (b) Cl^- for the USGS and 1995 ISGS data sets. There are 279 and 29 data points for the USGS and ISGS (1995) reports, respectively.

2.4.1.2 Produced water from CBM

Table 2-13 shows water quality data for four CBM projects in the Illinois Basin. Data were obtained from BPI Energy (one of the industrial collaborators of this project) and Pioneer Oil, and were either averaged over several wells from a producing region or represent water sampled from a tank that collected water from multiple wells.

The overall quality of the produced water from CBM projects is better than that from oil fields. That is, the concentration of most dissolved components in the CBM is less than in the oilfield brines. There is a wide range of quality; the smallest TDS value is just over 2,500 mg/L, and the largest value is about 84,000 mg/L. Sodium and chloride are the dominant ions present in all waters. No data are available for dissolved organic compounds in the water.

Table 2-13: Water quality parameters from existing CBM projects in the Illinois Basin. Concentrations are in mg/L.

Project	pH	TDS	Na	Ca	Mg	Fe	K	Ba	Sr	Mn	Cl	HCO_3	SO_4
Delta	8.10	2,532	552	9.07	3.79	1.66	2.0	0.5	0.32	0.03	500	1,464	1
Shelby	7.00	83,920	27,911	2,271	970	3.27	62.0	37.0	182.6	0.58	52,300	244	1
Macoupin	7.69	12,611	4,304	241	194	2		3			7,300	561	6
Pioneer	7.3	32,291	10,105	1,307	646			35			19,506	705	

2.4.1.3 Produced water from coal mines

A literature search provided limited water quality data for Illinois coal mines. Gluskoter (1965) reported water quality data for 21 water samples obtained from underground mines associated with the Herrin Coal seam in Christian, Douglas, Franklin, Jefferson, Montgomery, Randolph, and Williamson Counties in Illinois. Statistics calculated from these data are presented in Table 2-14. It is notable that although all

water samples were obtained from the Herrin Coal seam, the TDS and other water quality parameters varied over a wide range from freshwater to high-salinity water.

Table 2-14: Statistics of 21 groundwater samples associated with Herrin coal in Illinois.

			Concentration in water samples from different undergound mines(ppm)										
	Depth (ft)	pH	TDS	Cl	SO4	Na and K	Fe	Mn	Ca	Mg	SiO2	Alkalinity*	Hardness*
Min	120.0	7.0	994.0	150.0	0.0	406.0	0.0	0.0	2.0	1.0	6.8	160.0	8.0
Max	795.0	8.6	48,306.0	29,250.0	622.0	17,059.0	9.6	1.0	1,008.0	452.0	22.1	1,004.0	4,380.0
Mean	390.6	7.8	18,313.0	10,443.1	39.0	6,592.2	1.8	0.4	293.1	145.5	9.4	456.4	1,331.1
St Dev	225.5	0.4	16,970.8	10,662.0	133.9	6,023.8	2.7	0.3	328.0	152.1	3.5	254.3	1,441.0

* As CaCO3

2.4.2 Sample collection for this study

Water samples were collected from several oil fields, coal mines, and CBM projects throughout the Illinois Basin (Figure 2-8). Site selection and sample collection were coordinated with oil companies, CBM developers, and coal mine owners. The five selected oilfields (Main Consolidated, Union Bowman, Louden, Dale, and Sugar Creek) are among the largest fields and are spread throughout the basin. The three selected coal mines (Galatia and Millenium, Pattiki, and Royal Falcon) are the only active mines in the Illinois Basin with significant water production. Water samples from three active CBM projects (ACT, Pioneer, and Pulse Energy) were also collected. The sources and the number of samples collected from each source are listed in Table 2-15.

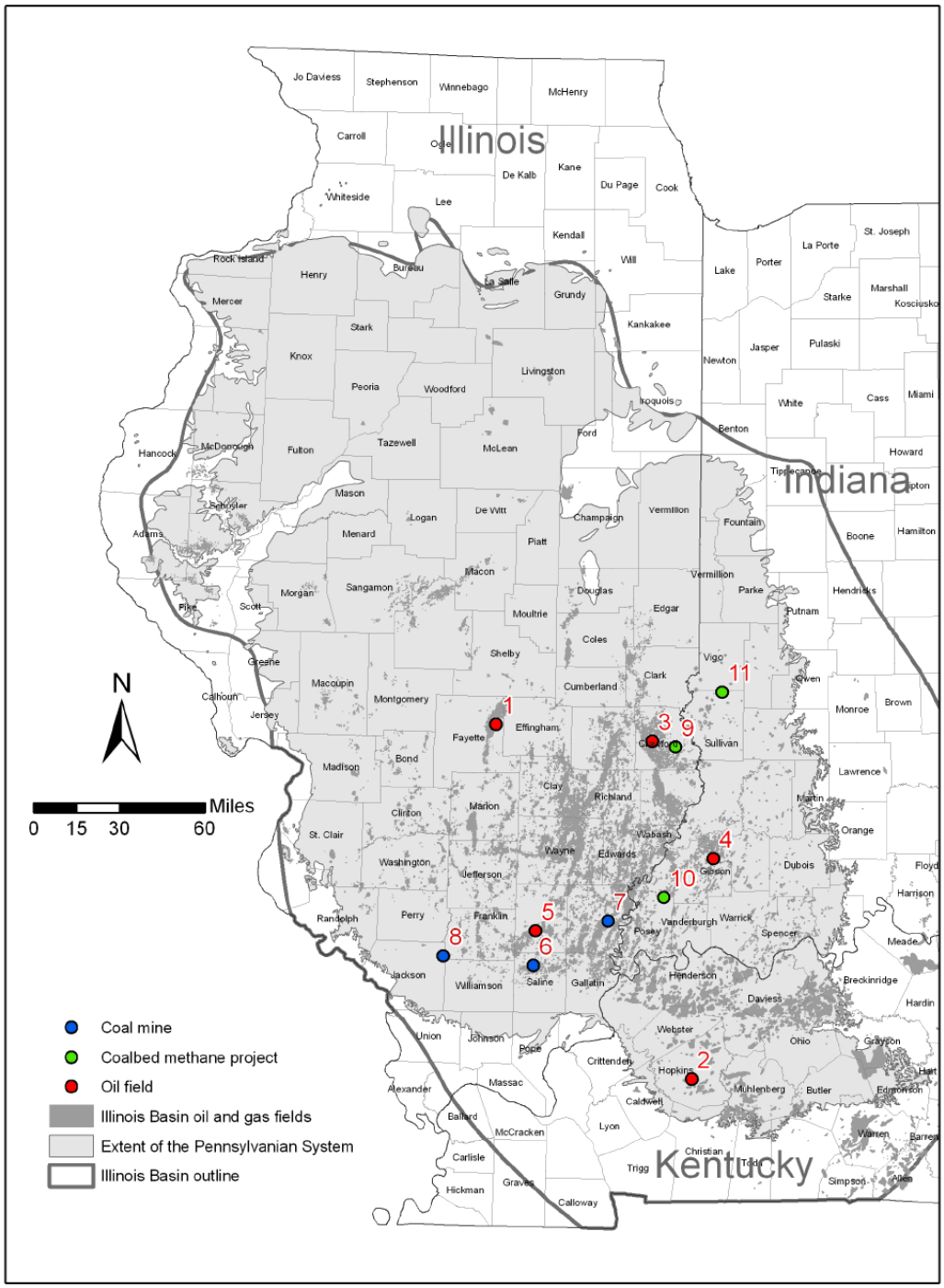

Figure 2-8: Water sampling locations of oil fields, coal mines, and CBM projects in the Illinois Basin.

Water from the sampling sites was collected primarily from composite sources rather than from individual wells. For coal mines, water was collected from settling ponds or discharge pipes; and for oil fields and CBM projects, water was collected from storage tanks for multiple producing wells. At the Pioneer CBM project, water was collected from individual wells because they are not connected. Water collection procedures followed the guidelines established by the USGS water sampling field manual

(USGS, 2006). For water collected from tanks, the tank's drainage valve was opened and two to six gallons of water were drained before sample collection. Depending on the valve configuration, water was poured directly into the bottles or transferred to the bottles by a Nalgene bucket. At two coal mines, water was collected from settling ponds. Water bottles were submerged 6 inches below the surface at an arm's reach from the shore. We collected 12 L of water from the primary source and 1 L from each additional source. Water was collected in pre-washed, amber glass bottles, filled to the top with no headspace, and sealed with a Teflon lid. Primary samples were placed in 4-L bottles, and secondary samples were placed in 1-L bottles. Bottles were then placed in a cooler with bags of ice. Upon returning to the laboratory, bottles were transferred to a refrigerator at 4°C.

Table 2-15: List of sources for produced water samples obtained during this project.

Produced Water Source	County, state	# of samples	Produced Water Source	County, state	# of samples
1. Main Consolidated oil field	Crawford, IL	3	7. Pattiki coal mine	White, IL	1
2. Union Bowman oil field	Gibson, IN	2	8. Royal Falcon coal mine	Franklin, IL	3
3. Louden oil field	Fayette, IL	3	9. ACT CBM project	Posey, IN	1
4. Dale oil field	Hamilton, IL	2	10. Pioneer CBM project	Crawford, IL	3
5. Sugar Creek oil field	Hopkins, KY	1	11. Pulse Energy CBM project	Sullivan, IN	3
6. Galatia and Millenium coal mines	Saline, IL	3			

2.4.2.1 Produced water sample preparation and analysis

Sample preparation and analysis procedures are schematically shown in Figure 2-9. Preliminary experiments indicated that sand/grit in our samples retained by 100 μm filters were negligible, so total petroleum hydrocarbon (TPH) analysis for the filtered residuals through 100 μm filter was unnecessary. The difference between the TPH values in the unfiltered water and the water filtered through 0.7 μm filters indicates that TPH was associated with suspended particles and colloids. Conductivity was measured for the filtered water samples only because conductivity represents the soluble ions in aqueous solutions. Alkalinity is a measure of the capacity of water to neutralize acids and has important implications for water treatment. It is influenced by solid particles in water, so alkalinity was measured on unfiltered water samples. Total organic carbon (TOC) was measured for filtered water, so it represents only dissolved organic carbon (DOC). Total inorganic carbon (TIC) was not measured because alkalinity can be used to determine concentrations of carbonates and bicarbonates. Nitrate and ammonia were measured instead of the total nitrogen (TN). Cations and/or elements including Na, Ca, Mg, Sr, and Si were measured in both filtered and unfiltered water samples to characterize those cations or elements associated with suspended particles and colloids. Primary samples with volumes greater than 4L were subjected to the analyses presented in Figure 2-9. Secondary samples with volumes of 1L were subjected to all of the analyses in Figure 2-9 except TPH.

Measurements of pH, conductivity, and ammonia concentration for water samples were obtained by a pH/mV/ion/conductivity meter with the corresponding probes (Denver Instrument, Denver, CO) following the Standard Methods (SM) (SM 4500 for pH and ammonia and SM 2510 for conductivity) (Clesceri et al., 1998). The meter was calibrated with corresponding standard solutions before measurement. Turbidity of the unfiltered samples and the water samples filtered with 0.7 μm glass

microfiber filters were determined with an HF Scientific Micro 100 Laboratory Turbidimeter (HF scientific,inc., Fort Myers, FL) following SM 2130B (Clesceri et al., 1998) or EPA method 180.1 (EPA, 2010). The turbidimeter was calibrated with standard turbidity suspensions provided by the manufacturer. Alkalinity of the unfiltered water samples was measured with a Mettler Toledo autotitrator (Mettler-Toledo Inc., Columbus, OH) following SM 2320 (Clesceri et al., 1998) or EPA method 310.1 (EPA, 2010). TDS of unfiltered samples was measured following SM 2540C (Clesceri et al., 1998). Total Suspended Solids (TSS) of unfiltered samples was measured following SM 2540D (Clesceri et al., 1998). TPH of unfiltered samples and samples filtered with 0.7 μm glass microfiber filters was measured following the modified EPA Method 1664, Revision A (EPA, 2010).

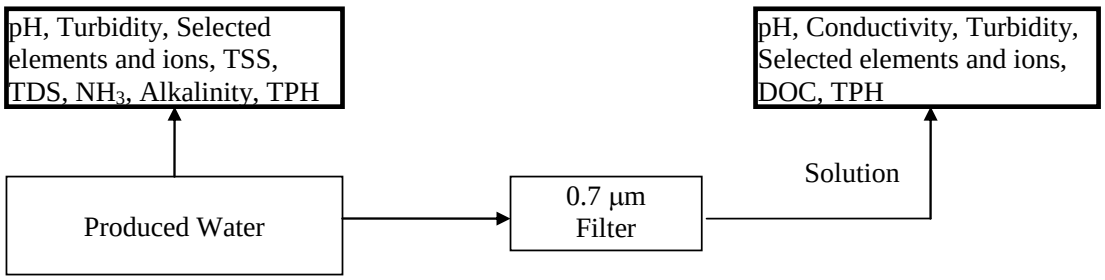

Figure 2-9: A schematic diagram of produced water sample preparation and analysis.

DOC/TOC in filtered samples was measured at the Illinois Sustainable Technology Center (ISTC) laboratory with a TOC analyzer following SM 5310 (Clesceri et al., 1998). Concentrations of thirty cations and/or elements in the unfiltered samples and the filtered samples were measured with inductively coupled plasma mass spectroscopy (ICP-MS) at the Illinois State Water Survey (ISWS) using standard methods. Selected anions (e.g.; NO_3, Cl, SO_4, and F) in filtered samples were analyzed with ion chromatography (IC) at the ISTC laboratory using standard methods. Quality assurance for analysis was provided by analyzing selected duplicate samples, blank samples, and spiked samples.

Statistical differences in water quality parameters among different produced water samples from the oilfields, CBM fields, and coal mines were performed using analysis of variance (ANOVA), with least significant difference (LSD) test at a 95% confidence interval for an alpha level of 0.05. The multiple comparisons were performed using SAS® (Statistical Analysis System, Version 9, SAS Institute Inc., Cary, NC).

2.4.2.2 Produced water characteristics

Water quality parameters, including pH, turbidity, conductivity, TDS, TSS, alkalinity, DOC, and ammonia content, are presented in Table 2-16. Included in the table are the average values and standard deviations of these parameters for each source of produced water (water from oilfields, CBM projects, and coal mines). Averaged results from previous studies are shown in Table 2-17.

Table 2-16: pH, turbidity, conductivity, TDS, TSS, alkalinity, DOC, and ammonia in produced water samples (mean values for each source with same letter are not significantly different).

Source	Site	pH	Turbidity (NTU)		Conductivity (mS/cm)	TDS (mg/L)	TSS (mg/L)	Alkalinity (mg/L as $CaCO_3$)	DOC (mg/L)	Ammonia (mg N/L)
		Unfiltered	Unfiltered	Filtered	Filtered			Unfiltered	Filtered	Unfiltered
Main Consolidated	1	7.0	420	0.21	32	19,010	101.0	1,148	507.5	4.4
	2	7.2	96	0.94	24	22,043	135.7	595	14.4	0.3
	3	7.4	97	0.61	33	20,807	74.3	1,109	11.0	0.2
Louden	1	7.4	33	0.10	120	101,734	8.5	285	8.5	25.4
	2	6.7	13	0.18	140	102,650	103.7	163	5.8	24.6
	3	6.9	49	0.42	100	90,557	47.5	238	7.1	23.7
Dale	1	6.7	36	0.06	160	126,949	8.0	90	20.2	31.8
	2	7.1	74	0.16	89	78,200	75.1	178	7.3	35.5
Sugar Creek	1	6.4	168	0.22	39	25,317	16.5	776	15.2	5.1
Mean of Oilfield		7.0±0.3[A]	110±125[A]	0.3±0.3	82±52[A]	65,252±43,185[A]	33.5±45.2[A]	509±415[A, B]	66.3±165.5[A]	16.8±14.1[A]
ACT	1	7.5	5.98	0.16	34	25,114	57.0	636	7.3	11.2
Pioneer	1	7.2	446	0.79	45	27,705	151.5	672	2.2	8.8
	2	7.8	156	1.38	42	31,327	40.7	627	0.9	9.9
	3	7.9	106	0.03	55	33,083	45.5	555	0.8	11.8
Pulse Energy	1	8.8	1.96	0.49	2.40	1,956	1.4	1,469	0.4	0.5
	2	8.7	7.41	0.12	1.95	1,310	1.0	902	1.0	<0.05
	3	8.5	0.91	0.04	2.00	1,340	10.0	1052	2.7	<0.05
Mean of CBM		8.1±0.6[B]	103±163[A]	0.4±0.5	26±23[B]	17,405±15,061[B]	70±76[A]	845±327[A]	2.2±2.4[A]	6.0±5.6[B]
Galatia	1	7.9	11	0.04	31	17,982	5.4	260	8.0	6.3
	2	7.5	24	0.28	14	10,517	36.4	144	13.0	3.6
Millenium	1	7.6	274	0.16	26	16,004	2,644.0	482	14.5	8.4
Pattiki	1	7.5	91	0.90	34	20,392	113.0	296	1.3	4.7
Royal Falcon	1	8.1	0.56	0.53	0.74	522	0.8	353	0.5	<0.05
	2	7.8	375	0.13	3.10	2,863	359.7	295	1.7	<0.05
	3	7.9	12.1	0.02	2.10	1,587	20.2	152	0.9	<0.05
Mean of Coal Mine		7.7±0.2[B]	113±150[A]	0.3±0.3	16±14[B]	9,981±8,362[B]	690±1,300[A]	283±117[B]	5.7±6.1[A]	3.3±3.4[B]

Table 2-17: Compiled water quality data of produced water from the fields of interest in the Illinois Basin. Oilfield data represent calculated average water quality parameters of 20 largest oilfields in the Illinois Basin (Demir, 1995)). Coal mine data represent calculated average water quality parameters of 21 water samples from the Herrin coal seam (Gluskoter, 1965) (Concentrations in mg/L).

		pH	TDS	Alkalinity (as $CaCO_3$)	Na^-	Ca^{2-}	Mg^{2-}	HCO_3^-	Cl^-	SO_4^{2-}
Oil	Mean	6.6±0.6	110,000±34,000	NA	37,000±11,000	4,300±2,600	1,300± 490	220±230	68,000±21,000	810±890
	Min	5.2	6,000	NA	0	5	380	0	2,800	0
	Max	8.0	210,000	NA	73,000	26,000	2,300	1,800	13,0000	4,900
Coal Mine	Mean	7.8±0.4	18,313±16,971	456±254	6,592±6,024*	293±328	146±152	NA	10,443±10,662	39±134
	Min	7.0	994	160	406*	2	1	NA	150	0
	Max	8.6	48306	1004	17,059*	1,008	452	NA	29,250	622

NA: not available

*: Combined concentration of Na and K

For the samples analyzed for this study, the pH values are between 6.4 and 7.4 for samples from the oilfields, between 7.2 and 8.8 for samples from the CBM projects, and between 7.5 and 8.1 for samples from coal mines. The pH values of samples from CBM fields (8.1±0.6) and coal mines (7.7±0.2) are not significantly different, but are significantly higher than those from the oilfields (7.0±0.3) (Table 2-16). Our pH results for the water samples from the four selected oilfields are consistent with those of the 20 largest oilfields in the Illinois Basin that range from 5.2 to 8.0 with a mean of 6.6±0.6 (Table 2-16). Our results for the water from four coal mines are also consistent with the study by Gluskoter (1965) (Table 2-17).

The turbidity of unfiltered samples ranged over as much as four orders of magnitude: from 13 to 420 NTU for samples from the oilfields, from 0.91 to 446 NTU for samples from the CBM fields, and from 0.6 to 375 for samples from the coal mines (Table 2-16). The turbidity of samples from the same sampling source also varied widely among different sites, suggesting the turbidity may not be determined by the geological formation, but more influenced by the site operation of wells or coal mines. The samples collected from Main Consolidated Site 1, Pioneer Site 1, and Royal Falcon Site 2 had the highest turbidity (420, 446, and 375 NTU) among all samples from the same types of sources. The water samples from the Royal Falcon coal mine Site 1 and Pulse Energy CBM Site 3 were relatively clear with turbidity of less than 1 NTU. After filtration, all samples had turbidities of less than 1 NTU except the sample from Pioneer CBM Site 2. The turbidity of some filtered samples is even lower than the drinking water treatment standard (<0.3 NTU) for conventional and direct filtration combined filter effluent (U.S. EPA, 2001). The mean turbidities of produced water from the three sources are not significantly different from each other either before or after being filtered.

The conductivity of samples from oilfields ranges from 24 to 160 mS/cm, of the CBM fields from 1.95 to 55 mS/cm, and of the coal mine samples from 0.74 to 34 mS/cm (Table 2-16). The water sample from Dale Site 1 had the highest conductivity (160 mS/cm). The water from Royal Falcon Site 1 had the lowest conductivity of 0.74 mS/cm. The mean conductivity of water samples from oilfields was significantly higher than those from coal mines and CBM sources, while the latter two were not significantly different.

TDS ranged from 19,010 to 126,949 mg/L for samples from oilfields, from 1,310 to 33,083 mg/L for samples from CBM fields, and from 522 to 20,392 mg/L for samples from coal mines (Table 2-16). For comparison, the TDS value for the national drinking water standards recommendation for potable water is 500 mg/L (U.S. EPA, 2009); the TDS of seawater is about 35,000 mg/L (Crittenden et al., 2005); and the TDS of produced water in the Western United States ranges from 1,000 to 400,000 mg/L (Benko and Drewes, 2008). As suggested by the conductivity, TDS is significantly higher in water samples from oilfields (average of 65,252±43,185 mg/L) than those from CBM fields (17,405±15,061 mg/L) and coal mines (9,981±8,362 mg/L). The mean TDS of the samples from oilfields is four times that of samples from CBM fields and seven times that of samples from coal mines. TDS values for samples from CBM fields and coal mines are not significantly different, but samples from Pulse Energy and Royal Falcon have much lower TDS values than other samples of the same type (i.e., CBM or coal mines). The mean TDS of our samples from the four oilfields is lower than the reported mean value for the twenty largest oilfields (110,000±34,000 mg/L) (Table 2-17).

A significant correlation between TDS and conductivity was observed in all samples: TDS (g/L) = Conductivity (mS/cm) × 0.79 (R^2=0.98). And the coefficient of 0.79 is within the reported range of 0.54 – 0.96 for natural water (APHA, 1992). Significant correlations were also observed in each source of produced water: the coefficient was 0.80 for samples from the oilfields (R^2=0.97), 0.66 for samples from CBM sites (R^2=0.97), and 0.61 for samples from coal mines (R^2=0.99).

TSS ranged from 8.0 to 135.7 mg/L for samples from oilfields, from 1.0 to 151.5 mg/L for samples from CBM sources, and from 0.8 to 2644.0 mg/L for samples from coal mines (Table 2-16). The highest and lowest TSS values were observed in the samples from coal mines. Because the water sample from Millenium coal mine was collected directly from the discharge pipe without settling, this sample has the highest TSS of 2,644.0 mg/L. The sample from Royal Falcon Site 1 had the lowest TSS of 0.8 mg/L, since it was collected from a settling pond. No significant difference was observed among the means of the three types of produced water.

The alkalinity ranged from 90 to 1,148 mg/L for samples from oilfields, from 627 to 1,469 mg/L for samples from CBM sources, and from 144 to 482 mg/L for samples from coal mines (Table 2-16). The mean alkalinity of samples from CBM fields (845±327 mg/L) was significantly higher than that from coal mines (283±117 mg/L), but there was no significant difference between samples from oilfields and those from CBM fields, or between samples from oilfields and those from coal mines. The mean alkalinity of samples from the four coal mines was higher than the mean value of the 21 samples from selected coal mines in the previous study by Gluskoter (1965) (456±254 mg/L) (Table 2-17).

DOC concentrations ranged from 5.8 to 507.5 mg/L for samples from oilfields, from 0.9 to 7.3 mg/L for samples from CBM fields, and from 0.5 to 14.5 mg/L for samples from coal mines. The highest DOC concentration was observed in a sample from Main Consolidated oilfield and the lowest DOC was observed in samples from Pulse Energy CBM Site 1 and Royal Falcon coal mine Site 1 (Table 2-16). The mean DOC value for the oilfields (66 mg/L) was an order of magnitude larger than those from CBM fields and coal mines (2.2 and 5.7 mg/L, respectively). However, large variations of DOC were observed within each type of source, so the values are not significantly different.

The concentration of ammonia (primarily in the form of NH_4^+ within the sample pH ranges) ranged from 0.2 to 35.5 mg N/L for samples from oilfields, from 0.05 to 11.8 mg N/L for samples from CBM fields, and from <0.05 to 8.4 mg N/L for samples from coal mines. The mean value for ammonia in samples from the oilfields (16.8 mg N/L) was significantly higher than the values from CBM fields and coal mines (6.0 and 3.3 mg/L, respectively). Mean dissolved ammonia concentrations of samples from CBM fields and coal mines were not significantly different from each other.

The TPH contents of selected samples before and after filtration are presented in Figure 2-10. For unfiltered samples, the average TPH in samples from oilfields (80 mg/L) is 40 times of that in Royal Falcon coal mine Site 1 and 20 times of that in ACT CBM site. The TPH content of samples from oilfields (ranging from 26 to 107 mg/L) was reduced by 71 to 95% after passing through the 0.7 µm filter, which indicates that the majority of TPH in water samples was associated with suspended small droplets,

colloids, and particles. For comparison, the oil and grease contents of produced water in the Western United States range from 40 to 2,000 mg/L (Benko and Drewes, 2008).

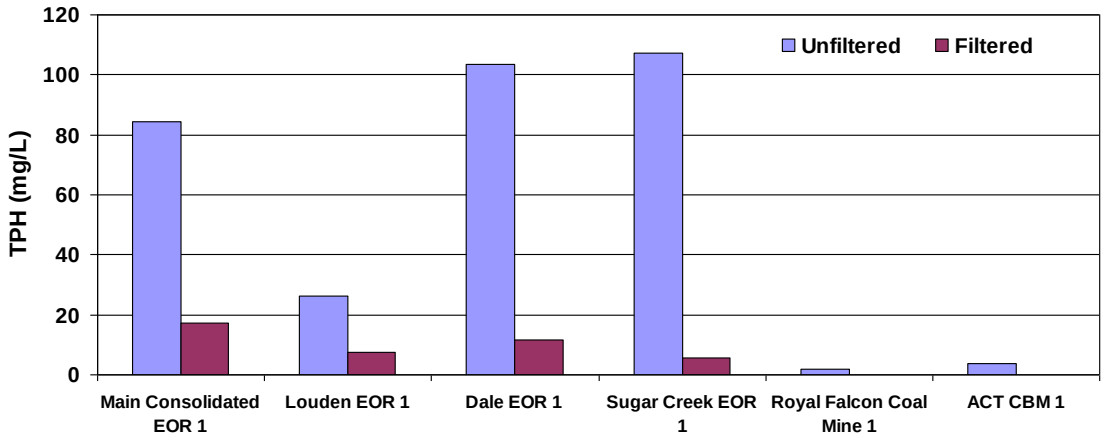

Figure 2-10: TPH contents in selected samples before and after filtration (0.7 µm).

Concentrations of major cations (Na^+, K^+, Ca^{2+}, Mg^{2+}, Ba^{2+}, and Sr^{2+}) and anions (Cl^-, Br^-, SO_4^{2-}, and HCO_3^-) in sampled produced water are presented in Table 2-18. The table also shows the average values and standard deviations calculated for each type of produced water.

Na^+ is the dominant cation in all samples, followed by Ca^{2+}. The average concentrations of Na^+, Ca^{2+}, Mg^{2+}, K^+, Ba^{2+}, and Sr^{2+} in samples from oilfields were all significantly higher than those from CBM fields and coal mines, while there was no significant difference between the averages for the samples from CBM fields and coal mines. The mean concentration of Na^+ in samples from oilfields (23,000±15,000 mg/L) was four times that of samples from CBM fields (6,100±5,300 mg/L) and six times that of samples from coal mines (3,900±3,400 mg/L). The mean concentration of Ca^{2+} in samples from oilfields (2,000±1,700 mg/L) was 22 times that of samples from CBM fields (91±86 mg/L) and 11 times that of samples from coal mines (190±60 mg/L) (Table 2-18). Similar to TDS (Table 2-16), the concentrations of the six cations (Table 2-18) were all relatively lower in samples from Pulse Energy and Royal Falcon compared to those of the oilfield samples, indicating that water with a relatively good quality was produced from the coal seams. The mean Na^+ and Ca^{2+} concentrations in samples from the four oilfields were lower than the mean values for the 20 largest oilfields reported in the previous study by Demir (1995) (37,000±11,000 mg/L for Na^+ and 4,300±2,600 mg/L for Ca^{2+}) (Table 2-17). The mean Na^+ and Ca^{2+} concentrations in samples from the four coal mines was lower than the mean value for 21 samples from selected coal mines reported in the previous study by Gluskoter (1965) (6,592±6,024 mg/L for Na^+ and 293±328 mg/L for Ca^{2+}) (Table 2-17).

Table 2-18: Concentrations of major cations and anions in samples (concentrations in mg/L) (mean values for each source type with the same letter are not significantly different).

Source	Site	Na^+	K^+	Ca^{2+}	Mg^{2+}	Ba^{2+}	Sr^{2+}	Cl^-	Br^-	SO_4^{2-}	HCO_3^-
Main Consolidated	1	7,110.2	31.8	199.5	184.3	33.8	13.39	10,420.6	28.0	ND	1,399.7
	2	7,909.9	26.2	374.3	166.7	137.5	26.11	12,410.4	26.8	ND	724.2
	3	7,302.4	26.4	299.2	177.5	99.0	20.67	11,634.9	32.8	ND	1,350.1
Louden	1	33,567.9	100.5	2,602.6	968.6	609.5	219.22	60,341.4	95.1	ND	346.3
	2	32,547.1	100.2	2,615.3	998.8	314.3	185.40	58,277.1	90.4	ND	198.8
	3	31,876.6	99.6	2,508.8	984.4	429.8	195.09	58,117.7	89.6	ND	290.1
Dale	1	38,958.3	243.7	4,891.5	1,603.2	1.6	302.83	74,883.7	123.5	60.0	110.2
	2	37,356.3	238.7	3,987.7	1,325.1	0.5	194.38	65,813.9	110.0	100.0	216.4
Sugar Creek	1	7,960.7	19.3	603.3	219.1	2.6	330.73	14,011.8	70.8	31.7	946.3
Mean of Oilfield		23,000±15,000	98±88 [A]	2,000±1,700 [A]	740±560 [A]	180±220 [A]	170±120 [A]	41,000±28,000 [A]	74±37 [A]	64±34 [A B]	620±505 [A B]
ACT	1	7,234.7	27.5	124.2	67.9	6.2	4.62	10,418.1	37.1	< 0.5	773.3
Pioneer	1	10,583.6	31.8	155.1	133.3	19.7	15.65	15,995.8	40.3	ND	818.4
	2	11,089.1	39.1	156.3	153.7	42.9	18.02	17,085.7	46.1	ND	759.6
	3	11,936.6	40.8	196.9	168.7	46.5	21.15	18,900.3	49.1	ND	672.2
Pulse Energy	1	753.0	1.9	2.7	1.1	0.4	0.12	139.3	1.7	0.5	1,685.1
	2	456.3	1.1	1.5	0.4	0.2	0.05	44.3	1.4	25.0	1,050.4
	3	581.9	1.6	2.5	1.0	0.2	0.07	148.7	1.6	46.0	1,243.8
Mean of CBM		6,100±5,300 [B]	21±18 [B]	91±86 [B]	75±76 [B]	17±20 [B]	8.5±9.4 [B]	9,000±8,700 [B]	25±23 [B]	24±23 [B]	1,000±361 [A]
Galatia	1	6,312.2	33.4	265.5	150.0	0.5	8.18	9,486.6	29.5	200.0	314.2
	2	6,699.5	35.6	221.1	153.0	0.7	8.22	9,935.8	32.0	200.0	174.9
Millenium	1	5,818.7	33.3	173.4	102.5	1.0	6.45	8,195.9	26.1	150.0	585.3
Pattiki	1	7,234.3	29.0	234.8	102.2	0.8	8.45	10,777.9	34.8	160.0	360.1
Royal Falcon	1	48.0	1.1	80.4	24.8	0.2	0.18	21.1	1.4	5.0	425.8
	2	339.8	5.2	133.8	61.7	0.4	1.18	700.1	2.3	100.0	357.9
	3	508.1	7.0	211.7	88.4	0.5	1.77	1063.2	2.9	110.0	183.7
Mean of Coal Mine		3,900±3,400 [B]	21±15 [B]	190±60 [B]	97±46 [B]	0.6±0.3 [B]	4.9±3.7 [B]	5,700±4,900 [B]	18±15 [B]	132±68 [A]	343±142 [B]

Chloride was the most abundant anion in all samples from the oilfields and the majority of samples from CBM fields and coal mines. Bicarbonate concentrations were calculated from alkalinity and pH values. Bicarbonate was the dominant anion for the three samples from Pulse Energy and the sample from Royal Falcon Site 1. The concentrations of I^-, NO_3^-, and PO_4^{3-} were not reported because either their concentrations were below the detection limit or their peaks could not be distinguished from peaks of other ions with higher concentrations. Chloride and bromide concentrations in the samples from oilfields were significantly higher than those from CBM and coal mine sources, but their mean concentrations in the CBM and coal mine samples were not significantly different. The mean concentration of Cl^- in the samples from oilfields (41,000±28,000 mg/L) was five times that of the CBM samples (9,000±8,700 mg/L) and seven times that of the samples from coal mines (5,700±4,900 mg/L) (Table 2-18). The mean Cl^- concentration of the samples from the four oilfields was lower than the mean value for the 20 largest oilfields (68,000±21,000 mg/L) (Table 2-17). The mean Cl^- concentration in samples from the four coal mines also was lower than the mean value of the 21 coal samples (10,443±10,662 mg/L) (Table 2-17).

Linear correlations were observed between TDS and Na^+ concentrations for the three sources of produced water (R^2=0.92, 0.87, and 0.98 for water from oilfields, CBM fields, and coal mines), and between the TDS and Cl^- concentrations (R^2=0.94, 0.87, and 0.98 for water from oilfields, CBM fields, and coal mines) (data not shown).

Sulfate was not detected in all samples from oilfields and CBM fields. Like the previously mentioned anions, sulfate detection by ion chromatography can be affected by the high Cl^- background. Among the sampled sites, the mean SO_4^{2-} concentration was significantly higher in samples from coal mines (132±68 mg/L) than those from CBM fields (24±23 mg/L). The mean sulfate concentration of oilfields (64±34 mg/L) was not significantly different from that from coal mines and CBM fields; however, the average value of sulfate concentration in produced water samples from the twenty largest oilfields in the Illinois Basin was 810±890 mg/L (Demir, 1995) (Table 2-17). Hem (1992) suggested that SO_4^{2-} concentration has a direct influence on the barium concentration because barium sulfate precipitation generally controls the level of dissolved barium in most natural waters. In our study, water samples from Main Consolidated oilfield, Louden oilfield, and ACT and Pioneer CBM fields have relatively higher levels of Ba and lower levels of sulfate compared with other sources (Table 2-18).

Concentrations of HCO_3^- were calculated from alkalinity and pH values. Within the pH range of our samples, HCO_3^- is the dominant inorganic carbon ion. The mean HCO_3^- concentration was significantly higher in the samples from the CBM fields (1,000±361 mg/L) than those from coal mines (343±142 mg/L). The mean HCO_3^- concentration in oilfield samples (620±505 mg/L) was not significantly different from those from coal mines and CBM fields.

Concentrations of trace elements in samples are shown in Table 2-19. Concentrations of Al, As, Be, Cd, Co, Cr, and Pb were below the detection limit. Boron and Si were detected in all samples. The mean concentration of B was 2.6±1.6 mg/L for samples from oilfields, 1.3±0.2 mg/L for samples from CBM fields, and 1.0±0.4 mg/L for samples from coal mines. Boron concentrations in samples from the Dale Consolidated oilfield (4.8 and 5.6 mg/L) were comparable to that of seawater (4.5 mg/L) (Hem, 1992).

The mean concentration of Si was 5.6±1.0 mg/L for samples from oilfields, 3.8±0.4 mg/L for samples from CBM fields, and 5.9±0.4 mg/L for samples from coal mines. The average concentrations of B and Si for 41 water samples from selected oilfields in the Aux Vases Formation in the Illinois Basin were 3.90±1.39 and 4.50±1.60 mg/L, respectively; and the average concentrations of B and Si for 36 water samples from selected oilfields in the Cypress Formation in the Illinois Basin were 2.58±0.57 and 5.00±2.80 mg/L, respectively (Demir and Seyler, 1999); not significantly different from our results. The average concentration of Li in oilfield water samples was 5.1±3.2 mg/L, similar to that in 41 water samples from selected oilfields in the Aux Vases Formation (8.22±3.04 mg/L), and in 36 water samples from selected oilfields in the Cypress Formation (4.96±0.36 mg/L) (Demir and Seyler, 1999), but these values are more than an order of magnitude greater than normal concentration of Li in seawater (0.17 mg/L) (Hounslow, 1995). Lithium in samples from CBM fields and coal mines was below the detection limit. Concentrations of Cu, Mn, and Ni in most samples were less than 1.0 mg/L. The concentration of Fe was low (equal or less than 1.0 mg/L) in most samples, except in the Pioneer CBM Site 1 (32.0 mg/L) and the Louden oilfield Site 2 (6.4 mg/L).

Table 2-19: Concentrations of trace elements in samples (concentrations in mg/L).

Source	Site	B	Cu	Fe	Mn	Ni	Si	Li
Main Consolidated	1	1.2	BD	0.1	1.7	0.2	5.4	BD
	2	1.4	0.1	0.1	0.5	BD	6.2	BD
	3	1.2	1.1	0.1	0.6	BD	7.6	BD
Louden	1	2.8	BD	BD	0.2	0.5	4.6	3.0
	2	2.5	BD	6.4	0.5	0.4	4.3	2.8
	3	2.1	BD	0.2	0.6	0.5	4.5	2.7
Dale	1	4.8	BD	0.6	0.5	0.8	6.2	9.3
	2	5.6	BD	0.1	0.7	0.6	5.7	7.7
Sugar Creek	1	1.5	BD	0.3	0.5	BD	5.6	BD
Mean of Oilfield		2.6±1.6	0.6±0.7	1.0±2.2	0.7±0.4	0.5±0.2	5.6±1.0	5.1±3.2
ACT	1	1.6	0.046	0.1	0.2	BD	3.9	BD
Pioneer	1	1.4	BD	32.0	0.7	0.1	3.7	BD
	2	1.2	BD	0.9	0.3	0.2	3.2	BD
	3	1.3	BD	BD	0.2	0.1	3.3	BD
Pulse Energy	1	1.1	0.042	BD	BD	BD	4.0	BD
	2	1.4	BD	0.4	0.0	BD	4.1	BD
	3	1.2	BD	0.1	0.0	BD	4.1	BD
Mean of CBM		1.3±0.2	0.044±0.003	6.7±14.1	0.2±0.3	0.16±0.03	3.8±0.4	NA
Galatia	1	0.8	BD	BD	BD	0.3	1.3	BD
	2	0.8	0.9	BD	0.1	0.3	1.6	BD
Millenium	1	0.8	0.1	1.0	0.3	0.2	3.1	BD
Pattiki	1	1.5	BD	BD	0.7	0.1	3.5	BD
Royal Falcon	1	BD	0.0	BD	0.1	BD	14.1	BD
	2	BD	0.0	BD	0.1	BD	7.4	BD
	3	BD	0.0	BD	0.4	BD	10.2	BD
Mean of Coal Mine		1.0±0.4	0.2±0.4	1.0	0.3±0.3	0.2±0.1	5.9±4.9	NA

BD: below detection
NA: not available

2.5 Conclusions

The potential flow rate of produced water for CO_2-EOR from Illinois basin oil fields was estimated to be between 15 and 110 million liters per day (4 and 29 MGD), based on several assumptions. Potential flow rate of produced water from coal mines and CBM sources are estimated to be up to 144 million liters per day (38 MGD), assuming a lifetime of 50 years for CBM recovery. Water sources are located throughout the southern half of the Illinois Basin.

Significant uncertainties make estimation of water availability difficult. Development of CO_2-EOR and CBM projects depend on the cost and availability of CO_2, the energy price (both oil and methane), and future regulations for brine disposal injection. For CO_2-EOR the fraction of produced water available for beneficial use is not precisely known. For CBM more data are needed to predict long term water-to-gas ratios and water quantities available in the Illinois Basin.

Water quality of each of the sources of produced water varies significantly. TDS concentrations of water samples collected in this study ranged between 500 and 127,000 mg/L. The dominant components in all produced waters were sodium and chloride. In order to beneficially use produced water, TDS must be reduced to approximately 1,000 mg/L by either a water treatment process or by blending with other water sources.

Based on results from this project, the following recommendations for future studies and projects are suggested. Investigate the quantity of produced water production available from CO_2-EOR under different scenarios (e.g., injected CO_2-to-water ratio). The costs of produced water injection and treatment for beneficial use should be compared. Characterize additional produced water samples in the Illinois Basin using the methodology of this work. Particularly, the volume and quality of water in mine pools and the quantity of water influx into abandoned coal mines should be investigated.

2.6 References

American Petroleum Institute (API) Production Waste Survey prepared by Paul G. Wakim, June 1988.

American Public Health Association (APHA), Standard Methods for the Examination of Water and Wastewater. 18th ed., Washington, DC, 1992.

Baviere, M., Basic Concepts in Enhanced Oil Recovery Processes, Elsevier Applied Science, 1991.

Benko K. L., Drewes J. E., Produced water in the Western United States: Geographical distribution, occurrence, and composition. Environmental Engineering Science 25, 239-246, 2008.

Clark C. E., Veil J. A., Produced Water Volumes and Management Practices in the United States, 2009.

Clesceri, L. S., Greenberg A. E., Eaton A. D., Franson M. H., Standard methods for the examination of water and wastewater 20th edition, American Public Health Association, American Water Works Association, Water Environment Federation, 1998.

Crittenden J. C., Trussell R. R., Hand D. W., Howe K. J., Tchobanoglous G., Water Treatment: Principles and Design. John Wiley & Sons, Inc., Hoboken, NJ, 2005.

Demir, I., Formation Water Chemistry and Modeling of Fluid-rock Interaction for Improved Oil Recovery in Aux Vases and Cypress Formations, Illinois basin, Illinois Petroleum 148, 1995.

Demir I., Seyler B.,) Chemical composition and geologic history of saline waters in Aux Vases and Cypress Formations, Illinois Basin. Aquatic Geochemistry 5, 281-311, 1999.

DOE/EIA, Annual Coal Report, DOE/EIA-0884, 2009.

DOE/NETL, Estimated Freshwater Needs to Meet Future Thermoelectric Generation Requirements, DOE/NETL-400/2007/1304, September 24, 2007.

DOE/NETL, Use of Non-traditional Water for Power Plant Applications: An Overview of DOE/NETL R&D efforts, DOE/NETL-311/040609, November 1, 2009.

Doran G. F., Williams K. L., Drago J. A., Huang S. S., Leong L. Y. C., Converting oilfield produced water to reusable quality. J. Pet. Technol. 51, 62-63, 1999.

Electric Power Research Institute (EPRI), Enhanced Oil Recovery Scoping Study, Palo Alto, CA, TR-113836, 1999.

Electric Power Research Institute (EPRI), Use of Produced Water in Recirculated Cooling Systems at Power Generating Facilities. http://www.osti.gov/bridge/purl.cover.jsp?purl=/935386-AygWJW/, 2006.

Energy Information Administration, www.eia.doe.gov, accessed 2010.

EPA Web site for Analytical Methods for Drinking Water, accessed 2010.

Feeley T. J., Green L., McNemar A., Carney B. A., Pletcher S., Department of Energy/Office of Fossil Energy's Water-Energy Interface Research Program, DOE/FE's Power Plant Water Management R&D Program Summary, April 2006.

Finley R. J., An Assessment of Geological Carbon Sequestration Options in the Illinois Basin, Final Report for U.S. DOE contract DE-FC26-03NT41994., December 31, 2005.

Frailey S. M., Oil Reservoirs: CO_2 Storage and EOR, Illinois State Geological Survey, MGSC PAG Meeting, September 13, 2005.

Gillette J. L., Veil J. A., Identification of Incentive Options to Encourage the Use of Produced Water, Coal Bed Methane Water, and Mine Pool Water. Prepared by Argonne National Laboratory for U.S. Department of Energy, Office of Fossil Energy, National Energy Technology Laboratory, 2004.

Gluskoter, H. J., Composition of Ground Water Associated with Coal in Illinois and Indiana, Econ. Geology, v. 60, p. 614-620, 1965.

Hem J. D., Study and interpretation of the chemical characteristics of natural water. U.S. Geological Survey, Water Supply Paper 2254, 1992.

Holtz M. H., Nance P., Finley R. J., Reduction of Greenhouse Gas Emissions through Underground CO_2 Sequestration in Texas oil Reservoirs; Final Contract Report prepared for EPRI through U.S. Department of Energy, under contract no. W04603-04, 1999.

Holtz M. H., Nance P., Finley R. J., Reduction of Greenhouse Gas Emissions through Underground CO_2 Sequestration in Texas oil Reservoirs", Environmental Geosciences, v. 8, 187–199, 2001.

Hounslow A. W., Water Quality Data: Analysis and Interpretation. CRC Press LLC, Boca Raton, FL, 1995.

Hutson S. S., Barber N. L., Kenny J. F., Linsey K. S., Lumia D. S.,Maupin M. A., Estimated Use of Water in the United States in 2000, U.S. Geological Survey 1268, 2004.

Klett M. G., Kuehn N. J., Schoff R. L., Vaysman V., White J. S., Power Plant Water Usage and Loss Study, prepared for the United States Department of Energy, National Energy Laboratory, August 2005, Revised May 2007.

Koren A.,Nadav N., Mechanical vapor compression to treat oil-field produced water. Desalination 98, 41-48, 1994.

Meents, W. F., Bell A. H., Rees O. W., Tilbury W. G.,, Illinois Oil-field Brines: Their Geologic Occurrence and Chemical Composition, Illinois Petroleum No. 66, 1952.

Sirivedhin T., Dallbauman L., Organic matrix in produced water from the Osage-Skiatook Petroleum Environmental Research site, Osage county, Oklahoma. Chemosphere 57, 463-469, 2004.

Solley W. B., Pierce R. R., Perlman H. A., Estimated Use of Water in the United States in 1995, U.S. Geological Survey 1200, 1998.

Spellman, F. R., The Science of Water: Concepts and Applications, CRC Press, 2nd Edition, 2007.

Tao F. T., Curtice S., Hobbs R. D., Sides J. L., Wieser J. D., Dyke C. A., Tuohey D. and Pilger P. F., Reverse-Osmosis Process Successfully Converts Oil-field Brine into Fresh-water. Oil Gas J. 91, 88-91, 1993.

U.S. Department of Energy, Energy Demands on Water Resources: Report to Congress on the Interdependency of Energy and Water, December 2006.

U. S. Environmental Protection Agency (U. S. EPA), Interim Enhanced Surface Water Treatment Rule: A Quick Reference Guide, 2001.

U. S. Environmental Protection Agency (U. S. EPA), 2009 Edition of the Drinking Water Standards and Health Advisories, 2009.

U.S. Geological Survey (USGS), Assessing the Coal Resources of the United States. USGS Fact Sheet FS-157-96 http://energy.usgs.gov/factsheets/nca/nca.html, 1996.

USGS, Water Production with Coal-bed Methane, Fact Sheet FS-156-00, November 2000.

USGS, Collection of Water Samples (ver. 2.0): U.S. Geological Survey Techniques of Water-Resources Investigations, book 9, chap. A4, U.S. Geological Survey, September, at http://pubs.water.usgs.gov/twri9A4/, 2006.

USGS, USGS Produced Water Database, http://energy.cr.usgs.gov/prov/prodwat/data2.htm. Accessed 2010.

Veil J. A., Kupar J. M., Puder M. G., Feeley T. J., Beneficial Use of Mine Pool Water for Power Generation, Ground Water Protection Council Annual Forum, Niagara Falls, NY, September 13-17, 2003.

Veil J. A., Puder M. G., Elcock D.,Redveik R. J., Jr. A white paper describing produced water from production of crude oil, natural gas, and coal bed methane. U.S. Department of Energy, National Energy Technology Laboratory, 2004.

Winter E. M., Chen Z. Y., Disposal of Power Plant CO_2 in Depleted Oil and Gas Reservoirs in Texas: Energy Conversion and Management PD Bergman, v. 38, Suppl. 1, p. S211–S216, 1997.

Chapter 3 Techno-economic assessment

3.1 Cooling and process water demand at Illinois Basin power plants to 2030

Available data on current water demand at coal-fired power plants in the Illinois Basin was examined. Projections of electricity demand were calculated in order to estimate future water demand of power plants in the Illinois Basin through the year 2030.

3.1.1 Current water demand by power plants in the Illinois Basin

Projections of U.S. coal-based power generation capacity through the year 2030 are available from the Energy Information Administration (EIA). However, no projections for individual states are reported by EIA. In this section of the report, we explain how we predicted the changes in coal-based electricity generation capacity for Illinois, Indiana, and Kentucky in the Illinois Basin.

Data on the power generation and cooling water withdrawals/discharges of current coal-based power plants in the Illinois Basin were extracted from the DOE/NETL 2007 coal power plant database. Coal-based power plants in the three Illinois Basin states were classified according to their cooling systems, and estimates for their water withdrawal and consumption were calculated for both cooling and process uses. Process water makeup for boiler and FGD makeup (when applicable) were estimated from the power plants' net generation data, using water consumption factors of 249.1 and 16.7 L/MWh (65.8 and 4.4 gal/MWh) for the flue gas desulfurization (FGD) system and the boiler, respectively (DOE/NETL, 2005). For power plants with recirculating cooling systems, cooling tower makeup (evaporation and blow-down) was calculated using the factor of 4,160.2 L/MWh (1099 gal/MWh) (DOE/NETL, 2005). Cooling water loss in open-loop systems was calculated from the difference between withdrawal and discharge data reported in the NETL database.

The net electricity generation for coal-based power plants in the U.S. and for Illinois, Indiana, and Kentucky (in the Illinois Basin) were calculated separately based on the NETL 2007 Coal-based Power Plants Database (Table 3-1). In 2007, coal-based power plants in Illinois, Indiana, and Kentucky (in the Illinois Basin) generated 70,470,231; 87,186,582; and 51,519,726 MWh electricity, respectively, while the total national coal-based power generation was 2,016,456,000 MWh. Therefore, coal-based power generation in the Illinois, Indiana, and Kentucky sections of the Illinois Basin were 3.5, 4.3, and 2.6% of the total U.S. coal-based power generation in that year.

Table 3-1: Coal-based power generation in the US and Illinois Basin in 2007.

	Generation, MWh	Fraction of US generation
Total coal-based in USA	2,016,456,000	1.000
Illinois (in Illinois Basin)	70,470,231	0.035
Indiana (in Illinois Basin)	87,186,582	0.043
Kentucky (in Illinois Basin)	51,519,726	0.026
Illinois Basin Total	209,176,539	0.104
Source of power generation data: NETL 2007 coal power plant database		

Coal-based power generation projections (including additions and retirements) for the three states in the Illinois Basin were estimated by assuming that 50% of additions would be supercritical plants and

50% would be Integrated Gasification Combined Cycle (IGCC) plants. Furthermore, it was assumed that 10% of the added supercritical plants would use dry FGD systems and 90% wet FGD. This 90/10 ratio was selected based on the current national split in FGD systems of PC power plants and following the NETL/DOE methodology for estimating the freshwater demand of future power plants (DOE/NETL-2007). All added power plants were assumed to be equipped with freshwater recirculating cooling systems. For retirements, all plants were assumed to be subcritical plants burning pulverized coal (PC) without FGD units and using freshwater, once-through cooling systems.

Changes in future water withdrawal/consumption of coal-based power plants (due to additions and retirements) in the Illinois Basin were estimated based on the projected power generation and water withdrawal/consumption factors listed in Table 3-2. Water demand factors of model power plants were obtained from a recent NETL report (DOE/NETL, 2007), while water demand factors for retiring subcritical plants (once-through, no FGD) were derived from the Illinois Basin power plants data (obtained from DOE/NETL 2007 Coal-based Power Plants Database).

Table 3-2: Water withdrawal and consumption factors for different types of coal-based power plants.

Coal-based Power Plants	Withdrawal Factor (gal/kWh)	Consumption Factor (gal/kWh)
Model supercritical PC, recirculating freshwater, wet FGD	0.669	0.518
Model supercritical PC, recirculating freshwater, dry FGD	0.648	0.496
Model IGCC(E-Gas), recirculating freshwater	0.226	0.173
Illinois existing subcritical PC, once-through freshwater, no FGD	28.1	0.150
Indiana existing subcritical PC, once-through freshwater, no FGD	28.5	0.004
Kentucky existing subcritical PC, once-through freshwater, no FGD	51.3	0.004

Notes: (1) Factors for model plants were obtained from DOE/NETL (2007) (2) Withdrawal and consumption factors for existing plants were estimated from current water consumption of power plants.

Cooling and process water consumptions of added power plants were estimated by multiplying the total projected water consumption of new power plants by the average water consumption factors listed in Table 3-3.

Table 3-3: Expected cooling and process water consumption factors of future power plants.

Cooling/process Make Up Water Consumption	Consumption* (gal/kWh)	Consumption Fraction
IGCC(E-gas), cooling	606.7	0.895
IGCC, process	71.5	0.105
PC Sup, wet FGD, cooling	979.8	0.940
PC Sup, wet FGD, process	62	0.060
PC Sup, dry FGD, cooling[1]	979.8	0.996
PC Sup, dry FGD, process[1]	3.9	0.004
Average cooling[2]		0.9203
Average process[2]		0.0797

[1] Assuming supercritical wet case with no FGD water usage.

[2] Average values are weight averaged based on 0.5*IGCC, 0.5*0.9 Sup wet and 0.5*0.1 Sup dry.

* From DOE/NETL, 2005.

Water demand data for Illinois Basin power plants are presented in Table 3-4 and Table 3-5. The total water withdrawal and consumption of coal-based power plants in Illinois are 13.8 and 0.151 million cubic meters per day (MCMD) (3.64 and 0.04 billion gallons per day (BGD)), respectively. The USGS estimates that the total water withdrawal rate is 64.7 MCMD (17.1 BGD) and the consumption rate is 1.51 MCMD (0.4 BGD) for all thermoelectric power plants in the state of Illinois (Solley et al., 1998). About 50% of the total electricity generation in Illinois is from coal-based power plants. The rest is mostly from nuclear plants that withdraw more water compared to coal-based power plants with similar power generation. In the state of Illinois coal-based power plants with once-through systems account for the withdrawal of more than 85% of the cooling water for all coal-based power plants.

An analysis of water withdrawal and consumption by coal-based power plants in the Illinois Basin using different recirculating or once-through cooling systems is shown in Table 3-6. The data indicate that in 2007, coal-based power plants equipped with various once-through cooling systems accounted for 40% of the total power generation and 18% of total water consumption by all coal-based power plants. The remaining 60% of the power generation by coal-based power plants was generated by power plants with recirculating cooling systems that accounted for 82% of water consumption.

Table 3-4: Estimated yearly water withdrawal and consumption of current coal-based power plants with different cooling systems in the Illinois Basin.

	# of plants	Net generation (MWh)	Water withdrawal (million gal)	Boiler makeup (million gal)	FGD makeup (million gal)	Total process makeup (million gal)	Cooling tower makeup (million gal)	Water loss in open-loop systems (million gal)	Raw water consumption (million gal)	Consumption (gal/kWh)	Withdrawal (gal/kWh)
Illinois	24	70,470,231	1,328,464	310	371	681	5,400	8,285	14,366	0.20	19.83
Indiana	16	87,186,582	1,095,379	384	2,250	2,634	23,766	7,591	33,991	0.39	12.56
Kentucky	12	51,519,726	1,023,822	227	2,264	2,491	14,583	262	17,336	0.34	19.87
Total	**52**	**209,176,539**	**3,447,665**	**921**	**4,885**	**5,806**	**43,749**	**16,138**	**65,693**	**0.31**	**16.48**

Table 3-5: Classification of cooling systems of current coal-based power plants in the Illinois Basin.

	# of Plants	Cooling systems	# of Plants/cooling systems	Net generation (MWh)	Annual water withdrawal (million gal)	Annual water consumption (million gal)	Consumption (gal/kWh)	Withdrawal (gal/kWh)
Illinois	24	Recirculating with cooling tower	6	3,954,952	25,651	1,437	0.36	6.54
		Recirculating with cooling pond	5	29,825,908	167,668	4,913	0.16	5.62
		Once-through with fresh water	6	19,231,021	643,482	2,434	0.13	33.46
		Once-through with cooling pond	6	15,866,684	491,218	5,560	0.35	30.96
		Other	1	1,591,666	140	168	0.11	0.09
Indiana	16	Once through, fresh water	9	29,323,482	848,148	1,052	0.03	28.92
		Recirculating with cooling tower	6	28,646,061	34,274	31,718	1.11	1.20
		Recirculating with cooling pond	2	29,217,039	212,911	1,258	0.04	7.29
Note: there is one plant in Indiana that has two primary cooling systems. One is once through, fresh water and the other is recirculating with cooling tower.								
Kentucky	12	Once through, fresh water	5	18,648,749	842,805	505	0.03	45.18
		Recirculating with cooling tower	7	32,870,977	181,310	16,830	0.51	5.52

Table 3-6: Water withdrawal and consumption by coal-based power plants in the Illinois Basin that use recirculating or once-through cooling systems.

All recirculating systems						
	Generation, MWh/yr	% MWh of the total generation	Consumption (million gal/yr)	% of total water consumption	Withdrawal (million gal/yr)	% of total water withdrawal
IL	35,372,526	50.2	6,518	44.9	193,458	14.6
IN	57,863,100	66.4	32,976	96.9	247,185	22.6
KY	32,870,977	63.8	16,830	97.1	181,310	17.7
Total	**126,106,603**	**60.3**	**56,324**	**85.5**	**621,953**	18.0

All once-through systems						
	Generation, MWh/yr	% MWh of the total generation	Consumption (million gal/yr)	% of total water consumption	Withdrawal (million gal/yr)	% of total water withdrawal
IL	35,097,705	49.8	7,994	55.1	1,134,700	85.4
IN	29,323,482	33.6	1,052	3.1	848,148	77.4
KY	18,648,749	36.2	505	2.9	842,805	82.3
Total	**83,069,936**	**39.7**	**9,551**	**14.5**	**2,825,652**	82.0

3.1.2 Water demand projections for the Illinois Basin

The projections for US coal-based electricity generation capacity including power plant additions and retirements from 2005 to 2030 are obtained from EIA's Annual Energy Outlook 2008. The projections for US power generation capacity in GWh are shown in Table 3-7**Error! Reference source not found.**. Assuming that the general trends of the coal-based power generation additions and retirements in the Illinois Basin and the US will be the same and by using the coal-based power generation factors from Table 3-1, coal-based power generation capacity is projected up to 2030 in Table 3-7.

Table 3-7: Projections for coal-based electricity generation capacity for Illinois Basin.

Year	2010	2015	2020	2025	2030
	Net electricity generation (GWh)				
USA	2,528,000	2,592,000	2,744,000	2,976,000	3,248,000
IL (in IL Basin)	88,347	90,584	95,896	104,004	113,510
IN (in IL Basin)	109,304	112,072	118,644	128,675	140,436
KY (in IL Basin)	64,589	66,225	70,108	76,036	82,985
Illinois Basin	262,241	268,880	284,648	308,715	336,930
	Net electricity generation addition (GWh)				
USA	64,000	80,000	152,000	232,000	272,000
IL (in IL Basin)	2,237	2,796	5,312	8,108	9,506
IN (in IL Basin)	2,767	3,459	6,572	10,031	11,761
KY (in IL Basin)	1,635	2,044	3,884	5,928	6,950
Illinois Basin	6,639	8,299	15,768	24,066	28,216
	Net electricity generation retirement (GWh)				
USA	16,000	8,000	8,000	0	0
IL (in IL Basin)	559	280	280	0	0
IN (in IL Basin)	692	346	346	0	0
KY (in IL Basin)	409	204	204	0	0
Illinois Basin	1,660	830	830	0	0

Note: A factor of 8000 GWh/GW was used for conversion. Electricity generation, addition, and retirements for Illinois Basin coal power plants = US data * national fractions for Illinois Basin power plants. National fractions for IL, IN, and KY were estimated as 0.035, 0.043, and 0.026, respectively.

Estimations for the types of coal-based power generation systems that will be added and retired in the Illinois Basin from 2010 to 2030 are shown in Table 3-8. For each five-year time interval, the added power generation capacity for IGCC and PC supercritical (equipped with wet or dry FGD) as well as the power generation retirements of existing PC subcritical are tabulated. Additions and retirements of coal-based power capacity in the Illinois Basin are proportional to the U.S. predictions.

Projections for additional water demand of future coal-based power plants in the Illinois Basin are summarized in Table 3-9. Tabulated numbers show excess cooling and process water consumption and water withdrawal demand for each five-year interval from 2010 to 2030, compared to the 2005 baseline demand. Cumulative additional water demands for coal-based power plants are also tabulated in Table 3-9 and plotted in Figure 3-1 relative to the amounts used in 2005.

Results of this work project a continuous decrease in the cumulative water withdrawal demand of coal-based power plants in the Illinois Basin, reaching 378.5 million cubic meters less water withdrawn per year (100,000 million gallons per year (Mgal/yr)) by 2020 due to retirements of PC subcritical power plants with once-through cooling. From 2020 to 2030, when no retirements are assumed, the cumulative water withdrawal demand will increase but the total water withdrawal demand at 2030 will be 280 million cubic meters per year (~75,000 Mgal/yr) less than that of the baseline demand (Figure 3-1). The current water withdrawal demand of coal-based power plants in the Illinois Basin is ≈1,300 million m^3 (≈3,450,000 Mgal) per year, indicating a 2% reduction.

The consumptive demand of coal-based power plants is predicted to increase. The cumulative additional raw water consumption demand is estimated to increase to ≈106 million cubic meters per year (≈28,000 Mgal/yr) by 2030. About 92% of the new demand will be for cooling water make up (Table 3-9). Current raw water consumption of coal-based power plants in the Illinois Basin is estimated as ≈250 million cubic meters per year (≈66,000 Mgal/yr), suggesting that consumption will increase by more than 40% by 2030.

These results suggest that if new power plants are built at or close to the location of retiring power plants and if the current water resources for the power plants can provide the same flow rate of water, no new water resources will be needed through 2030. However, if power plants are built in other locations or if current water resources of power plants are not available (e.g., due to new regulations or excess water demand of agricultural and other industrial sectors), other water resources including non-traditional water sources, such as treated municipal wastewater or produced water, should be considered.

Table 3-8: Electric energy addition/retirement estimates (MWh) for future coal-based power plants in the Illinois Basin.

Illinois Basin	2010 additions			2010 retirements
	Supercritical, wet FGD	Supercritical, dry FGD	IGCC	Subcritical, no FGD, once-through
Illinois	1,006,490	111,832	1,118,322	559,161
Indiana	1,245,241	138,360	1,383,601	691,801
Kentucky	735,830	81,759	817,588	408,794
Total	2,987,561	331,951	3,319,512	1,659,756

Illinois Basin	2015 additions			2015 retirements
	Supercritical, wet FGD	Supercritical, dry FGD	IGCC	Subcritical, no FGD, once-through
Illinois	1,258,112	139,790	1,397,903	279,581
Indiana	1,556,551	172,950	1,729,501	345,900
Kentucky	919,787	102,199	1,021,986	204,397
Total	3,734,451	414,939	4,149,390	829,878

Illinois Basin	2020 additions			2020 retirements
	Supercritical, wet FGD	Supercritical, dry FGD	IGCC	Subcritical, no FGD, once-through
Illinois	2,390,414	265,602	2,656,015	279,581
Indiana	2,957,447	328,605	3,286,052	345,900
Kentucky	1,747,595	194,177	1,941,773	204,397
Total	7,095,456	788,384	7,883,840	829,878

Illinois Basin	2025 additions			2025 retirements
	Supercritical, wet FGD	Supercritical, dry FGD	IGCC	Subcritical, no FGD, once-through
Illinois	3,648,526	405,392	4,053,918	0
Indiana	4,513,998	501,555	5,015,554	0
Kentucky	2,667,382	296,376	2,963,758	0
Total	10,829,907	1,203,323	12,033,230	0

Illinois Basin	2030 additions			2030 retirements
	Supercritical, wet FGD	Supercritical, dry FGD	IGCC	Subcritical, no FGD, once-through
Illinois	4,277,582	475,287	4,752,869	0
Indiana	5,292,274	588,030	5,880,304	0
Kentucky	3,127,276	347,475	3,474,751	0
Total	12,697,132	1,410,792	14,107,925	0

Table 3-9: Estimated additional water demand (Mgal) for future coal-based power plants in the Illinois Basin due to additions of new and retirements of old power plants, through 2030. Cumulative changes use 2005 as the starting point.

	2010				2010 cumulative			
Illinois Basin	Withdrawal	Consumption	Process water make up	Cooling water make up	Withdrawal	Consumption	Process water make up	Cooling water make up
Illinois	-14,714	686	55	632	-14,714	686	55	632
Indiana	-18,481	950	76	875	-18,481	950	76	875
Kentucky	-20,241	562	45	517	-20,241	562	45	517
Total	-53,436	2,198	175	2,023	-53,436	2,198	175	2,023
	2015				**2015 cumulative**			
Illinois Basin	Withdrawal	Consumption	Process water make up	Cooling water make up	Withdrawal	Consumption	Process water make up	Cooling water make up
Illinois	-6,608	964	77	887	-21,322	1,650	132	1,519
Indiana	-8,314	1,191	95	1,096	-26,795	2,142	171	1,971
Kentucky	-9,573	704	56	648	-29,814	1,266	101	1,165
Total	-24,495	2,859	228	2,631	-77,931	5,057	403	4,654
	2020				**2020 cumulative**			
Illinois Basin	Withdrawal	Consumption	Process water make up	Cooling water make up	Withdrawal	Consumption	Process water make up	Cooling water make up
Illinois	-5,485	1,788	142	1,645	-26,807	3,438	274	3,164
Indiana	-6,924	2,262	180	2,082	-33,719	4,404	351	4,053
Kentucky	-8,752	1,337	107	1,230	-38,566	2,602	207	2,395
Total	-21,160	5,386	429	4,957	-99,091	10,444	832	9,611
	2025				**2025 cumulative**			
Illinois Basin	Withdrawal	Consumption	Process water make up	Cooling water make up	Withdrawal	Consumption	Process water make up	Cooling water make up
Illinois	3,620	2,792	223	2,570	-23,187	6,230	497	5,734
Indiana	4,478	3,455	275	3,179	-29,240	7,858	626	7,232
Kentucky	2,646	2,041	163	1,879	-35,920	4,644	370	4,274
Total	10,744	8,288	661	7,628	-88,347	18,732	1,493	17,239
	2030 additional water demand				**2030 cumulative**			
Illinois Basin	Withdrawal	Consumption	Process water make up	Cooling water make up	Withdrawal	Consumption	Process water make up	Cooling water make up
Illinois	4,244	3,274	261	3,013	-18,943	9,504	757	8,746
Indiana	5,251	4,050	323	3,728	-23,990	11,909	949	10,960
Kentucky	3,103	2,393	191	2,203	-32,817	7,037	561	6,476
Total	12,597	9,718	774	8,943	-75,750	28,450	2,267	26,182

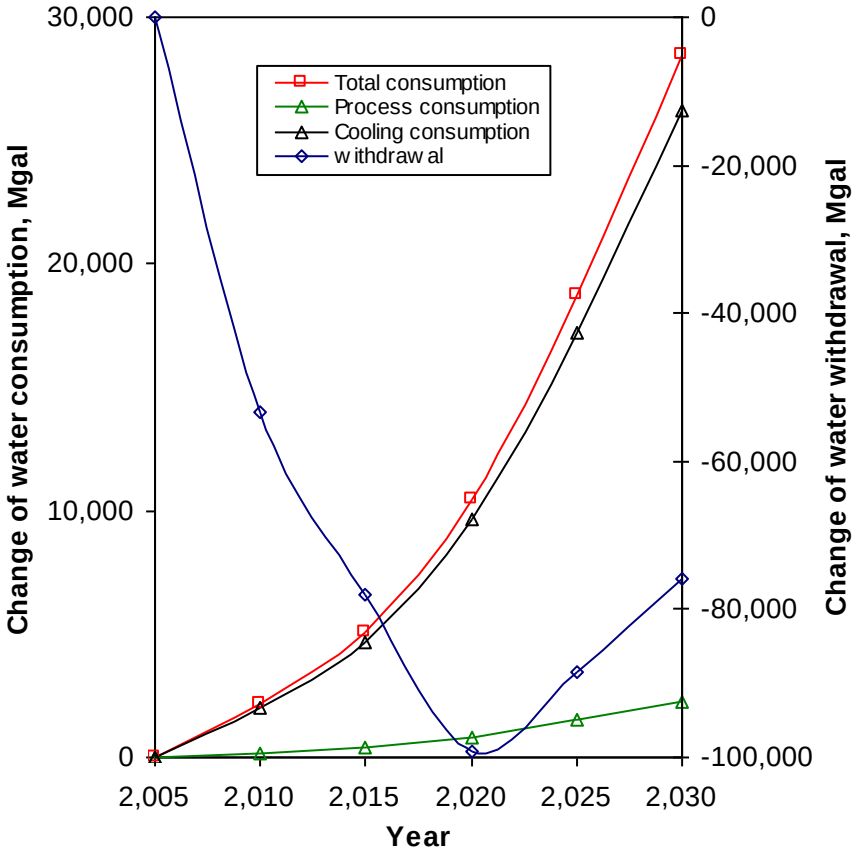

Figure 3-1: Projections for cumulative additional annual water consumption and withdrawals of coal-based power plants in the Illinois Basin.

3.2 Cost estimates for produced water treatment

3.2.1 Introduction

The approach for estimating the cost of treating produced water is shown in Figure 3-2. The first step is to develop a process flow diagram for the treatment system for each source of produced water. The second step is to obtain information resources for the estimation of direct capital costs (DCC) and operation and maintenance (O&M) costs for the various treatment systems. Costs of the various treatment units, estimated based on cost information available for different dates, must be updated using cost estimation indexes. In the last step, the costs of the different treatment units required for a particular type of produced water are summed to obtain the overall cost.

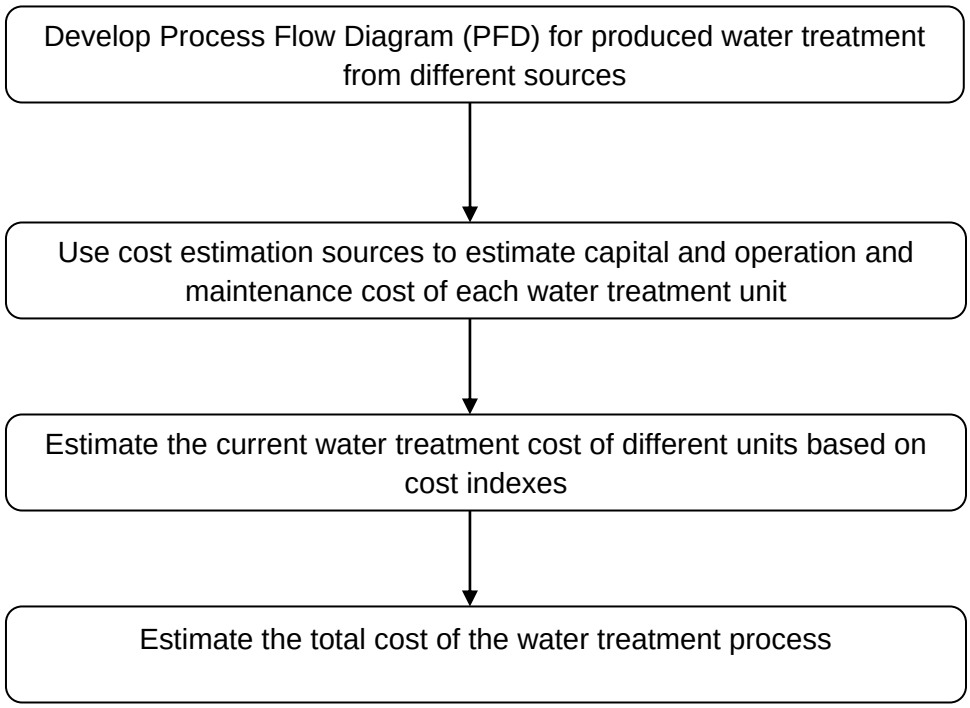

Figure 3-2: A summary of the approach to estimating produced water treatment costs.

Four produced water sources in the Illinois Basin were considered for the cost estimation task: Galatia (coal mine), ACT (CBM), Louden (oilfield), and Sugar Creek (oilfield). Two feed water flow rates, 1,900 and 19,000 m^3 per day (0.5 and 5 million gallons per day (mgd)), were assumed for each source. Due to limited flow rates of produced water from some sources, it was also desirable to include lower flow rates (e.g., 189 cubic meters per day (0.05 mgd)) for produced water treatment cost estimations. However, water treatment cost estimation resources are not available for such low flow rates because they focus on large-scale drinking water treatment operations. For each of the eight main scenarios (four water sources and two flow rates), up to ten different water treatment options for core treatments were considered. Half of the considered core treatment cases were zero liquid discharge (ZLD) processes which included crystallizers. For non-ZLD cases the cost for disposal of concentrated brine by other means was included in the treatment cost.

3.2.2 Cost estimations for treatment units

Produced water treatment processes were designed based on literature information and our treatability studies. Pretreatment process units for ACT and Galatia produced waters included coagulation/flocculation, sand filtration, and granular activated carbon (GAC) adsorption. For produced water from oilfields, walnut shell filtration and organoclay adsorption pretreatments are also included to remove suspended and dissolved oil compounds. Several combinations of established core treatment processes are considered, including reverse osmosis (RO), multiple effect distillation (MED), and multi-

stage flash (MSF). Brine from the core treatments is assumed to be either discharged to disposal wells or sent to crystallization units for ZLD.

Total produced water treatment cost was obtained by adding Direct Capital Costs (DCC) and Operation and Maintenance (O&M) costs of all treatment units. Total capital cost was the summation of total direct and indirect capital costs.

The Water Treatment Estimation Routine (WaTER) Excel file (Wilbert et al, 1999), designed by the US Bureau of Reclamation for drinking water treatment cost estimation, was used for cost estimations in this work. Existing WaTER worksheets were modified in order to apply them to produced water quality, and new worksheets (e.g., for MED, MSF, crystallizer, brine disposal by underground injection) were added. WaTER also was used for estimates of the DCC for eight principal components of produced-water treatment plants: excavation and site work, manufactured equipment, concrete, steel, labor, pipes and valves, electrical equipment and instrumentation, and housing.

According to the Desalting Handbook for Planners (RosTek Associates (2003), indirect capital cost consists of the following items:

- Freight and insurance (5% of DCC)
- Interest during construction period (≈3% of DCC)
- Construction overhead (≈15% of the DCC for total construction cost above US$100 million)
- Owner's direct expense (≈10% of the DCC)
- Contingencies (10% of the DCC)
- Working Capital (2 months of total O&M cost)

O&M cost in this project comprises several elements such as labor, materials, energy, and chemicals.

The Cost Estimating Manual for Water Treatment Facilities (McGivney and Kawamura, 2008) provides an Excel-based model for cost estimation. While the model enables users to update the cost index, it provides no other input parameters except capacity. This source is still useful for approximating the cost of processing unit components which do not have absolute dependency on water quality (e.g., feed and finished water pumps, mix tank, flocculator, and water storage tanks and basins).

Information related to cost indexes, electricity, labor costs, interest, and amortization periods were obtained from the Engineering News Record website (ENR). In all cost estimation calculations by WaTER, a plant life of 30 years and an interest rate of 3% were assumed. Cost estimation for most of the units in WaTER was performed based on the ENR 1978 and ENR 2010 cost indexes. The cost of RO was calculated based on the ENR 1995 cost index.

In the cost estimations using the Cost Estimation Manual Excel model, the cost indexes were based on the handy-Whitman 2010 index of public utility construction costs (Whitman, Requardt and Associates, 2010). In GAC cost estimations, ENR 1984 and current cost indexes were used. In addition an interest rate of 10% was assumed. The cost estimation for the crystallizer unit was calculated based on year 2004 cost information. Chemical prices used in this report were obtained from bulk price quotes from U.S. producers.

3.2.2.1 Raw and finished water pumps

Raw water pumps are used to deliver produced water from the settlement reservoir into the rapid mix tank. Finished water pumps are used to pump the treated water from the treatment plants' reservoirs to the nearby pumping stations. A set of back-up pumps ensures the safety and continuity of water delivery. The DCCs of raw and finished water pumps were obtained by utilizing two equations in Table 3-10 given in the Cost Estimation Manual Excel model. Historical cost data for annual O&M costs of raw and finished water pumps for various plant capacities are summarized in Table 3-11 (USEPA, 1979).

Table 3-10: DCC equations from Cost Estimation Manual excel model for water pumping.

DCC (US$) raw water pumping	8,947.7 x + 44,644
DCC (US$) finished water pumping	13,889 x + 103,488
X	Pump capacity MGD

Table 3-11: Components of raw and finished water pumping O&M cost.

Plant Capacity (MGD)	Raw Water Pumping			Finished Water Pumping		
	Electricity (kwh/yr)	Maintenance Cost (US$/yr)*	Labor (hr/yr)	Electricity (kwh/yr)	Maintenance Cost (US$/yr)*	Labor (hr/yr)
1	195,670	300	511	88,970	260	505
10	1,360,540	1,160	663	519,470	1,210	655

*The numbers are based on 1979 dollar values updated with cost indexes for unit cost calculations.

Annual O&M cost was calculated from the following:

Annual O&M cost (US$/yr) = Electricity + Maintenance + Labor

Electricity = Electricity (kWh/yr) × electricity rate (US$/kWh)

Maintenance = Maintenance cost (US$/yr)

Labor = Labor used (hr/yr) × Labor wage (US$/hr)

3.2.2.2 Mixing system

The mixing system consists of rapid mix basins with a set of propellers in each basin and a flocculator tank. Gradient velocity (G) and detention time (t) determine the quality of mixing in the rapid mix and flocculator tanks. Suggested values for G and t for the rapid mix tank are 900 sec^{-1} and 30 sec, and for the flocculator, they are 80 sec^{-1} and 10 minutes. The Cost Estimation Manual Excel model was used to estimate the cost for both units. Cost equations implemented in this tool, as summarized in Table 3-12, require a value for basin capacity. Calculation of the required capacity is given by:

Detention time flocculator ($t_{flocculator}$) = 10 minutes and $t_{rapid\ mix\ tank}$ = 30 seconds

Basin capacity = detention time × flow rate

The Cost Estimation Manual does not provide any information for the O&M of the mixing system. Hence, the O&M cost estimation was obtained from the US EPA (2000). Assuming the ratio between O&M and direct capital cost in 1992 will remain constant until 2010, the O&M cost for 2010 was determined by multiplying the O&M/DCC ratio by the DCC (2010 value).

Table 3-12: DCC equations from Cost Estimation Manual Excel model for various G values.

Rapid Mix G = 300 sec^{-1}	Direct Capital Cost (US$)	US$ = 3.2559 X + 31,023
Rapid Mix G = 600 sec^{-1}		US$ = 4.0668 X + 33,040
Rapid Mix G = 900 sec^{-1}		US$ = 7.0814 X + 33,269
Flocculator G = 20 sec^{-1}	Direct Capital Cost (US$)	US$ = 566,045 Y + 224,745
Flocculator G = 50 sec^{-1}		US$ = 673,894 Y + 217,222
Flocculator G = 80 sec^{-1}		US$ = 952,902 Y + 177,335
X	Tank Capacity (gal)	
Y	Flocculator Capacity (MGD)	

3.2.2.3 Acid, lime, coagulant, poly-electrolyte, and antiscalant

The costs of chemicals needed for coagulation and pH adjustment were estimated using WaTER, with the equations listed in Table 3-13 - Table 3-16.

Table 3-13: Cost equations for sulfuric acid addition (before RO unit) in WaTER.

DCC (US$)	$6{,}010.6\ X^{0.7934} + 8{,}180$
O&M (US$)	$-42{,}397.4\ e^{-0.00682\ X} + 43{,}670$
X	Dose rate by volume (m^3/day)

Table 3-14: Cost Equations for lime feed (before coagulation) in WaTER.

DCC	$-24{,}950.92 + 20{,}424.674\ Ln(X)$
O&M Cost	$866.285\ X^{0.514}$
X	Total amount of lime required (kg/hr)

Table 3-15: Cost equations for iron coagulation in WaTER.

Iron	Capital Cost (US$)	$10{,}613\ X^{0.319}\ e^{3.93\ E\text{-}4\ (X)}$
	O&M (US$)	$1{,}260{,}926\ e^{1.394E\text{-}5\ (X)}\ -1{,}257{,}710$
X = kg/hr of iron coagulant required		

Table 3-16: Cost equations for antiscalant in WaTER.

Description	Amount
DCC	$11{,}760.71\ e^{0.00665\ X} + 8{,}200$
O&M Cost	$3{,}000.8\ e^{0.00207\ X}$
X	Antiscalant rate (kg/day) – selected dose: 0.5 mg/L

3.2.2.4 Clarifier

A clarifier is a sloped-bottom tank or basin, used to separate a liquid from suspended solid particles. Cost estimation for this unit is available in WaTER, where the recommended depth (height of clarifier), retention time, and gradient velocity are 4.8 m, 180 minutes, and 110 sec^{-1}, respectively (USDOI, 2001). The general flow rate assumption for industrial clarifier design is 1.0 gpm/ft^2. Calculation of the required floor area of the clarifier is given by

$$\text{Floor Area} = \frac{\text{flow rate} \times \text{retention time}}{\text{height of clarifier}}.$$

Cost-capacity equations used in WaTER models are summarized in Table 3-17.

Table 3-17: Cost-Capacity Equations Used in WaTER .

DCC (US$)	Floor Area <400 m^2	62,801.114 + 416.77 X
	Floor Area >400 m^2	132,264.71 + 244.33 X
O&M (US$)	G=70 s^{-1}	5,967.95 + 5.312 X
	G=110 s^{-1}	5,806.57 + 8.805 X
	G=150 s^{-1}	5,939.82 + 12.38 X
X = Floor area (m^2)		

3.2.2.5 Gravity filtration

Gravity filtration is used to remove particulate matter from water. The filtration medium is assumed to be sand. Filtration units include a back flush system to remove collected material and to maintain sufficient permeability. The direct capital cost for gravity filtration units includes a cast-in-place concrete structure with an inlet channel, motor controlled butterfly valves, effluent gullet, and under-drain system.

The design of a gravity filtration unit is mainly determined by the amount of suspended solids in the water. Table 3-18 lists the parameters for a gravity filtration unit. Based on these input parameters, the total required volume and surface area of the filter medium can be calculated. Calculation of the required filter size is given by

$$\text{Filter Volume} = \frac{\text{Flow rate} \times \text{wash cycle} \times \text{TSS concentration}}{\text{TSS density} \times \text{maximum media capacity}}.$$

Cost estimation for gravity filtration is based on equations shown in Table 3-19.

Table 3-18: Input parameters for gravity filtration system design in this report.

Description	Value	Unit
Temperature	77.00	^{o}F
Wash Cycle	24	Hr
TSS Density	35	g/L
Medium Depth	1	m
Maximum Medium Capacity	110	L-TSS/m^3
Tank Depth	1.3	m
Backwash Duration	6	min

Table 3-19: Cost equations for gravity filtration unit in WaTER.

Gravity Filter	DCC (US$)	$35{,}483.47\ X^{0.591}\ e^{13.62\ E\text{-}4\ X}$
	O&M (US$)	$359.5\ X^{0.8568} + 8{,}100$
Backwashing	DCC (US$)	$36{,}000 + 1{,}254.21\ X - 0.1212\ X^2$
	O&M (US$)	$73.3\ X^{0.75} + 2{,}200$
X = media surface area (m^2)		

3.2.2.6 Walnut shell filtration and organoclay adsorption

A walnut shell medium filter effectively removes oil while an organoclay medium removes a wide range of hydrocarbons and trace amounts of heavy metals. In practice, walnut shell and organoclay filters are installed in fixed bed units. The costs of vessels and backwashing systems for these media are similar to those for an ion exchange vessel.

Absolute Filtration, Inc, the manufacturer of the HYDROFLOW walnut shell filtration system, suggested a 550.1 liter per minute per square meter (13.5 gpm/ft^2) flow rate for produced water. The fixed bed unit is composed of a vessel and a backwashing system. The costs for six HYDROFLOW Model 1767 filters (5 running + 1 standby) having 7.3 m (24 ft) diameters are considered in this design. Walnut shell medium fills 60% of the tank volume to accommodate media rise during backwashing. The walnut shell bulk price was obtained from Eco-Shell, Inc.'s website (Absolute Filtration).

Ecologix MCM-830P Pure OrganoClay, an organoclay filter manufacturer, suggested a 6.6 min Empty Bed Contact Time (EBCT) (Ecologix). Similar to the walnut shell vessels, only 60% of the filter volume is filled with organoclay to provide for rise of the medium during backflushing. Cost estimations for both units were done in WaTER by using the equations shown in Table 3-20.

<u>Walnut shell filtration</u>

Filtration rate of walnut shell filter = 13.5 gpm/ft^2

Required Vessel Area = $\frac{\text{Flow Rate}}{\text{Filtration rate}}$

Ratio of height to diameter heuristically = 2

Diameter of vessel = $(4 \times \text{Area} / 3.14)^{0.5}$

Height = 2 × Diameter

Volume of vessel = $\frac{3.14 \times \text{Diameter}^2 \times \text{Height}}{4}$

Medium Volume = 0.6 * Volume of Vessel (to accommodate media rise during backwashing)

<u>Organoclay adsorption</u>

Detention time $t_{\text{organo-clay}}$ = 6.6 minutes

Vessel volume = $t_{\text{organo-clay}}$ * Flow Rate

Media Volume = 0.6 * Volume of Vessel

Table 3-20: Cost estimation equations for walnut shell and organoclay filtration units.

Vessel	
DCC (US$)	$\$ = 10^{3.44609 + (0.561757 \log(X))}$
O&M (US$)	Total media volume × media price
Backwashing	
DCC (US$)	$\$ = 36{,}000+1{,}254.21\ Y - 0.1212\ Y^2$
O&M (US$)	$\$ = 73.3\ Y^{0.75}+2{,}200$
X	Vessel volume (m^3)
Y	Bed Area m^2

3.2.2.7 Granular activated carbon (GAC) adsorption

GAC adsorption is a process for removing organic contaminants. The estimated capital and O&M costs include the backwashing system. GAC can be periodically regenerated. The WaTER model provides GAC cost-capacity equations for three different bed lives— 3, 6 and 12 months. Considering the high salinity of the produced water, a concrete contactor and IR reactivation system were considered in order to prevent corrosion. Cost estimation information is summarized in Table 3-21 and Table 3-22. The cost information was based on the 1984 ENR CCI of 4,131, hence it was updated to the 2010 ENR CCI = 8,671. Each unit was designed to have 15-minute empty bed contact time (EBCT), 3.4-3.7 m (11-12 ft) bed depth, and onsite GAC reactivation four times per year.

As provided in Clark and Lykins (1989), the total DCC was attained by converting the amortized capital cost into its present value. Annual O&M cost can be obtained by subtracting the amortized capital cost from the total annual cost. The capital cost of the contactor includes contactor construction, site works, pumps and valves, virgin GAC storage construction, and purchase of the initial quantity of GAC. The DCC of the onsite reactivation unit includes site work, furnace and spare part purchases, and transport facility construction.

$$\text{Total Capital Cost of GAC} = \text{Amortized Capital Cost} \times \left[1 - \frac{1}{(1+i)^n}\right]$$

where (i) = 10% for GAC, (Clark and Lykins, 1989) and
Annual O&M cost = Total Annual Cost – Amortized Capital Cost.

Table 3-21: Annual Cost of Concrete Contactor.

	Annual Cost (US$/yr)		
Plant Capacity (MGD)	**1**	**5**	**10**
Electricity	2,903	9,138	16,549
Maintenance	1,166	3,202	5,252
O&M Labor	8,006	12,234	16,900
Labor overhead	6,437	11,335	16,994
Labor for GAC transfer	576	2,879	5,759
Cooling Water	167	835	1,671
Amortized Capital	57,979	120,418	234,872
Total Annual Cost	77,234	160,041	297,997

Table 3-22: Annual Cost of Onsite Infrared Reactivation.

	Annual Cost (US$/yr)	
Plant Capacity (MGD)	**5**	**10**
Electricity	48,816	94,424
Maintenance	11,236	14,797
O&M Labor	90,811	134,944
Labor overhead	68,108	101,208
Process water	8,771	17,542
Make Up GAC	151,233	288,740
Amortized Capital	68,423	86,930
Total Annual Cost	447,398	738,585

3.2.2.8 Wash water surge basin & filter waste wash water storage tank

In large capacity plants, surge basins and storage tanks are required. Filter wash water is stored in a surge basin before being pumped to backwash the filters. The waste of this filter wash water will be temporarily contained in some storage units which normally are twice the volume of the surge basin. Cost estimations for these two units can be approximated by utilizing two equations listed in Table 3-23 obtained from cost estimation manual. Due to the lack of information; O&M for these units is neglected.

Table 3-23: DCC equation for wash water surge basin and waste wash water storage in Cost Estimation Manual.

Description	Amount
Basin Cost	87.811 × (basin capacity in gal)$^{0.7505}$
Tank Cost	4.1619 × (storage volume in gal)$^{0.8473}$

Volume of Wash Water Surge Basin (gal) = 1,666.7 × (Plant Capacity (MGD)) + 73,333.33
Volume of Wash Water Storage Tank (gal) = 2× Volume of Wash Water Surge Basin

3.2.2.9 Reverse osmosis (RO)

RO was selected for use in treating waters with TDS concentrations less than 55,000 mg/L. Cost estimation for the RO unit was performed with the WaTER model. Cost estimation details of the various components of the process can be found in the WaTER manual (Wilbert et al., 1999); the manual includes the RO cost estimation information provided in Suratt (1991). The RO system considered in our design consists of two stages. Feed water quality determines the maximum water recovery achievable with RO. For CBM water, with 25,000 mg/L TDS, and coal mine water, with 18,000 mg/L TDS, the recovery rates were assumed to be 50% and 75%, respectively. For our estimation, FilmTec BW30-400 membranes supplied by Dow were used for desalination.

3.2.2.10 Distillation

Distillation was selected for the desalination of produced waters with TDS concentration greater than 55,000 mg/L. The most common distillation techniques used in treatment plants are Multi Stage Flash (MSF) and Multi Effect Distillation (MED).

Water recovery rates for distillation units depend on the dissolved salt solubility in water. We assume that the maximum salt concentration cannot exceed 370 g/L. The water recovery rate in distillation is calculated using

$$\text{water recovery} = \frac{\text{volume flow rate of recovered water}}{\text{Feed flow rate}}.$$

The Cost Estimation Manual Excel model (McGivney and Kawamura, 2008) was used to estimate distillation costs. Table 3-24 and Table 3-25 provide the capital and O&M costs for MSF and MED, respectively.

Table 3-24: MSF distillation-related costs obtained from McGivney and Kawamura (2008).

Description	Equation
DCC (million US$)	$32.28\ X^{0.6739}$
O&M Cost (million US$)	$1.8653\ X^{0.9808}$
X	feed flow rate (MGD)

Table 3-25: MED distillation-related costs obtained from McGivney and Kawamura (2008).

Description	Equation
DCC (million US$)	$23\ X^{0.6097}$
O&M Cost (million US$)	$1.2576\ X^{1.0549}$
X	feed flow rate (MGD)

3.2.2.11 Crystallizer

Crystallizers are commonly used in zero liquid discharge (ZLD) processes. The cost was estimated based on information in publications by Lozier et al. (2006) and Genck (2004). Lozier et al. (2006) reported that the crystallizer studied in their work required 250-300 kWh per 3.8 cubic meters (1,000 gallons) of water. Due to limited cost estimation information, the O&M cost for these units was assumed to consist of only electricity cost at a rate of US$ 0.07/kwh. Crystallizer cost estimation calculations are summarized below.

<u>Direct Capital Cost</u>

20 ton/d LiCl costs US$ 800,000 of crystallizer.

$$\frac{US\$\,800{,}000}{DCC_b} = \left(\frac{20\ ton/d}{Q_b}\right)^{0.65}$$

Q_b (ton/d) = TDS concentration * Flow Rate

$$\textit{Crystallizer O\&M cost} = \text{Flow Rate (gal/d)}\ \frac{365\,\text{day}}{year}\ \frac{300kwh}{1000gall}\ Electricity\ Rate$$

3.2.2.12 Clear water storage

Clear water storage provides a buffer between the output of the water treatment plant and the distribution system demand. This unit is a large cast-in-place concrete structure covered by a concrete roof with interior supporting columns. The cost equation for this unit given by McGivney and Kawamura (2008) is

DCC = 444,448 X + 158,177

where X is the water storage capacity (MG). Water storage capacity (MG) =0.07 x Plant Capacity (MGD) + 1.

3.2.2.13 Disposal

Brine disposal cost was considered for non-ZLD cases. The commonly used on-site disposal methods include underground injection, land spreading or other land treatment, evaporation, surface discharge, and recycling. In the Illinois Basin, most oil field wastes are disposed of on-site through injection into Class II disposal wells (Veil, 1997). Brine disposal cost in Kentucky is reported as $1/bbl (Veil, 1997). Based on our recent communications with oil companies in Illinois, the current typical cost of brine disposal is 0.10 - 1.25 $/bbl (personal communications). For this project, brine disposal cost was assumed to be $1/bbl.

3.2.3 Treatment cost estimates for produced water

The initial composition and intended end use of produced water determine the treatment processes to be used. Costs including capital, operations and maintenance, and power costs, have been calculated for a range of proposed treatment processes.

Process flow diagrams were developed for nine case studies in order to estimate the costs of treating produced water from several sources. These nine scenarios included three different types of produced water sources: CBM, CO_2-EOR (oilfield), and coal mine water, and two different flow rates (1,893 and 18,930 cubic meters per day (0.5 and 5 mgd)). In each scenario, combinations of different core treatments including Reverse Osmosis (RO), Multiple Effect Distillation (MED), Multi Stage Flash distillation (MSF), and crystallization (for zero liquid discharge, ZLD) were considered.

Process flow diagrams (PFDs) for produced water treatment, developed using Microsoft Office software, are shown in Figure 3-3 and Figure 3-4. The PFDs for produced water treatment for produced water from CBM projects and coal mines are the same (Figure 3-3) because of their similar water qualities. The PFD for produced water from oilfields (Figure 3-4) is similar, but includes additional pretreatment stages (walnut shell filtration and organoclay adsorption) for the removal of colloidal and dissolved hydrocarbons. Stream specifications for Figure 3-3, for different water treatment scenarios for ACT (CBM) and Galatia (coal mine) produced water are tabulated in Table 3-26 and Table 3-27, respectively. For each produced water, a total of ten treatment scenarios were considered: RO (only), MSF (only), RO&MSF, MED (only), RO&MED; all with and without the crystallizer unit. The variable 'X' in Table 3-26 and Table 3-27 represents the produced water flow rate and was assumed to be either 1,893 or 18,930 cubic meters per day (0.5 or 5, mgd) for cost estimation calculations. The parameters R_{ro}, R_d, and R_c represent water recovery ratios for RO, MED/MSF distillation, and crystallizer units, respectively. These ratios are defined as the ratio of the flow rate of purified water from the unit to the flow rate of the water being fed to the unit.

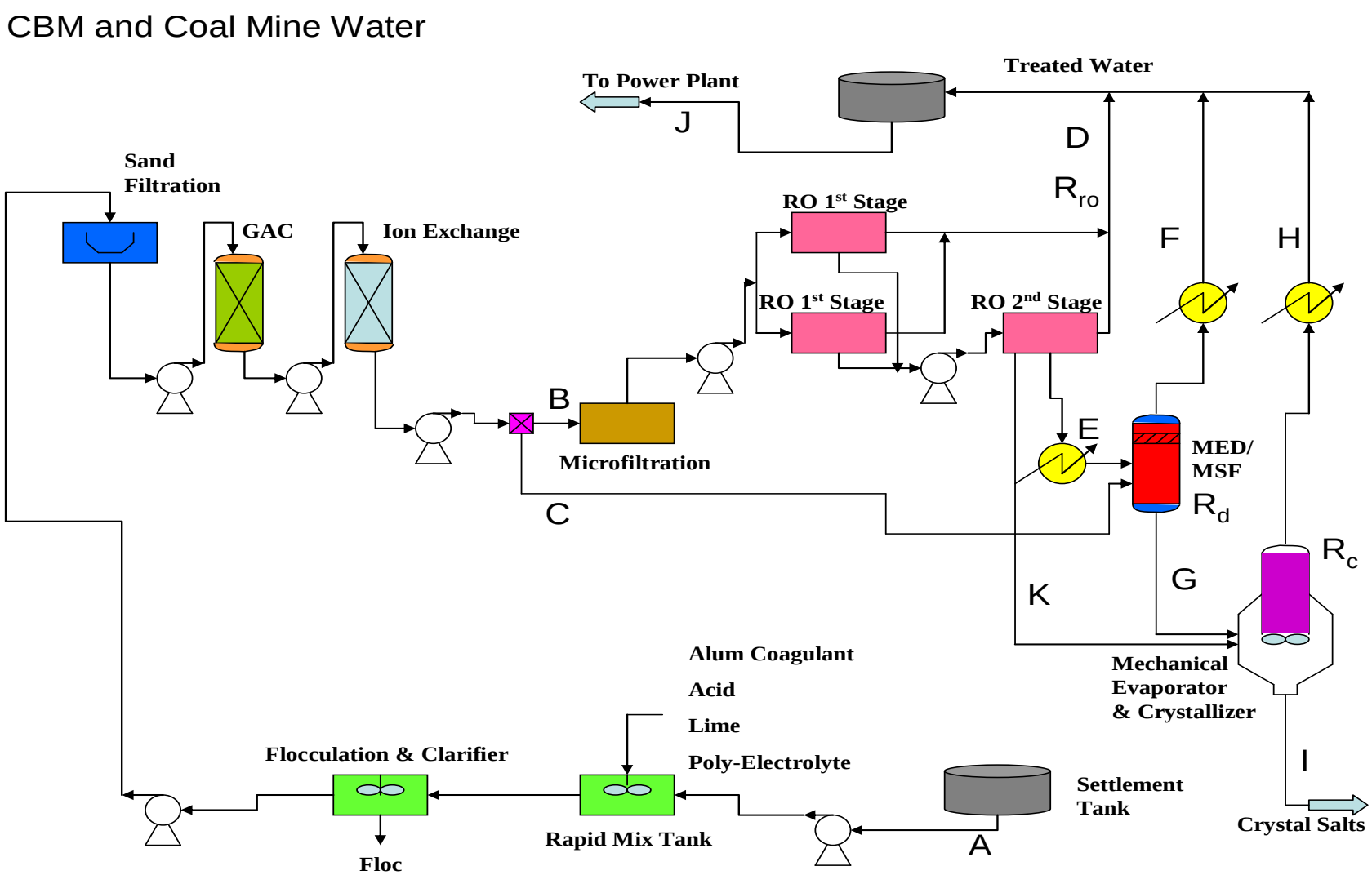

Figure 3-3: Conceptual process flow diagram (PFD) for treating produced water from CBM and coal mines.

Table 3-26: Stream specifications for Figure 3-3, for different water treatment scenarios of ACT (CBM) produced water. A total of ten treatment scenarios were considered: RO (only), MSF (only), RO&MSF, MED (only), RO&MED; all with and without crystallizer unit.

CBM

RO only (with crystallizer)			**RO only (without crystallizer)**	
Rro (overall): 50%, Rd: 0, Rc: 90%			**Rro (overall): 50%, Rd: 0, Rc: 0**	
Stream	Flow Rate	TDS (ppm)	Flow Rate	TDS (ppm)
A	X mgd	25000	X mgd	25000
B	X mgd	25000	X mgd	25000
C	0	0	0	0
D	0.5X mgd	0	0.5X mgd	0
E	0	0	0	0
F	0	0	0	0
G	0	0	0	0
H	0.45X mgd	0	0	0
I	94.625X ton/d	0	0	0
J	0.95X mgd	0	0.5X mgd	0
K	0.5X mgd	50000	0.5X mgd	50000

Multi-stage Flash Distillation only (with crystallizer)			**Multi-stage Flash Distillation only (without crystallizer)**		**Multi-effect Distillation only (with crystallizer)**		**Multi-effect Distillation only (without crystallizer)**	
Rro (overall): 0, Rd: 91%, Rc: 90%			**Rro (overall): 0, Rd: 91%, Rc: 0**		**Rro (overall): 0, Rd: 91%, Rc: 90%**		**Rro (overall): 0, Rd: 91%, Rc: 0**	
Stream	Flow Rate	TDS (ppm)	Flow Rate	TDS (ppm)	Flow Rate	TDS (ppm)	Flow Rate	TDS (ppm)
A	X mgd	25000	X mgd	25000	X mgd	25000	X mgd	25000
B	0	0	0	0	0	0	0	0
C	X mgd	25000	X mgd	25000	X mgd	25000	X mgd	25000
D	0	0	0	0	0	0	0	0
E	0	0	0	0	0	0	0	0
F	0.91X mgd	0	0.91X mgd	0	0.91X mgd	0	0.91X mgd	0
G	0.09X mgd	277777	0.09X mgd	277777	0.09X mgd	277777	0.09X mgd	277777
H	0.081X mgd	0	0	0	0.081X mgd	0	0	0
I	94.525X ton/d	0	0	0	94.525X ton/d	0	0	0
J	0.991X mgd	0	0.91X mgd	0	0.991X mgd	0	0.91X mgd	0
K	0	0	0	0	0	0	0	0

Multi-stage Flash Distillation after RO (with crystallizer)			**Multi-stage Flash Distillation after RO (without crystallizer)**		**Multi-effect Distillation after RO (with crystallizer)**		**Multi-effect Distillation after RO (without crytallizer)**	
Rro (overall): 50%, Rd: 81.5%, Rc: 90%			**Rro (overall): 50%, Rd: 81.5%, Rc: 0**		**Rro (overall): 50%, Rd: 81.5%, Rc: 90%**		**Rro (overall): 50%, Rd: 81.5%, Rc: 0**	
Stream	Flow Rate	TDS (ppm)	Flow Rate	TDS (ppm)	Flow Rate	TDS (ppm)	Flow Rate	TDS (ppm)
A	X mgd	25000	X mgd	25000	X mgd	25000	X mgd	25000
B	X mgd	25000	X mgd	25000	X mgd	25000	X mgd	25000
C	0	0	0	0	0	0	0	0
D	0.5X mgd	0	0.5X mgd	0	0.5X mgd	0	0.5X mgd	0
E	0.5X mgd	50000	0.5X mgd	50000	0.5X mgd	50000	0.5X mgd	50000
F	0.407X mgd	0	0.407X mgd	0	0.407X mgd	0	0.407X mgd	0
G	0.093X mgd	268817	0.093X mgd	268817	0.093X mgd	268817	0.093X mgd	268817
H	0.0837X mgd	0	0	0	0.0837X mgd	0	0	0
I	94.625X ton/d	0	0	0	94.625X ton/d	0	0	0
J	0.9907X mgd	0	0.907X mgd	0	0.9907X mgd	0	0.907X mgd	0
K	0	0	0	0	0	0	0	0

Table 3-27: Stream specifications for water treatment scenarios for Galatia (coal mine) produced water. A total of ten treatment scenarios were considered: RO (only), MSF (only), RO&MSF, MED (only), RO&MED; all with and without crystallizer unit.

Coal Mine

RO only (with crystallizer)			RO only (without crystallizer)	
Rro (overall): 50%, Rd: 0, Rc: 90%			**Rro (overall): 50%, Rd: 0, Rc: 0**	
Stream	Flow Rate	TDS (ppm)	Flow Rate	TDS (ppm)
A	X mgd	17982	X mgd	17982
B	X mgd	17982	X mgd	17982
C	0	0	0	0
D	0.75X mgd	0	0.75X mgd	0
E	0	0	0	0
F	0	0	0	0
G	0	0	0	0
H	0.225X mgd	0	0	0
I	68.06X ton/d	0	0	0
J	0.975X mgd	0	0.75X mgd	0
K	0.25X mgd	71928	0.25X mgd	71928

Multi-stage Flash Distillation only (with crystallizer)			Multi-stage Flash Distillation only (without crystallizer)		Multi-effect Distillation only (with crystallizer)		Multi-effect Distillation only (without crystallizer)	
Rro (overall): 0, Rd: 93%, Rc: 90%			**Rro (overall): 0, Rd: 93%, Rc: 0**		**Rro (overall): 0, Rd: 93%, Rc: 90%**		**Rro (overall): 0, Rd: 93%, Rc: 0**	
Stream	Flow Rate	TDS (ppm)	Flow Rate	TDS (ppm)	Flow Rate	TDS (ppm)	Flow Rate	TDS (ppm)
A	X mgd	17982	X mgd	17982	X mgd	17982	X mgd	17982
B	0	0	0	0	0	0	0	0
C	X mgd	17982	X mgd	17982	X mgd	17982	X mgd	17982
D	0	0	0	0	0	0	0	0
E	0	0	0	0	0	0	0	0
F	0.93X mgd	0	0.93X mgd	0	0.93X mgd	0	0.93X mgd	0
G	0.07X mgd	256885	0.07X mgd	256885	0.07X mgd	256885	0.07X mgd	256885
H	0.063X mgd	0	0	0	0.063X mgd	0	0	0
I	68.06X ton/d	0	0	0	68.06X ton/d	0	0	0
J	0.993X mgd	0	0.93X mgd	0	0.993X mgd	0	0.93X mgd	0
K	0	0	0	0	0	0	0	0

Multi-stage Flash Distillation after RO (with crystallizer)			Multi-stage Flash Distillation after RO (without crystallizer)		Multi-effect Distillation after RO (with crystallizer)		Multi-effect Distillation after RO (without crystallizer)	
Rro (overall): 75%, Rd: 73%, Rc: 90%			**Rro (overall): 75%, Rd: 73%, Rc: 0**		**Rro (overall): 75%, Rd: 73%, Rc: 90%**		**Rro (overall): 75%, Rd: 73%, Rc: 0**	
Stream	Flow Rate	TDS (ppm)	Flow Rate	TDS (ppm)	Flow Rate	TDS (ppm)	Flow Rate	TDS (ppm)
A	X mgd	17982	X mgd	17982	X mgd	17982	X mgd	17982
B	X mgd	17982	X mgd	17982	X mgd	17982	X mgd	17982
C	0	0	0	0	0	0	0	0
D	0.75X mgd	0	0.75X mgd	0	0.75X mgd	0	0.75X mgd	0
E	0.25X mgd	71928	0.25X mgd	71928	0.25X mgd	71928	0.25X mgd	71928
F	0.1825X mgd	0	0.1825X mgd	0	0.1825X mgd	0	0.1825X mgd	0
G	0.0675X mgd	266400	0.0675X mgd	266400	0.0675X mgd	266400	0.0675X mgd	266400
H	0.06075X mgd	0	0	0	0.06075X mgd	0	0	0
I	68.06X ton/d	0	0	0	68.06X ton/d	0	0	0
J	0.993X mgd	0	0.9325X mgd	0	0.993X mgd	0	0.9325X mgd	0
K	0	0	0	0	0	0	0	0

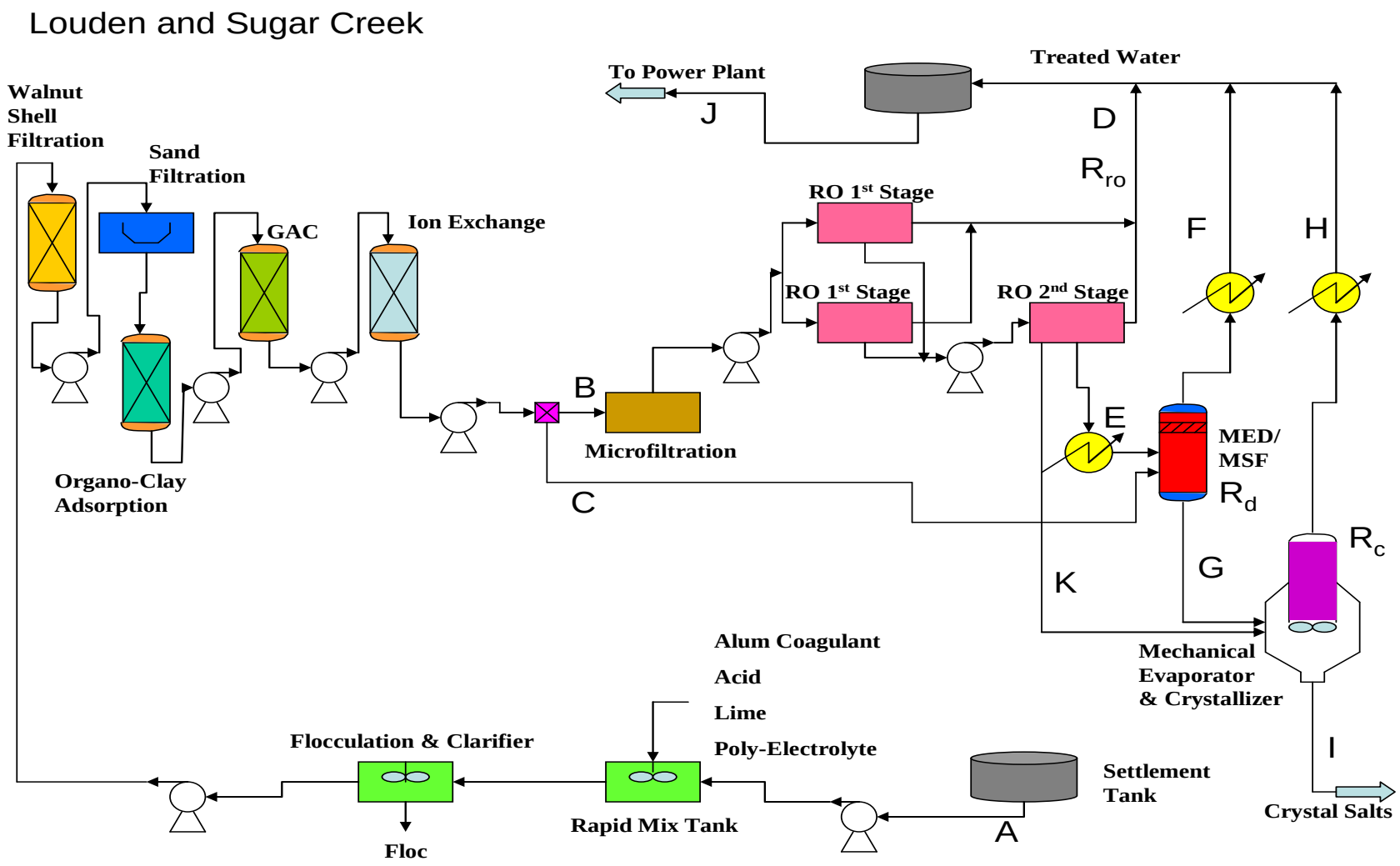

Figure 3-4: Conceptual process flow diagram for treating produced water from oilfields (Louden and Sugar Creek).

Table 3-28: Stream specifications for Figure 3-4, for different water treatment scenarios of Louden (oilfield) produced water. A total of four treatment scenarios were considered: MSF (only), MED (only); both with and without crystallizer unit.

Louden Oilfield

Multi-stage Flash Distillation only (with crystallizer)			**Multi-stage Flash Distillation only (without crystallizer)**		**Multi-effect Distillation only (with crystallizer)**		**Multi-effect Distillation only (without crystallizer)**	
Rro (overall): 0, Rd: 62%, Rc: 90%			**Rro (overall): 0, Rd: 62%, Rc: 0**		**Rro (overall): 0, Rd: 62%, Rc: 90%**		**Rro (overall): 0, Rd: 62%, Rc: 0**	
Stream	Flow Rate	TDS (ppm)	Flow Rate	TDS (ppm)	Flow Rate	TDS (ppm)	Flow Rate	TDS (ppm)
A	X mgd	101734	X mgd	101734	X mgd	101734	X mgd	101734
B	0	0	0	0	0	0	0	0
C	X mgd	101734	X mgd	101734	X mgd	101734	X mgd	101734
D	0	0	0	0	0	0	0	0
E	0	0	0	0	0	0	0	0
F	0.622X mgd	0	0.622X mgd	0	0.622X mgd	0	0.622X mgd	0
G	0.378X mgd	269138	0.378X mgd	269138	0.378X mgd	269138	0.378X mgd	269138
H	0.3402X mgd	0	0	0	0.3402X mgd	0	0	0
I	385X ton/d	0	0	0	385X ton/d	0	0	0
J	0.9622X mgd	0	0.622X mgd	0	0.9622X mgd	0	0.622X mgd	0
K	0	0	0	0	0	0	0	0

Table 3-29: Stream specifications for Sugar Creek (oilfield) produced water. A total of ten treatment scenarios are considered: RO (only), MSF (only), RO&MSF, MED (only), RO&MED; all with and without crystallizer unit.

Sugar Creek Oilfield

RO only (with crystallizer)			RO only (without crystallizer)	
Rro (overall): 50%, Rd: 0, Rc: 90%			Rro (overall): 50%, Rd: 0, Rc: 0	
Stream	Flow Rate	TDS (ppm)	Flow Rate	TDS (ppm)
A	X mgd	25317	X mgd	25317
B	X mgd	25317	X mgd	25317
C	0	0	0	0
D	0.5X mgd	0	0.5X mgd	0
E	0	0	0	0
F	0	0	0	0
G	0	0	0	0
H	0.45X mgd	0	0	0
I	95.8X ton/d	0	0	0
J	0.95X mgd	0	0.5X mgd	0
K	0.5X mgd	50634	0.5X mgd	50634

Multi-stage Flash Distillation only (with crystallizer)			Multi-stage Flash Distillation only (without crystallizer)		Multi-effect Distillation only (with crystallizer)		Multi-effect Distillation only (without crystallizer)	
Rro (overall): 0, Rd: 91%, Rc: 90%			Rro (overall): 0, Rd: 91%, Rc: 0		Rro (overall): 0, Rd: 91%, Rc: 90%		Rro (overall): 0, Rd: 91%, Rc: 0	
Stream	Flow Rate	TDS (ppm)	Flow Rate	TDS (ppm)	Flow Rate	TDS (ppm)	Flow Rate	TDS (ppm)
A	X mgd	25317	X mgd	25317	X mgd	25317	X mgd	25317
B	0	0	0	0	0	0	0	0
C	X mgd	25317	X mgd	25317	X mgd	25317	X mgd	25317
D	0	0	0	0	0	0	0	0
E	0	0	0	0	0	0	0	0
F	0.91X mgd	0	0.91X mgd	0	0.91X mgd	0	0.91X mgd	0
G	0.09X mgd	269789	0.09X mgd	269789	0.09X mgd	269789	0.09X mgd	269789
H	0.081X mgd	0	0	0	0.081X mgd	0	0	0
I	95.8X ton/d	0	0	0	95.8X ton/d	0	0	0
J	0.991X mgd	0	0.91X mgd	0	0.991X mgd	0	0.91X mgd	0
K	0	0	0	0	0	0	0	0

Multi-stage Flash Distillation after RO (with crystallizer)			Multi-stage Flash Distillation after RO (without crystallizer)		Multi-effect Distillation after RO (with crystallizer)		Multi-effect Distillation after RO (without crystallizer)	
Rro (overall): 50%, Rd: 82%, Rc: 90%			Rro (overall): 50%, Rd: 82%, Rc: 0		Rro (overall): 50%, Rd: 82%, Rc: 90%		Rro (overall): 50%, Rd: 82%, Rc: 0	
Stream	Flow Rate	TDS (ppm)	Flow Rate	TDS (ppm)	Flow Rate	TDS (ppm)	Flow Rate	TDS (ppm)
A	X mgd	25317	X mgd	25317	X mgd	25317	X mgd	25317
B	X mgd	25317	X mgd	25317	X mgd	25317	X mgd	25317
C	0	0	0	0	0	0	0	0
D	0.5X mgd	0	0.5X mgd	0	0.5X mgd	0	0.5X mgd	0
E	0.5X mgd	50634	0.5X mgd	50634	0.5X mgd	50634	0.5X mgd	50634
F	0.41X mgd	0	0.41X mgd	0	0.41X mgd	0	0.41X mgd	0
G	0.09X mgd	269945	0.09X mgd	269945	0.09X mgd	269945	0.09X mgd	269945
H	0.081X mgd	0	0	0	0.081X mgd	0	0	0
I	95.8X ton/d	0	0	0	95.8X ton/d	0	0	0
J	0.993X mgd	0	0.91X mgd	0	0.993X mgd	0	0.91X mgd	0
K	0	0	0	0	0	0	0	0

Total costs of the produced water treatment processes for different scenarios were determined for 1,893 and 18,930 cubic meters per day (0.5 and 5 MGD) flow rates from each produced water source. Direct capital, total capital, and O&M cost components for the ACT-CBM 1,893 cubic meters per day (0.5 MGD) cases are shown in Table 3-30 - Table 3-32, respectively. The total costs of the 10 produced water treatment schemes ($/3.8 cubic meters ($/1000 gal)) were calculated from the annual capital recovery; O&M, and waste disposal costs and are summarized in Table 3-33. The cost fraction of each water treatment unit was also calculated and is shown in Table 3-34. Cost estimation details of other cases are not shown due to space limitations. However, cost estimation results of all produced water types are presented and compared graphically at the end of this section.

For the ACT 1,893 cubic meters per day (0.5 MGD) cases, pretreatment units account for 18-34% of the total cost. For RO cases, the cost of the RO unit accounts for only 6-12% of the total cost, while the distillation-based units account for 32-73% of the total cost. The cost percentage of the crystallizer and brine disposal units varies in the range of 7-50% and 5-48% for the ZLD and non-ZLD cases, respectively (Table 3-34).

Water treatment costs for four types of produced water, with the designed plant input capacities of 1,893 and 18,930 cubic meters per day (0.5 and 5 MGD), without considering the salt sale credit in ZLD processes, are shown in Figure 3-5. The estimated total costs of produced water treatment range from less than $10 (for Galatia coal mine water) to about $70 per 3.8 cubic meters (1000 gallons) of treated water. Louden oilfield produced water was the most costly water to treat due to its high TDS value (≈100,000 mg/L). RO-ZLD was identified as the least expensive process for treating coal mine (Galatia), CBM (ACT), and low-salinity oilfield (SC) produced waters, with estimated costs of $16, $23, and $24 per 3.8 cubic meters (1000 gal) purified water, respectively, for 1,893 cubic meters per day (0.5 MGD) plants. The least expensive process for treating the high-salinity (Louden) oilfield water was the multi-effect distillation (ZLD) process at the estimated cost of $37 per 3.8 cubic meters (1000 gal) purified water (Figure 3-5).

Disposal cost for solid salt from ZLD cases was not included in cost estimations because the salt product might have economic value (e.g., for road deicing applications). Assuming the median cost of NaCl deicers as $42/ton (Kelting and Laxson, 2010), the potential credit for produced salt sale per 3.8 cubic meters (1000 gal) of purified water is ≈$4 for ACT water (TDS ≈25,000 mg/L) with ZLD processes. Considering the potential value of the recovered salt, the cost of produced water treatment with ZLD processes for ACT water could be reduced by about $4 per 3.8 cubic meters (1000 gal) purified water. For Louden produced water, the potential salt sale credit would be $16 per 3.8 cubic meters (1000 gal) purified water. With the assumption of the salt sale credit for the ZLD processes, the cost of produced water treatment for ZLD processes for 1,893 and 18,930 cubic meters per day (0.5 and 5 MGD) cases will be in the ranges of $13-37 and $6-24 per 3.8 cubic meters (1000 gal) purified water, respectively (Figure 3-6).

Produced water treatment with ZLD processes was found to be less expensive than treatment without ZLD, mainly due to high costs for concentrated brine disposal. The cost of brine disposal through underground injection in Class II wells was assumed to be $24 per 3.8 cubic meters (1000 gal).

Produced water treatment costs decrease with produced water flow rate. For all studied cases, the unit costs of produced water treatment for larger plants (5 MGD) are 63 $\pm$ 5% of their smaller counterparts (0.5 MGD). Nevertheless, the smaller capacity of 1,893 cubic meters per day (0.5 MGD) is a more realistic assumption considering current flow rates of produced water in the Illinois Basin.

Table 3-30: Direct capital cost (US$) of produced water treatment (ACT, 0.5 mgd).

Direct Capital Cost (ACT, 0.5 mgd)

Description	Zero Liquid Discharge							Without Crystallizer				
	Unit Construction Cost	RO	Flash	RO & Flash	Distillation	RO & Distillation		RO	Flash	RO & Flash	Distillation	RO & Distillation
Raw Water Pumping	213,088	213,088	213,088	213,088	213,088	213,088		213,088	213,088	213,088	213,088	213,088
Rapid Mix G=900	71,572	71,572	71,572	71,572	71,572	71,572		71,572	71,572	71,572	71,572	71,572
Flocculator G=80	381,640	381,640	381,640	381,640	381,640	381,640		381,640	381,640	381,640	381,640	381,640
Iron Coagulant Feed	137,358	137,358	137,358	137,358	137,358	137,358		137,358	137,358	137,358	137,358	137,358
Polymer Feed	60,099	60,099	60,099	60,099	60,099	60,099		60,099	60,099	60,099	60,099	60,099
Lime and Soda Ash Feed	233,270	233,270	233,270	233,270	233,270	233,270		233,270	233,270	233,270	233,270	233,270
Sulfuric Acid Feed - 93% Solution	34,361	34,361	34,361	34,361	34,361	34,361		34,361	34,361	34,361	34,361	34,361
Circular Clarifier (G=110)	255,759	255,759	255,759	255,759	255,759	255,759		255,759	255,759	255,759	255,759	255,759
Gravity Filter Structure +Backwashing	912,907	912,907	912,907	912,907	912,907	912,907		912,907	912,907	912,907	912,907	912,907
Wash Water Surge Basin	823,358	823,358	823,358	823,358	823,358	823,358		823,358	823,358	823,358	823,358	823,358
Wash Water Storage Tank	207,889	207,889	207,889	207,889	207,889	207,889		207,889	207,889	207,889	207,889	207,889
Organo Clay + Backwashing	0	0	0	0	0	0		0	0	0	0	0
Walnut Shell + Backwashing	0	0	0	0	0	0		0	0	0	0	0
GAC Filtration/Adsorption Bed	1,926,753	1,926,753	1,926,753	1,926,753	1,926,753	1,926,753		1,926,753	1,926,753	1,926,753	1,926,753	1,926,753
Antiscalant	60,099	60,099	60,099	60,099	60,099	60,099		60,099	60,099	60,099	60,099	60,099
Reverse Osmosis only	4,224,548	4,224,548	0	4,224,548	0	4,224,548		4,224,548	0	4,224,548	0	4,224,548
Multi-stage Flash Distillation only	41,977,613	0	41,977,613	0	0	0		0	41,977,613	0	0	0
Multi-stage Flash Distillation after RO	26,311,986	0	0	26,311,986	0	0		0	0	26,311,986	0	0
Multi-Effect Distillation only	31,270,741	0	0	0	31,270,741	0		0	0	0	31,270,741	0
Multi-Effect Distillation after RO	20,492,747	0	0	0	0	20,492,747		0	0	0	0	20,492,747
Clear Water Storage	1,282,519	1,282,519	1,282,519	1,282,519	1,282,519	1,282,519		1,282,519	1,282,519	1,282,519	1,282,519	1,282,519
Finished Water Pumping	472,629	472,629	472,629	472,629	472,629	472,629		472,629	472,629	472,629	472,629	472,629
Crystallizer (after RO)	1,399,988	1,399,988	0	0	0	0		0	0	0	0	0
Cyrstallizer (after flash)	1,399,988	0	1,399,988	0	0	0		0	0	0	0	0
Crystallizer (after RO and flash)	1,399,988	0	0	1,399,988	0	0		0	0	0	0	0
Crystallizer (after MED)	1,399,988	0	0	0	1,399,988	0		0	0	0	0	0
Crystallizer (after RO and MED)	1,399,988	0	0	0	0	1,399,988		0	0	0	0	0
Administration, Laboratory, etc.	66,096	66,096	66,096	66,096	66,096	66,096		66,096	66,096	66,096	66,096	66,096
Total direct capital cost		*12,763,933*	*50,516,998*	*39,075,919*	*39,810,126*	*33,256,680*		*11,363,945*	*49,117,010*	*37,675,931*	*38,410,138*	*31,856,692*

Table 3-31: Total capital cost of produced water treatment (US$) (ACT, 0.5 mgd).

	ZLD						Without Crystallizer				
	RO	Flash	RO & Flash	Distillation	RO & Distillation		RO	Flash	RO & Flash	Distillation	RO & Distillation
Total Direct Capital Cost	12,763,933	50,516,998	39,075,919	39,810,126	33,256,680		11,363,945	49,117,010	37,675,931	38,410,138	31,856,692
Freight and Insureance (5%)	638,197	2,525,850	3,907,592	3,981,013	3,325,668		568,197	2,455,851	3,767,593	3,841,014	3,185,669
Interest During Construction 3%	95,729	378,877	293,069	298,576	249,425		85,230	368,378	282,569	288,076	238,925
Construction Overhead 15%	1,933,736	6,971,346	5,509,705	5,613,228	4,838,847		1,721,638	7,072,849	5,425,334	5,531,060	4,635,149
Owner's Direct Expense 10%	1,404,033	4,647,564	3,673,136	3,742,152	3,192,641		1,250,034	4,616,999	3,579,213	3,648,963	3,058,242
Contingencies 10%	1,276,393	5,051,700	3,907,592	3,981,013	3,325,668		1,136,394	4,911,701	3,767,593	3,841,014	3,185,669
Total Depreciating Capital Cost	18,112,020	70,092,335	56,367,012	57,426,107	48,188,930		16,125,438	68,542,788	54,498,234	55,560,265	46,160,347
Working Capital 1/6 of annual cost	509,163	550,931	733,906	433,428	669,058		509,163	550,931	733,906	433,428	669,058
TOTAL CAPITAL COST	18,621,183	70,643,266	57,100,919	57,859,535	48,857,987		16,634,600	69,093,719	55,232,140	55,993,693	46,829,405

Table 3-32: Annual O&M cost of produced water treatment (US$) (ACT, 0.5 mgd).

O&M cost (ACT, 0.5 mgd)

Description		Zero Liquid Discharge						Without Crystallizer				
	Unit O&M Cost	RO	Flash	RO & Flash	Distillation	RO & Distillation		RO	Flash	RO & Flash	Distillation	RO & Distillation
Raw Water Pumping	56,944	56,944	56,944	56,944	56,944	56,944		56,944	56,944	56,944	56,944	56,944
Rapid Mix G=900	16,002	16,002	16,002	16,002	16,002	16,002		16,002	16,002	16,002	16,002	16,002
Flocculator G=80	20,350	20,350	20,350	20,350	20,350	20,350		20,350	20,350	20,350	20,350	20,350
Iron Coagulant Feed	167,934	167,934	167,934	167,934	167,934	167,934		167,934	167,934	167,934	167,934	167,934
Polymer Feed	9,796	9,796	9,796	9,796	9,796	9,796		9,796	9,796	9,796	9,796	9,796
Lime and Soda Ash Feed	142,061	142,061	142,061	142,061	142,061	142,061		142,061	142,061	142,061	142,061	142,061
Sulfuric Acid Feed - 93% Solution	24,734	24,734	24,734	24,734	24,734	24,734		24,734	24,734	24,734	24,734	24,734
Circular Clarifier (G=110)	16,945	16,945	16,945	16,945	16,945	16,945		16,945	16,945	16,945	16,945	16,945
Gravity Filter Structure + Backwashing	48,880	48,880	48,880	48,880	48,880	48,880		48,880	48,880	48,880	48,880	48,880
Filtration Media - Stratified Sand	16,307	16,307	16,307	16,307	16,307	16,307		16,307	16,307	16,307	16,307	16,307
Organo Clay Vessel + Backwashing	0	0	0	0	0	0		0	0	0	0	0
Organo Clay Media	0	0	0	0	0	0		0	0	0	0	0
Walnut Shell Vessel + Backwashing	0	0	0	0	0	0		0	0	0	0	0
Walnut Shell Media	0	0	0	0	0	0		0	0	0	0	0
GAC	410,226	410,226	410,226	410,226	410,226	410,226		410,226	410,226	410,226	410,226	410,226
Antiscalant	9,796	9,796	9,796	9,796	9,796	9,796		9,796	9,796	9,796	9,796	9,796
Reverse Osmosis	149,312	149,312	0	149,312	0	149,312		149,312	0	149,312	0	149,312
Multi-stage Flash Distillation	1,960,861	0	1,960,861	0	0	0		0	1,960,861	0	0	0
Multi-stage Flash Distillation after RO	993,566	0	0	993,566	0	0		0	0	993,566	0	0
Multi-Effect Distillation	1,255,840	0	0	0	1,255,840	0		0	0	0	1,255,840	0
Multi-Effect Distillation after RO	604,474	0	0	0	0	604,474		0	0	0	0	604,474
Clear Water Storage	0	0	0	0	0	0		0	0	0	0	0
Finished Water Pumping	49,648	49,648	49,648	49,648	49,648	49,648		49,648	49,648	49,648	49,648	49,648
Crystallizer (after RO)	1,916,042	1,916,042	0	0	0	0		0	0	0	0	0
Crystallizer (after flash)	355,106	0	355,106	0	0	0		0	0	0	0	0
Crystallizer (after RO and flash)	2,270,939	0	0	2,270,939	0	0		0	0	0	0	0
Crystallizer (after MED)	355,106	0	0	0	355,106	0		0	0	0	0	0
Crystallizer (after RO and MED)	2,270,939	0	0	0	0	2,270,939		0	0	0	0	0
Disposal Cost (RO)	1,955,357	0	0	0	0	0		1,955,357	0	0	0	0
Disposal Cost (flash)	362,392	0	0	0	0	0		0	362,392	0	0	0
Disposal Cost (RO and flash)	362,179	0	0	0	0	0		0	0	362,179	0	0
Disposal Cost (MED)	362,392	0	0	0	0	0		0	0	0	362,392	0
Disposal Cost (RO and MED)	362,179	0	0	0	0	0		0	0	0	0	362,179
Total O&M cost		*3,054,976*	*3,305,588*	*4,403,439*	*2,600,567*	*4,014,347*		*3,094,291*	*3,312,875*	*2,494,678*	*2,607,854*	*2,105,587*

Table 3-33: Total cost (US$/1000gal) of produced water treatment (ACT 0.5 mgd).

ACT 0.5 MGD					
Zero Liquid Discharge					
Description	RO	Flash	RO & Flash	Distillation	RO & Distillation
Total Capital Cost	18,621,183	70,643,266	57,100,919	57,859,535	48,857,987
Capital Recovery	950,039	3,604,167	2,913,247	2,951,951	2,492,698
Annual Cost	3,054,976	3,305,588	4,403,439	2,600,567	4,014,347
Disposal Cost	0	0	0	0	0
Water Production Cost US$/kgal	*23*	*38*	*40*	*31*	*36*
Without Crystallizer					
Description	RO	Flash	RO & Flash	Distillation	RO & Distillation
Total Capital Cost	16,634,600	69,093,719	55,232,140	55,993,693	46,829,405
Capital Recovery	848,685	3,525,110	2,817,903	2,856,757	2,389,202
Annual Cost	1,138,934	2,950,483	2,132,499	2,245,462	1,743,408
Disposal Cost	1,955,357	362,392	362,179	362,392	362,179
Water Production Cost US$/kgal	*43*	*41*	*32*	*33*	*27*

Table 3-34: Cost fraction of different produced water treatment units (ACT 0.5 mgd).

Description	Zero Liquid Discharge						Without Crystallizer				
	% (RO)	% (Flash)	% (RO&Flash)	% (Distillation)	% (RO&Distillation)		% (RO)	% (Flash)	% (RO&Flash)	% (Distillation	% (RO&Distillation)
Raw Water Pumping	1.82	1.04	1.00	1.31	1.12		1.85	1.05	1.60	1.32	1.92
Rapid Mix G=900	0.53	0.31	0.29	0.38	0.33		0.54	0.31	0.46	0.39	0.55
Flocculator G=80	1.22	0.69	0.67	0.88	0.75		1.30	0.70	0.89	0.89	1.06
Iron Coagulant Feed	4.45	2.57	2.44	3.21	2.74		4.43	2.57	4.20	3.21	5.09
Polymer Feed	0.36	0.20	0.20	0.26	0.22		0.37	0.21	0.30	0.26	0.36
Lime and Soda Ash Feed	3.98	2.30	2.18	2.87	2.45		3.99	2.30	3.67	2.87	4.44
Sulfuric Acid Feed - 93% Solution	0.68	0.39	0.37	0.49	0.42		0.68	0.39	0.63	0.49	0.77
Circular Clarifier (G=110)	0.90	0.51	0.49	0.65	0.56		0.95	0.52	0.68	0.66	0.80
Gravity Filter Structure +Backwashing	2.92	1.65	1.60	2.10	1.80		3.11	1.68	2.14	2.14	2.53
Wash Water Surge Basin	1.53	0.85	0.84	1.10	0.95		1.72	0.87	0.87	1.14	0.99
Wash Water Storage Tank	0.39	0.21	0.21	0.28	0.24		0.43	0.22	0.22	0.29	0.25
Filtration Media - Stratified Sand	0.41	0.24	0.22	0.29	0.25		0.40	0.24	0.39	0.29	0.48
Organo Clay + Backwashing	0.00	0.00	0.00	0.00	0.00		0.00	0.00	0.00	0.00	0.00
Walnut Shell + Backwashing	0.00	0.00	0.00	0.00	0.00		0.00	0.00	0.00	0.00	0.00
Organo Clay Media	0.00	0.00	0.00	0.00	0.00		0.00	0.00	0.00	0.00	0.00
Walnut Shell Media	0.00	0.00	0.00	0.00	0.00		0.00	0.00	0.00	0.00	0.00
GAC Filtration/Adsorption Bed	13.82	7.93	7.57	9.96	8.52		14.13	7.97	11.93	10.03	14.34
Antiscalant	0.36	0.20	0.20	0.26	0.22		0.37	0.21	0.30	0.26	0.36
Reverse Osmosis only	11.58	0.00	6.35	0.00	7.16		12.50	0.00	8.07	0.00	9.45
Multi-stage Flash Distillation only	0.00	71.72	0.00	0.00	0.00		0.00	72.89	0.00	0.00	0.00
Multi-stage Flash Distillation after RO	0.00	0.00	40.39	0.00	0.00		0.00	0.00	51.78	0.00	0.00
Multi-Effect Distillation only	0.00	0.00	0.00	64.38	0.00		0.00	0.00	0.00	65.84	0.00
Multi-Effect Distillation after RO	0.00	0.00	0.00	0.00	32.89		0.00	0.00	0.00	0.00	42.35
Clear Water Storage	2.38	1.32	1.31	1.71	1.48		2.68	1.36	1.36	1.78	1.54
Finished Water Pumping	2.12	1.21	1.16	1.53	1.31		2.21	1.22	1.70	1.55	2.02
Crystallizer (after RO)	50.44	0.00	0.00	0.00	0.00		0.00	0.00	0.00	0.00	0.00
Cyrstallizer (after flash)	0.00	6.58	0.00	0.00	0.00		0.00	0.00	0.00	0.00	0.00
Crystallizer (after RO and flash)	0.00	0.00	32.46	0.00	0.00		0.00	0.00	0.00	0.00	0.00
Crystallizer (after MED)	0.00	0.00	0.00	8.27	0.00		0.00	0.00	0.00	0.00	0.00
Crystallizer (after RO and MED)	0.00	0.00	0.00	0.00	36.51		0.00	0.00	0.00	0.00	0.00
Administration, Laboratory, etc.	0.12	0.07	0.07	0.09	0.08		0.14	0.07	0.07	0.09	0.08
Disposal Cost (RO)	0.00	0.00	0.00	0.00	0.00		48.20	0.00	0.00	0.00	0.00
Disposal Cost (flash)	0.00	0.00	0.00	0.00	0.00		0.00	5.23	0.00	0.00	0.00
Disposal Cost (RO and flash)	0.00	0.00	0.00	0.00	0.00		0.00	0.00	8.74	0.00	0.00
Disposal Cost (MED)	0.00	0.00	0.00	0.00	0.00		0.00	0.00	0.00	6.51	0.00
Disposal Cost (RO and MED)	0.00	0.00	0.00	0.00	0.00		0.00	0.00	0.00	0.00	10.61
	100.00	100.00	100.00	100.00	100.00		100.00	100.00	100.00	100.00	100.00

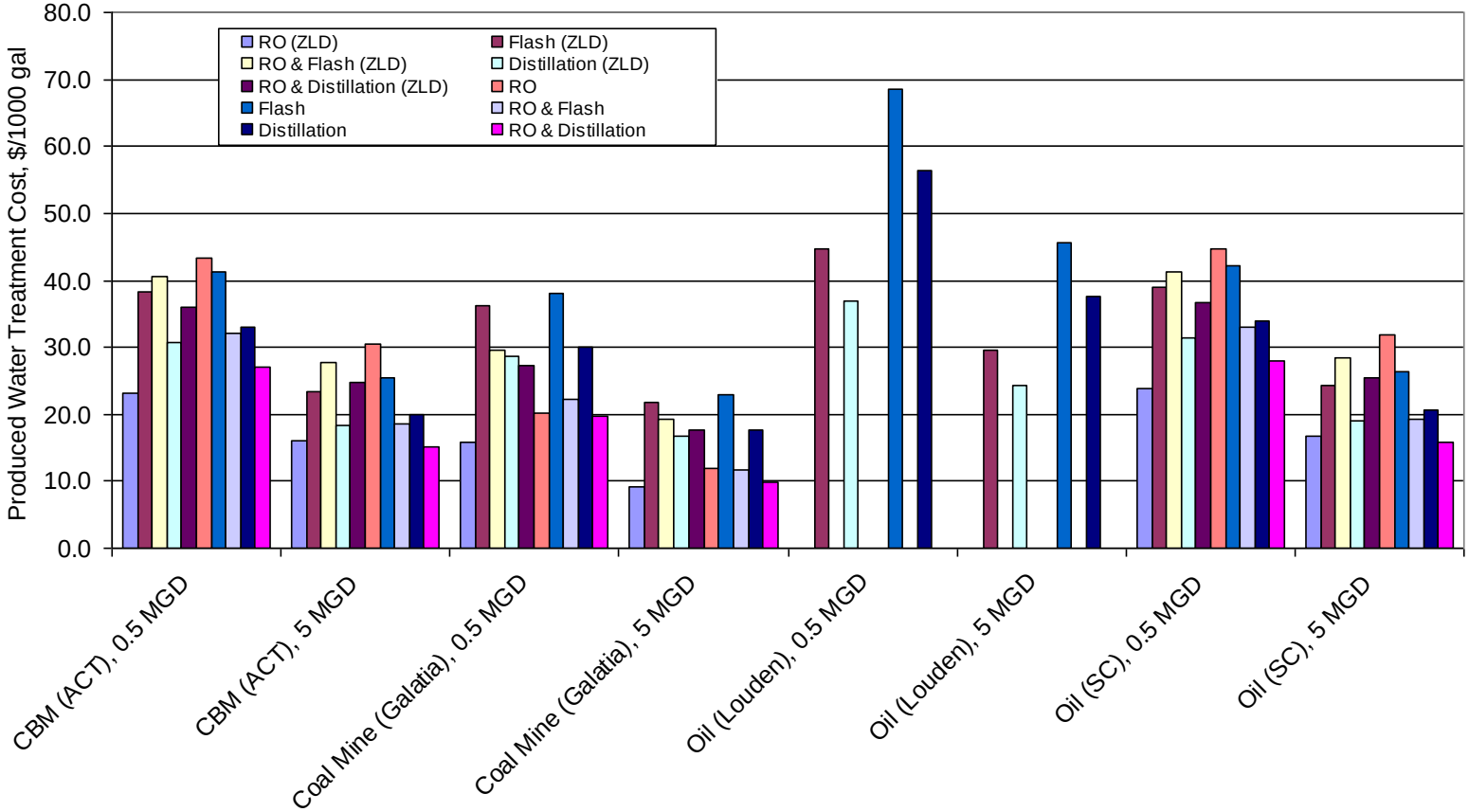

Figure 3-5: Estimated produced water treatment cost of different cases without including the salt sale credit for ZLD processes.

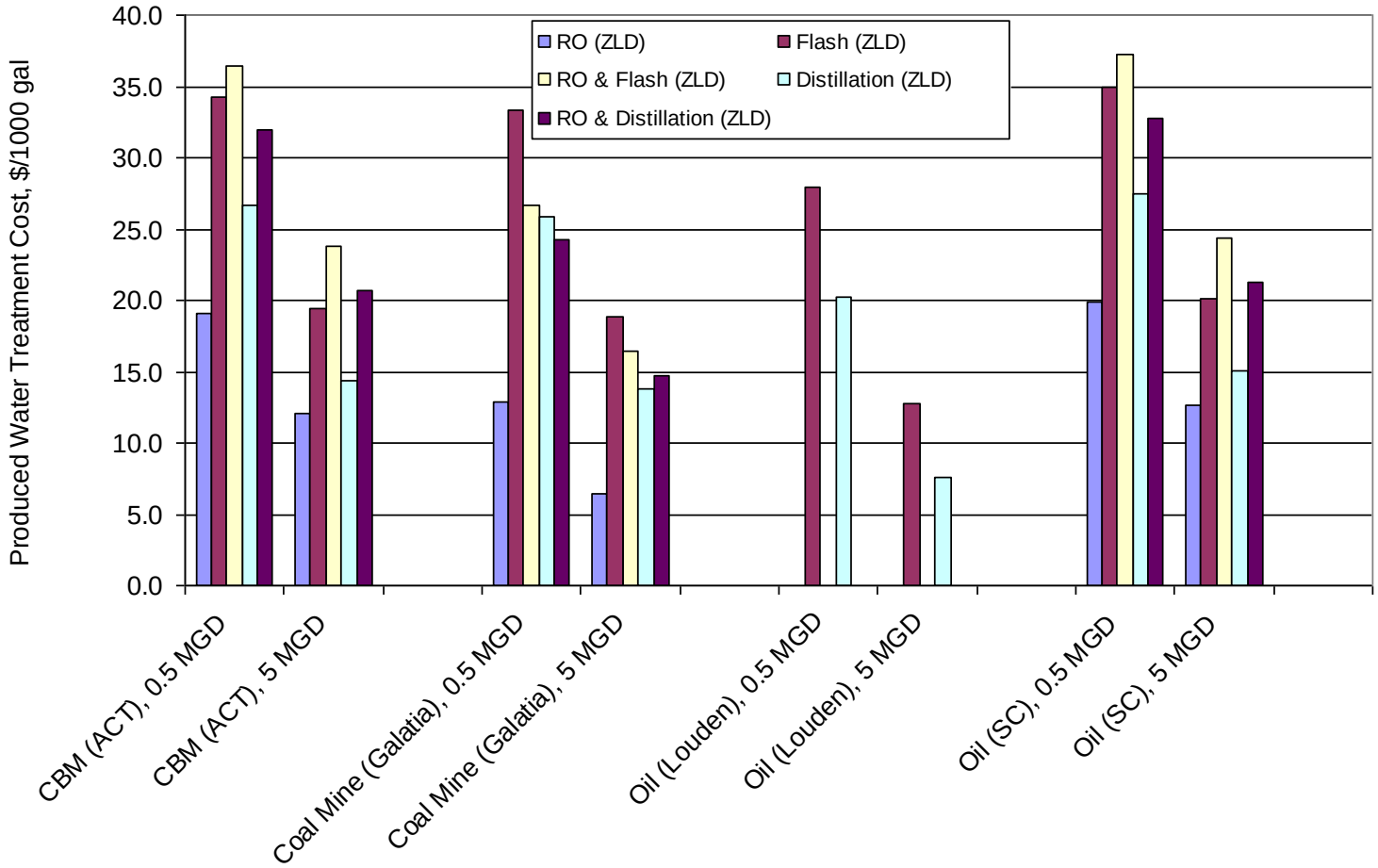

Figure 3-6: Estimated produced water treatment for ZLD processes considering the salt sale credit.

3.2.4 Comparison of costs to literature values

Sandia National Laboratories (SNL) has recently estimated the cost of treating brackish produced water from the Morrison saline formation as $5.32 per 3.8 cubic meters (1000 gallons) of treated water for a 2 MGD output capacity (DOE/NETL, 2009). Our estimated cost for the treatment of Galatia coal mine produced water, is about $9 per 3.8 cubic meters (1000 gal) using RO treatment for an 18,930 cubic meters per day (5 MGD) plant. When ZLD is considered the estimated cost is reduced to $6 per 1000 gal. Our higher estimation, compared to SNL's estimation, might be due to the higher salinity of Galatia coal mine water compared to the salinity of Morrison water (i.e., ≈18,000 ppm vs ≈6,000 ppm) and considering more pretreatment stages (e.g., GAC), higher brine disposal cost, and other differences in cost estimation methodologies.

A USBR/SNL publication estimates the cost of freshwater from conventional treatment plants as $ 0.30-0.40 per 3.8 cubic meters (1000 gal) and the cost of treating brackish water for residential use as $1-3 per 3.8 cubic meters (1000 gal) (USBR/SNL, 2003). The short-term (by year 2015) goal for freshwater conservation in re-circulating cooling systems of thermoelectric power plants is $4.40 per 3.8 cubic meters (1000 gal) water conserved. Our cost estimates for treatment of produced water for a 1,893 cubic meters per day (0.5 MGD) capacity plant range from about $13 to $20 per 3.8 cubic meters (1000 gallons). There will also be significant additional costs for transportation of treated produced water to power plants.

Table 3-35 provides cost estimates of current technologies for treating produced water from coal-bed methane and oil fields (AGV Technologies, 2004). As shown by the large ranges in these figures, costs for treatment of produced water will be very dependent on both the initial composition of the produced water and desired final composition of the output water, based on the criteria for its intended use. .

Table 3-35: Treatment costs of selected current produced water projects (from AGV (2004)).

Technology	Cost $/barrel
CBM Disposal	$0.10 to $1.75
CBM Electro-Dialysis	$0.29 to $1.04
CBM Freeze Crystallization	$0.24 to $1.04
Oil Field Reverse Osmosis	$0.20 to $1.68
Oil Field Distillation	$0.67

Table 3-36 summarizes the reported cost for water treatment unit operations in different processes.

Table 3-36: Cost estimation of representative produced water treatment systems (from Lawrence et al., 1995).

Treatment	Treatment Process System	Cost($/bbl) for a plant with a 354 m^3 per day (65 GPM) flow rate
Deoiling	API	0.0016
	Hydrocyclone	0.0028
	API with Chemical Polymer	0.0908
	Induced Gas Flotation	0.0172
Deoiling and Organic Removal	API and FBR	0.0230
	Hydrocyclone and FBR	0.0202
	API with Chemical Polymer and GAC	0.1517
Deoiling, Iron Removal and Organic Removal	API, Chemical Iron Removal and FBR	0.1286
	Hydrocyclone, Chemical Iron Removal and FBR	0.1289
	API with Chemical Polymer, Chemical Iron Removal and GAC	0.2613
Deoiling Chemical Iron Removal, Organic Removal and Partial Demineralization	API, Chemical Iron Removal, FBR w/sand Filter and Electrodialysis	0.2598
	Hydrocyclone, Chemical Iron Removal, , FBR w/sand Filter and Electrodialysis	0.2610
Organic Removal and Partial Demineralization	FBR w/sand Filter and Electrodialysis	0.1486
	Forced Evaporation	1.11
Deoiling, Organic Removal and Partial Demineralization	API,FBR w/sand Filter and Electrodialysis	0.1503
	Hydrocyclone, FBR w/sand Filter and Electrodialysis	0.1514
Surface Ponds	Oxidative Surface Pond with Setting	0.0529
	Oxidative Surface Pond with Setting and Storage	0.0948

3.3 Treatment options for beneficial use of produced water at power plants

3.3.1 Water quality requirements

The main uses of water at coal-fired power plants include cooling water, boiler water, and flue gas desulfurization (FGD) make-up water. In order to use produced water at a power plant, the quality must meet requirements for these uses.

General cooling water chemistry limits recommended by SPX Cooling Technologies, Inc., one of the largest U.S. suppliers of wet and dry cooling systems for thermoelectric power plants, include the following: Cl^- < 750 mg/L; 6 < pH <8; SO_4^{-2} < 1,200 mg/L. Additional cooling water chemistry limits recommended by Nalco, one of the largest U.S. vendors for cooling system water treatment technologies, include Si concentrations of no more than 200-250 mg/L, and Fe concentrations of no more than 5 mg/L (DOE/NETL, 2009). Table 3-37 shows the recommended water quality requirements to avoid corrosion of the materials typically used in cooling systems at power plants. , Based on these findings, we conclude that a realistic objective for using produced water for cooling make-up water is to achieve a TDS concentration of less than 1000 mg/L after treatment.

Table 3-37: Suggested guidelines for cooling water characteristics to reduce corrosion (from (EPRI, 2008)).

Component material	Chemical Constituent
Stainless steel	Chloride < 1,000 – 1,200 mg/L
Copper alloys	Ammonia < 2 mg/L
	Sulfide < 3 – 5 mg/L
Carbon steel pipe, rebar	TDS < 2,000 – 3,000 mg/L
Concrete	Sulfate < 2,000 – 3,000 mg/L

Water quality requirements for boiler feed water are more constrained than those for cooling water makeup. Maximum allowable concentrations of organic and inorganic species depend on the steam drum pressure. Some specific criteria are listed in Table 3-38. For high pressure conditions, high quality water with a specific conductance of less than 100 μS/cm is suggested. Therefore, if the objective is to use produced water as boiler feed water, treated water must reach a TDS concentration less than 10 mg/L.

Table 3-38: Guidelines for power plant boiler feed water (from (GE, 2010)).

	Drum Operating Pressure, MPa (psig)							
	0-2.07 (0-300)	2.08-3.10 (301-450)	3.11-4.14 (451-600)	4.15-5.17 (601-750)	5.18-6.21 (751-900)	6.22-6.89 (901-1000)	6.90-10.34 (1001-1500)	10.35-10.79 (1501-2000)
FEEDWATER								
Dissolved oxygen (mg/L O_2) measured before oxygen scavenger addition	<0.040	<0.040	<0.007	<0.007	<0.007	<0.007	<0.007	<0.007
Total iron (mg/L Fe)	0.100	0.050	0.030	0.025	0.020	0.020	0.010	0.010
Total Copper (mg/L Cu)	0.050	0.025	0.020	0.020	0.015	0.015	0.010	0.010
Total Hardness (mg/L $CaCO_3$)	0.300	0.300	0.200	0.200	0.100	0.100	--not detectable--	
pH range at 25° C	7.5-10.0	7.5-10.0	7.5-10.0	7.5-10.0	7.5-10.0	8.5-9.5	9.0-9.6	9.0-9.6
Chemicals for preboiler system protection	use only volatile alkaline materials							
Nonvolatile TOC (mg/L C)	<1	<1	<0.5	<0.5	<0.5	--as low as possible, <0.2--	<1	<1
Oily Matter (mg/L)	<1	<1	<0.5	<0.5	<0.5	--as low as possible, <0.2--	<1	<1
BOILER WATER								
Silica (mg/L SiO_2)	150	90	40	30	20	8	2	1
Total alkalinity (mg/L $CaCO_3$)	<350	<300	<250	<200	<150	<100	--not detectable--	
Free Hydroxide alkalinity (mg/L $CaCO_3$)	--not specified--						--not detectable--	
Specific conductance (µS/cm) (µmho/cm at 25° C without neutralization	<3500	<3000	<2500	<2000	<1500	<1000	<150	<100

The water treatment procedures for a produced water will depend both on the quality of the produced water and the treatment objective. For produced water with TDS values less than 60,000 mg/L, membrane desalination is the most cost effective approach. For produced water with larger TDS values, membranes cannot be used for desalination because the required hydraulic pressure would damage the membranes. In that case, thermal desalination methods such as MSF or MED must be used.

The focus of this section is on produced water that may be treated with membranes, which incur the least treatment cost. The baseline produced water for membrane studies is from the ACT-CBM project. Water from ACT has a TDS equal to 19,400 ppm. We show results from the same model for produced water having three different TDS values; TDS equal to ACT, two times this value, and 3 times this value. The permeate TDS values are determined when the maximum recovery is implemented for each produced water. Maximum recovery is determined assuming that the TDS of the concentrate is equal to 70,000 ppm. RO modeling is performed with ROSA, computational program developed by Dow Chemical.

An alternative method that can improve RO permeate quality is to use booster pumps prior to downstream membrane elements. Under typical operating conditions for RO plants, feed water is pressurized at the head of the RO system to a value that corresponds to the desired recovery rate. As a result, the pressure at the leading elements is much greater than necessary for producing permeate, while at the last element, the pressure is just sufficient to drive water across the membrane. When treating water with moderate TDS values (such as ACT) using this method, the critical system constraint is the permeate flow rate in the first element. The operating pressure is reduced to meet this constraint, and the reduced pressure results in greater TDS values for the permeate stream.

An alternative process design is to not mix permeate from different elements. The ROSA model is used to determine permeate quality from each element in the desalination process for two different membranes. This analysis shows that the TDS of permeate from upstream elements is of much higher quality than that of downstream permeate. This observation may motivate finding alternative uses for the streams with different quality or may suggest alternative process designs.

3.3.2 Treatment options results

Figure 3-7 shows ROSA modeling results for treating ACT produced water with high rejection (SW30XHR) and loose (XLE) RO membranes over a range of recovery rates. Neither membrane optimally achieves either of the treatment objectives (1,000 mg/L for cooling water and <10 mg/L for boiler feed water). Ideally, one would hope to achieve very high recovery rates at these target TDS values. High recovery rates are desired both so that more water is available for beneficial use and to reduce the volume of water to be disposed or sent to a zero liquid discharge process. The permeate TDS is approximately 260 mg/L at 77% recovery for the SW30XHR membrane, which is acceptable for cooling makeup water, but not for boiler feed water, and 4,100 mg/L at 60% recovery for the XLE membrane, which is unacceptable for either purpose.

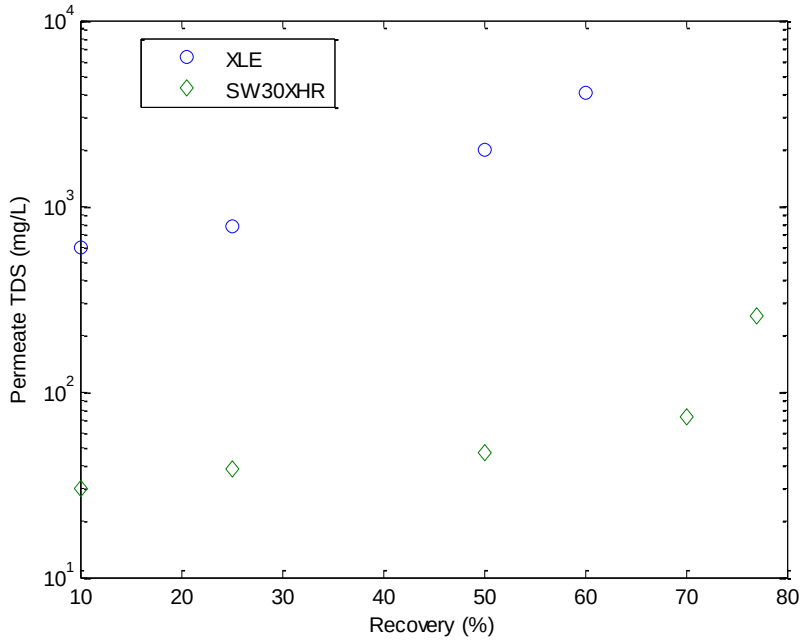

Figure 3-7: Permeate TDS values as a function of recovery for ACT produced water (feed TDS = 19 g/L) with XLE and SW30XHR membranes.

Figure 3-8 shows the permeate TDS values for the three different feed water TDS values using XLE and SW30XHR membranes operating at maximum recovery. The recovery for the feed waters was 71%, 43%, and 14% for feed TDS values of 19,400, 38,800, and 58,200 ppm, respectively. The TDS concentrations of permeate from the SW30XHR membrane all plotted well below the allowable maximum for cooling make-up water (1,000 mg/L) for each of the feed waters. The operating pressure for these three cases is between 1,100 and 1,200 psi, where 1,200 psi is the manufacturer's upper limit. For the lowest TDS feed water, the permeate TDS is 35 ppm, very close to the more stringent standard. To meet the relaxed standard, feed water can be mixed with permeate. To meet the lower standard, additional treatment with ion exchange is recommended.

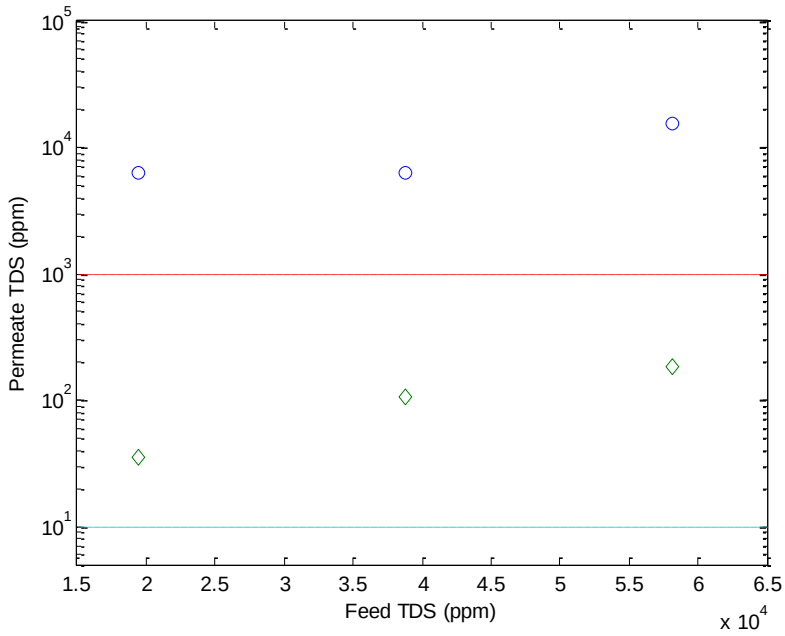

Figure 3-8: Permeate TDS values obtained at maximum recovery for the 3 produced waters. XLE (circles) and SW30XHR (diamonds) membranes are used in the simulations. Target TDS values for permeate are shown by the red and green dashed lines.

Results for the XLE membrane are not promising. The permeate TDS exceeds the upper standard for all three feed waters. The operating pressure for these simulations ranged from 400 to 600 psi, where 600 psi is the upper limit for the membrane. Alternative operating conditions such as reduced recovery or addition of booster pumps are needed in order to successfully use the XLE membrane.

Figure 3-9 shows the impact of using booster pumps for treating ACT produced water with XLE membranes. For recoveries less than 35%, operating the RO system in the usual manner allows the upper water quality standard to be met. For greater recoveries, the TDS concentration of permeate increases rapidly, but the use of booster pumps enables the recovery to exceed 55% while still meeting the 1,000 mg/L water quality target.

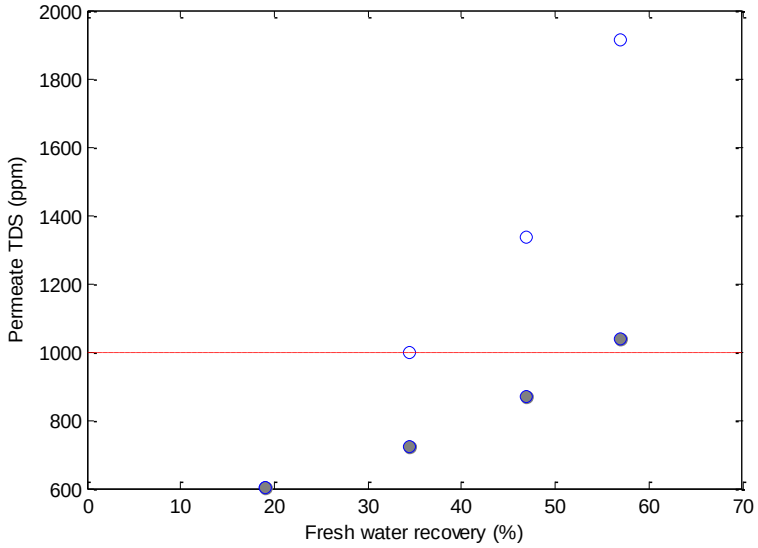

Figure 3-9: Permeate TDS values for ACT produced water with (filled circles) and without (open circles) booster pumps. Dashed line denotes target TDS value for cooling make-up water.

The booster pump method has some distinct advantages as well as some drawbacks. For the 57% recovery case presented in Figure 3-9, the pressures in each of the 4 elements are 416, 458, 511, and 594 psi. Though the recovery is much less than that achieved with the SW30XHR membrane (72% recovery including dilution water to get TDS equal to 1,000 ppm), the energy needed for this process is significantly less, despite the multiple pumps (operating pressure for SW30XHR is 1180 psi). Another advantage is that the higher pressures needed downstream are applied to decreasing feed water flows due to the removal of permeate. However, the engineering complexity of the system is increased because multiple pumps must operate with precision.

Results from the ROSA model using SW30XHR membranes are shown in Table 3-39. Permeate flux decreases by 85% from the first to last element, and permeate TDS increases from 28 to 440 ppm. The averaged TDS from all elements is 82 mg/L. Permeate from the first element does not achieve the water quality for boiler feed water, but only minor additional treatment would be required to reach that level. Nearly 80% of the permeate stream (elements 1-6) have TDS values less than 100 ppm that probably could be used for boiler feed water after an ion exchange treatment. The TDS of permeate from the last element is still well below the target maximum for cooling tower feed water.

Table 3-40 shows ROSA results for treating ACT water with XLE membranes. For this water source, the optimal number of elements is 16. For the XLE membranes, there is a dramatic reduction in performance as feed water proceeds through the elements. The permeate flow rate decreases by 95% and the TDS increases from 600 to 15,600 ppm from the first to last element. Permeate from the first two elements achieves the cooling tower water quality standard, and all other elements produce permeate that exceeds the treatment targets.

Table 3-39: ROSA model of full desalination system using SW30XHR membranes to treat ACT water.

Element	Perm Flow (gpm)	Perm TDS (mg/l)	Feed Flow (gpm)	Feed TDS (mg/l)	Feed Press (psig)
1	6.69	28.	55.0	19290.	932.
2	6.22	34.	48.3	21959.	927.
3	5.68	42.	42.0	25202.	922.
4	5.05	53.	36.4	29125.	918.
5	4.34	70.	31.3	33805.	915.
6	3.58	95.	27.0	39223.	912.
7	2.82	134.	23.4	45204.	910.
8	2.12	194.	20.6	51376.	908.
9	1.50	292.	18.4	57241.	901.
10	1.04	440.	17.0	62263.	900.

Table 3-40: ROSA model of full desalination system using XLE membranes to treat ACT water.

Element	Perm Flow (gpm)	Perm TDS (mg/l)	Feed Flow (gpm)	Feed TDS (mg/l)	Feed Press (psig)
1	6.93	596.	37.8	19290.	419.
2	4.75	956.	30.8	23489.	415.
3	3.15	1537.	26.1	27590.	413.
4	2.10	2390.	22.9	31161.	411.
5	1.47	3478.	20.8	34054.	409.
6	1.10	4698.	19.4	36369.	407.
7	0.87	5939.	18.3	38270.	406.
8	0.72	7156.	17.4	39885.	405.
9	0.59	8609.	16.7	41300.	399.
10	0.53	9613.	16.1	42502.	397.
11	0.50	10246.	15.5	43621.	396.
12	0.44	11555.	15.0	44735.	395.
13	0.39	12753.	14.6	45735.	394.
14	0.36	13838.	14.2	46649.	393.
15	0.34	14737.	13.8	47501.	392.
16	0.32	15611.	13.5	48315.	391.

Figure 3-10 shows that the permeate flux and TDS values are quite different between the two membranes. For the SW30XHR membrane, the permeate flow rate decreases linearly throughout the treatment system, and the permeate TDS increases parabolically. For the XLE membrane, the permeate flow rate decreases very rapidly in the first 3 elements and then asymptotically approaches zero. The permeate TDS increases nearly linearly with the number of elements. The poor overall performance of the XLE system may be explained by the very small permeate flow rates from most of the elements.

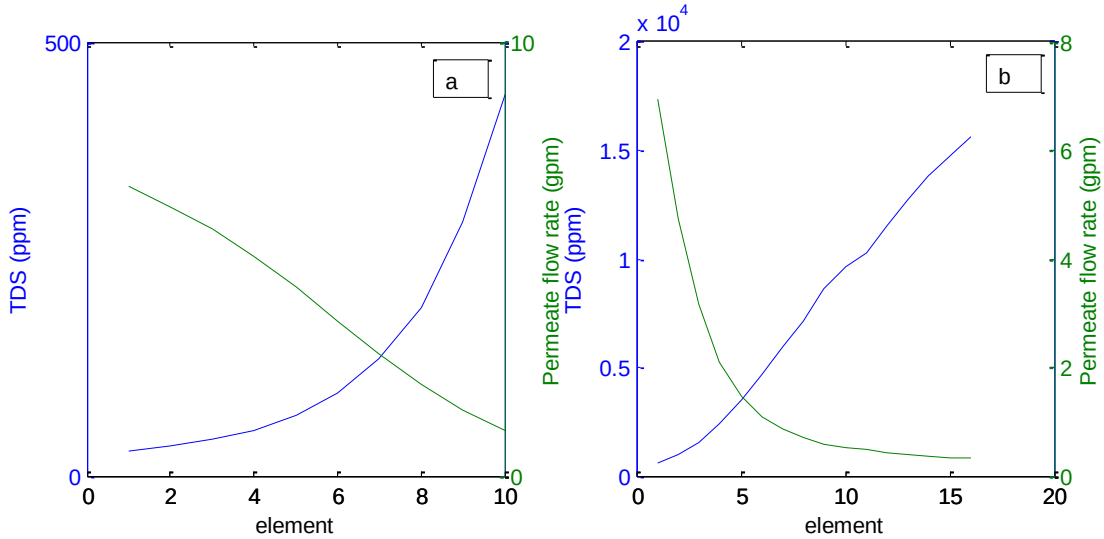

Figure 3-10: ROSA results for membrane treatment of ACT produced water using (a) SW30XHR and (b) XLE membranes.

Many different treatment systems may be designed to achieve the 1000 mg/L treatment target. Addition of booster pumps has been shown to significantly improve overall performance by increasing the permeate flow rate at downstream elements. An alternate design would be to use a combination of membranes. For example, XLE membranes might be used for the first two elements, followed by a set of SW30XHR membranes. Another possible design would be to collect permeate from the poorly performing elements in a system with XLE membranes and send it back to the head of the treatment system. ROSA does not have this feature available, so detailed calculations were not performed. A full analysis of the treatment options is beyond the scope of this project. However, it would be interesting and useful to compare costs for these and other design options to find the ones best suited for treatment of the various types of produced waters in the Illinois Basin. Such an analysis would also need to consider system complexity and operator skill.

3.4 Transportation cost estimate

3.4.1 Transportation cost methods

Costs related to pipeline transportation include pipeline right-of-way cost, pipeline material cost, construction cost, pipeline service cost, pump station cost, and the operating cost. The pipeline diameter will be calculated based on the water volume to be transported.

Literature was reviewed to identify resources for estimating the costs for pipeline transportation of water from produced water sources to the water treatment plants and for transport of treated water to power plants. Cost information for pipelines came from a variety of sources (EPRI, 2008; MGSC, 2004; MGSC, 2005; USEPA, 2006; ENR).

The costs of water transportation consist of the capital cost and O&M cost. Components of the capital cost were estimated from cost estimation resources and updated to the current dollar value using ENR cost estimation indexes. Cost of water transportation ($/3.8 cubic meters ($/1000 gal)) was estimated based on the capital and O&M costs, assuming a capital depreciation lifetime of 30 years and an interest rate of 3%.

3.4.2 Transportation cost calculations

The various components of pipeline water transportation costs are summarized in Table 3-41 and discussed below.

3.4.2.1 Pump Stations

Pump station cost is directly related to the size of the pipeline, water flow rate, and required pressure increase at each pump station. The cost of back up pumps is also included for possible pump failures. Two methods were used for estimation of pump station costs: USEPA and power-based correlations. USEPA (2006) provides a general cost estimation equation for pump stations for drinking water:

$$C = e^{12.466 + (0.5*1.0772)} \; D^{0.644} \times 1.096833,$$

where: C = the pump station cost in US$ and D = the design capacity (mgd).

The cost of pump stations will be significantly increased for pumping corrosive produced water that requires the use of more costly corrosion-resistant materials. However, this factor is not included in the cost estimations.

In the second method, the annualized cost of a pump station (Y) is estimated based on the required pump power (P, kW) using the equation $Y = 5560\ P^{0.723}$ obtained from a recent cost estimation reference (Swamee et al., 2008). This correlation is valid for a power range of 2-1500 kW.

Required power for the pump can be calculated from the following equation, where P = required power, S_b = standby friction, ρ = fluid density, g = gravitational acceleration, Q = fluid flow rate, h_0 = required head, and η = pump efficiency [Swamee et al., 2008].

$$p = \frac{(1+s_b)\,\rho g Q h_o}{1000\eta}$$

The required head (h_0) is equal to friction head losses in pipes (h_f) and in valves and fittings (h_v), and the required elevation head. The value of h_f can be calculated from equation:

$$h_f = \frac{2f\frac{L}{D}\left(\frac{4Q}{\pi D^2}\right)^2}{g}$$

where f = the pipe friction factor, L = length, D = diameter, and Q = flow rate.

The value of h_v can be calculated from the following equation:

$$h_v = 1/2g\ (4Q/\pi D^2)^2(e_v)$$

where e_v is the summation of the friction loss factors for valves, meters, etc. Friction loss factors for gate valves, control valves, backflow prevention devices, and water meters used in this work were 0.17, 10, 10, and 10, respectively (Sakiadis and Byron, 1984). Elevation head was assumed to be negligible due to the flat topography of the Illinois Basin.

The pipeline friction factor (f) was calculated from Reynolds number and the ratio of pipe roughness and diameter (e/D). The kinematic viscosity of fluid used for calculating Reynolds number was 9×10^{-7} m^2/s. Typical values of roughness for PVC and ductile iron pipe materials are 6×10^{-5} inch and 1×10^{-2} inch, respectively.

It was assumed that one gate valve, control valve, check valve, and water meter would be installed for each mile of the pipeline. The cost estimation information for these valves and meters was obtained from an EPA report (USEPA, 2006). The calculated cost was adjusted to the present value by multiplying it by the ratio of 2010 ENR cost index (8920.45) and the ENR cost index of year 2003 (6580.54).

Table 3-41: Components of pipeline water transportation cost.

Description	Amount
Pump Stations	
Pipeline Material	
PVC, HDPE, Steel, Ductile Iron, RCP, FRP	
Valves	
Pipeline Construction Cost	
Agricultural Lay	
Congested Lay	
Special Crossing Techniques (Microtunneling, Bore and Jack)	
Right-of-Way Cost	
Pipeline Service Cost	12-20% of pipeline material, construction, and right-of-way cost
Subtotal Construction Cost	
Contractor Overhead and Profit	15% of Subtotal Construction Cost
Mobilization, Demobilization, and Bond	6% of Subtotal Construction Cost
Current Construction Costs	
Escalation	6% of Current Construction Cost
Total Construction Cost	
Contingency	30% of Total Construction Cost
Engineering Design	15% of Total Construction Cost and Contingency
Construction Management	10% of Total Construction Cost and Contingency
Sales Tax	7.5% of Total Construction Cost and Contingency
Total Capital Cost	
O&M	
Electricity	
Labor	
General Maintenance	

3.4.2.2 Pipeline Material

A suitable piping material resistant to the corrosive produced water must be selected. The transmission pipeline for produced water may require a monitored secondary containment system, which may increase the cost 150-300%, compared to a conventional single pipe system. Oilfield water often requires this secondary containment to prohibit oil/hazardous material leakage.

There are six different pipe materials suitable for transporting produced water. These include: ductile iron, steel, polyvinyl chloride (PVC), high density polyethylene (HDPE), fiber reinforced plastic (FRP) and reinforced concrete pipe (RCP). Polyethylene encasement may be required to protect ductile iron pipe under corrosive environments. Each of the 6 materials has particular advantages and disadvantages. PVC

and HDPE pipes are not only much cheaper than ductile iron and stainless steel pipes, but also more resistant to corrosion. However, they have limited pressure-handling capability. Some piping materials have also specific limitations on the size of pipe that can be manufactured. For example, the cost of RCP will be extremely high for pipe diameters smaller than 61 cm (24in); PVC pressure pipe generally is not fabricated for diameters above 91 cm (36”). Information on pipe material cost can be obtained from the graphs of pipe material cost versus pipe diameter in the EPRI (2008) report.

3.4.2.3 Pipeline Construction Cost

In usual practice, the area where a pipeline is to be constructed is divided into three types of areas: agricultural lay, congested lay (city), and alternative installation procedures, such as microtunneling and bore and jack (for roads and rivers/streams).

The EPRI (2008) report provides the cost of trenching labor and equipment, daily output of pipe with various materials, and alternative installation techniques as a function of pipe diameter and types. It should be noted that these are rough estimates. Local contractors should be consulted for more accurate estimates. Selection of a proper water transportation route can significantly impact the pipeline construction cost. Route selection would require a detailed study that was beyond the scope of this work.

3.4.2.4 Pipeline Service Cost

In some cases, the pipeline requires professional services including engineering, surveying, mapping, right-of-way acquisition, legal, permit application and acquisition, environmental consulting, geotechnical analysis, vendor inspection, and construction inspection. The suggested value for this cost is 12-20% of the subtotal of the right-of-way, material, and construction costs.

3.4.2.5 Pipeline Right-of-Way Cost

Pipeline Right-of-Way cost represents the cost directly related to the value of property on which the pipeline is constructed and also the interruption of business currently associated with that property. Right-of-way costs for pipelines of various diameters were obtained from MGSC (2004) and are shown in Table 3-42.

Table 3-42: Pipeline right-of-way cost in the Illinois Basin.

Diameter (inch)	US$/mile	US$/diameter inch/mile
4	36,713	9178
6	36,713	6119
8	44,500	5563
10	44,500	4450
12	51,731	4311
16	66,750	4172
18	66,750	3708
20	66,750	3338
22	66,750	3034
24	66,750	2781

Based on the previously described methodology, the cost of water transportation was estimated under several scenarios. The cost components for water transportation by a PVC pipeline are tabulated in Table 3-43. The cost was estimated for several pipe diameters (from 15 cm to 71 cm (6" to 28")) and two selected flow rates (1,893 and 18,930 cubic meters per day (0.5 and 5 MGD)). The cost of pump stations for different cases shown in Table 3-43 is calculated based on a power-based correlation. No cost estimation was performed for cases (pipeline diameters) that the estimated power was outside the power range of the correlation.

Similar cost estimations were performed for PVC pipelines by using the above EPA capacity-based correlation for the pump station cost (Table 3-44). For DIP pipelines both EPA capacity-based and power-based correlations were used to estimate the cost of pump stations. A summary of all cost estimation results is shown in Table 3-44. For most cases, cost estimations for costs of pumping stations by the power-based or capacity-based correlations provided similar results. However, the cost estimation for pump stations based on power requirement appears to be more accurate because the impact of both pipe diameter (and head loss) and water flow rate are included whereas the EPA correlation is based only on the water flow rate.

The cost of water transportation strongly depends on the water flow rate. For a flow rate of 1,893 cubic meters per day (0.5 MGD), the cost of water transportation in a 15 cm (6") diameter PVC pipeline is estimated as ≈ $ 1 per 2.35 m^3/km (1000 gal/mile). For the flow rate of 18,930 cubic meters per day (5 MGD) the lowest cost of ≈$ 0.25 per 2.35 m^3/km (1000 gal/mile) was estimated for 51-71 cm (20-28") diameter PVC pipelines. Slightly greater, but similar, costs were estimated for DIP pipelines with the same range of diameters (Table 3-44).

The cost of water transportation for small flow rates (e.g., < 189 cubic meters per day (< 0.05 mgd)) from scattered and unsteady sources of produced water can be significantly higher when high capital cost of pipeline transportation cannot be justified and the practical option is to use truck tankers for water transportation. In a recent report, the cost of water transportation by a 19 m^3 (5000 gal) truck was reported as $200/hr (Brown and Caldwell, 2007). If we assume 1 hour for loading and unloading and 1 hour to travel 16 km (10 miles) round trip, the cost would be estimated as ≈$16 per per 2.35 m^3/km (1000 gal/mile).

Table 3-43: Cost components of water transportation by PVC pipelines for 1 mile (pump station cost estimated from power requirement).

	0.5 mgd, 6" dia.	5 mgd, 12" dia.	5 mgd, 14" dia.	5 mgd, 16" dia.	5 mgd, 18" dia.	5 mgd, 20" dia.	5 mgd, 22" dia.	5 mgd, 24" dia.	5 mgd, 28" dia.
Cost Items									
Pump Stations (PVC)	$522,613	$6,022,041	$3,633,617	$2,321,110	$1,588,238	$1,119,297	$816,963	$613,733	$379,040
Pipeline Material									
PVC pipe (1mile)	$41,634	$93,851	$114,946	$137,887	$162,672	$189,302	$217,778	$248,098	$314,274
Gate valve (1)	$1,690	$7,838	$10,697	$10,697	$17,698	$17,698	$31,952	$31,952	$31,952
Control Valve (1)	$11,737	$14,827	$29,257	$29,257	$91,053	$91,053	$91,053	$91,053	$91,053
Water Meter (1)	$6,958	$16,013	$16,013	$16,013	$16,013	$16,013	$16,013	$16,013	$16,013
Check valve (1)	$6,535	$26,298	$36,065	$47,420	$60,366	$74,900	$91,024	$108,738	$148,932
Pipeline Construction Cost									
Trenching Labor and Equipment Cost (1 mile)	$107,981	$184,676	$210,719	$237,000	$263,521	$290,280	$317,278	$344,515	$399,705
Bore and Jack or Microtunneling (200 ft)	$30,780	$64,472	$75,723	$86,978	$98,236	$109,495	$120,753	$132,010	$154,517
Right-of-Way Cost (ROW)	$49,767	$70,126	$70,126	$90,485	$90,485	$90,485	$90,485	$90,485	$90,485
Total of pipeline material, construction, ROW	$257,083	$478,101	$563,546	$655,738	$800,044	$879,227	$976,337	$1,062,865	$1,246,932
Pipeline Service Cost	$51,417	$95,620	$112,709	$131,148	$160,009	$175,845	$195,267	$212,573	$249,386
Subtotal Construction Cost	$831,112	$6,595,763	$4,309,872	$3,107,996	$2,548,291	$2,174,370	$1,988,567	$1,889,171	$1,875,358
Contractor Overhead and Profit	$124,667	$989,364	$646,481	$466,199	$382,244	$326,156	$298,285	$283,376	$281,304
Mobilization, Demobilization, and Bond	$49,867	$395,746	$258,592	$186,480	$152,897	$130,462	$119,314	$113,350	$112,521
Current Construction Cost	$1,005,646	$7,980,873	$5,214,945	$3,760,675	$3,083,432	$2,630,988	$2,406,166	$2,285,896	$2,269,183
Escalation	$60,339	$478,852	$312,897	$225,640	$185,006	$157,859	$144,370	$137,154	$136,151
Total Construction Cost	$1,065,984	$8,459,725	$5,527,842	$3,986,315	$3,268,438	$2,788,847	$2,550,536	$2,423,050	$2,405,334
Contingency	$319,795	$2,537,918	$1,658,353	$1,195,895	$980,532	$836,654	$765,161	$726,915	$721,600
Total of total construction cost and contingency	$1,385,780	$10,997,643	$7,186,194	$5,182,210	$4,248,970	$3,625,502	$3,315,697	$3,149,965	$3,126,935
Engineering Design	$207,867	$1,649,646	$1,077,929	$777,331	$637,345	$543,825	$497,355	$472,495	$469,040
Construction Management	$138,578	$1,099,764	$718,619	$518,221	$424,897	$362,550	$331,570	$314,997	$312,693
Sales Tax	$103,933	$824,823	$538,965	$388,666	$318,673	$271,913	$248,677	$236,247	$234,520
Total Capital Cost	$1,836,158	$14,571,877	$9,521,708	$6,866,428	$5,629,885	$4,803,790	$4,393,299	$4,173,704	$4,143,188
Annualized Capital Cost (30 yrs, 7% interest)	$147,969	$1,174,295	$767,320	$553,341	$453,692	$387,120	$354,040	$336,344	$333,885
O&M									
Electricity	$9,167	$49,937	$49,937	$49,937	$49,937	$49,937	$49,937	$49,937	$49,937
Labor	$18,092	$20,828	$20,828	$20,828	$20,828	$20,828	$20,828	$20,828	$20,828
Total Annual Cost	$175,228	$1,245,060	$838,085	$624,106	$524,457	$457,885	$424,805	$407,109	$404,650
Cost per 1000 gallons (for 1 mile)	**$0.96**	**$0.68**	**$0.46**	**$0.34**	**$0.29**	**$0.25**	**$0.23**	**$0.22**	**$0.22**

Table 3-44: Cost of water transportation by PVC and DIP pipelines.

	0.5 mgd, 6" dia.	0.5 mgd, 8" dia.	5 mgd, 12" dia.	5 mgd, 14" dia.	5 mgd, 16" dia.	5 mgd, 18" dia.	5 mgd, 20" dia.	5 mgd, 22" dia.	5 mgd, 24" dia.	5 mgd, 28" dia.
PVC pipeline *	$0.96 ***		$0.68	$0.46	$0.34	$0.29	$0.25	$0.23	$0.22	$0.22
PVC pipeline **	$0.87 ***		$0.28	$0.29	$0.30	$0.32	$0.33	$0.34	$0.35	$0.37
DIP pipeline *	***	$0.98	$0.83	$0.56	$0.43	$0.36	$0.33	$0.31	$0.31	$0.32
DIP pipeline **	***	$1.18	$0.31	$0.33	$0.35	$0.37	$0.39	$0.41	$0.43	$0.46

Pump station cost calculated from the power required (*) or EPA capacity-based correlation (**).
*** Not estimated because the estimated power requirement was outside the power range of the correlation.

3.5 Optimization of the transportation network

3.5.1 Introduction

The objective of this work is to estimate the cost of treating and transporting water from produced water sources to power plants. Treatment costs depend on the flow rate as well as the TDS of the produced water. Transportation costs depend on the flow rate and pipeline length. Demand for water at power plants is constrained by the cooling water needs, which scale linearly with electricity production. Water cost curves as a function of water supplied are analyzed for two cases. For the first case, all treated water is sent to a single power plant, and for the second case, water is distributed to power plants throughout the basin.

Except under extreme drought, water availability is not a problem for cooling systems at power plants within the Illinois Basin. Increased water demand by population growth, irrigation, or expansion of thermal-electric generation at some point in the future may reach freshwater supply limits. The EIA projects a national 30% increase in electricity demand by 2030. As a result, freshwater availability for power production in some areas may be limited. Results from this optimization study may assist decision-makers in determining which alternative to pursue for power plant cooling systems.

This task attempts to answer the following question: what is the best way to distribute the potentially available produced water? If power plants request produced water for cooling, the objective is to find the pipe network that achieves the least cost for the full treatment and transportation system. Results may be significantly different under different assumptions. If water demand is not even at the power plants, the optimal water distribution will be altered. For example, a single power plant may expand power production, but no additional freshwater is available.

3.5.1.1 Problem statement

The produced water optimization problem is a variation of the minimum cost-flow problem. Oil fields, coal mines, and coal bed methane projects are the sources for produced water, and coal fired power plants are the sinks. Because the locations of future demand for cooling water are unknown (e.g., new power plants, expansions at existing plants), the maximum flow to any given sink is set equal to the current demand. For some plants, this means that produced water may replace freshwater. The capacity of the pipelines is not constrained because the pipe diameters can be designed to accommodate the optimal flow rates. The problem objective is to minimize the total cost of the treatment and transportation network.

The problem constraints are the following. Any source may send water to any sink, but sources do not need to be used. A source must send its water to either a source or a sink. Closed loop pipelines may be selected in the model, where water flows along a path and returns to the source. For simplicity, any such pipelines are neglected in the cost calculation. A power plant cannot accept more treated produced water than it needs for the cooling system. Because of potential leaks in the pipeline, all water must be treated prior to pumping in pipelines, which means that water treatment plants are located at each produced water source.

The optimization problem is challenging to solve because of the large number of possible solutions. The number of solutions scales as $(n_{sources} + n_{sinks})^{nsources}$, where n_i refers to the number of either sources or sinks. For the scale of the IL basin (we assume 60 sources and 11 sinks), the number of possible solutions is 10^{111}. Evaluating every possible permutation is not possible, so a genetic algorithm is used to search for optimal solutions. The solution determined from the genetic algorithm is unlikely to be the optimal solution, but it does provide guidance for which sources and sinks should be connected. In practice, a pipeline designer would need to make finals decisions for pipe routing.

The genetic algorithm used to solve the optimization problem is a slightly modified form of Matlab's genetic algorithm (Mathworks, 2010). The default algorithm uses real numbers for the decision vector. For the pipe network optimization problem, the decision vector corresponds to the downstream source or sink that will receive the source's water. The integer range is from 1 to the number of sources plus sinks. In the model, a source is allowed to send water to itself. Practically, this means that the water from that source is not used. No treatment or transportation costs are calculated for that source. The length of the decision vector is equal to the number of sources.

3.5.1.2 IL Basin produced water data

Table 3-45 shows power plants used and water withdrawal rates, assuming circulating cooling systems and current electricity production rates.

Table 3-45: Electric power production and water demand (assuming recirculating cooling) for power plants included in the study.

Sink #	Power plant	Electricity production (MW)	Water demand* (kgal/d)	latitude	longitude
1	Gibson	3145	38500	38.37233	-87.76716
2	Paradise	2273	27800	37.25981	-86.97814
3	AES	2203	27000	38.52822	-87.25198
4	Clifty Creek	1300	15900	38.9365	-88.2771
5	Powerton	1786	21860	39.22739	-87.57344
6	Warrick	775	9490	37.91503	-87.33268
7	Wabash	668	8180	39.52892	-87.424
8	Coffeen	1005	12300	39.05958	-89.40287
9	Marion	274	3350	37.62	-88.953
10	Holland**	630	4630	39.225	-88.759
11	Pinckneyville**	316	2320	38.113	-89.346

* Assuming water demand is 0.5 gal/kWh or 12.2 kgal/day/MW for coal plants and 0.3 gal/kWh for natural gas combined cycle plants. ** Natural gas power plant

Oil fields used in this study are listed in Table 3-46. Oil production rates are taken from 2004 data, and the water/oil ratio is assumed to be equal to 40. For fields with unknown values of TDS, the TDS value used in the model is randomly selected from a normal distribution with mean = 109,000 and SD = 36,000 mg/L.

Table 3-46: Data for oil fields in the IL basin used for the optimization model.

Oil field	Oil production (1000 barrels / year)	TDS (mg/L)	latitude	longitude
Albion	101.3	110,800	38.3422	-88.034
Allendale	156.6	92,100	38.4699	-87.7615
Clay city	1175.6	133,900	38.9889	-88.0338
Dale	49.4	134,400	38.0161	-88.5743
Goldengate	104.4	136,800	38.2107	-88.1952
Griffin	194.1	76,000	38.203	-87.9401
Johnsonville	191.9	140,800	38.3886	-88.5268
Lawrence	1004	36,400	38.6195	-87.7339
Louden	600.9	111,600	39.0714	-88.8544
Main	860	70,800	38.9075	-87.8067
Mattoon	37.1	100,600	39.3969	-88.3898
New Harmony	524.2	120,300	38.3286	-87.8736
Parkersburg	25.4	122,600	38.5685	-88.0099
Phillipstown	194.7	81,200	38.109	-88.0485
Sailor Springs	254.7	116,500	38.6509	-88.4291
Salem	670.5	122,600	38.481	-88.9945
Union Bowman	177.162	91,200	38.3977	-87.4327
Benton	143.3	118,700	37.9711	-88.9409
Divide	67.2	131,200	38.3936	-88.8097
Dudley	62	49,100	39.5985	-87.8539
Enfield	107.7		38.0539	-88.3386
Herald	71.3		37.8815	-88.2117
Inman	95.6	71,100	37.82	-88.1011
Marine	61.1	58,000	38.8034	-89.7655
Miletus	1086	130,700	38.7627	-88.7523
Mill Shoals	95.9		38.2403	-88.359
Roland	132.4	96,800	37.9324	-88.3029
St James	120.7	88,800	38.9274	-88.9171
West Frankfort	67.1		37.8917	-88.9202
Westfield	149.8		39.3798	-87.978
Apex			37.0801	-87.3406
Greensburg			37.3096	-85.5059
Poole			37.6503	-87.6497

The only active coal mines in the Illinois basin with significant produced water are Pattiki, Galatia, and Royal Falcon. The estimated produced water flow rate is: mean = 200, SD = 20 kgal/d. The TDS has mean = 20,000, SD = 3,000 mg/L.

Simulations have been performed with both current CBM projects and with potential future development. For simulations with current CBM projects, two coal bed methane sites are included in the model (ACT and Pioneer). In the model, the produced water flow rate from each project has mean = 100 and SD = 10 kgal/d. The TDS has mean = 20,000 and SD = 3,000 mg/L.

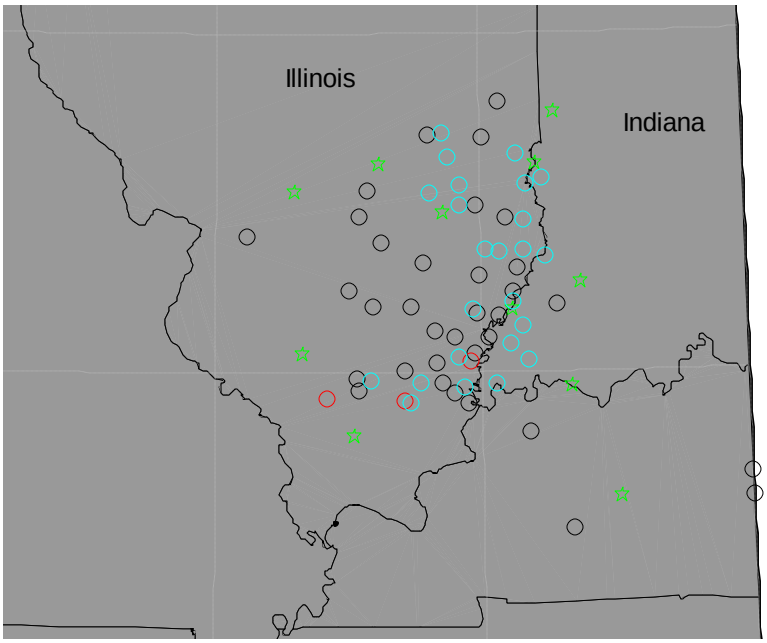

Figure 3-11: Locations of power plants (green stars) , oil fields (black O), coal mines (red O), and potential coal bed methane projects (cyan O) used for the optimization model.

A map of power plants and produced water sources used in the model is shown in Figure 3-11. Since most of the produced water sources are located in the southern half of the basin, the numerous power plants in northern Illinois were not included in the model. Figure 3-12 provides another means of measuring distances between sources and three power plants. There is effectively a shift of 10-20 miles in the curves between Gibson (the best location) and Powerton (typical location). There is another 20 mile shift to Coffeen (one of the worst locations).

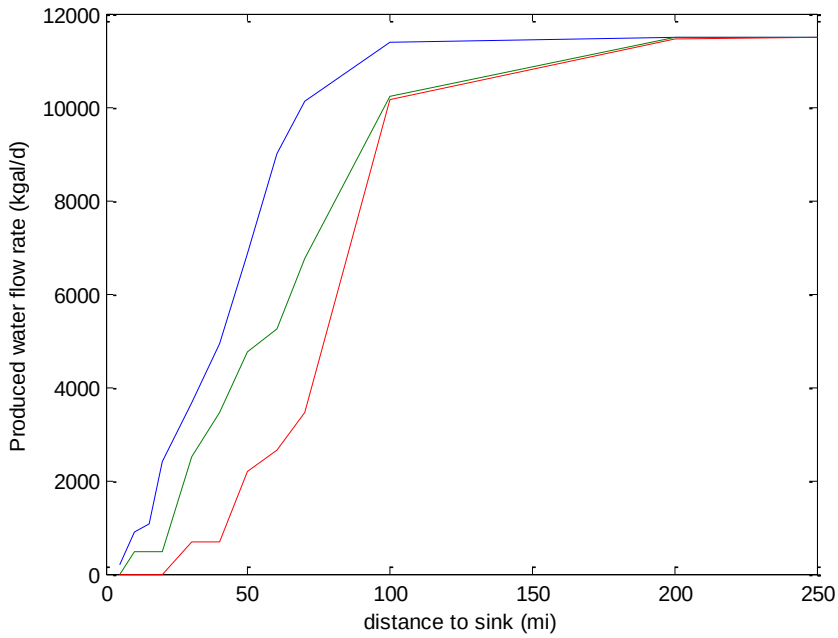

Figure 3-12: Cumulative raw water production of the modeled sources plotted as a function of distance from the Gibson (blue), Powerton (green), and Coffeen (red) power plants.

An additional view of the distances between sources and sinks is shown in Figure 3-13. The flow rate as a function of distance to the nearest sink is determined by binning flow rate from each source located within a specified distance from its nearest power plant. Most produced water must travel between 10 and 30 miles to reach a power plant.

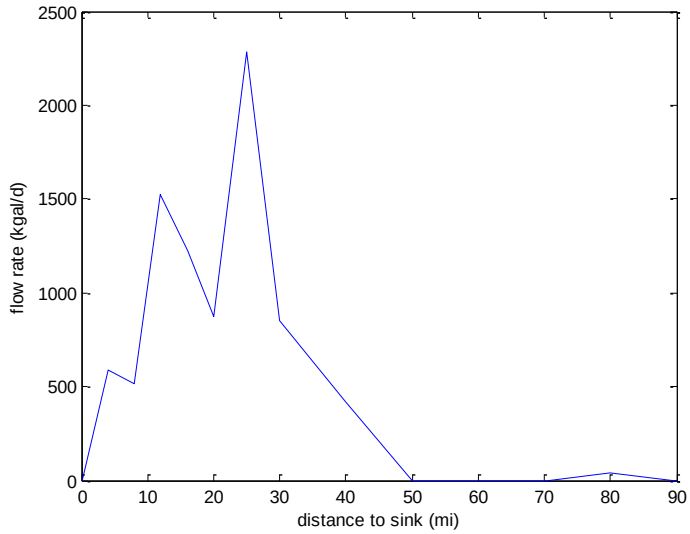

Figure 3-13: Total flow rate as a function of the distance from sources to the closest sink in IL basin.

3.5.1.3 Produced water from CBM development in Illinois Basin

Currently coal bed methane production in the Illinois Basin is very limited. During the course of this project, 5 different sites have produced CBM, and at least one of these sites has been shut off due to the removal of tax breaks for CBM production and the reduced price of natural gas. Because of these conditions, it is very difficult to predict if or when large-scale coal bed methane projects will be started.

Numerous assumptions were made to estimate the produced water volume generated by large scale CBM development in the IL basin. Based on investigations by MGSC/ISGS, the IL basin is assumed to contain 16.4 $x10^{12}$ scf of CBM reserves. The largest project in the IL basin to date (Delta) was able to produce 800,000 scf per day. Gas production from drilled wells appears to last less than 5 years. If we assume that the gas is produced over the time frame of 50 years, then approximately 900 Delta projects could be undertaken. This means that at any given time, there could be 90 projects in operation. To be slightly conservative, we have estimated that 24 fields are in production.

The peak concentrations of CBM in the basin are approximately 2 million scf per acre. Assuming gas production equal to 1,000,000 scf/day, each project requires 1000 acres, or a square region with 1.25 mile long sides. Since these projects take small areas, we assume that once a production has ceased, development of the next project will occur adjacent to the existing project. In this way, locations of the projects are within 2 miles of the original project, so that water transportation costs are relatively unaffected. We assume that development is spread relatively uniformly throughout regions with high gas concentrations. The locations of the projects are listed in Table 3-47.

In the optimization code, water quantity and quality from these sources are randomly selected from normal distribution functions. Water flow rates have mean and standard deviation equal to 140 kgal/day and 40 kgal/day, respectively. The mean TDS of produced water is assumed to have mean and standard deviation equal to 20,000 and 3,000 mg/L, respectively.

Table 3-47: Locations of potential CBM projects in the IL basin used for simulations.

number	county	city	latitude	longitude
1	Coles	Lerna	39.417943	-88.288957
2	Cumberland	Toledo	39.272115	-88.242778
3	Jasper (1)	Newton	38.988119	-88.164390
4	Jasper (2)	Rose Hill	39.103998	-88.148464
5	Effingham	Dieterich	39.060156	-88.378994
6	Richland	Claremont	38.720346	-87.972731
7	Lawrence (1)	Sumner	38.715935	-87.859910
8	Lawrence (2)	Lawrenceville	38.725686	-87.684538
9	Edwards	Albion	38.377300	-88.061028
10	Wabash	Mt. Carmel	38.414859	-87.768596
11	White	Carmi	38.088333	-88.168056
12	Gallatin	New Haven	37.907113	-88.126954
13	Saline	Raleigh	37.827084	-88.533738
14	Franklin	Hanaford	37.957485	-88.839177
15	Hamilton	Broughton	37.934104	-88.463027
16	Clark	Choctaw	39.282222	-87.721389
17	Crawford (1)	Hutsonville	39.109142	-87.659262
18	Crawford (2)	Flat Rock	38.902220	-87.672402
19	Sullivan	(no town)**	39.144324	-87.528081
20	Knox	Vincennes	38.678329	-87.516067
21	Gibson	Owensville	38.271769	-87.690652
22	Posey (1)	Poseyville	38.169290	-87.783632
23	Posey (2)	Mt. Vernon	37.936766	-87.898780
24	Vanderburg	St. Joseph	38.066111	-87.646944

** midway between Shellburn, IN and Hutsonville, IL.

3.5.1.4 Produced water cost functions

The total cost of using produced water for cooling water at power plants includes treatment, transportation, and waste disposal costs. Treatment, transportation, and disposal cost functions have been developed by comparing results from previous reports to additional literature sources. All costs are assumed to follow a power law scaling with flow rate (RosTek Associates, 2003). Water treatment costs depend on the TDS of the produced water source. These cost functions all have significant uncertainties because currently there are no large scale produced water treatment systems for beneficial use. To assess the sensitivity of the optimal solutions to the individual cost functions, simulations have been performed with double and one half the costs given by the functions listed below.

The transportation cost function has a simplified form. Additional factors that must be considered, including elevation, right of way, etc., are neglected in order to make the model tractable. Transport function (flow rate (q) in kgal/d and distance in miles):

$$\text{Transport cost (\$/d)} = 15.8\ q^{0.55}\ \text{distance}$$

RO treatment costs are estimated from the available references (RosTek, 2003; Sandy and DiSante, 2010). Water recovery for a produced water source is limited by the maximum allowed membrane pressure, typically 1,200 psi. RO Treatment (TDS in mg/L and flow rate in kgal/d):

RO treatment cost ($/d) = 0.25 $TDS^{0.4}$ $q^{0.6}$

For thermal treatment, MED and MSF are limited to TDS concentrations close to 60 g/L (RosTek, 2003). Thus, any desalination of water with TDS greater than 70 g/L will be done using brine concentrators (possibly with crystallizers if ZLD is worthwhile). The cost function of a brine concentrator is given by

Distillation cost ($/d) = 17 $q^{0.94}$,

where the flow rate (q) is in kgal/d (Mickley and Associates, 2006). The range where this equation is accurate is from 500 to 3,000 kgal/day, but the function will be applied for all possible flow rates.

The cost function for a crystallizer is given by

ZLD crystallizer cost ($/d) = 60 $q^{0.88}$,

where the flow rate (q) is in kgal/d. This equation is accurate for flow rates in the range 10 to 70 kgal/d, but this equation also is applied to all flow ranges.

To date, no information has been found regarding disposal costs scaling. Costs are typically quoted at around $1-3 per barrel of water. For now, cost is assumed as a power function of flow rate:

Disposal cost ($/d) = 171 $q_{disposed}^{0.6}$,

where the scaling constants are determined by setting the cost of disposing 200 kgal/day equal to $1 per barrel of water. An interesting issue with disposal of produced water is this. Currently, all produced water in the IL basin is disposed, though in different ways. If the water is desalinated, less water will be disposed, so for most cases disposal costs will actually decrease. Coal mines are the exception because they currently discharge produced water to surface water. It is highly unlikely that they will be allowed to discharge concentrate from desalination plants. If the cost reduction is considered, the new disposal cost function has the form k_{disp} $(q_{IN}-q_{disposed})^{k2}$, where k2 is the power law scaling.

Disposal costs are neglected in the optimization model. For some produced water sources, this assumption will lead to significant errors for the total water cost, but for most the difference will be within the error estimates for the treatment and transport processes. First, all current produced water sources have disposal methods in place. Very little capital investment is needed to handle retentate from desalination processes, and the flow rates of retentate will be less than the initial produced water flow rates. For most oil sources, the water is reinjected to maintain formation pressure. For CBM and coal mine produced water, the water is either surface discharged or injected to a high-permeability, low-pressure formation with large TDS values. For small recovery rates, the disposal volumes are marginally affected. Surface discharge may be allowed to continue if salt loads remain relatively constant.

Figure 3-14 shows the costs of disposal of all produced water along with treatment only costs and treatment plus concentrate disposal costs. Compared to disposal costs of $1 per barrel of water, the treatment costs of water are quite small. As the TDS of produced water increases, disposal costs of the

concentrate increase rapidly due to increasing volumes of concentrate. For produced water with low TDS, the disposal costs tend to be roughly equal to treatment costs.

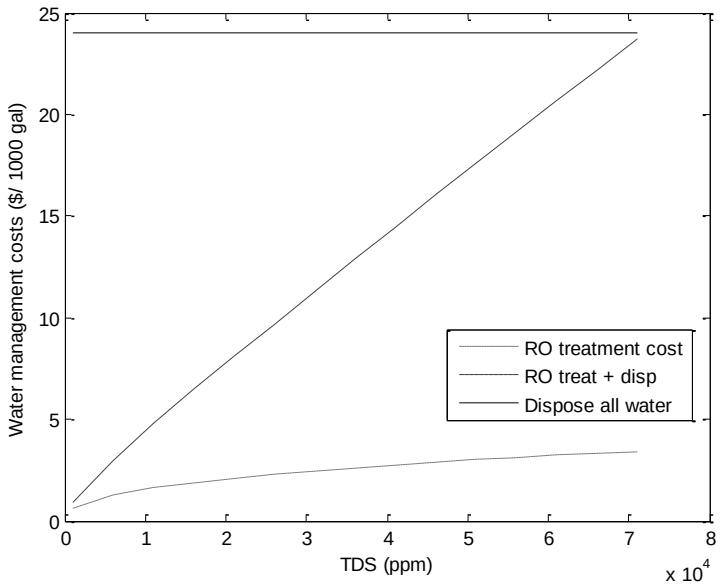

Figure 3-14: Cost of water management for RO treatment of produced water. Curves show costs for RO treatment only, RO treatment plus concentrate disposal, and direct disposal of all produced water.

3.5.2 Optimization model analysis

3.5.2.1 Computational demand

Before modeling the entire IL basin, it is helpful to consider the implications of the cost functions selected for the model. The relative costs of treatment and transportation are investigated for varying TDS values of produced water, flow rates, and distances from sources to sinks.

For the linear cost function, the optimal pipe network is always single connections between each source and the closest sink. This can be proven as follows. Consider sources 1 and 2 with flow rates q1 and q2, and source 2 is closer to sink A than source 1. Compare the cost of the two possible pipe networks: (1) from 1 to A and 2 to A and (2) the pipe connecting 1 to 2 to A. The cost of (1) is the left hand side (LHS) and the second option is the right hand side (RHS):

LHS cost = $k(q1 \times d_{1A} + q2 \times d_{2A})$

RHS cost = $k(q1 \times d_{12} + (q1+q2) \times d_{2A})$

where d_{ij} refers to the distance between points i and j, and k is the linear cost scaling. The cost scaling can be neglected. Both options have the term q2×d2A, this term is neglected. Also, given that q1 > 0, we can divide both equations by q1. We are left with

LHS = d_{1A}

RHS = $d_{12} + d_{2A}$.

This is simply a statement of the triangle inequality, so we conclude that

$d_{1A} <= d_{12} + d_{2A}$,

and that the cost of the first option is the minimum pipe network cost.

For nonlinear cost functions, the optimal solution is more difficult to find. A test code was developed to calculate the total cost for the water system for all possible pipe network permutations. For this analysis, permutations that have closed loop pipelines are ignored. The pipe network optimization model was used to simulate between 7 produced water sources with randomly generated locations and 2 sinks located at the corners of a region (0,0 and 1,1). A histogram of the costs for all feasible solutions is generated.

Computational performance of the test code is shown in Table 3-48. The computational time and number of feasible solutions scale roughly linearly with the number of possible solutions. As the number of sources increases beyond 9, a more sophisticated solver is required.

Table 3-48: Computational performance of permutation code using Matlab/Windows Vista.

Number of sources	Number of possible solutions	Number of feasible solutions	Computational time (Matlab/intel core2) (min)
7	8.2×10^5	5.8×10^4	0.13
8	1.7×10^7	7.3×10^5	3
9	3.9×10^8	7.0×10^6	87
10	1×10^{10}	1.7×10^8 (approx)	2000 (predicted)

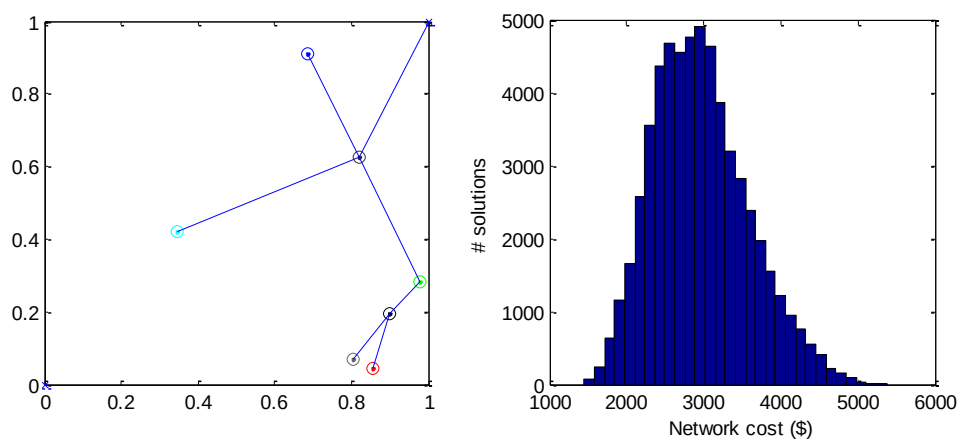

Figure 3-15: Model results from randomly generated locations and flow rates for 7 produced water sources (circles). Sinks (x) are located at (0,0) and (1,1). Transport cost is given by power law cost function. Optimal pipe network solution (left) and histogram of the costs for all feasible solutions (right).

The cost of the optimal pipe network with seven sources and two sinks shown in Figure 3-15 is $1,449. The cost of the network in which all sources are directly piped to the nearest sink is $2,106. Both costs are less than the mean of all feasible solutions, as shown in the histogram of Figure 3-15. This suggests that the majority of feasible solutions are poor choices. A method to neglect these solutions would be quite useful for problems involving large numbers of sources.

3.5.2.2 Cost function analysis

Figure 3-16 shows overall costs for water treatment and transport for TDS values of 20 and 100 g/L and pipe distances equal to 5 and 30 miles. Overall costs per kgal increase rapidly as flow rates decrease to values smaller than 100 kgal/day. At large flow rates (1 MGD) the overall costs flatten to approximately $10 / kgal for the 20 g/L case and $25/kgal for the 100 g/L case.

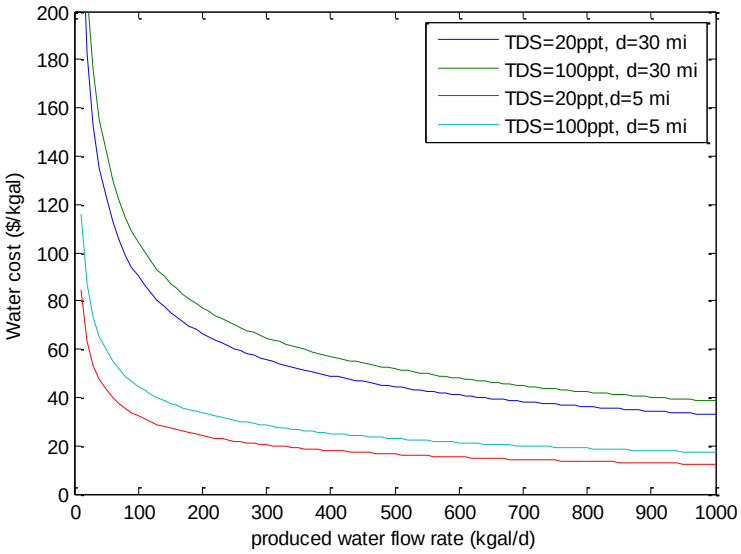

Figure 3-16: Total water costs (treatment and transportation) for two different distances and raw water TDS values using a single sink and source.

Figure 3-17 shows the distance at which transportation costs are equal to treatment plus disposal costs for a range of TDS values, flow rates and treatment processes (either RO or thermal desalination). Costs depend on local conditions such as distances from sources to sinks, quantity of water, and TDS of the water. Distances are quite short, generally less than 20 miles, which suggests that transportation costs dominate the system cost for the IL basin.

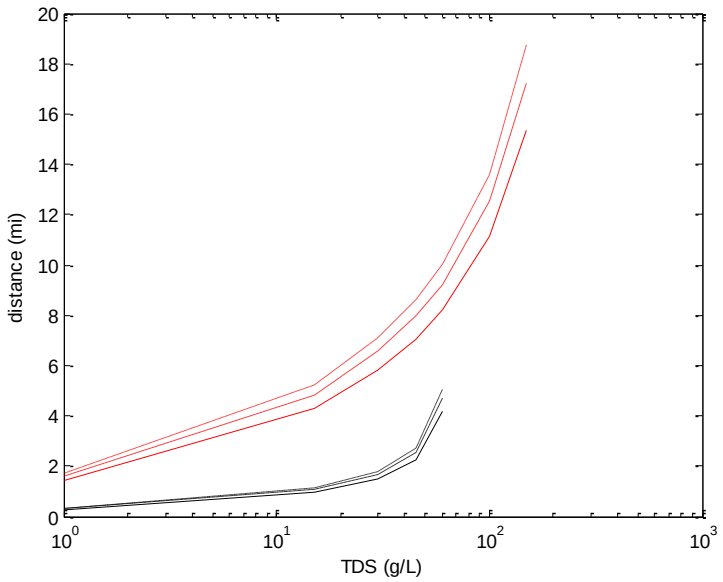

Figure 3-17: Pipe length at which transportation costs are equal to treatment plus disposal costs. Black lines indicate RO treatment, red lines indicate thermal treatment, and flow rates are 20, 100, and 500 kgal/d (solid, dashed, and dash-dot, respectively).

Figure 3-18 demonstrates a method for comparing two potential water sources for use at a power plant. The first source is located closer to the sink than the second, but its water has a greater TDS concentration. The difference between the distances from the sources to the sinks that equalizes the overall costs for each source is determined. For sources that may be treated with RO (TDS values are less than 60,000 ppm), the distance separating the best and worst TDS values is only 10 miles. Thus, the water source with lower TDS will be chosen for nearly all cases. For thermal treatment, the distance is only 2 miles, so again the better quality water will be selected for all sources in the IL basin.

When one source may be treated with RO and the other must be thermally treated, the difference between the distances from the sink is much greater. For RO treated source water with TDS equal to 20 g/L, the distance approaches 35 miles for thermally desalinated water with TDS equal to 250 g/L. On the other hand, for RO treated water with TDS equal to 60 g/L, the overall costs are greater than thermal costs for TDS values between 70 and 250 g/L. For 70 g/L thermally treated water, the RO treated source must be nearly 20 miles closer to the sink in order to match the overall costs.

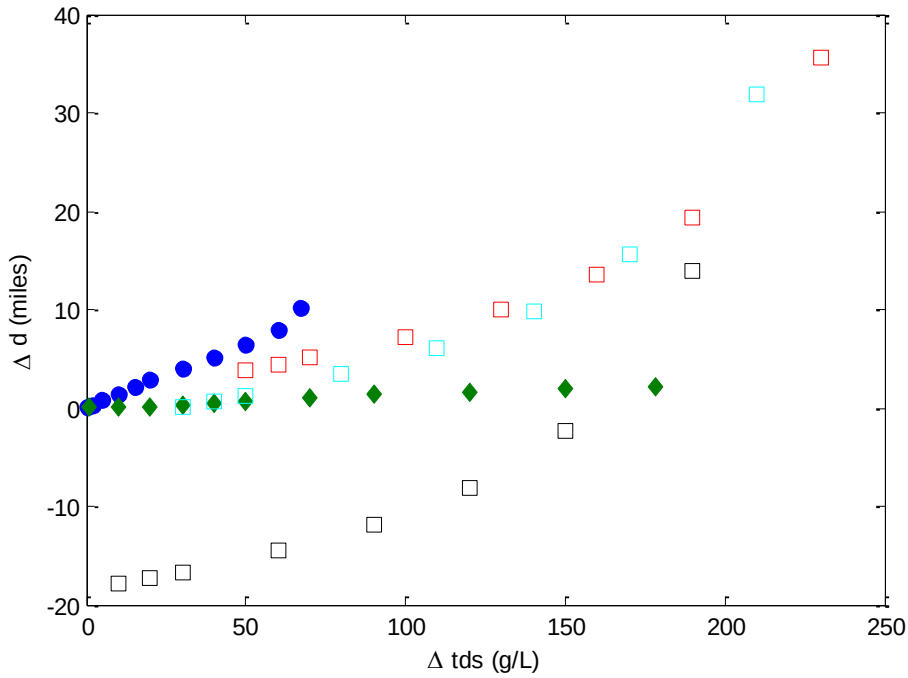

Figure 3-18: Distance differences for equal water costs, comparing sources with different values of TDS. Circles denote RO treatment for both sources, diamonds denote thermal treatment for both sources, and squares one source with RO and one with thermal, where RO treats a source with TDS equal to 20 (red), 40 (cyan), and 60 (black) g/L.

3.5.2.3 Simple pipe configurations

A test case considered 3 sources and 1 sink located at the corners of a square. Using the cost functions described above, the total costs of the treatment and transport of water were analyzed for the following cases:

1. separate pipelines and treatment plants
2. combined pipelines, treatment at all sources
3. combined pipelines, treatment at the 2 downstream sources.
4. combined pipelines, treatment at 1 source.

Results from this square geometry case are shown in Figure 3-19. For distances less than 5 miles, case 4 is the optimal configuration. For small distances, treatment costs are more significant than transportation costs, so combining the raw produced water for treatment at a single plant achieves improved economy of scale. At increased distances, case 2 is optimal. For large distances, transport costs begin to dominate, so decreasing the flow rates through all pipes has the greatest impact on overall costs.

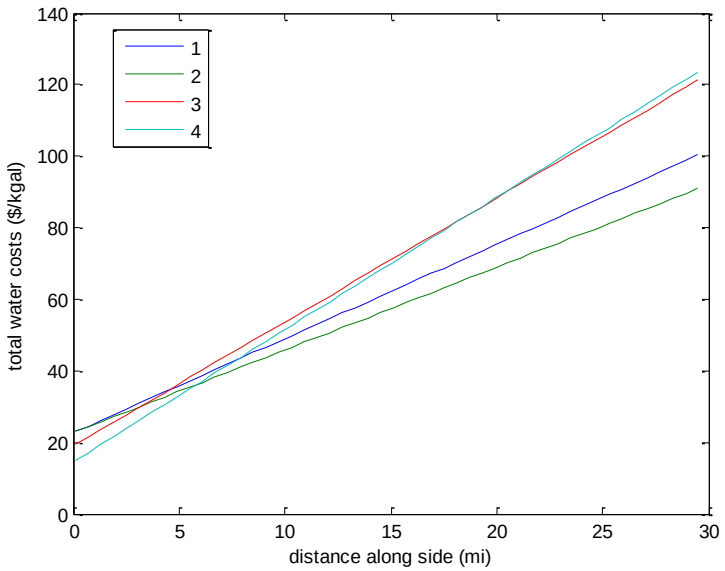

Figure 3-19: Costs for water treatment and pipe network configurations for the sample square problem.

The implications from this square model for the IL basin are significant. Since very few sources and sinks are separated by less than 5 miles (see Figure 3-12 and Figure 3-13), the lowest cost configuration is to have treatment plants located at each source. This greatly simplifies the number of variables in the optimization problem. Without this simplification, the solver must determine which sources contain treatment plants, and this decision depends on the configuration of the pipe network. For example, the last source along a pipeline upstream of a sink must always have a treatment plant (otherwise untreated water is sent to the sink).

As water demand for a power plant increases, the plant must seek additional water that is either further away or of poorer quality or possibly both. To quantify this increase, a simplistic model of sources and sinks was developed. We consider a set of sources located co-linearly with a sink. Distance from each source to the subsequent downstream source is constant. Flow rate from each source is 100 kgal/day with TDS equal to 20 g/L. The distance between sources is varied with values set equal to 1, 2, 5, and 10 miles.

The set of geometries for the sources and sinks is shown in Figure 3-20. Sources that are equidistant from a sink are located along a circle with center at the sink. For the linear case, each upstream source is located a fixed distance from its downstream neighbor. For fractal cases, each source sends water to a single, downstream source (or sink if it is the final source). The number of sources that send water to the sink is set equal to 2, 3, or 4. Only the configuration (not drawn to scale) for the 2 upstream sources is shown in Figure 3-20.

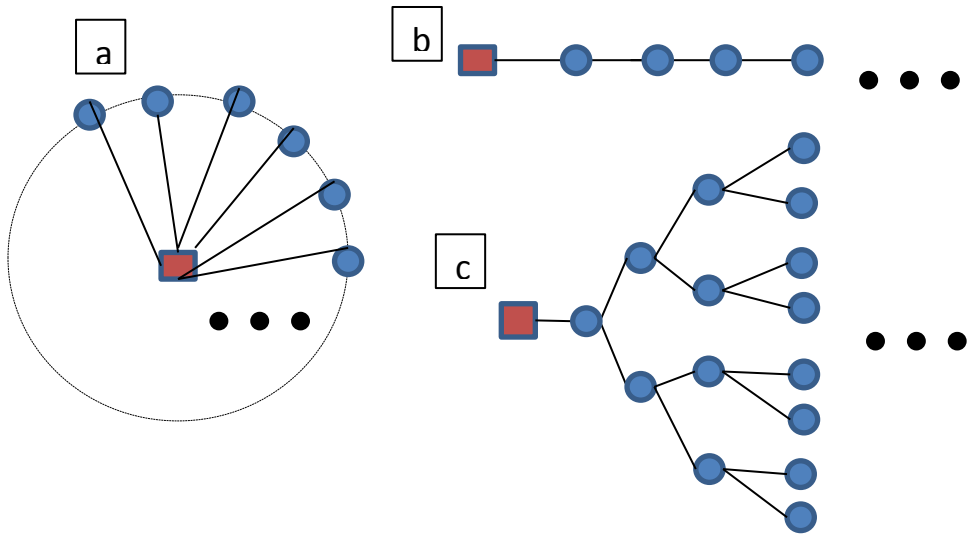

Figure 3-20: Source configuration problem. Each source (blue circles) has the same flow rate and TDS value. a: sources are equidistant from the sink (red). b: Linked linear pipe network. c: Linked fractal pipe network.

A second sample problem considers the effect of increasing TDS value to quantify the impact of using more degraded water. A number of potential sources are located equidistant from the sink (power plant). The TDS value of the sources increases by 5,000 mg/L with each additional source used. The TDS of the first source is 10,000 mg/L. Two different flow conditions cases are considered for this toy problem. In the first case, each source flows through a unique pipeline to the sink, and in the second, all treated source flows are combined in a single pipe. For the second case, all sources are located at exactly the same location.

Figure 3-21 shows the overall water cost as a function of the number of sources along a pipeline that connects sources in series. The cost functions grow as a power law with additional sources. The distance between the sources strongly influences the cost. Even at 25 times the water flow rate (and 2.5 times the total distance), water cost from the pipeline with 1 mile between sources is still less than one half the cost of the first source for the 10 mile case. Costs for the 1 mile spacing case are greater than $10 per 1,000 gallons when 25 sources are used, an amount much greater than the cost of municipal water (typically $4 per 1,000 gallons). Costs become extremely large when distances between sources exceed 5 miles. These costs are probably low estimates because disposal costs are excluded. Including disposal costs simply increases the overall costs uniformly for all source numbers.

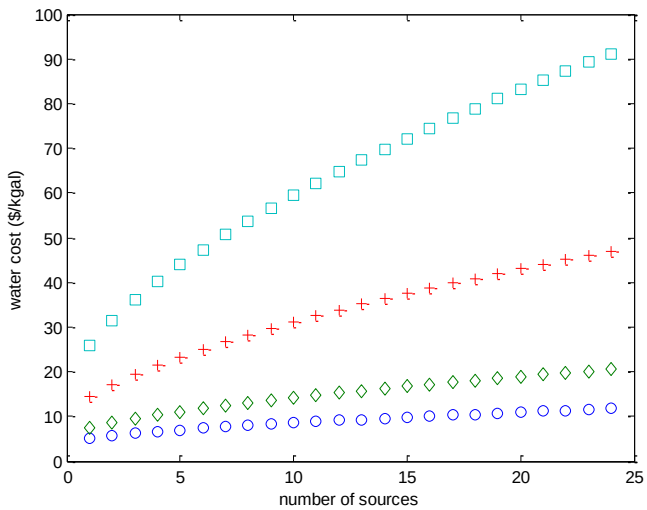

Figure 3-21: Linearly located sources linked along a single pipeline with distances between sources equal to 1(o), 2 (diamonds), 5 (+), and 10 (squares) miles.

Figure 3-22 shows the incremental costs for each new source added along a single pipeline. The overall shape of the curves is nearly identical to that in Figure 3-21, but the costs rise more quickly with increasing numbers of sources. Water sources that are further away along the pipeline are more expensive than those near the beginning of the pipeline, even including the scaling of water transport costs.

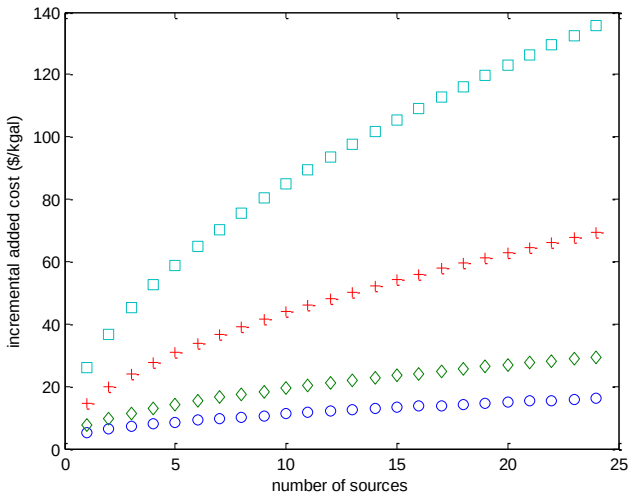

Figure 3-22: Incremental costs for each additional water source added for the single pipeline case. (Same distance symbols as in Figure 3-21).

Figure 3-23 shows the effect on water costs for the problem where the distances between successive additional sources remain fixed (i.e., all the sources are 1 mile from the sink), but the TDS of the water supplied by each additional source increases by 5 g/L. The cost increases slowly for the first 13 sources (all these sources can be treated with RO), but then rapidly increases due to the need for thermal

treatment of water with TDS concentrations exceeding 70 g/L. The magnitude of the cost increase is much greater than the cost increase observed in Figure 3-21. The savings from combining the water flows into a single pipeline is small compared to the cost increase from adding lower quality sources. These results also suggest that thermal desalination should be avoided if possible.

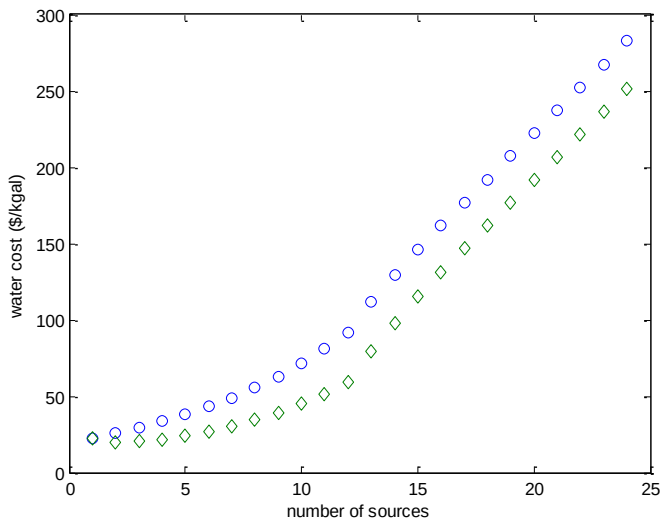

Figure 3-23: Cost of water from sources equidistant from the sink that have TDS concentrations that increase by 5 g/L with each source. The blue curve is for using separate pipelines, with the green curve us a single pipe connects all the sources to the sink. Linear disposal costs are included.

The model results shown in Figure 3-23 provide no clear cut-off for a decision maker regarding either distance or water quality. The possible exception is the transition between successful RO treatment up to 13 added sources, and the need for thermal treatment after that point, but water quality already is quite poor at this transition. For a power plant that needs to get an additional supply of water from produced water sources, consideration of both budget and water demand may be needed to determine how far to extend the supply pipeline.

Figure 3-24 shows the effect of branching pipe networks where sources with identical flow rates and TDS concentrations are linked. The lowest cost (red curve) corresponds to the case where all sources are equidistant from the sink, case (a) in Figure 3-20. Green diamonds represent case c in Figure 3-20, where the sink receives flow from a fractal pipeline network (with 1, 3, 7, 15, 31, and then 63 sources) where each source receives water from 2 upstream sources. The blue (o) data represent the linear pipeline, case b, in Figure 3-20. The uppermost cyan curve represents sources at increasingly larger distances (5 miles further for each source, starting at 5 miles for source 1) with each source connected to the sink by its own pipeline. Clearly, the lowest costs are observed for sources located close to the sink. As sources are spaced further apart, costs may be reduced by increasing the branching of the network.

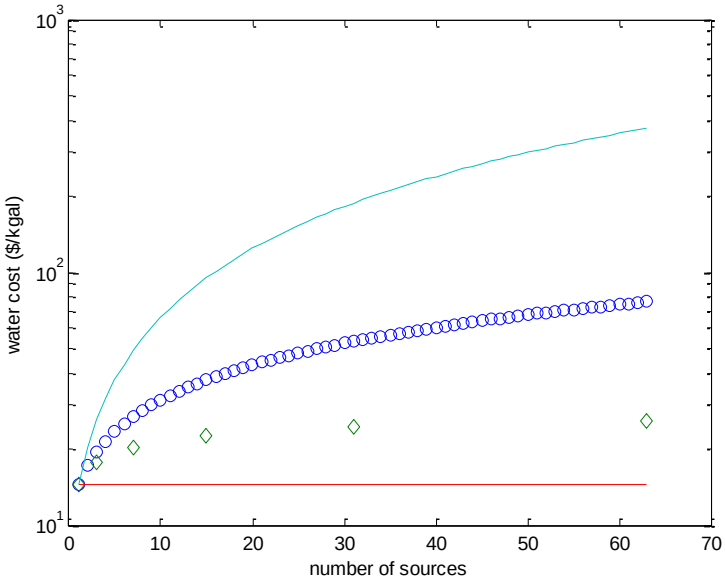

Figure 3-24: Water costs for linear chain (O), fractal (diamond), independent constant distance (red), and independent increasing distance (blue).

The degree of branching in the fractal case is investigated in more detail in Figure 3-25. The distances between the sets of sources are adjusted so that the flow rate as a function of distance for all fractal cases are identical (fitted function to binary fractal series is $d = 0.5699 \exp(0.7896^{isource})$, where 'isource' is the number of new sources in set number i (e.g., for fractals with 3 branches, the series 1,2,3,4, …i have 1,3,9,27, …3^(i-1) additional sources) and d is the distance from the sink to set i. The binary fractal case has lowest cost because it has the fewest number of pipelines, which results in greater flow rates per branch. Differences between the fractal cases are small compared to the difference between fractal configurations and the linear pipe configuration (Figure 3-24).

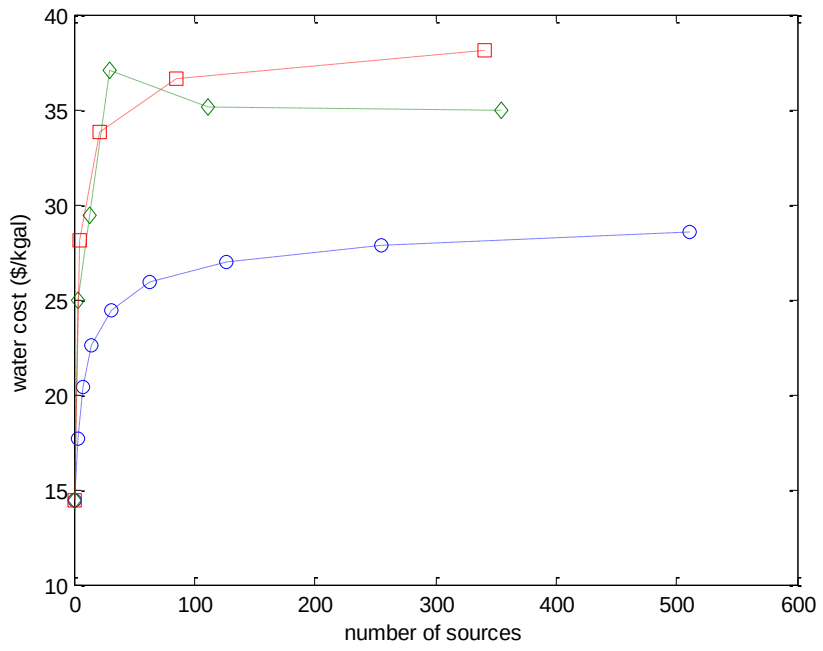

Figure 3-25: Number of connections in the fractal network varied (2 (blue O), 3 (red squares) or 4 (green diamonds) sources sent to each source in the network), but the flow rate as a function of distance is equal for all cases.

3.5.3 Illinois basin optimization results

Optimization simulations are performed for the Illinois basin for two types of scenarios. The first scenario is that a single power plant demands water, so any produced water that is treated is sent to that power plant. For the second scenario, all power plants demand produced water.

For the single sink scenario, the optimization algorithm determines the least cost pipe network that meets the needs of the power plant. Simulations are performed using either Gibson, Clifty Creek, or Marion (see Table 3-45) as the power plant that demands water.

For the all power plants case, we assume that all power plants are able to use produced water, and the total produced water flow rate from the IL basin is varied. The objective of the optimization problem is to find the pipe network that minimizes the cost of the system as a whole. The constraint for this problem is that each plant has a maximum water demand, above which a cost penalty is assessed.

For both scenarios, the overall costs for the pipe network are determined for a number of realizations (typically 70) and assumptions about water treatment and transportation costs. The cost of water that each power plant must pay is determined and values are compared for each sink in the whole basin.

3.5.3.1 Water demand at a single sink

Figure 3-26, Figure 3-27, and Figure 3-28 show the optimal pipe networks for single sink simulations when the receiving sink is Gibson, Clifty Creek, and Marion, respectively. The total water flow rates for each case are approximately 3 MGD. The produced water sources used for pipelines to Gibson and to

Marion are similar, although these sinks are located far from each other. A line of sources located between 4200 and 4350 km north at 425 east in the figures forms the main water pipeline in each case. For the Clifty Creek case, water sources farther west are used before extending the pipeline to the main line of sources. The water costs (including treatment and transportation costs) for the cases are Gibson $32.33, Clifty Creek $36.99, and Marion $55.42 per kgal. The extra distances from sources to sink evident in the figures are responsible for the greater costs for Clifty Creek and Marion.

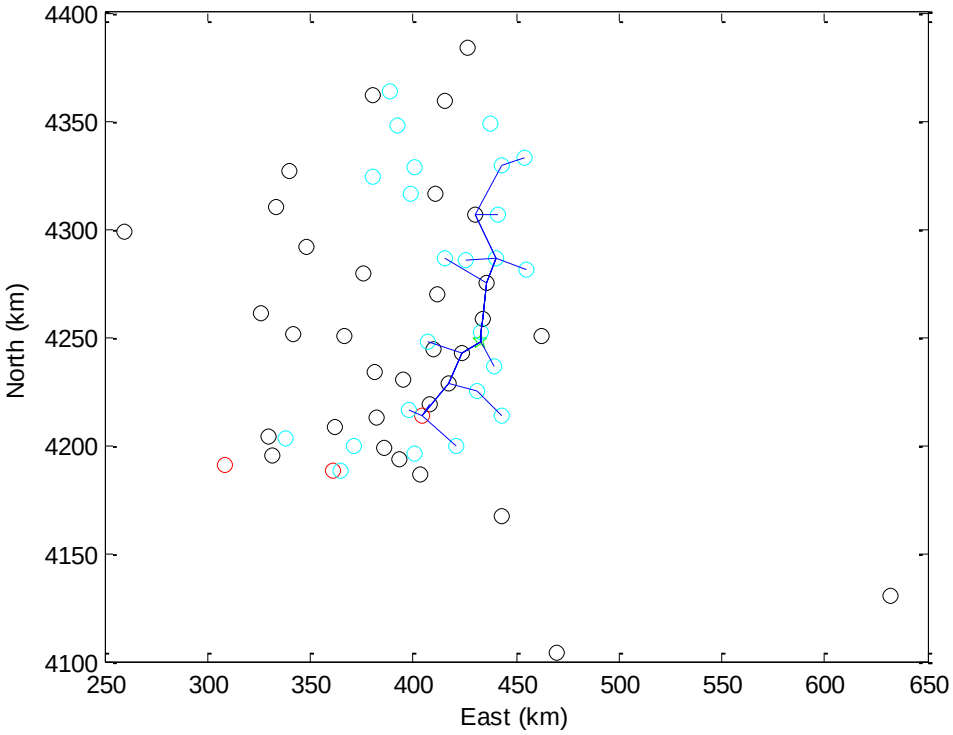

Figure 3-26: Optimal pipe network for water sent to Gibson only, where total flow rate is 3087 kgal/d. Oil fields (black O), CBM projects (cyan O), coal mines (red O), send produced water to Gibson power plant (green star).

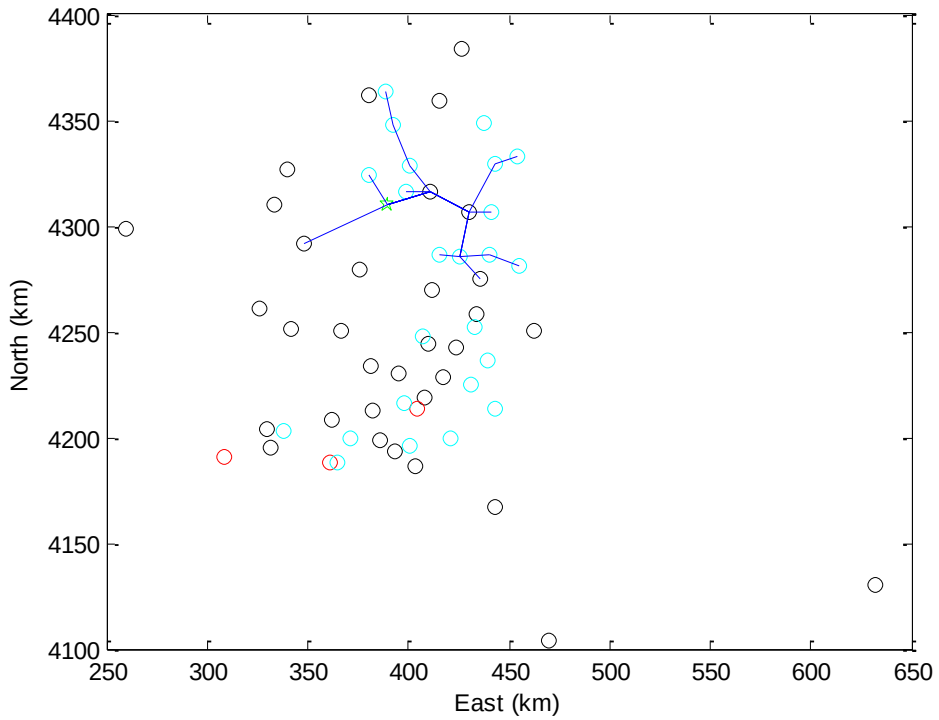

Figure 3-27: Optimal pipe network for water sent to Clifty Creek only, where total flow rate is 3126 kgal/d. Symbols are the same as used in Figure 3-26.

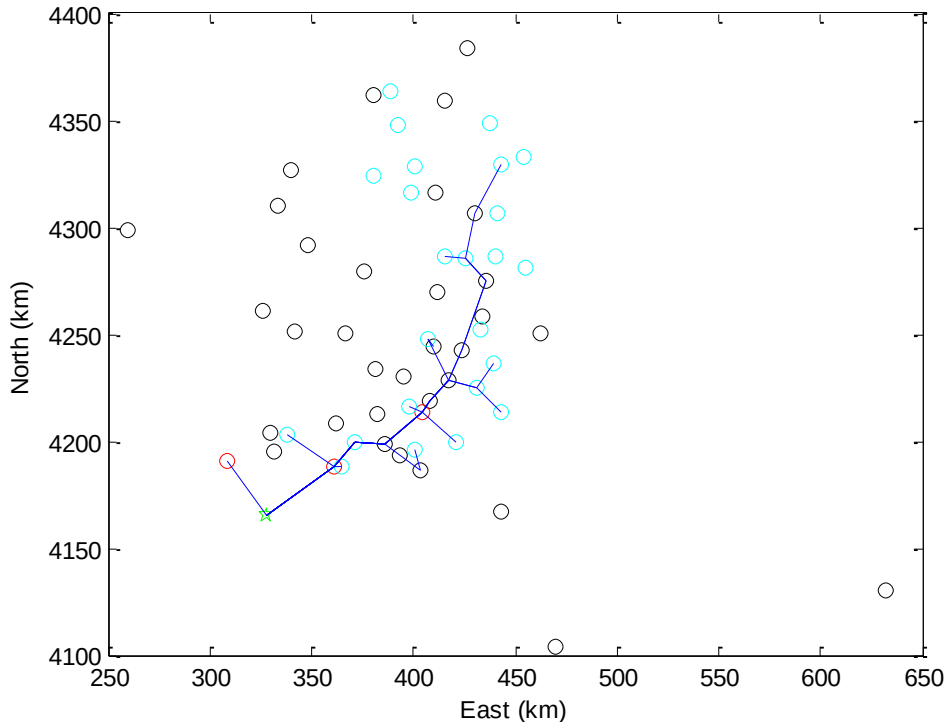

Figure 3-28: Optimal pipe network for water sent to Marion only, where total flow rate is 3347 kgal/d. Symbols are the same as used in Figure 3-26.

Figure 3-29 shows cost and flow rate results from a set of realizations for demand at either Gibson or Clifty Creek power plant. The cost of water ranges from $15 to $60 per 1000 gallons at each sink, with cost increasing with flow rate. At the upper and lower range of flow rates, the costs at the two sinks are nearly identical. For very low flow rates, less than 5 sources located nearby are used at the sinks, so costs are low. For very large flow rates, all of the water in the basin is sent to the sinks, so the ultimate destination of the water is less significant. For intermediate flow rates, the water costs at Gibson are slightly less than those at Clifty Creek because Gibson is more centrally located within the modeled area of the IL basin.

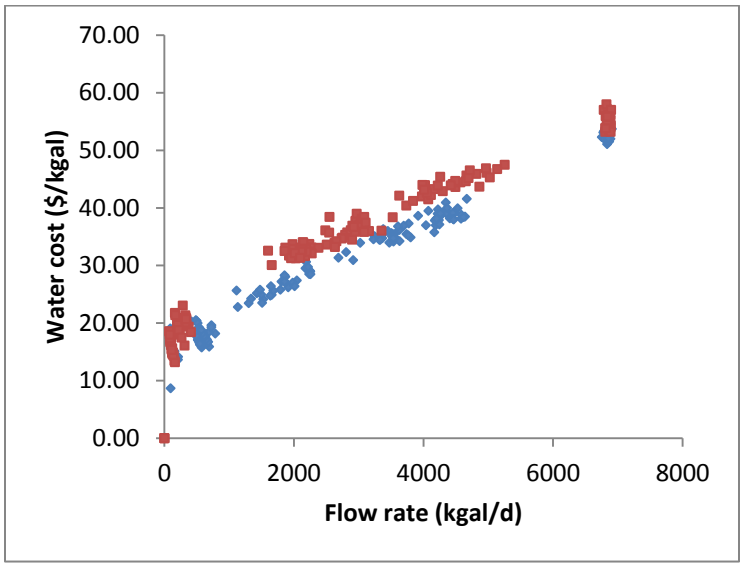

Figure 3-29: Water costs for demand at a single sink, where blue diamonds and red squares indicate Gibson and Clifty Creek, respectively.

Figure 3-30 shows the degree branching (defined as the sum of the number of links to each source divided by the number of sources). The Clifty Creek power plant pipe network is slightly more branched than the pipe network for Gibson for intermediate flow rates. Both pipe networks are slightly less branched than a binary fractal pipe network, but more branched than a linear case (where branching is equal to one). The degree of branching grows more slowly compared to the binary case as the number of sources increases.

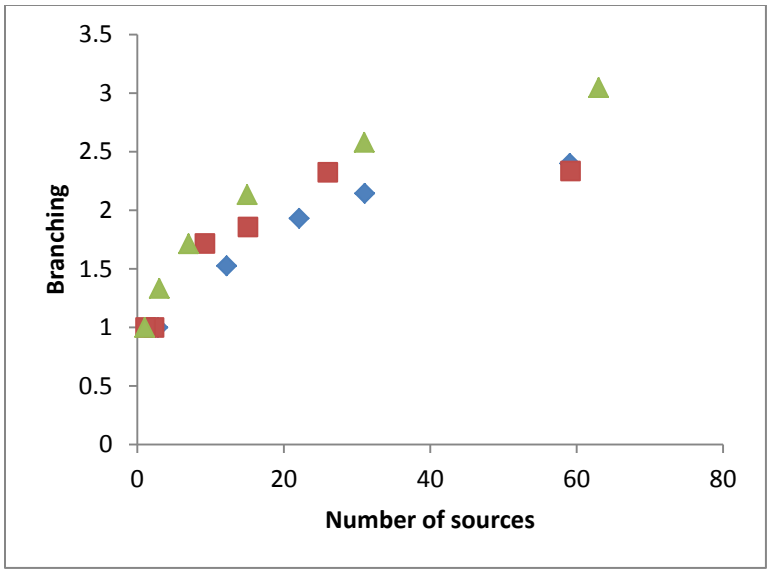

Figure 3-30: Degree of branching as a function of the number of sources connected to Gibson (blue) and Clifty Creek (red) power plants, and the theoretical branching of a binary fractal network (green).

The total water demand at the 11 power plants considered for this study is 171 MGD. The flow rate of treated produced water is estimated to be 7 MGD, or 4% of the total water withdrawn at these plants. The power plants with the most suitable locations for using produced water are Gibson and Clifty Creek, where the demands are 38 and 16 MGD, respectively. All of the treated produced water from sources used in this model of the IL basin is not sufficient to supply all the needs of either plant. If more produced water were needed, the concentrate could be harvested with a crystallizer, but costs would increase.

3.5.3.2 Water demand at all sinks

The optimal pipe network for a realization utilizing large scale CBM development and all of the other sources of produced water described above is shown in Figure 3-31. The distribution of water to the eleven sinks is highly uneven. For sinks receiving the bulk of the water, long pipelines are constructed with short branches extending off the primary line. These sinks are located near the center of the water-producing region. Two sinks receive no water at all, and four sinks receive water from 2 or fewer sources.

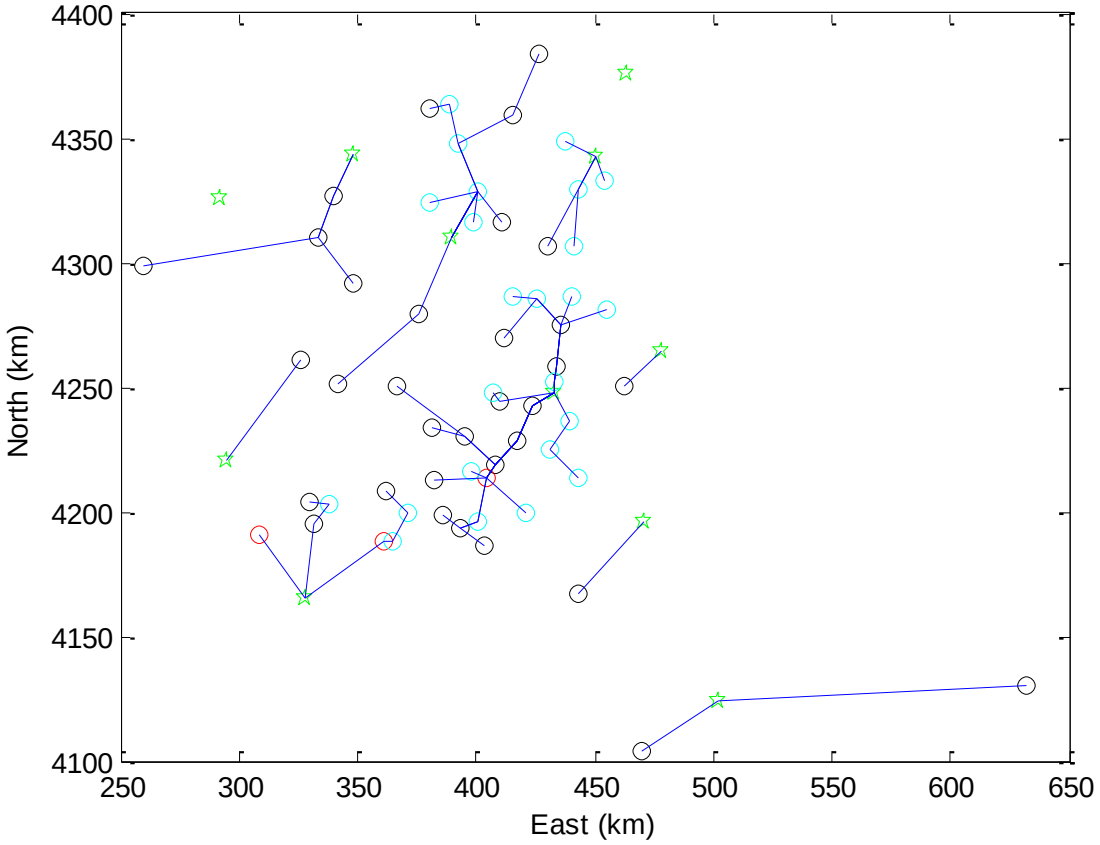

Figure 3-31: Optimal pipe network for a single realization using large scale CBM development where all sinks demand water. Oil fields (black O), CBM projects (cyan O), coal mines (red O), send produced water to power plants (green stars).

Because finding the exact optimal pipe network is exceedingly difficult, the true optimal pipe network may differ from results shown in this section. For identical raw water conditions, the water costs for solutions obtained by the solver are typically within $2 per kgal of each other.

Figure 3-32 shows water costs for the optimal pipe network connecting all sources and sinks for both minimal and large-scale CBM development. Minimal CBM production corresponds to current conditions, where only a few sites are undergoing production. Large scale development corresponds to the CBM projects listed in Table 3-47. Large scale development of CBM in the IL basin increases the volume of treated water available for use at power plants by 56% (from about 4.5 MGD to about 7 MGD). The water cost ranges from about $15 to more than $50 per kgal over the range of flow rates, where the cost increases approximately linearly with flow rate. For very low water flow rates in the Basin, the impact of additional CBM produced water on cost is minimal. The water cost for large-scale CBM development is approximately $15 per kgal less than the cost of minimal development when the total flow rate is 4.5 MGD.

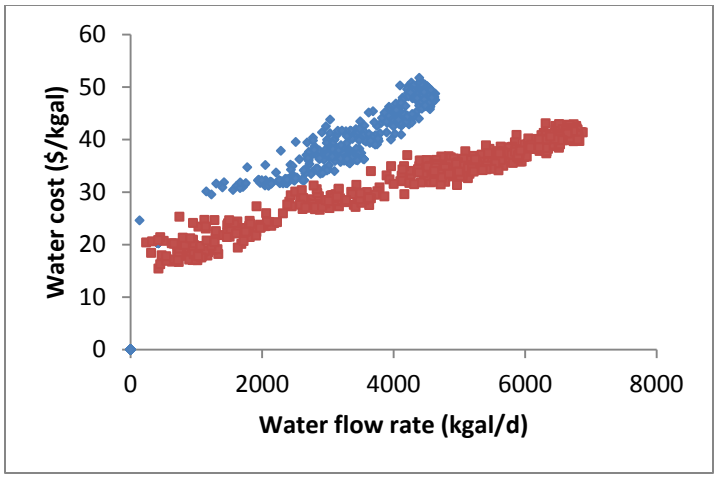

Figure 3-32: Water costs for delivery of produced water to all sinks, with minimal (blue diamonds) and large-scale (brown squares) CBM development.

Water flow rates and total costs for representative sinks are shown in Figure 3-33. Gibson and Clifty Creek receive the majority of available water because the water costs are the least for these plants for the whole range of flow rates available. As a comparison, water costs at Marion are $20 per kgal greater than costs at Gibson. This strongly encourages additional water to be transported to Gibson. For very small total water demand, each power plant obtains water from very nearby sources, so there is effectively no competition for the available water. As the demand increases, there is competition for the available water, and sinks with the lowest costs get more water.

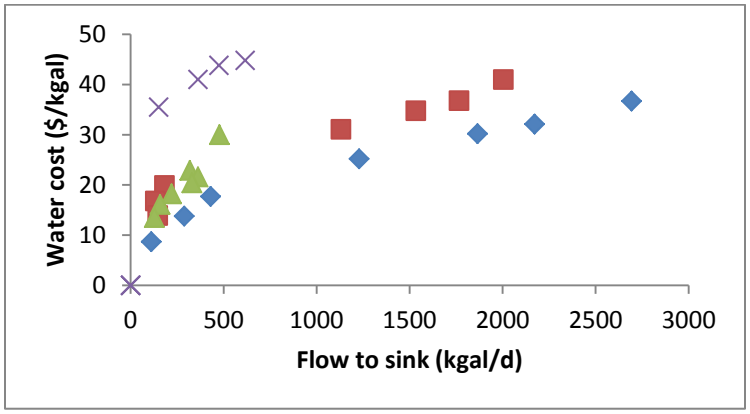

Figure 3-33: Water flow rates and costs at individual sinks for all sinks simulations. Sinks are Gibson (blue diamonds), Clifty Creek (red squares), Powerton (green triangles), and Marion (x).

Flow and cost results for each of the sinks in the all sinks simulations are shown in Table 3-49. Results are averaged over a set of 60 simulations for each total water demand. For total flow rates less than 1 MGD, only 3 power plants receive water. When all produced water is used, all of the power plants tend to obtain water. Since these results are averaged, some power plants may not obtain water for an individual realization (e.g., Figure 3-31). Gibson obtains the most water for all flow rates and generally has the lowest cost water. This is not true for larger flow rates, where sink 5 (Powerton) has the lowest

cost, albeit at a much lower flow rate. When all water in the Basin is used, Gibson obtains approximately 40% of the water available.

Table 3-49: Total water costs for the IL basin using all CBM sources broken down by sink and demand. Flow rate (q) is kgal/day and cost is $/kgal.

Sink	q	cost	q	cost	q	cost	q	cost	q	Cost	q	cost
1	288.6	13.80	1023.00	23.50	1228.2	25.20	1865.2	30.20	2172.3	32.10	2693.7	36.70
2	0	0	0	0	0	0	0	0	0	0	37.4	210.30
3	0	0	156.60	30.80	268.9	33.20	143.7	43.30	113.8	45.80	130.9	46.70
4	132.8	16.80	240.80	22.50	1130.2	31.10	1533.4	34.80	1765.3	36.80	2003.9	41.00
5	158.6	16.10	281.30	19.30	329.6	20.40	362.4	21.60	318.4	22.90	477.6	30.00
6	0	0	152.80	34.90	142.2	36.30	104.2	42.10	95.1	44.20	44.9	150.20
7	0	0	0	0	0	0	92.8	50.10	76.8	55.20	16	119.00
8	0	0	0	0	0	0	0	0	354.3	58.80	15.8	174.20
9	0	0	157.10	34.00	151.1	35.50	362	41.00	475.2	43.80	616.5	44.80
10	0	0	0	0	287.2	35.70	467.3	39.70	557.4	42.10	533.8	43.10
11	0	0	0	0	177.7	33.70	140.1	37.80	310.4	59.40	381.5	67.80
All	580	15.12	2012	25.05	3715	29.21	5071	33.81	6239	38.34	6952	42.75

At small water demand for the whole basin, the water costs at the sinks receiving water are similar. With increasing demand for the basin, a range of costs at the sinks is observed. The maximum cost observed is $210 per kgal, and four plants have water costs greater than $100 per kgal. By excluding the most expensive sources of water, the overall water cost decreases from $43 to $38 per kgal. The average cost of the excluded water is $81 per kgal. This especially expensive water would likely be avoided unless water demand is extreme.

Figure 3-34 shows averaged cost and flow rate data for all sinks simulations as well as for single sink simulations using Gibson and Clifty Creek. For the all sinks case, the cost and flow data is also shown for the water that goes to Gibson and Clifty Creek. The water costs at each sink increase for the all sinks case as a result of competition for water. For flow rates less than 1 MGD, the water cost at individual plants when all sinks demand water is essentially identical to the cost when a single sink demands water. For these conditions, the presence of other power plants does not influence which sources send water to Gibson or Clifty Creek. As demand increases, the water cost for all sinks demanding water increases faster than the individual case because other sinks compete water sources at intermediate distances. Clifty Creek and Gibson receive 68% of the available water.

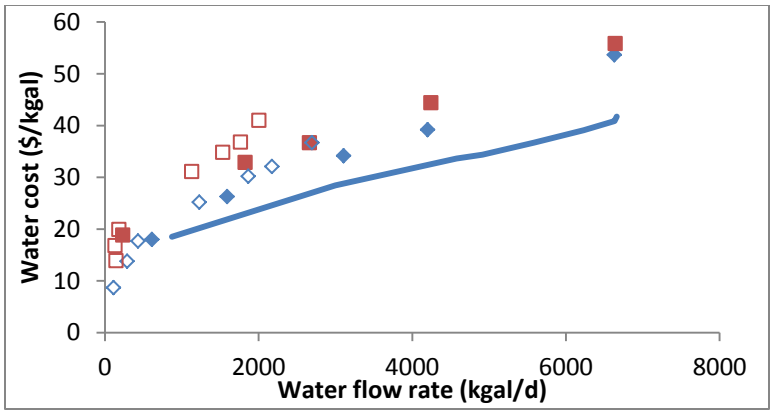

Figure 3-34: Water cost versus flow rate averaged over a set of realizations. Results are for all-sinks (solid line), Gibson (solid blue diamonds), and Clifty Creek (solid brown squares). Open symbols denote data from single sink simulations.

The degree of branching at individual sinks for the all-sinks simulations is shown in Figure 3-35. Degree of branching is significantly reduced compared to the individual cases (Figure 3-30) due to competition for nearby water sources. The maximum number of sources used at each sink is also reduced as a result of competition for existing water.

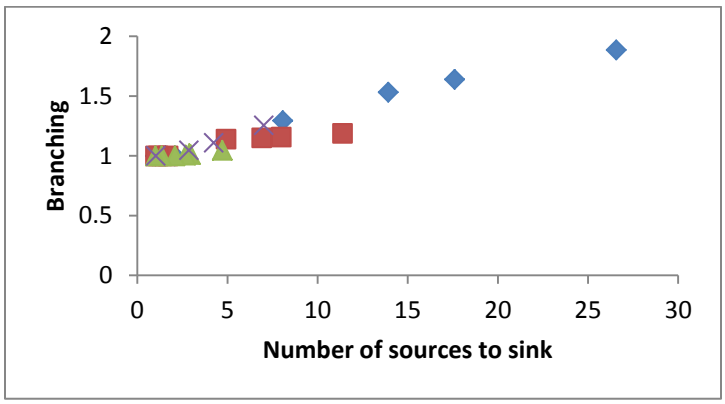

Figure 3-35: Degree of branching at several sinks for the all-sinks case. Sinks are Gibson (blue diamonds), Clifty Creek (red squares), Powerton (green triangles), and Marion (x).

Figure 3-36 shows the percentage of the total cost that is contained in the transportation cost for the all-sinks case as well as single sink cases for Gibson and Clifty Creek. For most cases, transportation costs are the largest water cost by far. The fraction decreases slightly with increasing flow rate to sinks. This is due to the use of lower quality water sources and the increased economies of scale for transportation.

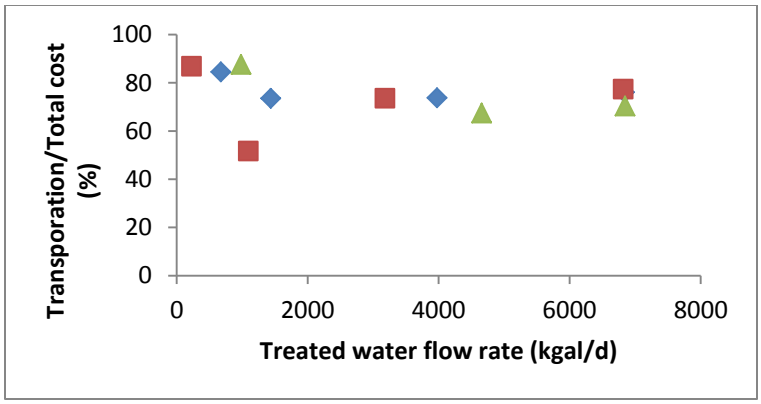

Figure 3-36: Percentage of total water cost comprised of transportation costs for Gibson only (blue diamonds), Clifty Creek only (red squares), and all-sinks (green triangles).

3.5.4 Electricity production increase allowed by produced water development

The maximum produced water flow rate available for use is estimated at 7 MGD. Current estimated water withdrawals from the 11 power plants studied in this project is 171 MGD. The produced water volume only adds 4% more water to the current supply. In order to increase electricity production by 30%, alternative cooling techniques must be considered to reduce water demand.

3.5.5 Paying for water treatment and transportation

The cost of water treatment and transportation are considered in the context of the revenues and expenses for fossil fuel producers and power plants. Future prices of oil, gas, and coal are highly uncertain in the next several decades, but current prices do provide guidelines for interpreting the water treatment costs calculated from our model.

An open question is who should pay for produced water treatment and transportation. Fossil fuel producers have the environmental responsibility to manage produced water, but treating it to a quality approaching drinking water standards is far beyond what is currently expected. Power plants may be expected to pay for the additional water obtained from produced water sources, but this additional cost would likely be passed along to electricity customers. The magnitude of water treatment costs in relation to both fuel producers' and power plants' revenues are explored.

Because future prices are unknown, current prices are used to estimate the bounds available for future water treatment costs. First, consider the amount of money available for water treatment from the oil producers. The current price of oil is roughly $100/barrel. Based on previous estimates, the water to oil ratio is 40 for producers in the IL basin. Current disposal costs for produced water are estimated at $1 per barrel of water. Converting these numbers to 1000 gallons (for easier comparison to water treatment costs), there is $60 of oil sales revenue for each 1000 gallons of water produced, and the current cost to dispose the water is $24 per 1000 gallons. Thus, to remain within current cost structures, the water treatment plus transportation costs plus disposal of concentrate should not exceed $24 per 1000 gallons. The absolute upper limit is $60 per 1000 gallons.

Another option is for the power plants to pay for treatment and transportation of produced water. For a 500 MW power plant, cooling water demand is approximately 6 MGD. For water costs of $5 and $30 per 1000 gallons, the daily costs of supplying water are $30,000 and $180,000 per day, respectively. Assuming the electricity price is $0.03/kw-h, the income to the plant is $360,000/day. The fraction of revenue spent on procuring produced water for cooling or other purposes would be 8.3% and 50% of total daily revenue, respectively, or that the price of electricity would need to be increased by those percentages to ensure similar profit margins. We can also compare the potential water cost to the cost for coal. Assuming that cost is $30 per short ton and that the energy density of coal is 6.67 kW-h/kg, a very rough estimate is $60,000 /day for coal. So, the cost of treated produced water for cooling could be similar to the coal cost.

Total water costs determined from the optimization model range from about $20 to $60 per 1000 gallons, where disposal costs are neglected. These costs may differ from actual costs of the installed network, but large changes to transportation costs must occur before the costs are affected in a major way. At this cost level, large-scale use of produced water at power plants will not be undertaken without large price increases for either oil or electricity or both. This suggests that produced water is a poor source of cooling water for power plants in the Illinois Basin. Studies of alternative cooling water sources or alternative cooling procedures should be undertaken to find lower cost alternatives.

An additional issue that should concern power plants is the quantity of produced water available. Assuming that most produced water will be treated with membranes and that the concentrate will be disposed, the total flow rate available is estimated to be approximately 6 MGD. The total water demand at the 11 power plants considered for this work is 170 MGD, assuming recirculating cooling systems. Additional water may be available from several sources. CBM may develop faster than assumed in this work. Produced water from more oil fields may be available if CO_2 EOR develops on a large scale. Finally, crystallizers may be used to increase the recovery from produced water sources. The cost of water in this case may increase even beyond the $60 maximum per 1000 gallons estimated in this section.

3.5.6 Alternative cooling technologies

A full comparison of costs for produced water to those for other alternative water sources and cooling types is beyond the scope of this work. Alternative cooling, including recirculated cooling systems, dry cooling and hybrid cooling processes, may be installed where once-through systems currently exist. Additionally, other alternative water sources may be considered.

The most abundant alternative source of water for power plant cooling is municipal wastewater. According to Cooley et al. (2006), the relative treatment costs for sources of drinking water are as follows: surface freshwater (1.25), recycled water (1.8), and desalinated sea water (2.6). So treatment costs for municipal waste water are typically 30% less than those for produced water with TDS equal to that for sea water (TDS = 35 g/L). A significant challenge for using treated municipal wastewater is that many power plants are located far from population centers. Using Gibson as an example, the nearest town to the power station is Mt. Carmel , IL (population 12,000). The wastewater treatment plant in Mt. Carmel has a present load of 2.2 MGD (Mt. Carmel, 2012). Gibson's water withdrawal is assumed to be

3100 MW × 12.2 kgal/d/MW = 38 MGD. The wastewater treatment load from Mt. Carmel could provide only an additional 6% of the water needed for the power plant. Using wastewater from more distant sources, however, incurs significant transportation costs.

Since transportation costs are typically more than two-thirds of the total delivered cost of produced water, alternative transportation methods may be considered. One possibility would be to discharge treated water into streams that flow downstream to water sources presently used by power plants. This will be limited to those produced-water sources that are connected to sinks by existing streams.

Finally, the pipe network should be designed to handle a range of possible flow rates. This may be difficult for pipelines located near the sinks. Sources may be taken on and offline due to maintenance or due to future development (particularly for CBM). The pipe diameters are going to be significant for this case. If the newly added water quantity is large compared to the existing flows, the pipe diameters may be too small in some sections of the pipeline to carry the additional water. To solve the problem, either parallel lines must be developed, or the additional water may have to be transported to a different location.

3.6 Conclusions

The Illinois Basin has no shortage of water for existing thermal electric power plants. Electricity demand is expected to increase by up to 30% by the year 2030, which would require additional generating stations with additional water demand. Because future power plants as well as modified existing plants are expected to use recirculating cooling water systems, the overall water withdrawal for power plants is expected to decrease by 2%, but water consumption is expected to increase by 40%.

Produced water from the Illinois Basin could be used to either supplement or replace freshwater withdrawals from rivers, lakes, and groundwater. However, either the water must be treated to nearly freshwater standards, or the cooling systems must be adapted to accommodate very saline water. For either case, water must be transported long distances from the sources to the sinks, and the cost of transportation is much greater than the treatment cost. Perhaps a solution to this problem would be to build future power plants much closer to regions with large volumes of produced water.

A method has been developed to estimate the least cost of using produced water as cooling water at power plants. The functions used for treatment and transportation costs are very rough estimates of the actual costs, but they are probably within a factor of 2 of the actual current costs of implementing such a system. The model results suggest that using a large fraction of the produced water from CBM will cost approximately $50 per kgal without further CBM development and $40 per kgal with large scale CBM development. The total available water for the two cases is 4 and 7 MGD, the larger of which is less than 6% of the current water withdrawals by power plants in the IL Basin.

3.7 References

Absolute Filtration Industries Corporation, “HydroflowTM Nut Shell Filter.” <http://www.walnutshellfilter.com/hydroflow.html>

AGV Technologies, Inc., Improving produced water quality for coal bed methane. RPSEA-R-518, Final report, September 30, 2004.

Brown and Caldwell Environmental Engineers and Scientists, Port of Milwaukee onshore ballast water treatment facility feasibility report. October 12, 2007. http://dnr.wi.gov/org/water/greatlakes/projects/WDNROnshoreBallastWaterTreatmentStudy_FinalReport.pdf

Clark, R. M., Lykins, Jr., B. W., Granular Activated Carbon Design, Operation, and Cost. Lewis Publishers, Inc., Michigan, 1989.

Cooley, H., Gleick, P. H., Wolff G., Desalination with a grain of salt. a California perspective. Pacific Institute, Oakland, CA, 2006.

DOE/NETL, Power Plant Water Usage and Loss Study. DOE/NETL Report, 2005.

DOE/NETL, Estimated Freshwater Needs to Meet Future Thermoelectric Generation Requirements. DOE/NETL-400/2007/1304, September 24, 2007.

DOE/NETL, Coal power plant database, 2007. Available for download from: http://www.netl.doe.gov/energy-analyses/hold/technology.html .

DOE/NETL, Use of non-traditional water for power plant applications: an overview of DOE/NETL R&D efforts. DOE/NETL-311/040609, November 1, 2009.

Dow Water and Process Solutions, FilmtecTM BW30-400.<http://www.dow.com/liquidseps/prod/bw30_400.htm>

Ecologix Environmental Systems, MCM 830P Organo Clay. <http://www.ecologixsystems.com/v_filtration_mcm830p.php>

Electric Power Research Institute (EPRI), Use of alternate water sources for power plant cooling. Technical Report 1014935, 2008.

Engineering News Record, <http://enr.construction.com/features/coneco/recentindexes.asp>

Genck, W. J., Guidelines for Crystallizer Selection and Operation. Chemical Engineering Progress, pp. 26-32, 2004.

GE Water and Process Technologies, Handbook of Industrial Water Treatment, <http://www.gewater.com/handbook/index.jsp>. (accessed on January 25, 2010)

Hutson, S. S., Barber N. L., Kenny, J. F., Linsey, K. S., Lumia, D. S., Maupin M. A., Estimated use of water in the United States in 2000, U.S. Geological Survey Circular 1268, 2004.

Kelting, D. L., Laxson, C. L., Review of Effects and Costs of Road De-icing with Recommendations for Winter Road Management in the Adirondack Park, New York, 2010.

Lawrence, A. Wm., Miller, J. A., Miller, D. L., Hayes, T. D., Regional assessment of produced water treatment and disposal practices and research needs, SPE/EPA Exploration and Production Environmental Conference, Houston, TX, 1995.

Lozier, J. C., Erdal, U. G., Lynch, A. F., Schindler, S., Evaluating Traditional and Innovative Concentrate Treatment and Disposal Methods for Water Recycling at Big Bear Valley, California. CH2M HILL, 2006.

MathWorks Inc., MATLAB version 7.10.0. Natick, Massachusetts, 2010.

McGivney, W., Kawamura, S., Cost Estimating Manual for Water Treatment Facilities. John Wiley & Sons, Inc., New Jersey, 2008.

Mickley & Associates, Membrane concentrate disposal: practices and regulation, Reclamation: managing water in the west, Desalination and water purification research and development program report no. 123 (second edition), 2006.

Midwest Geological Sequestration Consortium (MGSC), An Assessment of Geological Carbon Sequestration Options in the Illinois Basin, Topical Report, Task 3, 2004.

Midwest Geological Sequestration Consortium (MGSC), An Assessment of Geological Carbon Sequestration Options in the Illinois Basin, Final Report, Phase I, 2005.

Mount Carmel, IL <http://www2.illinoisbiz.biz/communityprofiles/profiles/MOUNTCARMEL.htm> (visited 4/24/12).

RosTek Associates, Inc., Desalting Handbook for Planners 3rd Edition, Desalination and water purification research and development program, Report No. 72, 2003.

Sakiadis, B. C., Fluid and Particle Mechanics. Perry's Chemical Engineers' Handbook., 6th ed. McGraw-Hill, pp. 5-38, 1984.

Sandy, T., DiSante, C., Review of available technologies for the removal of selenium from water, North American Metals Council, 2010.

Solley W. B., Pierce, R. R., Perlman, H. A., Estimated use of water in the United States in 1995, U.S. Geological Survey Circular 1200, 1998.

Suratt, W. B., Estimating the Cost of Membrane Water Treatment Plants. Camp, Dresser & McKee, 1991.

Swamee, P. K., Sharma, A. K., Cost Considerations, Design of Water Supply Pipe Networks. John Wiley & Sons, Hoboken, NJ. pp 79-95, 2008.

Tsang, P. B., Economic evaluation of treating oilfield produced water for potable use, SPE86948, March16-18, 2004.

US Bureau of Reclamation/ Sandia National Laboratories, Desalination and water purification technology roadmap – a report of the executive committee, 2003.

U.S. Department of the Interior (USDOI), Cost Assumptions for Contaminant Fact Sheets, 2001.

US EPA, EPA-600/2-79-162a August 1979: Vol 1 – Summary, 1979.

USEPA, Development Document for Final Effluent Limitations Guidelines and Standards for Commercial Hazardous Waste Combustors, EPA-821-R-99-020, 2000.

USEPA, Drinking Water Infrastructure Needs Survey – Modeling the Cost of Infrastructure, 2006.

Veil, J. A., Costs for Off-Site Disposal of Nonhazardous Oil Field Wastes: Salt Caverns Versus Other Disposal Methods. National Petroleum Technology Office, U.S. Department of Energy, DOE/BC/W-31-109-Eng-38-2, 1997.

Wilbert, M. C., Pellegrino, J., Scott, J., Zhang, Q., Water Treatment Estimation Routine (WaTER) User Manual.Water desalination research and development program report No. 43, U. S. Bureau of Reclamation, 1999. <http://www.usbr.gov/pmts/water/media/pdfs/report043.pdf>

Whitman, Requardt and Associates, The Handy-Whitman index of public utility contraction costs, 2010.

Chapter 4 **Sulfate removal from produced water**

4.1 Introduction

This chapter reports results from studies of two methods to remove sulfate from produced water. The first approach was an attempt to reduce sulfate with zero-valent iron doped with electron transfer agents. For this approach, the objective is to reduce the sulfur atom in sulfate molecules from (+6) to (-2) by transferring electrons from iron. Results from this approach were not promising, so this report does not provide a thorough literature review and does not give complete details of the experiments performed.

The second approach was to use commercially available anion exchange resins to remove sulfate.

For some produced water sources, sulfate concentrations may be sufficiently high to pose problems for beneficial reuse. Sulfate has been found to cause pitting and stress corrosion cracking in stainless steel. Reported concentrations in the steam that induced this behavior were between 5 and 20 ppm sulfate (Congleton and Li, 1999; Jones, 1992). EPRI suggests that sulfate levels must be below 2,000 – 3,000 mg/L to prevent concrete corrosion (EPRI, 2008), but levels closer to 966 mg/L in the cooling tower make-up water have been suggested to cause concrete corrosion (Engelbrecht and Swart, 2004).

4.2 Sulfate reduction by zero-valent iron

4.2.1 Methods

Preliminary experiments to test sulfate reduction with zero-valent iron were conducted using both iron powder and nano-sized zero-valent iron (NZVI) at two temperatures (25°C and 60°C). Based on a literature survey of similar iron reduction experiments, dosages of 100 g/L for iron powder and 5 g/L for NZVI were used.

The typical experimental procedure was as follows. Batch experiments were performed in 120 mL serum bottles sealed with septum-bearing stoppers. Nitrogen gas was continuously sparged through the bottles to ensure anoxic conditions. The bottles contained sulfate solutions with concentrations ranging from 100 to 600 mg/L. For some experiments nitrate replaced sulfate because nitrate is more readily reduced than sulfate. Iron along with any additional electron transfer agents and pH controls were then added. Bottles were placed on a shaker table to ensure good mixing. Initial and final pH values were measured. Solution samples were periodically taken, and concentrations of sulfate (or nitrate) were measured by ion chromatography.

The zero-valent iron materials were modified to attempt to improve their performance in reducing the anions. Iron particles were doped with rhenium (Re) and 4-dimethylaminopyridine (DMAP) in an attempt to increase electron transfer rates. We hypothesized that DMAP acts to stabilize the Re and increase adsorption to NZVI. Re(VII) may be reduced to Re(V) using hydrogen generated from Fe(0) oxidation in water. A water ligand is removed from Re(V) leaving an open site on Re(V) to coordinate with an oxygen atom from sulfate. We had hoped that sulfate would transfer an oxygen to the Re(V) oxidizing it back to Re(VII), and would ultimately be reduced to sulfide.

Additional experiments were performed to test the effectiveness of iron doped with electron transfer agents as a sulfate reducer. NZVI was synthesized in the laboratory, and both new NZVI and iron powder were doped with Re and DMAP. Typical experimental conditions for testing the influence of Re and DMAP as electron transfer agents in enhancing the performance of iron in reducing sulfate were as follows: 1) continuous nitrogen sparging of the bottles; 2) pH was initially 2.7 and then maintained at around pH 5 by a pHstat (except for the NZVI only case, where the final pH was 8.8); 3) 6% Re (by mass); 3) DMAP to Re ratio is 2 to 1; 4) 5 hour Re + DMAP sorption time before SO_4 and/or NZVI introduced. HPLC was used to measure concentrations of DMAP in solution at the end of the experiment. Conditions were varied to assess the impact of each component.

Two methods for pH control were evaluated, an acetate buffer and a pHstat using HCl addition. An experiment was conducted without Re (but with iron), and another was conducted with silica gel as an inert support medium in place of iron.

An x-ray photoelectron spectroscopy (XPS) analysis, using standard conditions, was conducted to examine the outer 5-10 nm of nanoscale NZVI surface after one of the standard experiments was completed.

Another possible means of reducing sulfate is to employ biological catalysts (Carroll et al., 2005). In sulfate-reducing bacteria, sulfate is first activated by the enzyme ATP sulfurylase and ATP (adenosine 5'-triphosphate) to APS (adenosine 5'- phosphosulfate). By activating sulfate the standard redox potential is shifted, and the sulfate reduction reaction is much more favorable:

$E^{o\prime}$ (APS / AMP + HSO_3) = - 60 mV

whereas

$E^{o\prime}$ (SO_4/ HSO_3) = - 516 mV.

The S-O-P moiety of APS is cleaved, yielding 80 kJ/mol, and APS reductase reduces APS to sulfite plus adenosine monophosphate AMP. APS reductase has two [4Fe-4S] clusters which are reduced to provide electrons for APS reduction. Sulfite is then reduced to hydrogen sulfide by sulfite reductase.

We hypothesized that NZVI could be used in place of APS reductase for the APS reduction step, and we performed several experiments to test this. Experiments were performed that attempted to reduce APS with NZVI without the presence of the enzyme APS reductase. The four experiments are summarized in Table 4-1. APS was mixed with NZVI with and without a buffer in serum bottles. Control experiments were run because APS is susceptible to hydrolysis at room temperature. A 3-(N-morpholino) propanesulfonic acid (MOPS) buffer was used to maintain constant pH for some of the experiments. Samples were frozen immediately after being taken to preserve any APS in solution. HPLC analysis was used to track APS concentration. A lead acetate indicator was used to test for the presence of hydrogen sulfide gas. HPLC analysis indicated that the MOPS buffer does not affect the APS peak. The MOPS buffer also does not interfere with sulfate or sulfite measurements during ion chromatography analyses.

Table 4-1: APS and NZVI experiments.

Experiment	Initial pH	[APS]/[SO4] (mg/L)	NZVI loading (g/L)	N_2 sparge?
Control- APS + MOPS buffer	7	142.5 / 32	0	Yes
Control- APS + MOPS buffer	7	142.5 / 32	0	Yes
APS + NZVI + MOPS buffer	7	142.5 / 32	22	Yes
APS + NZVI	5.5	142.5 / 32	22	Yes

4.2.2 Results from sulfate/nitrate reduction experiments with NZVI and iron powder

Results from the experiments testing the reduction of sulfate with zero-valent iron are shown in Table 4-2. For the preliminary batch experiments containing only NZVI or iron powder at room temperature and at 60°C, no sulfate reduction was observed. The pH increased by 0.4 from initial conditions in NZVI experiments but slightly decreased for iron powder experiments.

For experiments with Re-doped iron and an acetate pH buffer, no sulfate reduction was observed. The pH increased to approximately 10, the same value observed without buffer present.

For experiments performed using nitrate rather than sulfate, nitrate concentrations were reduced by 60% after 48 hours by both iron powder and NZVI. Iron powder showed faster kinetics than NZVI per unit surface area (determined by BET method). This suggests that an oxidation layer is formed on the surface of NZVI, which reduces its reactivity. Removal rates observed from nitrate experiments are much slower than literature results which report 60% nitrate removal within 1 hour (Yang and Lee, 2005).

Results of XPS analyses of Re-doped NZVI particles revealed the presence of several oxidation states of Re, including Re(0), Re(I) and Re(IV/V). Concentrations of Fe(II) on the NZVI surfaces were 10 times greater than Fe(0) concentrations. The S peak in the XPS spectra was difficult to interpret, but most likely indicated a sulfate or sulfite peak. A sulfide peak was not confirmed.

For the experiments with NZVI doped with Re and DMAP, the sulfate concentration decreased by 20%. Closing the system (no nitrogen sparging) resulted in no sulfate decrease, and removing pH controls (by acid addition) or adding sulfide resulted in less sulfate removal. Switching from NZVI to iron powder had no effect. Increasing DMAP concentrations resulted in increased sulfate removal, but the overall increase was not linear with the increase of DMAP concentration. When Re was not present, the sulfate concentration was reduced by about the same fraction as observed when Re was present. When iron was replaced with silica gel, no reduction in sulfate concentration was observed.

Table 4-2: Experimental results for Re-NZVI + DMAP system designed to reduce sulfate.

Experimental Conditions	Decrease of sulfate concentration at 48 hrs (%)
Re NZVI DMAP	20
Re NZVI DMAP, closed system	0
Re NZVI DMAP, No pH adjustment	10
Re NZVI DMAP, sulfide added	13
Fe Powder Re DMAP	22
5x (Re + DMAP), NZVI	30
NZVI, Re, 2x DMAP	36
NZVI, DMAP, Re not included	25
Iron replaced by silica gel, Re, DMAP	0

Experimental results suggest that electrostatic attraction between DMAP and sulfate is responsible for the observed decrease in sulfate concentrations. DMAP may be attracted to NZVI surfaces via coordination or electrostatics interactions. DMAP is protonated at pH below the estimated pKa of 10.1, where pKa was estimated using the Hammett correlation. During experiments, the pH was between 5 and 7.5, so DMAP molecules were protonated. DMAP may need to diffuse into corroded iron surfaces in order to adsorb, which may explain the slow sulfate sorption rate. The positive region of the protonated DMAP and sulfate anions may be bonded by electrostatic attraction.

After 5 hours of equilibration between DMAP and Re, the concentration of DMAP in solution was 43 mg/L. After addition of NZVI and sulfate, less than 5 mg/L DMAP (less than 3% of total DMAP) in solution was observed after 20.5 hours. Since DMAP was not desorbing from iron, DMAP desorption cannot account for the decrease of sulfate removal rate with time.

Results from the APS experiments listed in Table 4-1 using NZVI to reduce the sulfate present in APS are shown in Figure 4-1. H_2S was not detected in any of these experiments. Preliminary experiments under the same conditions as the APS experiments, but with a known amount of sulfide present, showed that the lead acetate indicators were working properly. APS concentration decreased rapidly in the presence of NZVI. The initial APS concentration was 142.5 mg/L but measured initial concentrations were 4 and 27 mg/L with and without MOPS, respectively. No sulfate reduction products were observed in the solutions.

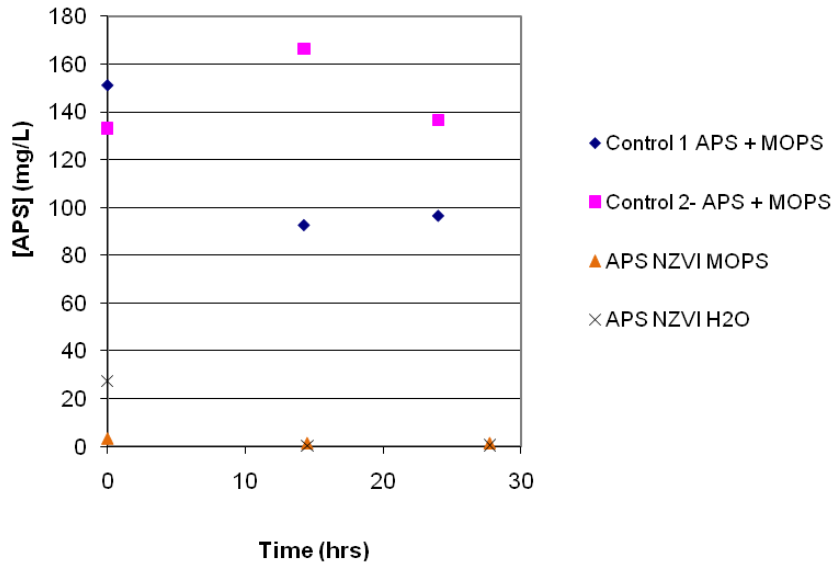

Figure 4-1: APS experiments shown with two controls.

APS/Fe solids were acid digested to release any H_2S from possible FeS precipitate. The solids were put in a sealed ion chromatography vial with a lead acetate indicator strip, and HCl was added with a syringe. No sulfide was detected.

4.3 Sulfate removal by ion exchange

4.3.1 Introduction

Ion exchange is an established treatment technology for the removal of common anions and cations from water. Synthetic anion exchange resins have ionizable groups that become charged upon loading with exchangeable anions such as chloride and hydroxide, which exchange with more favorable anions in solution. Typical ionizable groups include quaternary ammonium and amine groups (Reynolds and Richards, 1996). Reactions for strong base (Liberti et al., 1987) and weak base (Boari et al., 1974) anion exchange resins for sulfate removal can be represented as follows:

$$2\ RCl + SO_4^{2-} \Leftrightarrow R_2SO_4 + 2\ Cl^-$$

$$2\ RHCl + SO_4^{2-} \Leftrightarrow (RH)_2SO_4 + 2\ Cl^-$$

where R is the ion exchange radical. The typical dilute solution anion selectivity sequence for both ion exchange resins is $SO_4^{2-} > I^- > NO_3^- > CrO_4^{2-} > Br^- > Cl^-$ (Reynolds and Richards, 1996).

Specific research objectives for this part of the project were as follows: (1) compare commercially available strong base and weak base anion exchange resins' ability to remove sulfate in high chloride solutions, (2) determine at what chloride concentrations sulfate removal is hindered, and (3) gain insight into factors affecting sulfate removal in real produced water and engineering implications of those factors. Results from this study should aid in the selection of anion exchange resins for removing sulfate from produced water.

4.3.2 Methods

Six commercially available anion exchange resins were tested. The following resins were provided by Resin Tech, Inc.: WBG-30, SBG1, SBG1-OH, SBG2, and SBACR-HP. Reilly Industries, Inc. ReillexTM 402 (R402) was purchased from Sigma Aldrich. Table 4-3 presents the characteristics of each resin used in this study. Sulfate, chloride, and potassium hydroxide (KOH) stock solutions were prepared with sodium sulfate (Na_2SO_4), sodium chloride (NaCl), and KOH, respectively, each with greater than 95% purity and purchased from Fisher Scientific. Nanopure water (NPW) (>17.8 MΩcm-1; Barnstead Nanopure system) was used for all experiments and stock solutions. Trace metal grade hydrochloric acid (HCl) from Fisher Scientific was used for weak base resin pretreatment and titrations. Produced water samples are from Dale oil field and Galatia coal mine. N_2 gas (99.9%) was purchased from Matheson Tri-Gas (Joliet, IL).

Table 4-3: Resin characteristics

Resin	Type	matrix	Functional group	Exchange group	Repeating structure
SBG1	Strong base, Type 1	Poly-styrene DVB	Quaternary amine	Cl^-	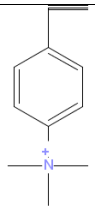
SBG2	Strong base, Type 2	Poly-styrene DVB	Quaternary amine	Cl^-	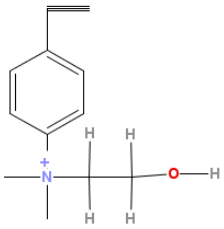
SBG1-OH	Strong base, Type 1	Poly-styrene DVB	Quaternary amine	OH^-	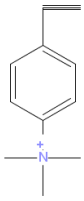
SBACR	Strong base, Type 1	Acrylic DVB	Quaternary amine	Cl^-	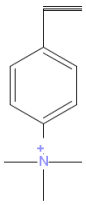
R402	Weak base	25% DVB	Pyridine	Cl^-	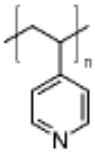
WBG-30	Weak base	Epoxy poly-amine	Secondary-tertiary amine	Cl^-	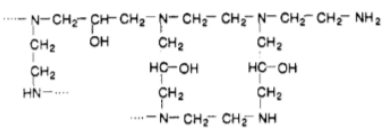

Batch equilibrium experiments were conducted for each anion exchange resin. All batch experiments were conducted in 120 mL glass serum bottles (Wheaton Industries Inc.) filled with 100 mL of aqueous solution (i.e. NPW, sulfate and chloride stock). A single 9 mL sample was then taken and analyzed to represent initial solution conditions. The resin to be tested was then added to the solution, and a 20 mm septum stopper (Bellco Glass, Inc.) and 20 mm aluminum seal (Fisher Scientific) were used to seal the

serum bottle. Solution concentrations and resin loadings varied depending on the experiment. Sealed serum bottles were secured in a gyratory shaker water bath (New Brunswick Scientific, Model G76D), which continuously shook the resins at 219 rpm at 25 +/- 0.1 degrees Celsius. At selected time points over a 24 hour period, the gyration was stopped and 1 mL samples were taken and analyzed to determine the time required to reach equilibrium.

Batch equilibrium experiments were performed using synthetic produced water solutions with varying chloride and sulfate concentrations and pH. Resin loadings were varied from 0.001 to 1,000 grams of resin per liter of solution (g resin/L) to obtain sorption isotherms. Strong base resins were used as-received, without pretreatment, but weak base resins were pretreated with acid titration as described below. For strong base resins, the pH was adjusted with KOH to pH 7.8 to model the pH of actual produced water samples. It is well known that the performance of strong base resins does not vary with pH. After a pretreated weak base resin was added to solution, the pH dropped to pH 3.5, which is necessary for the resin to remain protonated.

Acid titrations were performed with non-pretreated weak base resins, WBG-30 and R402, and the strong base resin, SBG1. The titrations indicate proton uptake capacity of the resin and are used to estimate proton concentration ranges for resin pretreatment. One hundred mL of 10,000 mg/L chloride solution was prepared in a 250 mL three neck flask for batch isotherm experiments. The three necks were filled with a pH meter electrode, a nitrogen gas line, and a rubber stopper, respectively. The solution in the flask was continuously stirred using a magnetic stir bar, and continuously sparged with nitrogen gas to eliminate the influence of carbon dioxide buffering. After one hour, one gram of resin was added to the solution and allowed to equilibrate. Increments of 1 M HCl were added to the solution and allowed to equilibrate, which took between one and twenty minutes. The pH meter was calibrated using 10,000 mg/L chloride standards at pH 4, 7, and 10.

Initial chloride concentrations were varied during batch equilibrium experiments to determine the influence of chloride on sulfate uptake. Synthetic produced water solutions were prepared with 100, 1,000, 10,000 and 40,000 mg/L chloride and 200 mg/L sulfate concentrations. Pretreated weak base resins were used at a resin loading of 10 g resin/L.

Batch equilibrium experiments were performed with synthetic and actual produced water solutions using pretreated weak base resins. Real produced water samples from Dale oil field and the Galatia coal mine were compared to synthetic produced water samples of the same sulfate and chloride concentrations. Measured concentrations were as follows, 576 mg/L sulfate and 87,364 mg/L chloride for Dale field, and 918 mg/L sulfate and 13,009 mg/L chloride for Galatia. Resin loadings were varied from 0.1 to 100 g resin/L to obtain sorption isotherms for each weak base resin.

Pretreated WBG-30 resin from Galatia produced water batch equilibrium experiments at 50 g/L resin loading were used to determine the resin's ability to be regenerated. After the initial batch equilibrium experiment, 100 mL of Galatia produced water was drained from the serum bottle and 100 mL of regenerant (6% NaOH) was added. The serum bottle with regenerant and resin were returned to the water shaker bath for 1 hour at 25+/- 0.1 degrees Celsius and rotation at 219 rpm. The regenerant

concentration and contact time were applied as directed by the resin manufacturer (Resin Tech). The resin was then washed 10 times with 30 mL NPW per 2.5 grams of resin before being pretreated again with HCl as described above. After pretreatment, the regenerated resin was then washed with NPW before being vacuum dried to the original weight. This describes one full regeneration cycle, after which the resin was ready for the next batch equilibrium experiment with a new volume of Galatia produced water.

Sulfate sorption data were modeled using a linear isotherm, and linearized Freundlich, and Langmuir isotherms as follows:

$$Cd = Kd\ Cw$$

$$\log(Cd) = (1/n)\log(Cw) + \log(Kf)$$

$$1/Cd = (1/(KL\ CSmax))(1/Cw) + (1/CSmax)$$

where:

Cd = adsorption capacity at equilibrium = (mg SO_4 sorbed /kg resin)

Cw = equilibrium sulfate concentration = (mg/L)

Kd = distribution coefficient = (L/kg resin) = slope of linear fit

n = Freundlich constant related to the sorption intensity of a sorbent = inverse of slope

Kf = Freundlich constant related to the sorption capacity = antilog of y-intercept

KL = Langmuir constant = (L/kg resin) = inverse slope multiplied by (1/ CSmax)

CSmax= maximum adsorption capacity = (mg SO_4 sorbed/kg resin) = inverse of y-intercept

The retardation factor was calculated for WBG-30 and R402 at each chloride concentration from sorption data as follows:

$$R = 1 + (p_b / n)K_d ,$$

where: K_d = distribution coefficient = (L/kg resin) from sorption data

n = porosity (assume n = 0.33)

p_b = bulk density = 0.6139 kg/L (WBG-30) and 0.5051 kg/L (R402)

For all batch experiments, concentrations of sulfate and chloride were analyzed using ion chromatography (IC; Dionex ICS-2000; Dionex IonPac AS18 column; 32 mM KOH eluent; 1.2 mL/min eluent flow rate). Calibration curves indicated a detection limit of less than 1 ppm sulfate. To protect the IC column, Dale and Galatia water samples were filtered with a 0.45µm syringe filter before ion chromatography analysis for sulfate and chloride.

4.3.3 Results

Acid titrations were performed for two weak base resins (WBG-30 and R402), the strong base resin (SBG1), and water. Results indicated that the weak base resins took up protons until 0.1 moles H^+ were added to the solution. By taking the difference between the pH of the water curve and the weak base resin curves, we estimated that WBG-30 and R402 have proton uptake capacities of 0.033 and 0.082 moles H^+ per gram of resin, respectively. The strong base resin, SBG1, took up no protons since it followed the water curve throughout the titration. These acid titrations motivated us to pretreat the weak base resins with 0.001, 0.01, and 0.1 moles H^+ per gram of resin to identify optimal acid pretreatment conditions.

The effects of varying the acid pretreatments on removal of 200 mg/L of sulfate from water containing 10,000 mg/L chloride by the two weak base resins are shown in Figure 4-2. Up to an 85% improvement in sulfate removal was observed for resins pretreated with 0.01 or 0.1 moles H^+ per gram of resin. For comparison, only 8% of the original sulfate was removed by resins pretreated with 0.001 moles H^+ per gram of resin. After the pretreated resin was added to solution, the pH remained constant during the 24 hour batch equilibrium experiment for R402 at all resin pretreatment conditions (i.e., from 0.001 to 0.1 moles H^+ per gram of resin). The pH value increased during the 24 hour batch equilibrium experiment for resin WBG-30 at the 0.001 level of pretreatment, which indicated that the resin still had proton uptake capacity and was not fully protonated. The pH decreased during the 24 hour experiment for the 0.01 and 0.1 levels of pretreatment using WBG-30 meaning that the initial equilibrium was not fully established. Overall, we observed a high equilibrium pH at the 0.001 level of pretreatment, in contrast to the 0.01 and 0.1 levels of pretreatment for both weak base resins. We attribute this to the poor sulfate removal at the 0.001 level of pretreatment.

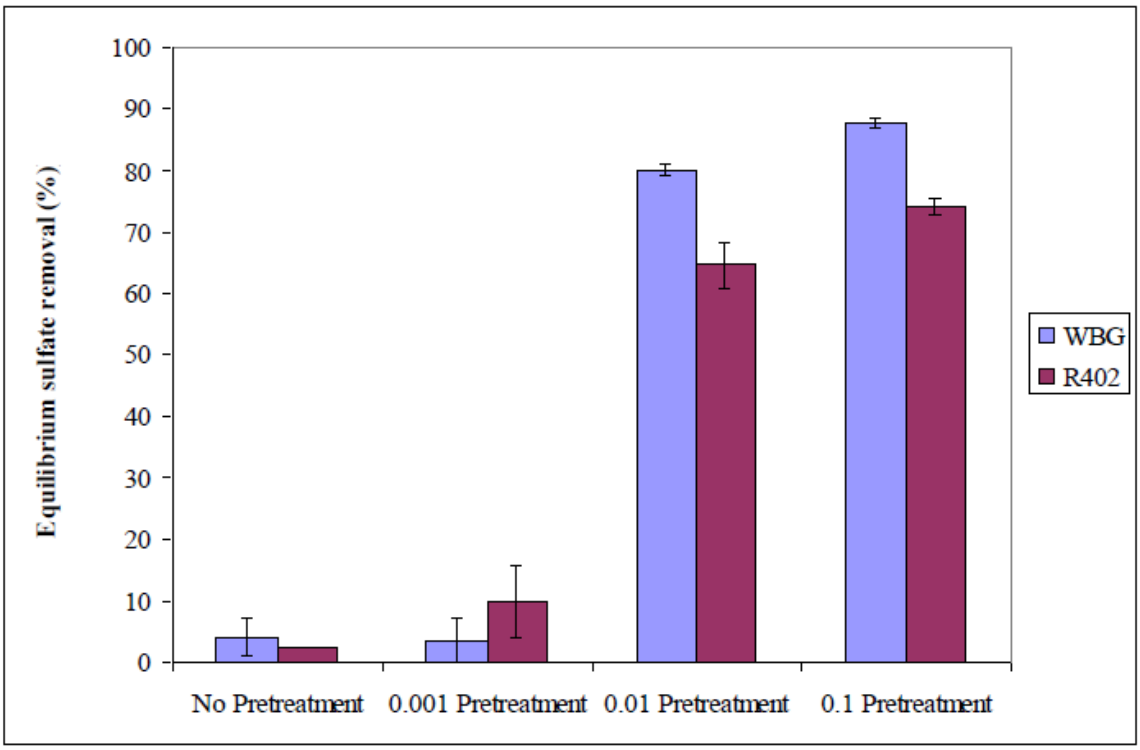

Figure 4-2: Effects of resin pretreatment on sulfate uptake for weak base resins.

Sorption isotherms for sulfate in the presence of 10,000 mg/L chloride for the six anion exchange resins are shown in Figure 4-3. Since weak base resins operate only at low pH and strong base resins function independent of pH, the experimental pH ranges differed between the two. The pH of solutions with strong base resins was adjusted to 7.9±0.2, and solutions with weak base resins were tested at pH 3.6. The pretreated weak base resins, WBG-30 and R402, markedly outperformed all the strong base resins. The weak base resins have secondary/tertiary amine functional groups or a pyridine group, which resulted in less steric hindrance compared to the quaternary functional groups of the strong base resins.

This is in agreement with Boari et al. (1974), who also showed that resins with secondary/tertiary amine functional groups preferred sulfate over resins with quaternary functional groups. Additionally, the suggested regenerant for strong base resins is a concentrated (i.e., >12,000 mg/L) chloride solution; this provides further insights into why strong base resins remove very little sulfate. Based on these isotherm results, the remainder of the study was carried out using only the pretreated weak base resins, WBG-30 and R402.

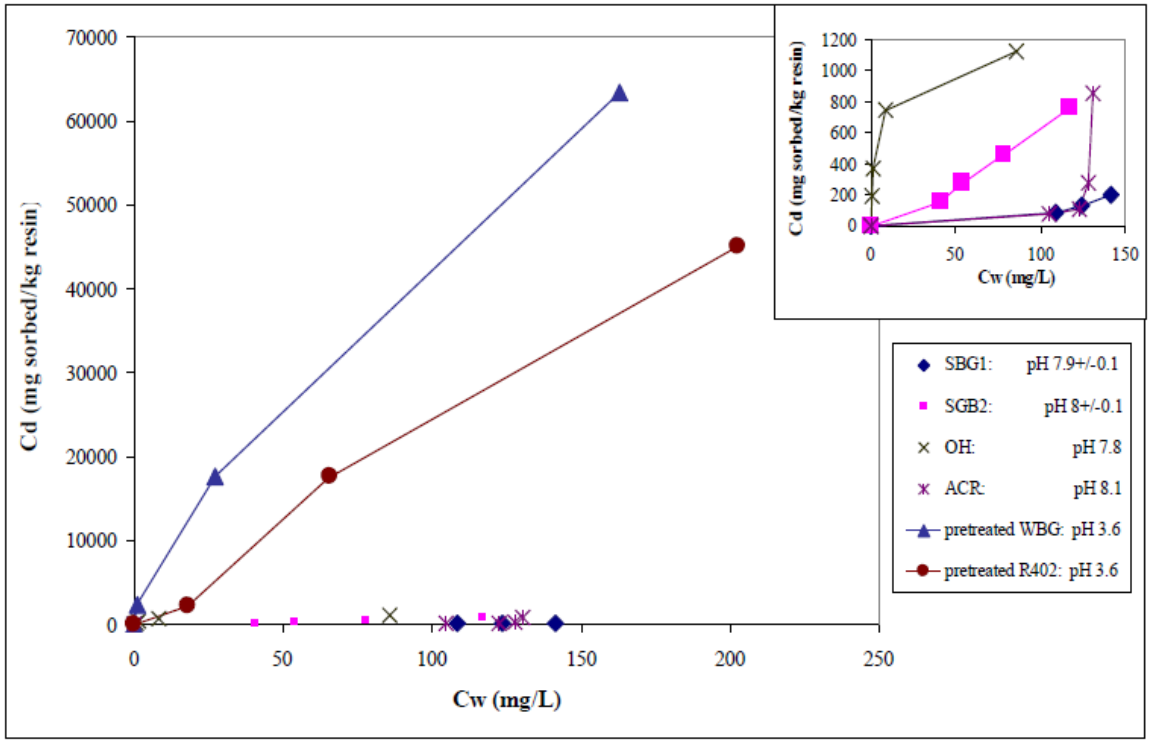

Figure 4-3: Sorption isotherms for commercially available weak base and strong base anion exchange resins. Inset plot shows strong base resin isotherms expanded.

As shown in the inset plot in Figure 4-3, the resin that used a hydroxide exchange group (SBG-OH) instead of a chloride exchange group had the greatest performance among the strong base resins. This result is in agreement with the typical anion selectivity sequence (Reynolds and Richards, 1996). Between Type 1 and Type 2 strong base resins, the Type 2 resin (SBG2) had better performance. In the case of the Type 2 resin, the functional group ($–C_2H_4OH$) is bulkier than the Type 1 resin's ($-CH_3$), but is more hydrophilic. This is further evidence that sulfate interacts more strongly with more hydrophilic resins.

Between the weak base resins, WBG-30 outperformed R402 due to its resin matrix and functional group. Sulfate is divalent and interacts with two anion exchange sites. The epoxy polyamine matrix of WBG-30 allows for more closely spaced exchange sites, which promotes exchange with divalent anions, compared to R402's DVB matrix that has wider-spaced exchange sites (Clifford and Weber, 1983). The WBG-30 resin also utilizes a secondary/tertiary functional group which has less steric hindrance than R402's pyridine functional group (see Table 4-3).

Results of batch studies used to determine the effect of chloride concentration on sulfate removal are shown in Figure 4-4. Sulfate removal was 99± 0.5% for both weak base resins at 500 and 1,500 mg/L chloride. At 10,000 mg/L chloride, sulfate removal dropped to 73 and 87% for R402 and WBG-30, respectively, and dropped to less than 40% at concentrations above 40,000 mg/L chloride. Sulfate removal decreases as chloride concentrations increase, but this result also suggests that there is a threshold chloride/sulfate ratio that must be achieved for the sulfate ion to be preferred.

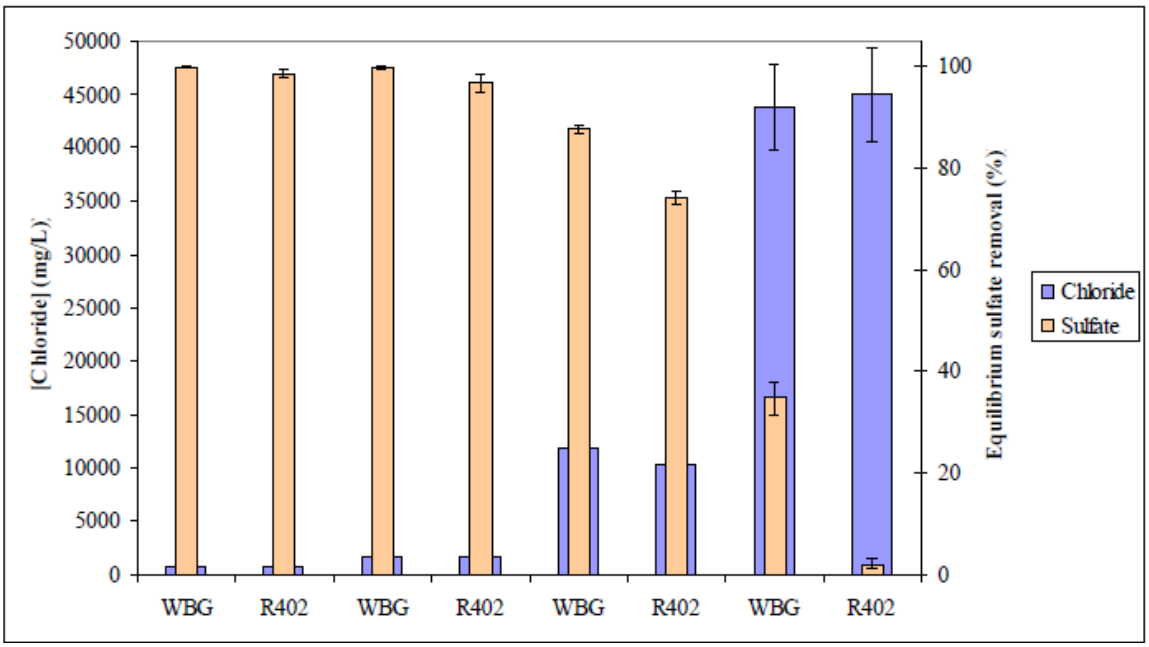

Figure 4-4: Chloride's effects on sulfate uptake by resins WBG-30 and R402.

Produced waters from enhanced oil recovery (Dale) and coal mining operations (Galatia) were analyzed for sulfate and chloride concentrations and used to conduct batch studies with weak base anion exchange resins. Chloride concentrations in Dale produced water samples averaged 87,364 mg/L and were approximately 150 times greater than their sulfate concentration. Sulfate removal for Dale was only 8±2% for the WBG-30 resin and 2.7±2% for R402. Chloride concentrations in Galatia produced water samples averaged 13,009 mg/L and were approximately 14 times greater than their sulfate concentration. More sulfate removal was observed for Galatia samples, 69.3 ±0.1% for the WBG-30 resin and 45.9±0.3% for R402. These performance differences are likely due to the epoxy polyamine matrix of WBG-30 and R402's bulkier and less hydrophilic DVB matrix.

During batch experiments, the pH dropped from pH 7.5±0.5 to pH 3.5 ±0.5 after the pretreated weak base resins were initially added to Dale and Galatia samples, which means that protons were released from the resins. The weak base resins lose between 0.2 and 1.5% of their total proton uptake capacities during this initial pH change, but their anion exchange capabilities are not significantly diminished.

Two synthetic produced water solutions consisting of the same chloride and sulfate concentrations as Galatia produced water samples, but with none of the other cations and anions in the real produced water, were batch-tested with the two resins for comparison. Sulfate removal from synthetic produced

water samples was within 3 and 10% of the sulfate removal from real produced water for WBG-30 and R402, respectively. Since the synthetic and real produced waters had statistically insignificant differences in sulfate removal, sulfate and chloride appear to be the dominant anions in determining the sulfate-removal performance of the resins, with minimal competition from competing anions.

Figure 4-5 shows sulfate removal for waters with different chloride/sulfate ratios but similar chloride concentrations. Real Galatia produced water has 13,009 mg/L chloride and a chloride/sulfate ratio of 38. In contrast, synthetic water used for results in Figure 4-4 had 10,000 mg/L chloride but a chloride/sulfate ratio of 160. Figure 4-5 shows that 3.6 and 2.9 times more moles of sulfate were removed from the real Galatia mine water by WBG-30 and R402, respectively, than from the synthetic solution with its much larger chloride/sulfate ratio. This suggests that both the absolute chloride concentration and the chloride/sulfate ratio in the water affect the performance of ion exchange resins in removing sulfate from water.

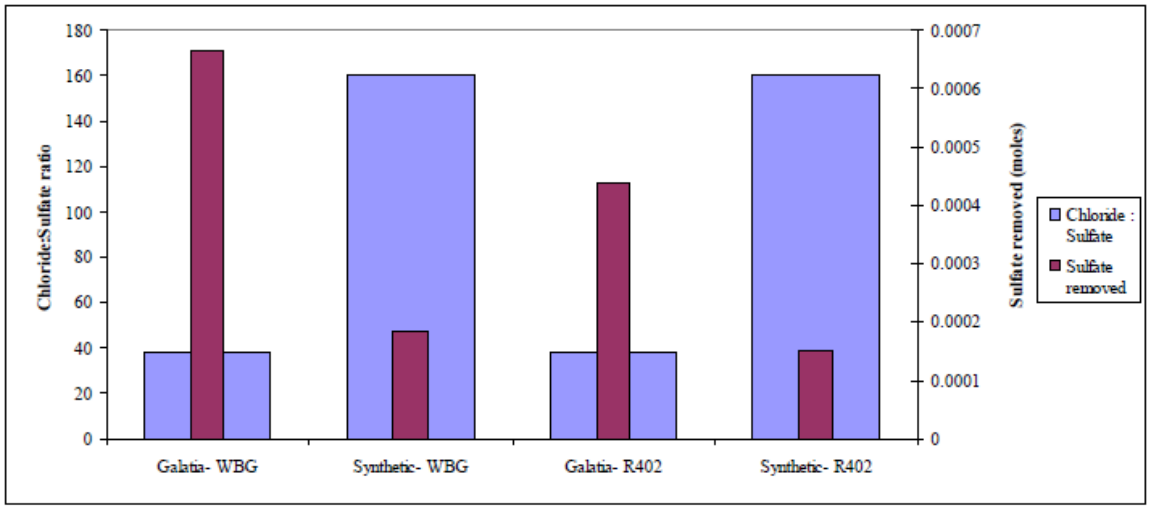

Figure 4-5: Sulfate removal for waters with similar chloride concentrations but differing chloride to sulfate ratios.

Sorption isotherms were determined for both synthetic and real Galatia mine water. Constants for linearized, Freundlich, and Langmuir isotherms are shown in Table 4-4. As expected, isotherm constants are significantly higher for WBG-30 compared to R402. The Galatia isotherm data appear to fit the Freundlich and Langmuir isotherms ($R^2 > 0.99$) better than the linear isotherm ($R^2 > 0.93$). The Freundlich and Langmuir isotherm fits are similar. Although isotherm tests were run with the produced water from Dale Field, less than 20% sulfate removal occurred at a resin loading of up to 100 g/L, thus making isotherm fitting impractical.

Table 4-4: Isotherm constants for real and synthetic Galatia produced water

		Isotherm							
		linear		Freundlich			Langmuir		
Water	Resin	K_d	R^2	K_f	1/n	R^2	K_L	C_{smax}	R^2
Synth.	WBG	358	0.988	766	0.859	0.997	0.0015	325000	0.999
Galatia	R402	98.0	0.978	166	0.917	0.982	0.000122	883000	0.984
Galatia	WBG	231	0.935	1520	0.667	0.992	0.00587	106100	0.999
Sample	R402	88.9	0.939	344	0.780	0.990	0.000986	139000	0.996

The ability for a resin to be regenerated is a key factor in determining whether it can be useful in practical applications. Batch experiments with real Galatia Mine produced water were conducted with WBG- 30. Weak base resins are typically regenerated by raising the pH, which causes the nitrogen sites to de-protonate and release sulfate anions. The resin was subjected to three regeneration cycles using a 6% NaOH solution as the regenerant. The resin was pretreated after each regeneration cycle. Sulfate removal differed by less than 0.2% between each regeneration, showing that WBG-30 can easily be regenerated without compromising performance.

To gain a better understanding of the feasibility of using anion exchange resins, we can calculate retardation factors (R) from isotherm Kd values, resin bulk density, and resin porosity in a packed bed. Assuming plug flow, we can estimate the reactor volume needed to treat produced water entering a power plant. For example, if R equals 430, we estimate that the resin can treat 430 bed volumes before sulfate breakthrough. If we assume we can supplement power plant water demand with 3.8 million liters per day (1 MGD) from produced water sources and we want to regenerate the resin once per day, a reactor treating real Galatia using WBG-30 would have the dimensions (length x width x height) of 2.1 m x 2.1 m x 2.0 m (7 feet x 7 feet x 6.5 feet). The suggested service flow rate for WBG- 30 from the manufacturer is 270 to 540 L/min.m^3 (2 to 4 gpm/ft^3), which corresponds to a service flow rate of 3.4 to 6.8 million liters per day (0.9 to 1.8 MGD) using the previous reactor dimensions. If we assume resin regeneration occurs once per week, the reactor dimensions increase to 4.0 m x 4.0 m x 4.0 m (13 feet x 13 feet x 13 feet), which corresponds to a service flow rate of 22.9 to 48.3 million liters per day (6.3 to 12.7 MGD). For both conditions, the service flow rate is well within the 3.8 million liters per day (1 MGD) water usage at the power plant.

The dependence of R on chloride concentrations is shown in Figure 4-6, where R is calculated from Kd values shown in Table 4-4. As expected, R markedly decreases at chloride concentrations greater than 40,000 mg/L, which corresponds to the resins' inability to remove sulfate in the presence of high chloride concentrations.

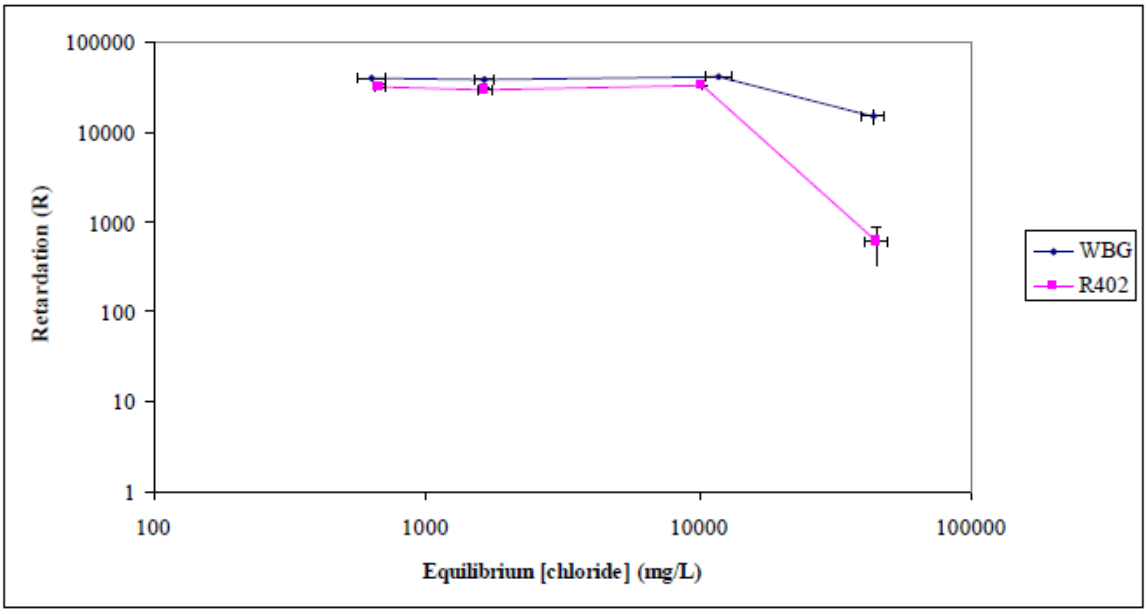

Figure 4-6: Chloride effect on retardation (R).

Pretreated weak base resins initially drop the pH of real produced water from pH 7.5±0.5 to pH 3.5±0.5 by releasing protons. This release insignificantly reduces the anion exchange capability of the resins in batch equilibrium experiments, but the long-term effects of this repeated loss were not studied. It could be favorable to drop the pH of incoming produced water to pH 3.5+/-0.5 before entering an anion exchange reactor so that the resin does not have to release any protons.

4.4 Conclusions

Abiotic catalytic reduction of sulfate remains an unsolved problem. Zero-valent iron, by itself or doped with electron transfer agents, cannot reduce sulfate. This project was also not able to observe sulfate reduction by zero-valent iron even after sulfate is activated to APS.

For optimum sulfate removal from high-chloride solutions, characteristics desired in an anion exchange resin are as follows: (1) type- weak base > strong base, (2) resin matrix- epoxy polyamine > DVB, and (3) functional group- secondary/tertiary amine > pyridine > quaternary ammonium. Weak base resins significantly outperformed strong base resins but must be pretreated with HCl and operated at low pH. Among the two weak base resins tested, WBG-30 consistently showed 15 to 25% higher sulfate removal than R402 throughout the study, which can arguably be attributed to its resin matrix and functional groups.

Sulfate removal by the weak-base resins significantly decreases above 40,000 mg/L chloride and more moles of sulfate can be removed at high chloride concentrations when the chloride/sulfate ratio is lower. For the two produced water samples tested, no anions other than sulfate competed for ion exchange sites. For practical use, weak base resins are able to be regenerated and their large retardation values allow for reasonable reactor dimensions.

4.5 References

Boari, G., Liberti, L., Merli, C.,Passino R., Exchange equilibria on anion resins. Desalination, 15, 145-166, 1974.

Carroll K. S., Gao H., Chen H. Y., et al., Investigation of the iron-sulfur cluster in Mycobacterium tuberculosis APS reductase: Implications for substrate binding and catalysis, BIOCHEMISTRY**,** 44(44)**,** 14647-14657, 2005.

Clifford, D.,Weber, W., The determinants of divalent/monovalent selectivity in anion exchangers. Reactive Polymers, 1, 77-89, 1983.

Congleton, J., Li, G. F., Stress corrosion cracking of a low alloy steel to stainless steel transition weld in PWR primary waters at 292 °C. Corrosion Science, 42(6), pp. 1005-1021, 1999.

Engelbrecht, J., Swart, J. S., Pilot scale evaluation of mine water (MW) as a cooling medium. Water SA, 30(5), 693-697, 2004.

Electric Power Research Institute (EPRI), Use of alternate water sources for power plant cooling. Technical Report 1014935, 2008.

Jones, R. H., ed., Stress corrosion cracking. ASM International, Materials Park, Ohio, 1992.

Liberti, L., Petruzzelli, D., Helfferich, F.,Passino, R.,. Chloride/sulfate ion exchange kinetics at high solution concentration. Reactive Polymers, 5, 37-47, 1987.

Reynolds, T. D., Richards, P., Unit Operations and Processes in Environmental Engineering. PWS Publishing, Boston, MA, 1996.

Yang G. C. C., Lee H. L., Chemical reduction of nitrate by nanosized iron: kinetics and pathways, WATER RESEARCH, 39(5), 884-894, 2005.

Appendix A. Innovative water treatment

This appendix has been submitted as a separate document because it contains proprietary information.